TRANSPORTATION RESEARCH
RECORD

No. 1255

Energy and Environment; Rail

Energy and Environment 1990: Transportation-Induced Noise and Air Pollution

A peer-reviewed publication of the Transportation Research Board

TRANSPORTATION RESEARCH BOARD
NATIONAL RESEARCH COUNCIL
WASHINGTON, D.C. 1990

Transportation Research Record 1255
Price: $23.00

Subscriber Categories
IB energy and environment
VII rail

Modes
1 highway transportation
2 public transit
3 rail transportation
4 air transportation

Subject Areas
12 planning
15 socioeconomics
17 energy and environment

TRB Publications Staff
Director of Publications: Nancy A. Ackerman
Senior Editor: Naomi C. Kassabian
Associate Editor: Alison G. Tobias
Assistant Editors: Luanne Crayton, Norman Solomon
Production Editor: Kieran P. O'Leary
Graphics Coordinator: Karen L. White
Office Manager: Phyllis D. Barber
Production Assistant: Betty L. Hawkins

Printed in the United States of America

Library of Congress Cataloging-in-Publication Data
National Research Council. Transportation Research Board.

Energy and environment 1990 : transportation-induced noise and air pollution.
p. cm.—(Transportation research record, ISSN 0361-1981 ; 1255)
ISBN 0-309-05009-X
1. Transportation noise. 2. Soundproofing. 3. Noise barriers. I. National Research Council (U.S.). Transportation Research Board. II. Series.
TE7.H5 no. 1255
[TD893.6.T7]
388 s—dc20
[363.73'1] 90-40567
CIP

Sponsorship of Transportation Research Record 1255

GROUP 1—TRANSPORTATION SYSTEMS PLANNING AND ADMINISTRATION
Chairman: Ronald F. Kirby, Metropolitan Washington Council of Governments

Environmental Quality and the Conservation of Resources Section
Chairman: Carmen Difiglio, U.S. Department of Energy

Committee on Transportation and Air Quality
Chairman: Susanne Pelly Spitzer, Minnesota Pollution Control Agency
Salvatore J. Bellomo, Paul E. Benson, David L. Calkins, John D. Dunlap III, Alan Eschenroeder, Steven J. Foute, Anne B. Geraghty, Howard A. Jongedyk, Roderick D. Moe, Sr., Carlton Thomas Nash, Christopher L. Saricks, Marilyn Skolnick, N. Thomas Stephens, John H. Suhrbier, Roger L. Wayson

Committee on Transportation-Related Noise and Vibration
Chairman: Domenick J. Billera, New Jersey Department of Transportation
Secretary: Win M. Lindeman, Florida Department of Transportation
Grant S. Anderson, Robert E. Armstrong, William Bowlby, Clifford R. Bragdon, Peter C. L. Conlon, Richard G. Dyer, C. Michael Hogan, M. Ashraf Jan, Harvey S. Knauer, Claude Andre Lamure, Bernard G. Lenzen, Christopher W. Menge, James Tuman Nelson, James R. O'Connor, Soren Pedersen, Kenneth D. Polcak, Joseph B. Pulaski, Karen L. Robertson, Simon Slutsky, Michael A. Staiano, Eric Stusnick, Dale K. Vander Schaaf

GROUP 2—DESIGN AND CONSTRUCTION OF TRANSPORTATION FACILITIES
Chairman: Raymond A. Forsyth, Sacramento, California

Railway Systems Section
Chairman: Robert E. Kleist, Ft. Washington, Maryland

Committee on Guided Intercity Passenger Transportation
Chairman: Robert B. Watson, LTK Engineering Services
Kenneth W. Addison, John A. Bachman, Raul V. Bravo, Richard J. Cassidy, Louis T. Cerny, Harry R. Davis, William W. Dickhart, Charles J. Engelhardt, Daniel J. Ferrante, George Haikalis, John A. Harrison, Richard P. Howell, Richard D. Johnson, Robert A. Kendall, W. J. Kleppinger, Jr., William J. Matthews, Myles B. Mitchell, James M. Rankin, Joseph J. Schmidt, Earl C. Shirley, Eric H. Sjokvist, Richard A. Uher

Wm. Campbell Graeub and Elaine King, Transportation Research Board staff

Sponsorship is indicated by a footnote at the end of each paper. The organizational units, officers, and members are as of December 31, 1990.

Transportation Research Record 1255

Contents

Foreword

Of the 15 papers in this Record, 3 deal with the subject of airplane noise and mitigation of its community impact. One paper discusses the rating system for sound insulation, two papers relate to public transportation issues, seven papers report research on traffic-induced noise, and two are related to high-speed rail (HSR) systems.

Public complaints have arisen in otherwise quiet locations about aircraft noise even from airplanes flying above 15,000 ft. Concerns continue regarding noise levels on the ground generated by new, advanced-design airplanes. Wesler reports on public reaction to low levels of aircraft noise. Because the noise levels involved do not exceed the usual criteria for community annoyance in the instances studied, Wesler suggests that there is need for better understanding of the intrusive effects of low levels of aircraft noise.

Sound insulation modification for buildings near airports has been found to be an effective way to mitigate aircraft noise impacts. Hougland reports on Denver's Stapleton Noise Insulation Program, which provides help to owner-occupied homes within the 70-L_{dn} contour and to schools and churches within the 65-L_{dn} contour. A study of before and after acoustical tests shows a 9- to 17-dB improvement in exterior-to-interior A-weighted noise reduction as a result of program modifications. The Shade paper describes noise reduction measures and their effects at three dwellings of the 1987 Pilot Residential Sound Insulation Program at Baltimore-Washington International Airport. The sound insulation modifications resulted in an improved reduction of aircraft noise intrusion by 4 to 10 dB over the existing noise reduction values. There also was a 3 to 18 percent cost savings in energy consumption.

Walker suggests the adoption of a new rating designation for sound insulation wall, named the Outdoor-Indoor Transmission Class. The author concludes that the calculation of this A-weighted reduction rating is simple and relatively easy to explain to the layman.

Wheel squeal is tonal noise heard when railcars travel around curves of small radii. This noise can be especially annoying to neighbors living near rail transit yards where there are many tight curves and train movements frequently occur during the night. Staiano and Sastry report on a comprehensive noise measurement and analysis program conducted for the Washington Metropolitan Area Transit Authority. The application of a proprietary alloy filler to a specially ground groove in the rail head was selected. Within 1 week of the installation, sound level showed a 23-dBA reduction and the complete elimination of squeal. However, after 6 months, chronic squeal reappeared.

Seven papers treat the issue of traffic noise prediction, mitigation, and abatement practices. Sung and Bowlby describe a knowledge-based preprocessor system that they developed to assist the engineer in creating detailed data input files to run a microcomputer version of the STAMINA 2.0 traffic noise prediction program. The system was tested on two major design projects previously done by human experts. The results indicated that the system produces a good, correct file from which to begin an analysis and is performing as desired.

Two additional papers in this Record cover the subject of traffic noise prediction. The first one, by Wayson and Bowlby, discusses atmospheric effects on traffic noise propagation. Although it has been generally accepted that these effects may produce large changes in receiver noise levels, they have largely been ignored during measurements and modeling. The paper reports several important conclusions. The STAMINA 2.0 computer program is the most commonly used method for prediction of traffic noise levels for impact analysis and noise barrier design. However, the program is based on the theory of freely flowing vehicles and constant speed. The paper by Bowlby et al. describes a methodology for using the program in nonconstant speed situations, such as signalized intersections, intersections with Stop signs, tollbooths, and highway loop and slip ramps.

Three papers deal with noise barriers. Situations arise in which noise barriers overlap to accommodate special highway geometrics. An arrangement of two parallel vertical barriers with traffic between may give rise to the overlapping noise barrier problem. The paper by Lee et al. describes an analytical procedure for investigating the reflection and diffraction

effects of such barrier designs. The second paper, by Rocchi and Pedersen, reports the preliminary investigations by the Ministry of Transportation of Ontario into the viability of transparent sheet glazing products made of glass or plastic for use in noise barriers. The third paper, by Cohn and Harris, reports noise barrier costs in the United States. A study was made of each state highway agency to codify all barriers constructed through 1987. New curves correlating cost per linear foot were developed using standard statistical techniques and made current to the fourth quarter of 1988.

Recently, many highway pavement projects have used open-graded asphalt overlays for increased skid-resistant properties. Subjective observations have noted a decrease in overall noise levels where such "pop-corn" pavement was used. The Polcak paper reports a field testing program for determining the difference in overall noise levels due to highway traffic on concrete versus open-graded asphalt pavement. The results showed a consistent 2- to 4-dBA reduction in L_{eq} that could be attributed to the open-graded pavement.

Santini and Rajan review numerous comparative studies on the emission characteristics of methanol- and diesel-fueled vehicles. The emission estimates are put on a common basis and applied to urban transit buses. The results imply that the replacement of clean diesel buses by methanol-fueled buses would not result in major air quality improvements.

Proposals for HSR passenger systems are under consideration for a number of locations around the country. Among the questions raised concerning environmental impacts of these systems is the issue of noise created by the operation of high-speed trains. Hanson discusses a noise-assessment procedure for the environmental impact analysis of HSR systems. This paper includes a comparison of the noise characteristics of conventionally tracked trains with those of magnetically levitated (maglev) vehicles. Hanson's conclusion is that these systems generate the same noise levels at speeds greater than 150 mph. Two high-speed systems under active development in Florida are a statewide HSR system and a regional maglev system. Lynch's paper reports analysis of the environmental, energy, and economic benefits for these two systems, which are projected to be fully permitted within the next 18 months and operational by the 1994 to 1996 period. A complex computer model integrates system characteristics for predicting benefits associated with proposals for different types of high-speed technology.

Public Reaction to Low Levels of Aircraft Noise

JOHN E. WESLER

In several recent instances, community annoyance has resulted from noise of airplanes flying at relatively high altitudes (or relatively far from airports). In none of these instances did the noise levels involved meet the usual criteria for community annoyance or interference with individual activity, either in terms of time-averaged noise levels or single-event noise levels. Five basic concepts are presented on which criteria may be established for assessing intrusiveness of low noise levels generated by aircraft in remote, quiet locations.

In several recent instances, community annoyance has resulted from noise of airplanes flying at relatively high altitudes (or relatively far from airports). For example, as the result of changes in flight patterns associated with the major New York airports, public complaints have arisen about airplane flights over northern New Jersey, even though in many instances the airplanes were flying at 15,000 ft or higher. Troublesome noise levels on the ground may also be generated by the new, swept-blade, advanced turboprop airplanes when flying at cruise altitudes of 30,000 ft or higher (*1*). Complaints about aircraft noise over national parks and wilderness areas have resulted in a Congressional requirement to measure these noises and determine their severity (Public Law 100–91, August 1987).

In these instances, the noise levels involved did not meet the usual criteria for community annoyance or interference with individual activity, either in terms of time-averaged noise levels or single-event noise levels. A better understanding of intrusive effects of low levels of aircraft noise is needed, specially in areas of relatively low ambient noise. In particular, practical criteria are needed for improving analyses of effects of changes in air traffic patterns, setting noise standards for airplanes at cruise altitudes, and assessing aviation noise impacts and minimum overflight altitudes for national parks.

ALTERNATIVE APPROACHES

Normally, the first approach to this type of issue would include a social survey to identify the extent of noise annoyance under the conditions presented. However, such an undertaking would be extremely complex and costly and would require an extensive effort and a considerable length of time to conduct properly. Schultz (*2*) observed that "for noise sources with A-weighted levels below about 65 dB, community annoyance reactions are quite variable and do not appear to be sufficiently strongly related to level of noise exposure to support confident prediction of annoyance or activity interference." Instead of extensive research, therefore, some guidelines that are already available may be used to reach a practical conclusion. Five basic concepts from which criteria may be established for assessing low-level aircraft noise in remote, quiet locations are described in the following paragraphs.

Because the public is little aware of civil airplanes flying at cruise altitudes today, even in quiet locations, the first concept is the flyover noise level of current turbofan airplanes. Few measurements of such noise-producing events are available, but unpublished FAA measurements indicate maximum A-weighted sound levels of 45 to 50 dB for flight altitudes of 30,000 to 35,000 ft above mean sea level. Thus, 50 dB would be considered an acceptable threshold of aircraft noise impact in remote locations. However, a higher level might also be acceptable.

The second concept (based on signal-to-noise ratio) would permit as an acceptable intrusion a maximum noise level of no more than, say, 10 dB above background level. For ambient A-weighted sound levels of 30 to 40 dB typical of remote areas, an acceptable A-weighted aircraft noise level would then be 40 to 50 dB.

However, both concepts address single-event noise levels and ignore the effects of repetitive occurrences. The third concept is based on a time-averaged measure of aircraft noise, such as day-night average sound level (DNL, symbolized L_{dn}). In the 1974 EPA Levels Document (*3*), a DNL of 55 dB was identified as acceptable for remote areas, described as "outdoors in residential areas and farms and other outdoor areas where people spend widely varying amounts of time and other places in which quiet is a basis for use." In fact, at many of the locations in northern New Jersey from which complaints about changed air traffic patterns were registered, the DNL measured was consistently less than 55 dB. If an average of 100 daily overflights is assumed, the mean sound exposure level (SEL) corresponding to a DNL of 55 dB for these overflights would be 85 dB, with a corresponding maximum A-weighted sound level of about 75 dB. This value is substantially higher than the noise levels currently created by high-altitude airplane flights.

The 1974 EPA Levels Document (*3*) also suggested the use of corrections to normalize DNL to account for different non-acoustic factors that could influence public reactions to noise. An empirical adjustment of 10 dB was suggested for situations involving a "quiet suburban or rural community remote from large cities and from industrial activity and trucking" (*3,4*). This adjustment suggests an acceptable exterior DNL threshold of 45 dB for remote areas. Again for 100 daily overflights, this condition would impose a limiting mean SEL of 75 dB,

Wyle Laboratories, 2001 Jefferson Davis Highway, Arlington, Va. 22202.

or a maximum A-weighted sound level of about 65 dB. This value also seems too high to be useful.

As a fifth concept, a threshold DNL not to exceed the ambient DNL could be established. Again, a typical ambient DNL of 30 to 40 dB in remote areas would be reasonable. For 100 daily overflights, this range corresponds to maximum A-weighted sound levels of 46 to 58 dB. These levels are generally consistent with current experience.

SUGGESTED GUIDELINE

Thus, as a reasonable recommendation, aircraft-related DNL should not exceed the ambient DNL as a threshold for aircraft noise intrusion in quiet areas remote from an airport. Because such a guideline inherently requires that the ambient DNL must be measured (or estimated accurately) in those areas in which low levels of aircraft noise are evaluated, this requirement may present some difficulty in its implementation.

VALIDITY OF A-WEIGHTED AND DNL MEASUREMENTS

It must be emphasized that the preceding discussion is appropriate only for remote areas away from airports. DNL remains the best measure of noise impact near airports and should continue to be used for assessing land-use compatibility (*5–7*).

Because of the greater atmospheric attenuation of higher frequencies, the noise spectra from high-altitude airplanes are dominated by lower-frequency sounds. Consequently, A-weighted sound level may not be the most representative metric for evaluating these noises. In a recent project in which the taped noise histories of 24 aircraft flyovers at altitudes of 7,000 to 15,000 ft above mean sea level were correlated, maximum A-weighted sound levels were compared with a number of other possible metrics (*8*). The A-weighted sound level correlated closely with all the other metrics, including the so-called "detectability level" (*9*). Hence, there would be no significant advantage in using any one metric over the others. In particular, A-weighted sound level remains entirely appropriate as a metric for assessing the effects of low levels of aircraft noise.

REFERENCES

1. *Noise and Emission Standards for Aircraft Powered by Advanced Turboprop (Propfan) Engines.* FAA Notice of Decision, Federal Register, Vol. 54, May 5, 1989, p. 19498.
2. T. J. Schultz. *Community Noise Rating*, (2nd ed.). Applied Science Publishers, London and New York, pp. 269–274.
3. *Information on Levels of Environmental Noise Requisite to Protect Public Health and Welfare with an Adequate Margin of Safety.* Report 550/9-74-004, U.S. Environmental Protection Agency, Washington, D.C., March 1974.
4. K. M. Eldred. Assessment of Community Noise. *Noise Control Engineering*, Institute of Noise Control Engineering, Washington, D.C., Sept.–Oct. 1974, pp. 88–95.
5. *Airport Noise Compatibility Planning.* Federal Aviation Regulations, Part 150 (14 CFR 150), FAA, U.S. Department of Transportation, Washington, D.C., 1989.
6. *Guidelines for Considering Noise in Land Use Planning and Control.* Federal Interagency Committee on Urban Noise, FAA, U.S. Department of Transportation, Washington, D.C., June 1980.
7. *Sound Level Descriptors for Determination of Compatible Land Use.* ANSI S3.23, American National Standard Institute, New York, 1980.
8. J. E. Wesler. *Effects of the Expanded East Coast Air Traffic Plan on Noise over Northern New Jersey.* Wyle Research Report WR 89-2, Arlington, Va., Mar. 1989.
9. Bolt, Beranek, and Newman, Inc. *The Relationship Between Annoyance and Detectability of Low-Level Sounds.* Report 3699, submitted to U.S. Environmental Protection Agency, Cambridge, Mass., Sept. 1978.

Publication of this paper sponsored by Committee on Transportation-Related Noise and Vibration.

Airport Noise Insulation of Homes Surrounding Stapleton International Airport

DANA HOUGLAND

The Stapleton Noise Insulation Program (SNIP) was initiated by the city and county of Denver, Colorado, to provide aircraft noise insulation modifications to owner-occupied homes within the 70-L_{dn} (equivalent day-night sound level) contour and to schools and churches within the 65-L_{dn} contour of Stapleton International Airport. SNIP is not a part of an FAA Part 150 study, and such a study has not been completed on this airport. The project area includes approximately 3,936 homes, 22 churches, and 8 schools. The primary data base for homes in the study area was acquired from assessor's records. A data base program was used to sort and arrange the homes into distinct categories from which representative samples were selected for a detailed engineering survey—a total of 52 homes. Twenty-six of these homes were selected and used for preconstruction sound insulation testing, and 24 were used for preconstruction air infiltration testing. Because the construction funds available for this program limited expenditures to $7,500.00 per home, recommended sound insulation modifications developed from results of the detailed engineering survey were given priority to achieve the maximum sound insulation for the least cost. Two sample homes were completed as a part of the design phase. Before-and-after A-weighted acoustical tests show a 9- to 17-dB improvement in exterior-to-interior noise reduction as a result of SNIP modifications.

In 1986, the city and county of Denver agreed to a $27 million program to insulate homes around the existing Stapleton International Airport. This program preceded the May 17, 1988, vote by Adams County in favor of allowing Denver to annex property for the construction of a new international airport.

Denver residents had known that a major new airport was imminent because of growing air traffic and the physical constraints of the Stapleton site (originally established in 1928). But because new airports take time to plan and build, Stapleton needed to expand in the interim to keep up with traffic growth until the new airport could be opened in the mid-1990s.

Airport operations affect three counties—Denver, Arapahoe, and Adams. Denver and Adams Counties are affected the most heavily. In order to expand the airport by adding a new runway, Denver entered into an Intergovernmental Agreement (*1*) with the commissioners of adjoining Adams County. This agreement conditionally approved expansion of Stapleton by adding a new east-west runway located partially on the Rocky Mountain Arsenal northeast of the existing airport. Remedial measures addressing the noise issue required as a condition for the Intergovernmental Agreement were a noise-monitoring system and a noise-insulation program. Stapleton had already enjoined a penalty system for noncompliance with its noise cap regulations. However, the monitoring system provided for the identification of individual noise events that were not in compliance with the noise cap regulations.

David L. Adams Associates, Inc., 1701 Boulder St., Denver, Colo. 80211.

SCOPE

The Stapleton Noise Insulation Program (SNIP) created by the Denver-Adams County Intergovernmental Agreement (*1*) is a municipal project with specific monetary commitments. SNIP is not an FAA Part 150 study (*2*) and no such study has been completed on this airport. The program allows reimbursement of up to $4.00 per ft^2 for churches and schools and up to $7,500.00 for each owner-occupied home. The monetary limits were negotiated amounts based on the estimated value of the aviation easement required from each participating homeowner. A monetary maximum went against conventional FAA program wisdom, but it does present an interesting challenge for the engineering team comprising David L. Adams Associates, Inc., acoustical consulting engineers; W. C. Muchow & Partners, Inc., architects; System Engineering Corporation, mechanical engineers; and Roos Szynskie, Inc., electrical engineers.

The homes designated as eligible by the Intergovernmental Agreement are those located within the 70-L_{dn} (equivalent day-night sound level) contour. A noise measurement verification program is not included in the scope of this project. In heavily developed areas where the contour intersects a block, the L_{dn} contours have been expanded to include whole blocks. The requirement of owner occupancy was implemented to prevent real estate speculation in an already crisis-stricken market. Figure 1 shows the basic areas affected.

The other major constraint that required the most creativity from the engineering team was the predetermined installation format. Before the request for proposal was even released, the Stapleton administration had determined that local existing rehabilitation agencies such as the Denver Urban Renewal Authority and Aurora Community Service would handle all contracting. Their responsibilities included contact with the homeowners, inspection of the homes, preparation of bid packages, bidding, and construction administration.

The process was complicated because lengthy negotiations with the installing agencies were not completed until 6 months to 1 year after the engineering team finished the study and

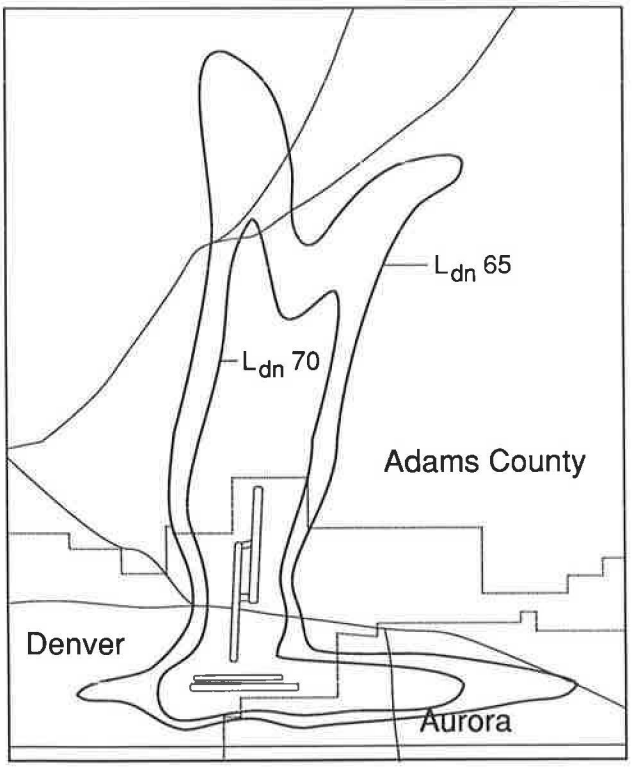

FIGURE 1 SNIP study area. The program includes owner-occupied homes within the 70-L_{dn} contour and schools and churches within the 65-L_{dn} contour.

design phases. The engineering team did not know exactly who would be doing the installation or what their capabilities would be. The time allotted for the engineering study was 6 months. The time allotted for the completion of the entire project was a maximum of 3 years.

RESEARCH PROCEDURE

The only material available with which to start the project was a map of the area showing the noise contours superimposed. The administrators had not gathered records or lists of the homes involved.

Research commenced with a search of all assessor's records for homes located within the contour area. Obtained from the assessor's records were owners' names and addresses, house addresses, house sizes, dates of construction, and basic construction types. Although the assessor's records were set up to record extensive information, their formats varied widely from one assessor to another, making the information unreliable. However, using a data base system, the engineering team was able to sort, categorize, and group the homes by basic construction type, size, age, and type of heating and ventilating system. The data base was also used for mass mailings that later proved to be very helpful.

The initial study of assessor's records established the following basic information about homes located in the study area:

1. There are 3,936 dwellings in the study area that could potentially be owner occupied—632 in Denver and 3,304 in Aurora or Adams County.
2. Most homes were built between 1949 and 1963, as shown in Figure 2. The peak year for construction was around 1952. The construction dates ranged from the 1880s to 1983.
3. At least 65 percent of the houses are of wood frame construction with forced air heating and ventilating systems, as shown in Figure 3.
4. Approximately 80 percent of all houses are single-story structures.
5. The average house size is approximately 1,000 ft².

From the basic information obtained from the assessor's records, a selection of homes was made including all categories of construction, heating systems, age, and location. A detailed engineering survey was initiated to cover at least 2 percent of the study population. It was the intent of the detailed engineering survey to document the conditions in the various home types in order to have a broad base of data from which to develop solutions.

Residents were contacted by mail soliciting voluntary participation in the engineering survey. A total of 52 homes were finally surveyed. The survey team consisted of architects, mechanical engineers, and electrical engineers and was headed by the acoustical engineering team. Tasks for survey responsibilities were divided among the team members so that everyone would complete field documentation in approximately 1 hr. A designated spokesperson was appointed to answer homeowner questions.

From the detailed engineering survey, information was compiled regarding types, locations, and frequency of exterior shell penetrations; wall construction; window construction;

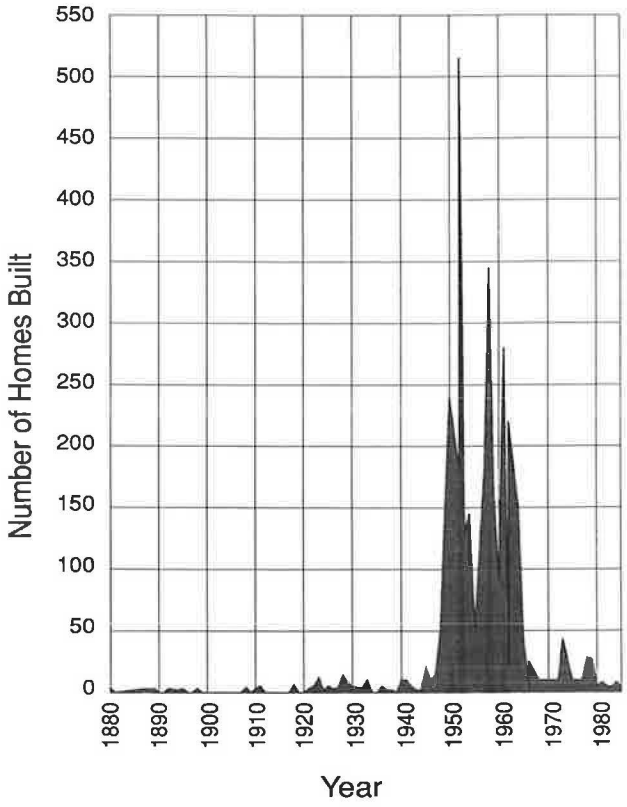

FIGURE 2 Number of homes built per year within the study area.

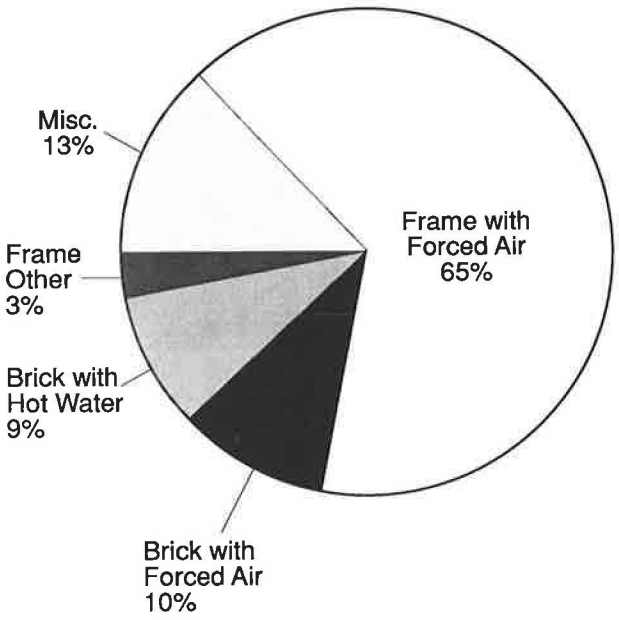

FIGURE 3 Distribution of basic construction and heating types in the study area.

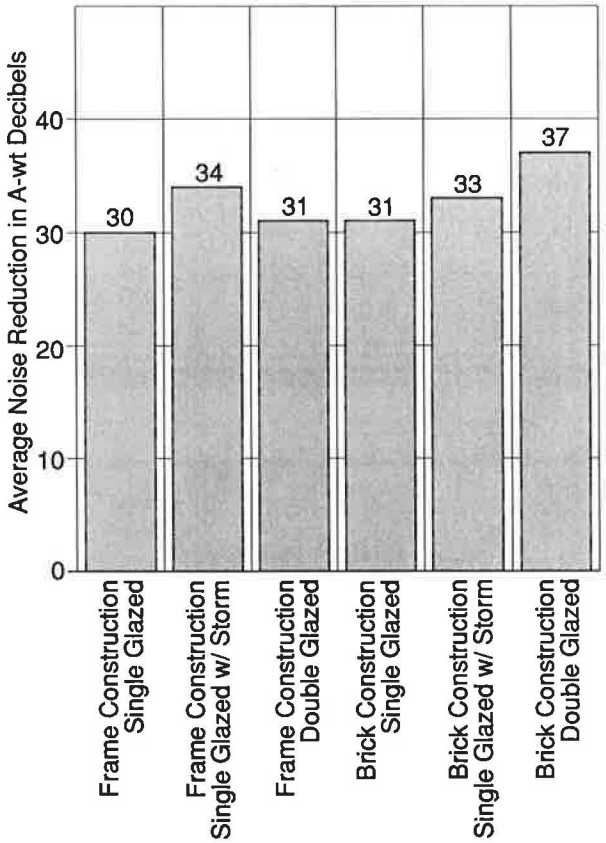

FIGURE 4 Results of preliminary acoustical testing showing average noise reduction (in A-weighted decibels) by composite exterior construction.

room layouts and sizes; type and condition of heating and cooling systems; and electrical service capacity. Photographic records were used extensively and were later very valuable in developing details.

Objective testing of the noise insulation capability of the exterior shell was completed on 26 residences. Average noise reductions in A-weighted decibels for the residences tested, grouped by construction, are shown in Figure 4. These tests were conducted using ASTM Standard E966-84 (*3*). There was typically a 7-dB spread between test results on houses within a given category. The widest deviations occurred on the homes with brick constructions, single-glazed windows, and aftermarket storm windows. The wide variety of storm window styles is the most likely source of this variation.

Infiltration testing was completed on the same 26 homes using the standard blower door method. The homes were tested to determine the amount of air leakage that a home experiences before any modifications made for sound insulation. The range of the results compiled is shown in Figure 5. To establish the effectiveness of the retrofit measures, all 26 homes will be retested after modifications are completed.

One of the primary reasons for including infiltration testing is the current high level of concern over radon gas levels in the Rocky Mountain region. Recent U.S. Environmental Protection Agency studies have shown Colorado to have higher than normal levels of radon gas. The public is generally very concerned about indoor air pollution and radon gas. Advanced documentation on air infiltration was acquired so that the program's impact on indoor air quality could be documented and homeowners' concerns could be addressed.

METHODS OF ANALYSIS

The goal of the analysis was to determine the most cost-effective methods of improving each home's exterior-to-interior sound insulation. The results of the field surveys were used as the data base, and the tested houses were used to verify the calculation methods.

The basic calculation method used to establish the acoustical effectiveness of various treatments was the external wall noise reduction method developed by Wyle Laboratories under contract to the U.S. Department of Housing and Urban Development (*4*). This method was later expanded to also address highway and aircraft noise under contracts to the FAA and the FHWA (*5*). Although there is still considerable controversy regarding this method, it had the largest existing data base on external wall constructions at the time of its compilation.

Calculations were made on a living room area and the worst case bedroom for each home. A computer program developed for the calculations incorporated a data base of exterior construction elements such as walls, windows, and roofs. A base-case calculation was completed along with a series of upgrades. As shown in Figure 6, major sound paths are well established from previous research and the engineering team's initial calculations. The following detailed priority list for the purpose of improving sound insulation was established from the detailed series of calculations:

1. Control direct penetrations into living areas such as mail slots, dryer vents, and exhaust fans.
2. Baffle penetrations into plenum areas such as attic vents directly adjacent to living areas not separated by a double-sided wall in the upper levels of the house.

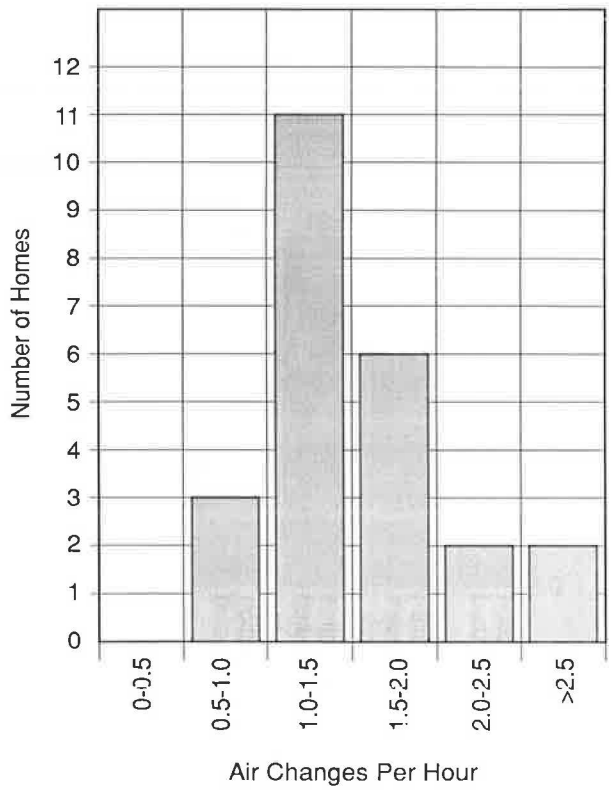

FIGURE 5 Results of preliminary air infiltration testing showing distribution of homes having various levels of air infiltration.

3. Introduce sufficient fresh air ventilation so that windows can remain closed on the large number of temperate days characteristic of the Colorado climate.
4. Add sound insulation in attics that are not insulated or are poorly insulated.
5. Upgrade sound insulation of the window units in bedroom and living areas.
6. Reduce sound and air infiltration of both standard and sliding glass doors.
7. Upgrade large building surfaces when the existing walls cannot perform as well as upgraded windows and doors.
8. Baffle penetrations into plenum areas such as crawl space vents directly adjacent to living areas not separated by a double-sided wall in the lowest levels of the house.
9. Add air conditioning or a specially designed evaporative cooling system, as money allows.

The priority item generating the most controversy is the preference given to small building elements such as windows and doors over large building elements such as the roof. The justification for this decision is best explained by a short series of illustrations. Figure 7 shows the effectiveness of typical wall constructions without any penetrations. Figure 8 shows the effectiveness of each of these walls when an average single-glazed window is placed in the wall. The poor sound insulation of the window quickly becomes the determining factor in the overall sound insulation. Figure 9 shows improvements in sound insulation gained through acoustical upgrades to the window system.

FIGURE 6 Major sound paths into typical residential construction: 1, air infiltration; 2, small building elements; 3, major building elements.

Extensive cost estimating has been done on all basic remedial constructions. The results of these cost estimates refined the priorities of some measures. Other measures had to be modified or eliminated altogether to comply with stringent local building codes. Such code limitations, for example, eliminated any modifications to existing flues or chimneys.

PROGRAM DESIGN FOR THE INSTALLING AGENCIES

Ideally, in such a program, the experienced engineering team could enter the individual homes, rapidly make an assessment, input the necessary information into a computer program, and directly generate the necessary drawings and specifications for each home in the program. The intentional separation of the engineering team from the decision-making process in the installing portion of the program forced a reconsideration of how to best convey the necessary information to the installing agencies. Although installing agency personnel are experienced in housing rehabilitation procedures, they can be expected to have no acoustical background and very little heating, ventilating, and air-conditioning experience. Neither of the installing agencies had any computer system or computer experience. The engineering team's responsibility was to devise a manual system to guide the installing agency personnel through the inspection, decision-making, and construction document process. The bidding and construction management processes were planned to be handled in a conventional manner.

The system that the engineering team devised is contained in the SNIP Installing Agency Manual (unpublished). Figure 10 shows the section-by-section breakout of the manual with a brief description of its contents. Not included in this figure are the lists of homes by jurisdiction. The lists are

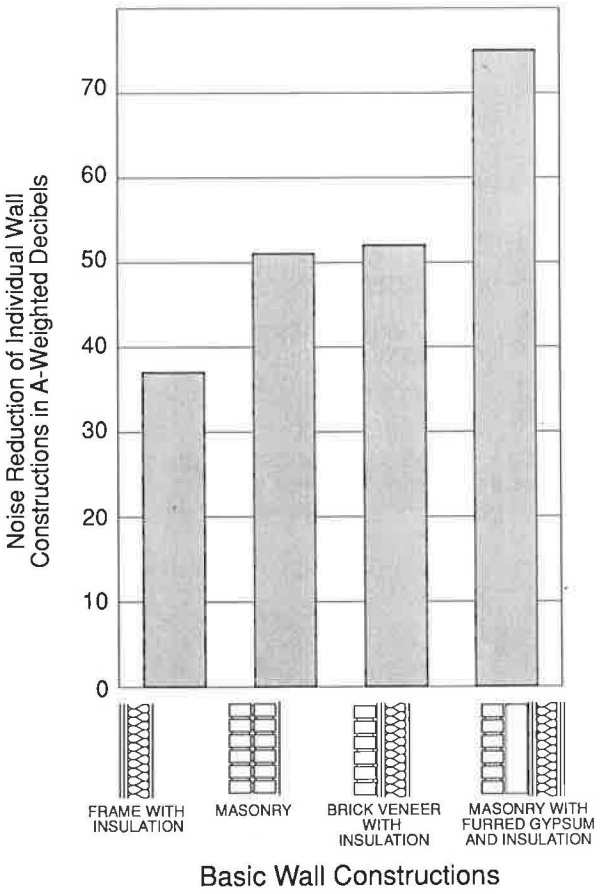

FIGURE 7 Comparison of noise reductions (in A-weighted decibels) of three common exterior wall constructions found in the field and one common modification used in the sound and energy insulation program.

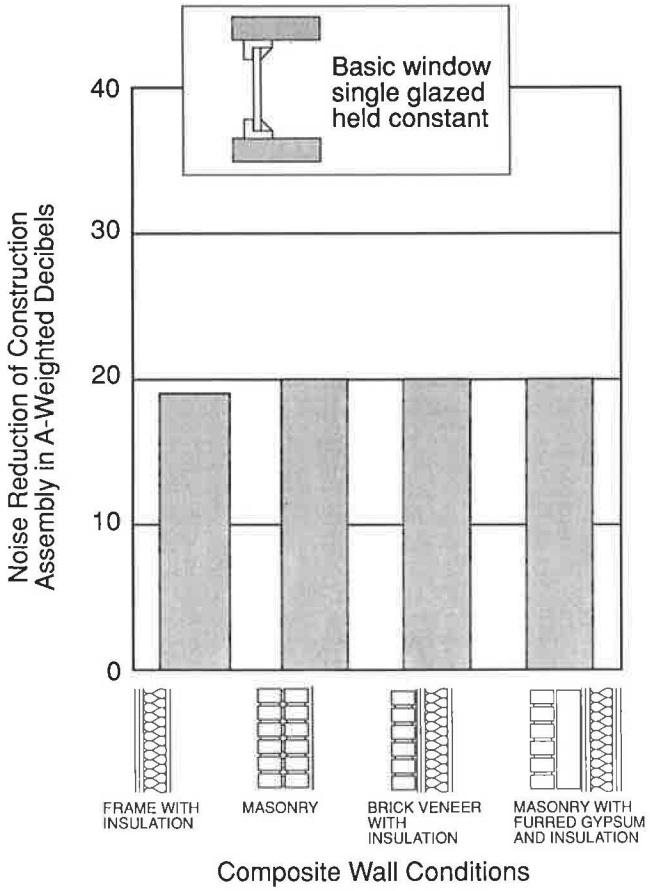

FIGURE 8 Comparison of composite noise reductions (in A-weighted decibels) of the same wall constructions as shown in Figure 7 with a standard single-glazed window installed in the wall.

ordered to directly correspond to utility billing lists. In this manner, they allow for a preliminary determination of whether or not a home is owner occupied.

The checklist system is designed to aid the inspector in recording information crucial to evaluating such items as the condition of a window or door. Even though there are many parallels, a window acceptable for energy efficiency is not necessarily acceptable for acoustical insulation. A small sample of a checklist is shown in Figure 11.

The corresponding decision tree is shown in Figure 12. The decision tree sections pose the questions necessary to evaluate the existing construction conditions. Though most of the decision trees are much more complex than the one shown here, they all direct the inspector to a reference in the priority blocks, applicable details, and appropriate specification sections to be included. The specification references are intended as guides and are not intended to be limiting.

Through use of the priority block system, the inspector is given direction not only to the relative importance of any item to the overall sound insulation but also to the cost-estimating procedure shown in Figure 13. The cost estimate for each item is included as a part of the priority block along with a description of the required action. The series of 11 priority blocks covering all actions allows for a running subtotal of ordered measures. These measures are also ordered by the room involved and that room's location within the home. By developing a list of items the estimated total cost of which is between 120 and 150 percent of the allotted $7,500.00, the installing agencies can prepare a package of details and specifications for competitive bid.

The program was designed to group 20 homes together in each bid package. The group of 20 homes was selected as being a cost-effective package for smaller contractors. To minimize disruption for the homeowner, the contractors are allowed only 1 week in each home.

Two sample homes were completed to check the effectiveness of the proposed modifications. The sample homes also served as the background for the filming of two videotapes. One was for acquainting the contractors with acoustical construction practices; the other was for introducing the homeowners to the program and explaining the important features of the program.

To acquire acoustical windows having a consistent standard of acoustical performance, the windows were bulk bid so that all custom replacement windows will be supplied by a single manufacturer. This process, though laborious and controversial while in progress, is proving very beneficial from a cost standpoint and is maintaining a high level of quality control throughout the program. When storm windows are used instead

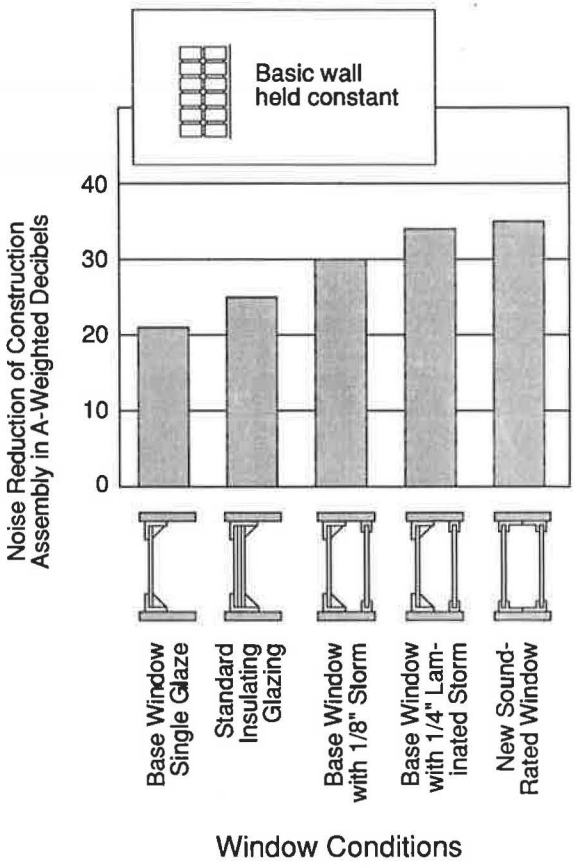

FIGURE 9 Comparison of the effect on the noise reductions (in A-weighted decibels) when window upgrades are applied for the same basic wall construction.

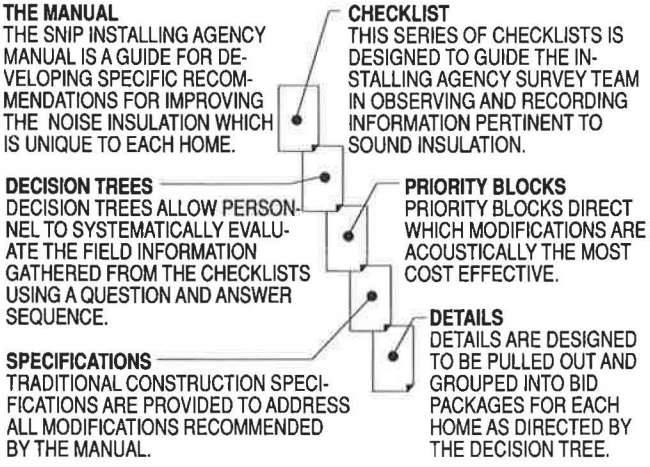

FIGURE 10 Organization of SNIP Installing Agency Manual.

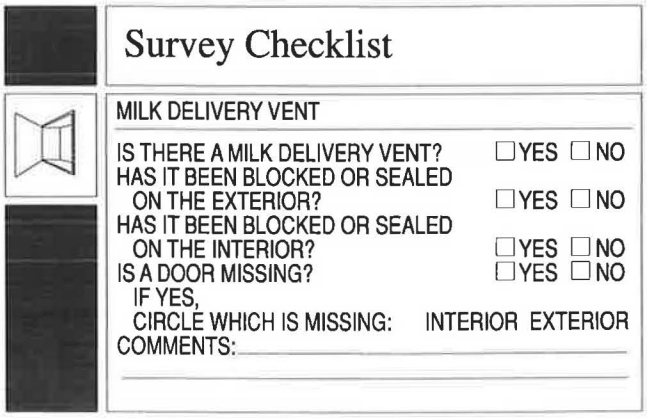

FIGURE 11 Sample section of a survey checklist from the SNIP Installing Agency Manual.

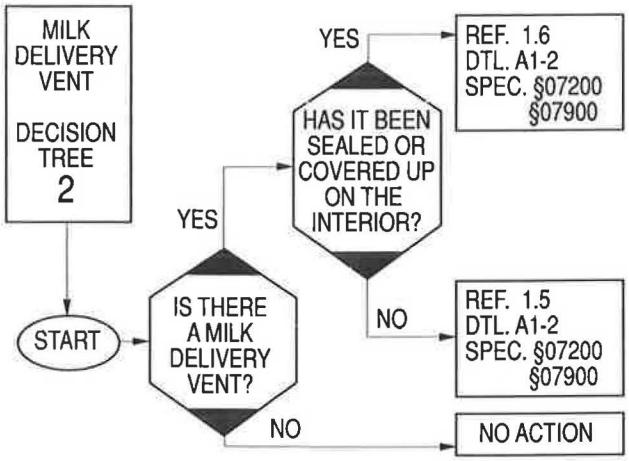

FIGURE 12 Sample section of a decision tree from the SNIP Installing Agency Manual.

REF.	CAT.	ACTION REQUIRED	ITEM COST	UNIT AMOUNT	COST	SUB-TOTAL
		PRIORITY BLOCK 1				
1.1	MAIL SLOT	NO ACTION REQUIRED.	$0/EA			
1.2		SEAL EXISTING MAIL SLOT. INSTALL NEW MAILBOX.	$78/EA			
1.3		REPLACE DOOR. INSTALL NEW MAILBOX.	$45/EA			
1.4		SEAL EXISTING MAIL SLOT.	$65/EA			
1.5	MILK DELIVERY VENT	FILL VENT WITH INSULATION. PROVIDE SEALANT ON PERIMETER OF BOTH DOORS.	$49/EA			
1.6		PROVIDE SEALANT ON PERIMETER OF BOTH SIDES.	$45/EA			

FIGURE 13 Sample section of a priority block from the SNIP Installing Agency Manual.

of replacement windows, there are several preapproved manufacturers, but the process allows continually evaluating new suppliers, if required. Currently, only two manufacturers have made the effort to apply for approval.

SUMMARY

Results of the program are expected to vary with respect to the basic construction of each house. Tentatively, modifications are designed to achieve approximately 10 dB of additional sound reduction from exterior to interior of the homes.

On the sample homes, before-and-after tests indicate improvements. The Aurora house, a frame house with aluminum siding over asbestos shingles, showed a 9-dB improvement. The Denver house, of solid masonry and brick construction, showed a 17-dB improvement. Floor plans of the Aurora and Denver homes with acoustical testing locations are shown in Figures 14 and 15, respectively. Results of the

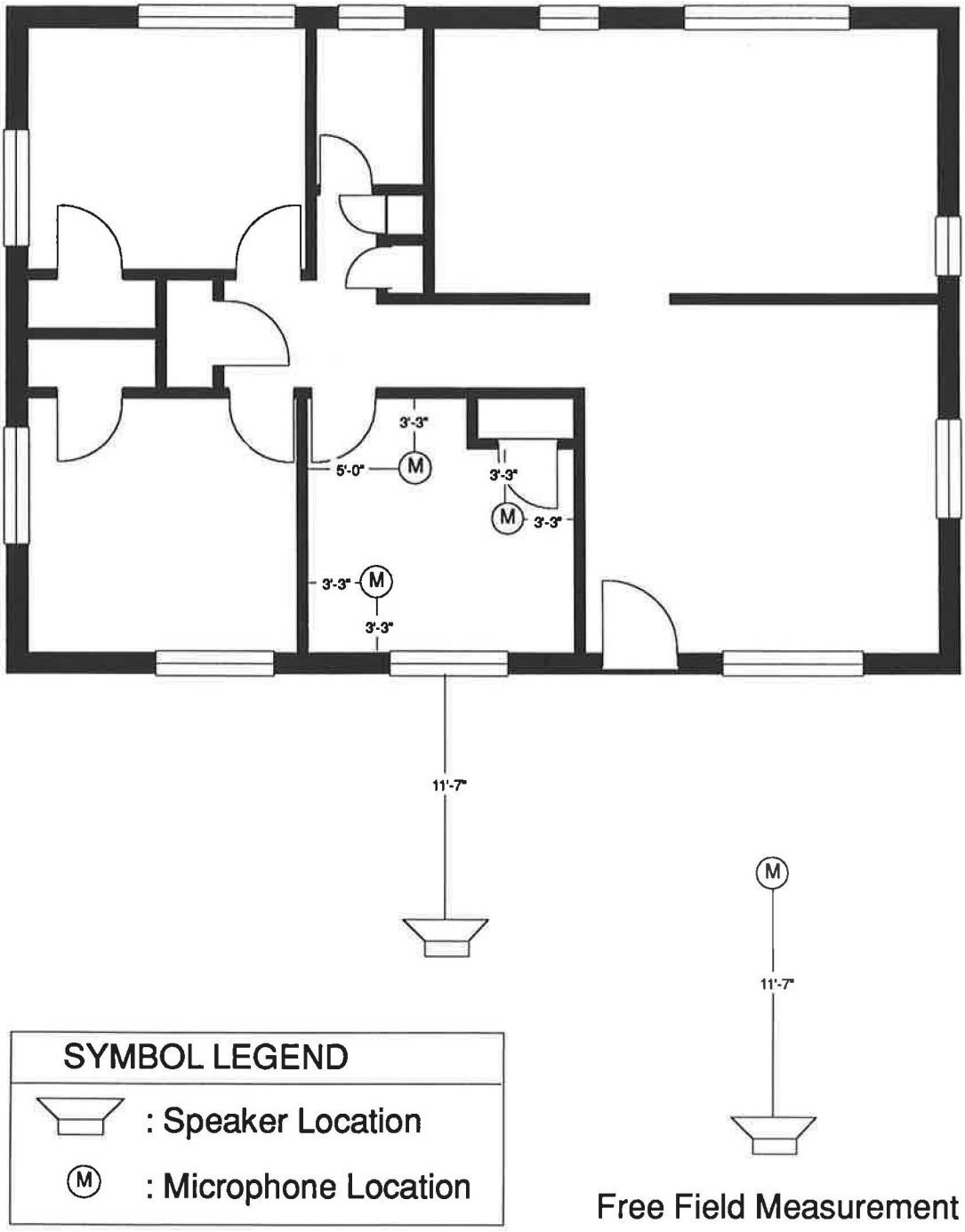

FIGURE 14 Floor plan of the Aurora sample home indicating acoustical test locations.

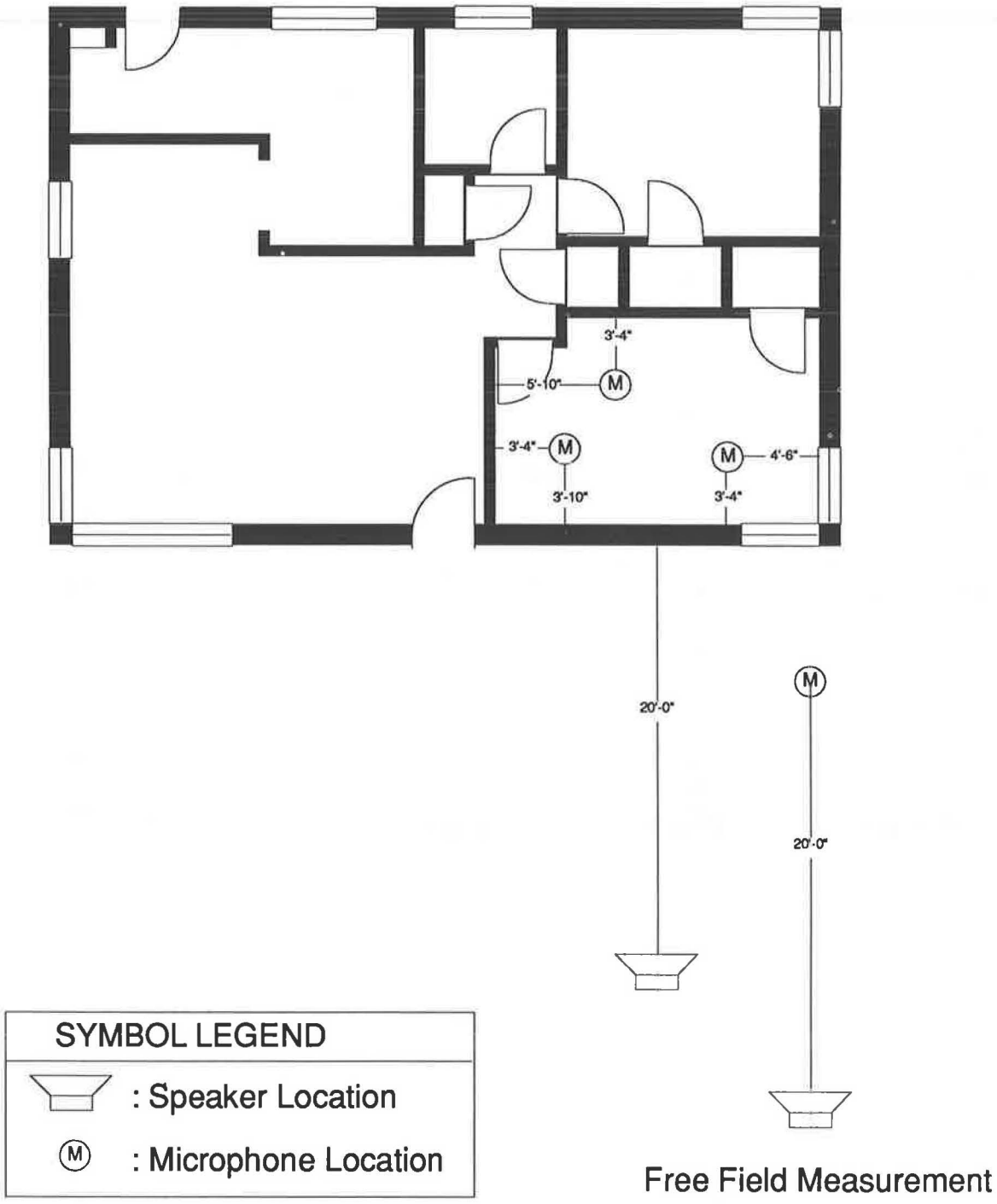

FIGURE 15 Floor plan of the Denver sample home indicating acoustical test locations.

before-and-after tests are shown in Figures 16 and 17, respectively.

The construction portion of the program was delayed because of delays in contract negotiations between the city and county of Denver and the two designated installing agencies. The program is currently in the construction phase with 390 homes completed to date. Because of the widely scattered location of the originally tested homes, only four homes completed to date were part of the original testing program. Postconstruction test results on these homes show a 12- to 23-dB improvement over the preconstruction test results. To document performance, all previously tested homes are slated for acoustical and air infiltration tests after completion.

From the initial construction phases, several observations can be made regarding the effectiveness of the SNIP Installing Agency Manual design. Although the checklist and decision trees are valuable as an initial training tool, each agency has reduced the survey process to reflect the typical construction condition found in its areas. The checklist and decision trees are still used for assessing the action required on less frequently observed conditions. The priority list has become the core document used by both programs for selecting and bidding modifications.

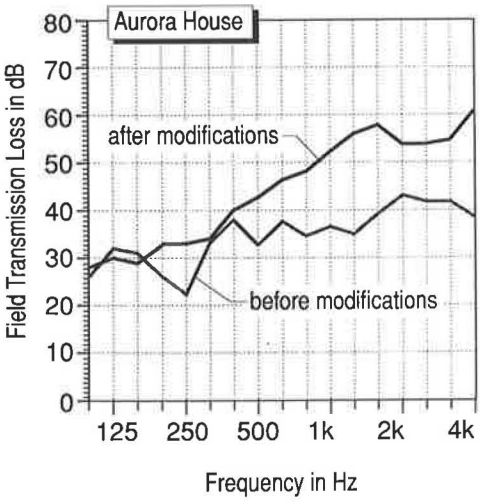

FIGURE 16 Before-and-after field transmission loss test results on a frame house with aluminum siding over asbestos shingles. Original steel casement windows are replaced with new dual-glazed sound-insulating windows.

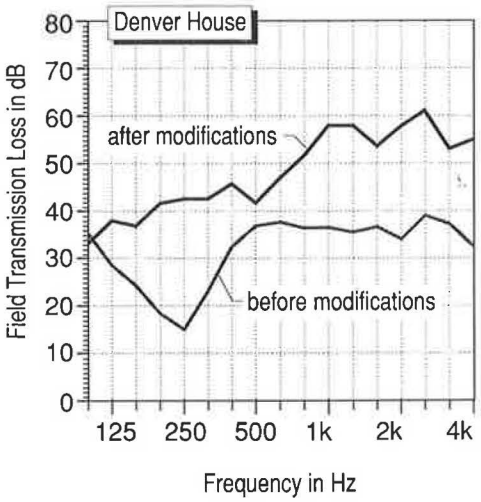

FIGURE 17 Before-and-after field transmission loss test results on a solid brick home. Original steel casement windows are replaced with new dual-glazed sound-insulating windows.

REFERENCES

1. *Denver-Adams Co. Intergovernmental Agreement.* 1988.
2. *Airport Noise Compatibility Planning.* Federal Aviation Regulations, Part 150 (14 CFR 150), FAA, U.S. Department of Transportation, Washington, D.C., 1989.
3. *Standard Guide for Field Measurement of Airborne Sound Insulation of Building Facade Elements.* ASTM Standard E966-84, ASTM, Philadelphia, Pa., 1988.
4. B. H. Sharp, B. A. Davy, and G. E. Mange. *The Assessment of Noise Attenuation Measures for External Noise.* Wyle Research Report WR 76-3, prepared for the U.S. Department of Housing and Urban Development, Arlington, Va., April 1976.
5. *Study of Soundproofing Public Buildings Near Airports.* Report FAA-AEQ-77-9, FAA, U.S. Department of Transportation, Washington, D.C., April 1977.

Publication of this paper sponsored by Committee on Transportation-Related Noise and Vibration.

Sound Insulation and Thermal Performance Modifications: Case Study for Three Dwellings Near BWI Airport

NEIL THOMPSON SHADE

In 1974, the Maryland General Assembly passed the Maryland Environmental Noise Act to provide citizen protection from transportation-related noise, including minimizing of residential dwelling aircraft noise exposure. In 1987, as part of this effort, the Maryland State Aviation Administration sponsored the Pilot Residential Sound Insulation Program for 17 dwellings to determine the feasibility and associated costs of reducing aircraft noise intrusion in residential dwellings. Dwellings within the Baltimore-Washington International Airport 65-dB yearly day-night noise level noise zone contour were selected for modification. Selection of dwellings and noise reduction measurements preceded design and specification of architectural modifications to reduce noise. These modifications included replacement of windows and doors, addition of gypsumboard to walls and ceilings, and installation of new heating, ventilating, and air-conditioning systems. The sound insulation modifications resulted in greater reduction of aircraft noise intrusion by 4 to 10 dB over the previously existing noise reduction values for the three dwellings studied. The energy savings due to the sound insulation modifications resulted in a 3 to 18 percent cost reduction compared to the existing conditions. Sound insulation design goals, construction modifications, pre- and postmodification noise reduction values, and thermal performance values are described for three dwellings that were part of this program.

In 1974, the Maryland General Assembly passed the Maryland Environmental Noise Act to provide citizen protection from transportation-related noise, including minimizing of residential dwelling aircraft noise exposure. As part of this effort, Baltimore-Washington International (BWI) Airport conducted the Pilot Residential Sound Insulation Program for 17 dwellings to determine the feasibility and associated costs of reducing aircraft noise intrusion in residential dwellings. This project involved determining the number and types of houses affected, selecting representative dwellings for study, measuring the present dwelling noise reduction properties, specifying noise control modifications, and implementing construction modifications to the dwellings. For illustrative purposes, the sound insulation modifications and effects on thermal performance are examined for three of the dwellings.

RESIDENTIAL SOUND INSULATION PROGRAM OVERVIEW

The FAA considers residential land use to be compatible for areas in which the exterior noise environment does not exceed a yearly day-night noise level (DNL) of 65 dB (*1*). DNL is a cumulative noise metric in units of A-weighted decibels. The DNL metric is an annual average noise level occurring during a 24-hr period with a 10-dB penalty added to noise events occurring between 10:00 p.m. and 7:00 a.m. Dwellings located in airport noise zones with exterior levels greater than DNL 65 dB are required to have interior noise levels below DNL 45 dB.

Interior noise level design criteria for this project were selected to provide measures of long-term reaction to aircraft noise (in DNL) and of the intrusion of individual aircraft flyover noise events (in mean maximum A-weighted noise levels). Habitable portions of the dwelling were not to exceed DNL 45 dB, whereas single-event aircraft flyovers were not to exceed 60 dBA in bedrooms and television rooms and 65 dBA in all other habitable rooms in the dwelling.

To identify construction elements that were most important in determining the present level of dwelling sound insulation, the first phase of the residential sound insulation program inventoried the number and architectural characteristics of the dwellings in the airport noise zones.

Next, representative dwellings were selected from a pool of homeowner applicants, and acoustic measurements were conducted to determine existing noise insulation. Analysis was then performed for each dwelling to determine a cost-effective design solution to satisfy the sound insulation goals.

Finally, architectural drawings and specifications describing sound insulation modifications for the dwellings were prepared.

After the construction modifications were completed, acoustic measurements were performed in each dwelling to verify that program sound insulation goals were satisfied.

FACTORS AFFECTING DWELLING SOUND INSULATION PERFORMANCE

Dwelling sound insulation is influenced by local construction styles, age, and condition of the structure; aircraft flight path orientation; and dwelling-specific conditions. Figure 1 indicates the numerous paths that enable sound to enter the interior of a dwelling.

Existing architectural features are important in a dwelling's sound insulation performance. Single-story and split-level dwellings expose larger areas of living space to noise from the exterior roof path than do bilevel and two-story dwellings. Vented attic spaces provide an acoustic void between the

Wyle Laboratories, Arlington, Va., 22202.

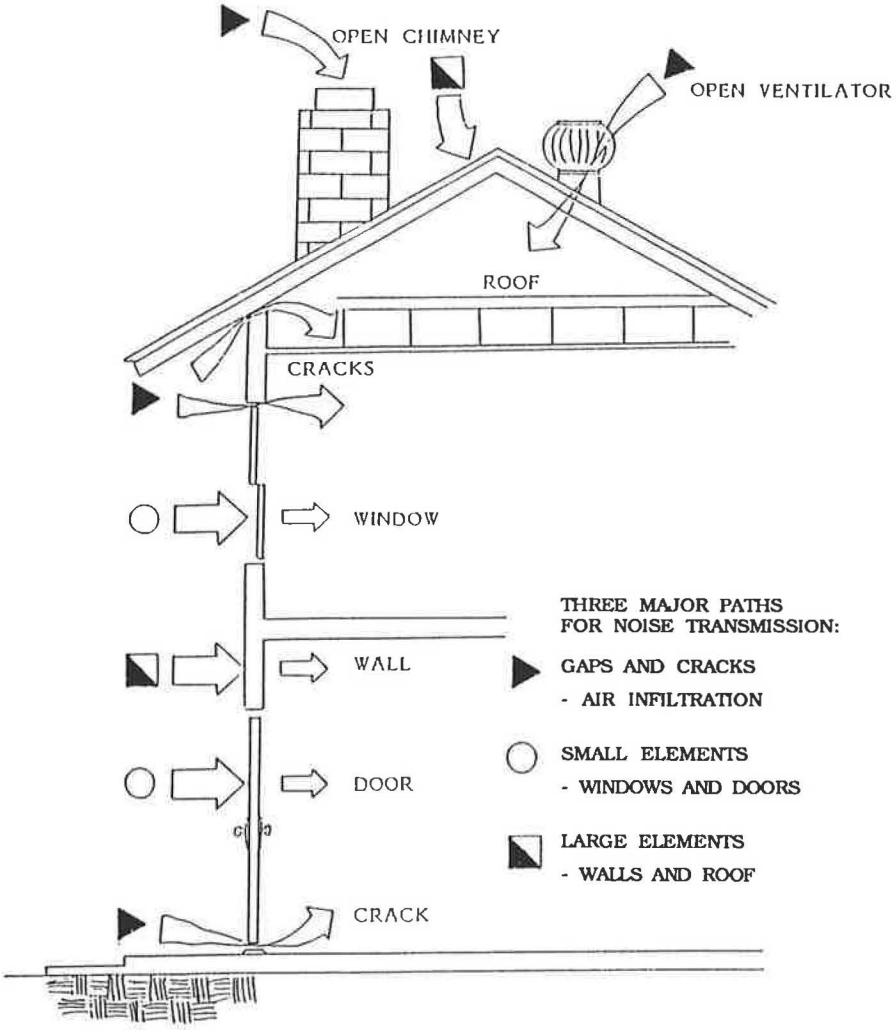

FIGURE 1 Major paths for noise transmission into dwelling interiors.

exterior and the occupied rooms that exposed ceilings and occupied attic spaces lack. Brick, stucco, and other cementitious exterior walls provide greater sound insulation than do lighter walls of wood and aluminum siding construction. Metal frame and thermal windows provide less sound insulation than wood frame and single-pane windows with exterior storm window assemblies.

Shielding of the dwelling from direct exposure to the flight path reduces the noise level at certain portions of the dwelling. Figure 2 shows measured A-weighted values of acoustical shielding at various dwelling locations. The shielding values can be reduced, typically by 5 dBA, because of sound reflections arriving at the dwelling elevation when other structures are nearby. This effect tends to be more pronounced for neighborhoods in which dwelling density is high and dwellings are closely spaced. The indicated shielding factors allow for a reduction in the required sound insulation at these portions of the dwelling.

Replacing the windows in the dwelling with acoustical windows typically does more to improve the sound insulation performance than other architectural modifications. Thermal and single-pane windows with storm assemblies provide little insulation of aircraft noise.

Exterior doors often require improved sound insulation, particularly when these doors open directly to kitchens and living rooms, which are common areas for family activities.

Interior walls and ceilings adjoining the exterior often require modifications to increase sound insulation. Typical modifications include adding gypsumboard layers directly to, or furred out from, existing surfaces with fiberglass batts installed in the cavity. Vented attic spaces are provided with 6-in. (R–19) fiberglass acoustical insulation. Exposed ceilings and occupied attic spaces normally have additional gypsumboard layers applied directly to the finished ceiling.

Table 1 presents possible modifications that can be readily adapted to residential construction and have been shown to require minimal contractor supervision to achieve successful acoustical performance.

SOUND INSULATION DESIGNS FOR THREE SELECTED DWELLINGS

Sound insulation designs were examined for three dwellings. Two of the dwellings were selected because the architectural characteristics are typical for dwellings within the DNL 65-

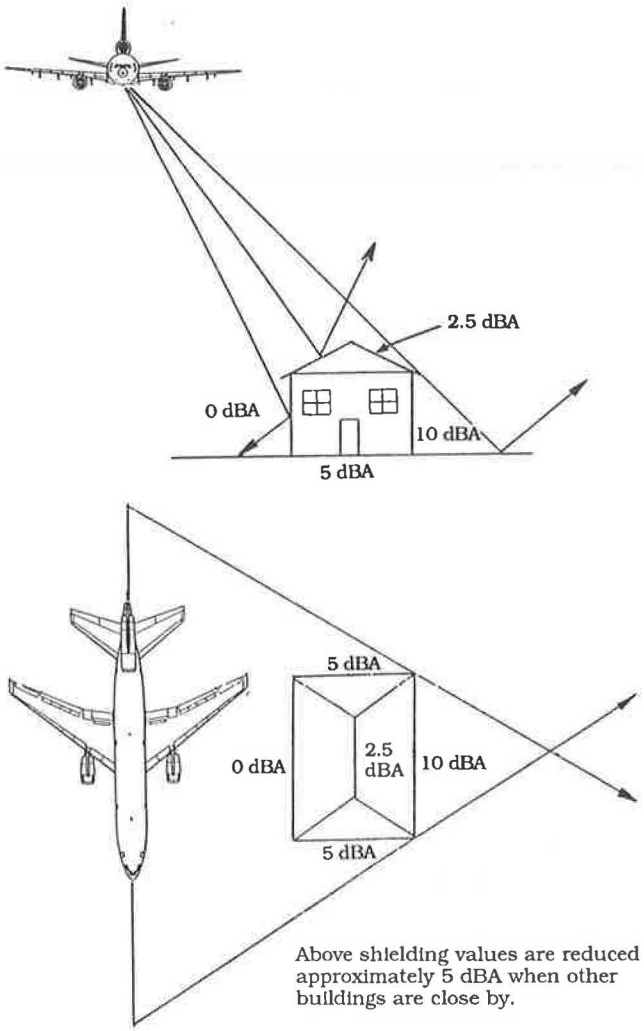

FIGURE 2 Measured values for acoustical shielding due to aircraft noise.

dB noise zone. The third dwelling was selected because of the unusual wall and heating, ventilating, and air-conditioning (HVAC) system configuration. The age, style, and construction features of the dwellings are different. Table 2 presents the existing characteristics of the three dwellings studied.

Dwelling noise reduction data were obtained as part of the initial acoustic survey by simultaneously measuring the exterior and interior sound levels due to aircraft overflights in each habitable room. At least eight room noise reduction values were obtained by taking differences between exterior and interior sound levels. Noise reduction values were then averaged to obtain a single value for each room.

Actual sound levels inside the rooms of the dwelling were obtained both in terms of the DNL and mean maximum A-weighted levels. The interior DNL values for each room were determined by subtracting each room's measured noise reduction value from the exterior DNL value as determined from the airport noise zone contours. The interior mean maximum A-weighted levels were obtained by subtracting each room's measured noise reduction value from the takeoff noise level footprint, calculated using the FAA Integrated Noise Model (INM) Computer Program, that a typical noisy aircraft (e.g., a Boeing 727–200) would produce while flying over the dwelling's location.

A computer program developed by Wyle Laboratories was used to compute the room noise reduction values on the basis of the architectural characteristics for each dwelling. This program accounts for the sound transmission paths, acoustical shielding, and room absorption. Comparing measured and computed noise reduction values resulted in differences of only 2 to 3 dB. The lower of the measured and computed values was taken as the noise reduction for each room. Table 3 presents existing and modified dwelling noise reduction and interior sound level characteristics for each room.

Selected noise reduction values were used in a computer design modification program developed by Wyle Laborato-

TABLE 1 TYPICAL CONSTRUCTION MODIFICATIONS FOR IMPROVED DWELLING SOUND INSULATION

Element	0–5 dB Noise Isolation Improvement	5–10 dB Noise Isolation Improvement	10–20 dB Noise Isolation Improvement
Windows	Seal cracks. Caulking.	Replace with STC 35 acoustic windows.	Replace with STC 40-45 acoustic windows.
Doors	Weatherstrip. Add storm doors.	Replace with STC 35 acoustic doors. Add storm doors.	Replace with STC 40 acoustic doors. Add storm doors.
Walls	Increase mass of interior surfaces.	Increase mass or resilient mounting of interior surfaces.	Resilient or furred-out mounting of new interior surfaces.
Ceiling	Add fiberglass insulation to attic space.	Increase mass of interior surfaces. Add fiberglass insulation to attic spaces.	Resilient mounting of new interior surfaces.

TABLE 2 CHARACTERISTICS OF THE DWELLINGS FOR EXISTING AND MODIFIED CONDITIONS

Element	Dwelling No. 1		Dwelling No. 2		Dwelling No. 3	
	Existing	Modified	Existing	Modified	Existing	Modified
Windows	21 single-pane, double-hung. 5 single-pane, fixed light.	15 double-hung, STC 35. 2 fixed light STC 35. 4 single-pane, double-hung. 5 single-pane, fixed light.	10 single-pane alum. sliders. 4 single-pane, fixed light.	2 double-hung STC 35. 7 double-hung, STC 40 4 single-pane, fixed light. 1 single-pane, alum. slider.	12 single-pane, double-hung, 6 single-pane, fixed light.	2 double-hung, STC 35. 7 double-hung, STC 40. 2 double-hung, STC 45. 1 double-hung, single-pane. 6 single-pane, fixed light.
Doors	3 solid-core wood. 1 single-pane glass panel.	Existing 3 solid-core wood. 1 glass panel, 1.4" lam. glass.	1 hollow-core wood. 1 panel wood.	1 solid-core STC 35. Existing 1 panel wood.	3 solid-core wood.	Existing 1 solid-core wood. 2 solid-core STC 35.
Walls	2 layers brick with plaster interior.	No modifications.	Brick veneer with 1 layer gypsumboard interior. Asphalt siding with 1 layer gypsumboard interior.	Existing brick veneer with 3 layers gypsumboard interior. Existing asphalt siding with 3 layers gypsumboard interior.	Shingle/wood clapboard with plaster interior.	Existing shingle/ wood clapboard with plaster and 2 layers gypsumboard interior.
Roof	Asphalt shingle gabled with plaster interior.	Existing asphalt shingle gabled plaster with 1 layer 5/8" gypsumboard at interior.	Asphalt shingle gable with gypsumboard interior.	No modifications.	Asphalt shingle gable with plaster interior.	No modifications.
Basement	Unfinished.	No modifications.	Unfinished.	No modifications.	Unfinished.	No modifications.
HVAC	Wood stove heat. Window air conditioning.	Gas split system HVAC (3 tons), Heat pump (2 tons), and ductwork.	Gas heating. Window air conditioning.	Gas heating and 3-ton central air conditioning.	Gas heating. Window air conditioning.	Gas heating and 3-ton central air conditioning.
Thermal	R-19 in attic knee space. No insulation in walls.	No modifications.	R-11 in attic and walls.	R-30 in attic. Existing walls.	R-6 in attic. No insulation in walls.	R-25 in attic. Existing walls.

ries. This program iteratively computes noise reduction values for various user-selected modification options and compares the result with design goals. Modifications for the three dwellings were selected from the program data base of approximately 75 construction modifications on the basis of their associated costs. This procedure allowed a cost-optimized sound insulation design to be generated for each modified room.

Existing windows in the major habitable rooms for the three dwellings were replaced with acoustical windows rated sound transmission class (STC) 35, 40, or 45. Specific window STC ratings were determined by the room's noise reduction and shielding factors. Dwelling 1, which consists of two layers of brick masonry construction, required STC 35 windows. The other two dwellings, of lightweight frame construction, required STC 40 and 45 windows. For each room, windows were selected, consistent with wall modifications, to achieve balanced acoustical design. Typically with this procedure, walls with high transmission loss values and small window dimensions require lower STC-rated windows than walls that have lower transmission loss values and larger window dimensions. In each dwelling, windows were replaced only for habitable rooms.

Because of the two layers of brick masonry forming the exterior wall construction, Dwelling 1 did not require wall modifications. This wall construction provides considerably higher transmission loss values than typical frame construction with exterior siding. Additional gypsumboard layers were applied to the exterior-facing walls for most of the habitable rooms in Dwellings 2 and 3. A single layer of $\frac{5}{8}$-in. gypsumboard was applied to the ceiling of the occupied attic space in Dwelling 1. Additional fiberglass insulation of thickness equivalent to R–19 was provided for the vented attics in Dwellings 2 and 3. Improvements in the existing noise reduction values ranged from 4 to 10 dB to satisfy the sound insulation design goals. The average cost for the modifications was $21,730 per dwelling. Specific costs for the various modifications are presented in Table 4.

TABLE 3 MEASURED NOISE REDUCTION AND INTERIOR SOUND LEVELS FOR EXISTING AND MODIFIED CONDITION

Dwelling No.	Room	Noise Reduction		Interior Sound Level			
				Existing		Modified	
		Existing	Modified	Ldn	A-Wtd.	Ldn	A-Wtd.
1	Kitchen	26	30	49	64	45	60
	Living Room	29	34	46	61	41	56
	Master Bedroom	26	33	49	64	42	57
	Boy's Bedroom	33	38	42	57	37	52
	Girl's Bedroom	31	36	44	59	39	54
	Guest Bedroom	26	31	49	64	44	59
2	Kitchen	21	26	49	69	44	64
	Living Room	20	30	50	70	44	60
	Master Bedroom	22	31	48	68	39	59
	Boy's Bedroom	23	31	47	67	39	59
	Child's Bedroom	23	31	47	67	39	59
3	Kitchen	22	26	48	68	44	64
	Living Room	23	30	47	67	40	60
	Dining Room	22	26	48	68	44	64
	Master Bedroom	23	31	47	67	39	59
	Spare Bedroom	22	30	48	68	40	60

TABLE 4 COSTS FOR SOUND INSULATION AND HVAC MODIFICATIONS

Dwelling No.	Acoustic Windows	Other Acoustic (Drywall + Doors)	R-19 Acoustic Insulation	Demolition/ Repair Work	Elec., HVAC, & Ducting	House Total
1	$6,300	$2,330	$1,050	$0	$12,020	$21,700
2	$9,500	$3,500	0	$2,330	$6,070	$21,400
3	$7,100	$7,000	$1,110	0	$6,880	$22,090

IMPACT OF SOUND INSULATION MODIFICATIONS ON DWELLING THERMAL PERFORMANCE

The HVAC system in each dwelling was modified to provide forced-air heating and cooling, primarily so that the dwelling occupants would be able to keep the acoustic windows closed during the warmer periods of the year.

The sound insulation modifications for the three dwellings improved the thermal resistance (R-value) of the windows, doors, walls, and ceiling elements, reducing the heating and cooling loads on the dwelling envelope.

Replacing the dwelling's windows and doors and adding new caulking and weather stripping substantially reduce the perimeter air infiltration rate. This effect is more noticeable during the winter months, due to the increased stack effect. The stack effect results when the warmer inside air rises and flows out the dwelling near its top and is replaced by cooler outside air near the dwelling's base. Comparison with calculations for the existing windows, in accordance with methods given by the American Society of Heating, Refrigerating, and Air-Conditioning Engineers (ASHRAE) (*2*) and with the acoustic window manufacturer's data, shows that the air infiltration rate for the acoustical window is one-tenth that for the existing window units.

Studies were done to determine the electricity and natural gas cost savings resulting from the sound insulation and HVAC modifications presented in Table 2. The effect of increasing

the thermal insulation over that specified as part of the sound insulation modifications was also studied.

A computer program based on ASHRAE (*3*) calculation methods simulated the yearly heating and cooling loads for the existing and modified sound insulation modifications. The computer program then examined the effect of increasing the thermal insulation to meet the American Institute of Architects (AIA) recommended practice (*4*). This recommended practice calls for walls to have R–19 insulation, roofs to have R–30 insulation, and glass to be of the double-pane heat-absorbing type.

The simulated yearly utility costs for heating, cooling, and fans for no modifications and after sound insulation and thermal insulation modifications are listed in Table 5. The latter two conditions studied include HVAC modifications. Results vary according to the different dwelling sizes and characteristics. An assumption was made in the calculations that the internal lighting equipment and domestic hot water loads would remain the same for each of the three conditions examined. Table 6 compares percent savings resulting from the sound insulation and thermal modifications with the existing conditions.

Dwelling 1, built in the 1850s, has little thermal insulation. The building envelope is in fair condition and it is the largest (2,100 ft²) of the three dwellings examined. The sound insulation modifications resulted in only a 3 percent savings for the total energy costs. If this dwelling were to be modified to conform to the AIA recommended practice for thermal insulation, the yearly energy costs could be reduced more than 30 percent.

Dwelling 2 (1,400 ft²) and 3 (1,100 ft²) were built in the 1950s and the 1920s, respectively. These dwellings have slightly better thermal insulation than Dwelling 1; however, air infiltration at the window perimeter is high. The sound insulation modifications would result in 15 and 18 percent savings, respectively, for the total energy costs for these two dwellings. Upgrading the insulation at these two dwellings to the AIA recommended practice for thermal insulation would reduce the yearly energy costs by 20 and 40 percent, respectively. The total utility costs illustrated include a portion of the fixed costs for lighting, appliances, and domestic hot water, which are assumed to be the same for the existing and modified conditions.

Table 6 also presents the percent savings relative to the recommended AIA thermal insulation practice directly attributable to the sound insulation modifications. For the three dwellings studied, these savings amount to between 10 and 75 percent.

TABLE 5 UTILITY COSTS IN DOLLARS FOR THREE MODIFICATION SCHEMES

	Dwelling No. 1			Dwelling No. 2			Dwelling No. 3		
	Exist	Snd Ins	Ther	Exist	Snd Ins	Ther	Exist	Snd Ins	Ther
Total	1,927	1,873	1,284	991	848	781	982	808	591
Heating	662	641	102	448	343	157	442	320	144
Cooling	277	267	241	114	99	74	115	93	81
Fans	175	153	129	95	71	46	105	76	46

Exist = Present utility costs without modifications.

Snd Ins = Utility costs after sound insulation and HVAC modifications.

Ther = Utility costs after sound insulation and thermal modifications per AIA recommendations.

TABLE 6 PERCENT SAVINGS FROM EXISTING THERMAL CONDITIONS FOR SOUND INSULATION AND THERMAL MODIFICATIONS

	Snd Ins	Ther	Percent Ther Savings Due to Snd Ins
Dwelling No. 1	3%	30%	10%
Dwelling No. 2	15%	20%	75%
Dwelling No. 3	18%	40%	45%

Snd Ins = Utility costs after sound insulation and HVAC modifications.

Ther = Utility costs after sound insulation, HVAC, and thermal modifications per AIA recommendations.

CONCLUSIONS

Sound insulation modification designs for three different dwellings have been described. Modifications included replacing windows and doors and increasing the mass of certain walls and ceilings. This procedure resulted in a measured improvement in the dwelling's existing noise reduction by 4 to 10 dB. The HVAC system in each dwelling was modified to provide forced-air heating and cooling capabilities. The sound insulation modifications resulted in a calculated energy savings of 3 to 18 percent over the existing conditions. Increasing the thermal insulation to meet current AIA recommended practices would improve the energy savings by 20 to 40 percent. The sound insulation modifications alone provide between 10 and 75 percent of the energy savings that would result if the AIA thermal insulation practice were to be implemented in the dwellings.

REFERENCES

1. *Airport Noise Compatibility Planning*. Federal Aviation Regulations, Part 150 (14 CFR 150), FAA, U.S. Department of Transportation, Washington, D.C., 1989.
2. American Society of Heating, Refrigerating, and Air Conditioning Engineers. *ASHRAE Handbook: 1989 Fundamentals*. Atlanta, Ga., 1989, Chapter 23.
3. American Society of Heating, Refrigerating, and Air Conditioning Engineers. *ASHRAE Handbook: 1989 Fundamentals*. Atlanta, Ga., 1989, Chapters 22–28.
4. *Architect's Handbook of Energy Practice*, The American Institute of Architects, Washington, D.C., 1987.

Publication of this paper sponsored by Committee on Transportation-Related Noise and Vibration.

Single-Number Ratings for Outdoor-Indoor Sound Insulation

KEITH W. WALKER

All of the single-number indices currently used to assess the sound insulation of walls use one-third octave band sound transmission loss data in the frequency range 125 to 4,000 Hz. Forty-two walls were measured over the range 50 to 5,000 Hz. None of the existing indices correlated well with the calculated 50- to 4,000-Hz loudness reduction using the International Organization for Standardization method. A new proposed rating, the outdoor-indoor transmission class (OITC), which is based on A-weighted sound reduction in the range 80 to 5,000 Hz, shows significant improvement over other methods. Typically, both the loudness reduction and OITC give lower numbers than sound transmission class for wall constructions.

Single-number sound insulation ratings have been used for many years to determine if the acoustical performance of interior walls between dwellings, offices, and rooms in general was adequate to provide speech privacy and control of radio and television sounds. The sound transmission class (STC) (*1*) and the International Organization for Standardization (ISO) weighted sound reduction index (R_w) (*2*) were designed for these purposes, but they were never intended for use in describing sound insulation performance against outdoor traffic and other sounds with strong low-frequency content. Despite these limitations, these rating methods have been used many times to select and compare the performance of exterior walls, windows, and doors, with resultant failure to achieve satisfactory results. The limitations of STC and similar ratings when comparing the loudness reduction of a series of lightweight design walls in the range STC 30 to 69, which were measured for sound transmission loss (TL) at 50 to 5,000 Hz, are demonstrated, and an alternative rating method based on A-weighted sound reduction is offered (*3*). There were no data available below 80 Hz for exterior wall or window constructions; however, the range of constructions used is believed to be adequately wide.

STATISTICAL STUDIES

Correlation between STC and the loudness reduction (D_L) calculated using ISO 532B (*4*) was studied by linear regression for a series of 42 gypsum board and steel stud walls subjected to three assumed transportation sound spectra (*5*, *6*) and speech (*7*) (Figure 1). The spectrum for railroad noise was unpublished (K. W. Walker, USG Corporation). The spectra have been moved relative to each other so that the shapes can be more easily seen. Figure 1 also shows an averaged spectrum that is used later. The slope, intercept, correlation coefficient, and standard deviation of the slope were calculated for STC versus D_L for each sound source. The loudness of each source was calculated in phons(GF) (G indicates the calculation is based on critical bands, F designates a free field condition). Phons were obtained by calculating the loudness in sones in one-third octave bands, taking the logarithm to the base 2 of the sones, and adding 40, all in accordance with ISO 532B. The building interior sound levels were then calculated by subtracting the measured TL from the sound source one-third octave band levels for the 50- to 5,000-Hz range; no correction was made for room sound absorption. The indoor loudness was calculated in phons(GD) (D designates a diffuse field condition) and subtracted from the source phons(GF) to obtain the D_L value. Figures 2, 3, 4, and 5 indicate plots of STC versus D_L for each sound source and display the statistical data. STC is shown to work well for speech but is seriously deficient as a descriptor when used with the other sources. For example, with a Y-intercept of 15.2 and a slope of 1.094 in Figure 4, STC 50 corresponds to a D_L value of approximately 32 dB with a standard deviation of 6.1 dB. Thus, STC overestimates the loudness reduction by a significant amount and is inconsistent, preventing the adoption of a simple correction factor. Similar studies on R_w and the FAA's exterior wall rating (EWR) (*8*) have shown little improvement over STC even though R_w includes the 100-Hz one-third octave band.

USG Corporation, P.O. Box 460, Round Lake, Ill. 60073.

DEVELOPMENT OF THE NEW RATING METHOD

Several attempts have been made to develop an improved version of the STC method. STC is obtained by fitting a grading curve to the transmission loss graph of a wall. The grading curve is a contiguous series of three straight lines as shown in Figure 6. The curve is moved on the vertical axis so that no part lies more than 8 dB above the transmission loss curve, and the total of the transmission loss deficiencies below the grade curve (at the center frequencies) does not exceed 32 dB. When these requirements are satisfied, the STC is read from the intersection of the grade curve and the Y-axis at the 500-Hz center frequency. Figure 6 demonstrates the concept.

Changing the STC grading curve shape only or changing the curve fit method to be more controlled by the low frequencies was not useful because the standard test range does not go below 125 Hz. Some improvement was achieved by extending the range down to 50 Hz. Few laboratories have rooms of a size that permits reasonable test accuracy down to 50 Hz. Even if large rooms were available, when the wavelength is longer than the test wall dimensions, the transmission loss is largely controlled by the wall stiffness and is often

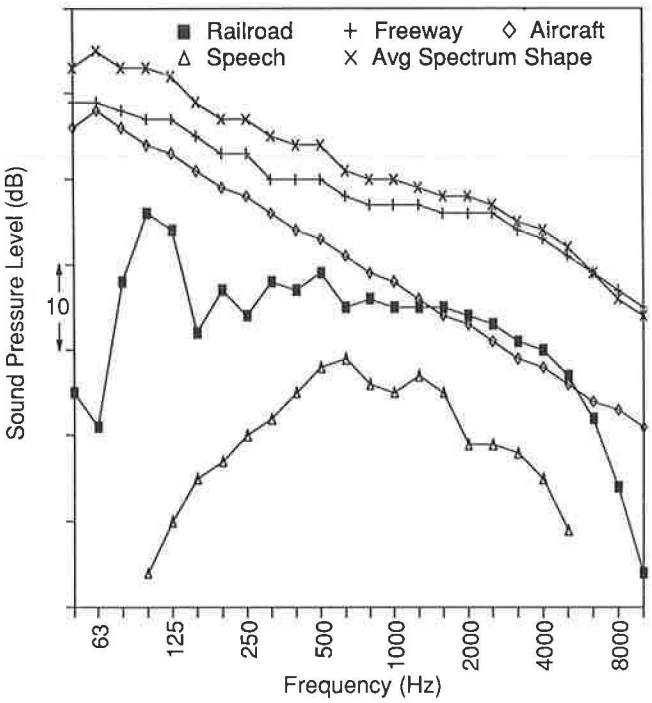

FIGURE 1 Four typical noise spectra and averaged spectrum used in study.

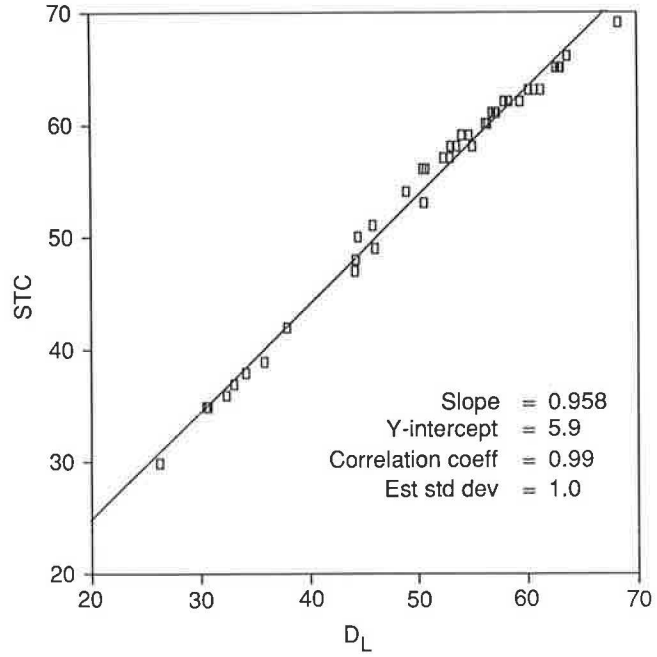

FIGURE 2 Scatter plot for STC versus D_L for speech noise source.

dependent on how the wall is tied into the surrounding test frame. The low-frequency TL dependence on the mounting method is significant because there is no way to ensure that the test wall stiffness can be replicated in the field, particularly in nonmasonry building structures. It is unreasonable to expect laboratories to provide data to 50 Hz on a routine basis, and even if available, the information would have a low credibility.

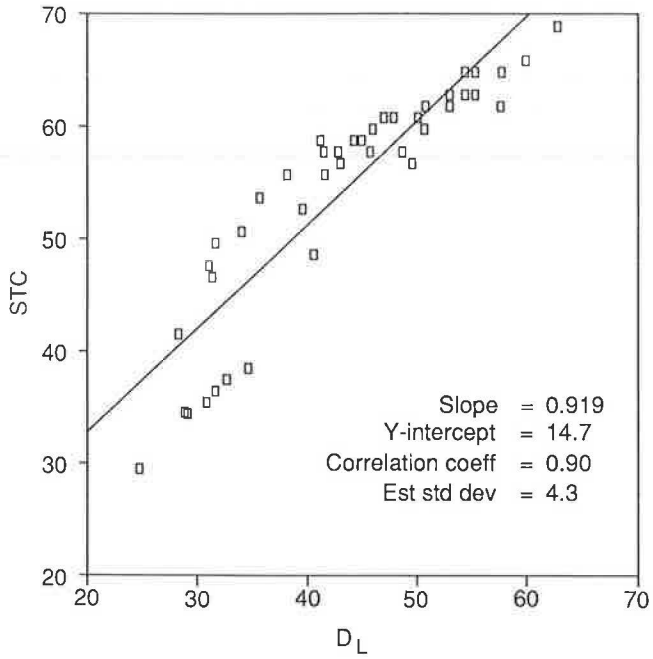

FIGURE 3 Scatter plot for STC versus D_L for railroad noise source.

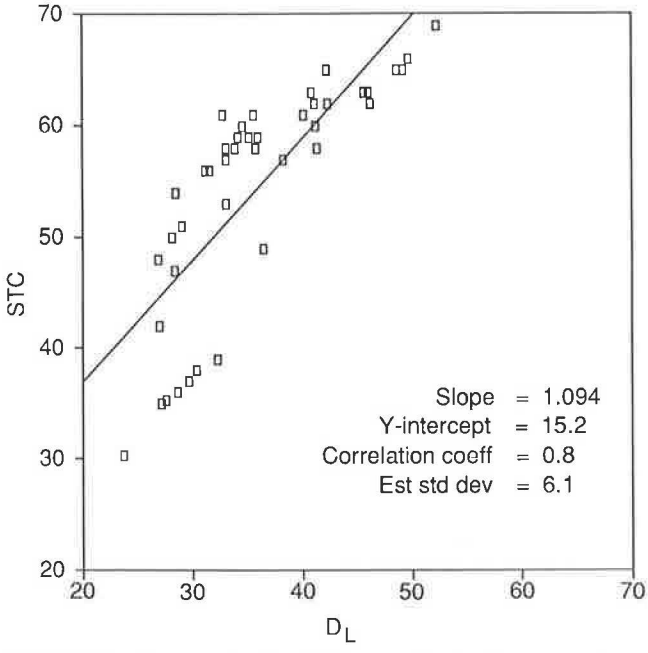

FIGURE 4 Scatter plot for STC versus D_L for freeway noise source.

Finally, it was determined that a calculation of A-weighted sound reduction provided a significantly improved correlation with D_L. A-weighted sound levels were calculated from Equation 1 by adding the corrections published in IEC 123 (*9*) to each one-third octave band sound level in the frequency range of interest and summing the corrected levels.

$$L = 10 \log \sum_f 10^{(SPL_f + W_f)/10} \quad \text{(dB)} \qquad (1)$$

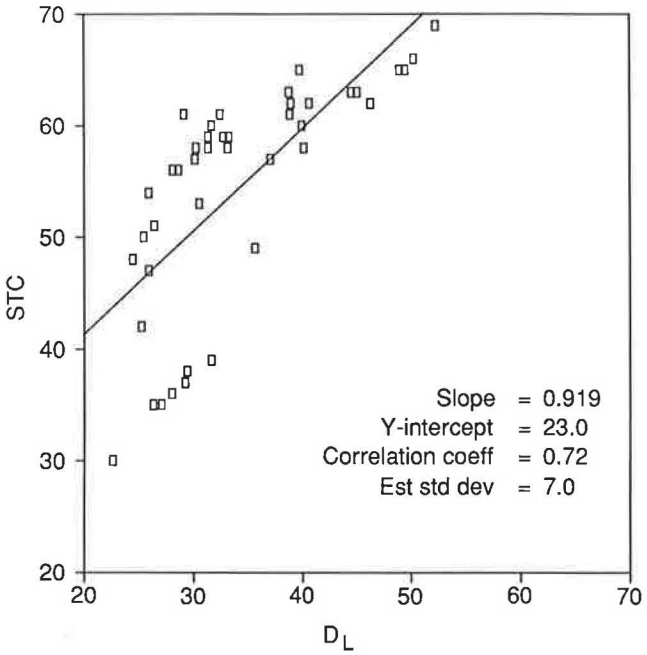

FIGURE 5 Scatter plot for STC versus D_L for aircraft noise source.

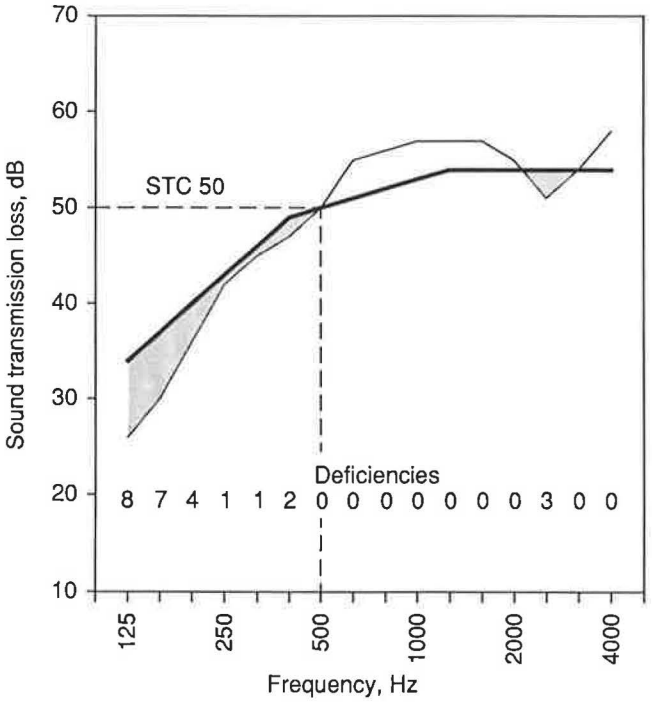

FIGURE 6 Application of the STC grading curve as described in ASTM E 413. The rating for the sound transmission loss graph in this example is STC 50.

where

L = A-weighted sound level,
f = one-third octave bands in the required frequency range,
SPL_f = sound pressure level in each frequency band, and
W_f = A-weighting correction for each frequency band.

The A-weighted sound level L_s for each source was calculated using Equation 1. L_r for the receiving side of each wall was obtained by substituting SPL_{rf} for SPL_f in Equation 1, SPL_{rf} being derived from

$$SPL_{rf} = SPL_{sf} - TL_f \quad \text{(dB)} \tag{2}$$

where SPL_{rf} is the sound level on the receiving side, SPL_{sf} is the sound level on the source side, and TL_f is the partition sound transmission loss for each one-third octave band.

The A-weighted sound reduction afforded by each wall is then

$$L_s - L_r \quad \text{(dB)} \tag{3}$$

Initially, a set of A-weighted reductions for each source was calculated for the range 80 to 5,000 Hz and correlated with D_L to determine the relationship. The data are presented in Table 1. In each case, the correlation with transportation noise was much better than for STC, and the correlation with speech was almost as good. Because it would not be reasonable to routinely perform calculations for every type of sound source, the three selected outdoor sound spectra were equalized in dBA level, and then sound intensity averaged to get the averaged spectrum shape shown in Figure 1. The A-weighted sound reduction using the averaged spectrum, designated outdoor-indoor transmission class (OITC), is then

$$OITC = L_s - L_r \quad \text{(dB)} \tag{4}$$

Separate OITC ratings were then calculated for each wall for each of three frequency ranges 50 to 5,000 Hz, 80 to 5,000 Hz, and 100 to 5,000 Hz and correlated with D_L for each sound source. Table 1 presents the statistical data. D_L is always calculated for the full 50- to 5,000-Hz range. The OITC value calculated for the 80- to 5,000-Hz range correlates with each transportation sound source to better than 0.9 and has much improved intercept and standard deviation characteristics than does STC. The ideal would be a slope of 1.0 and zero intercept, with a correlation of 1.0 and zero standard deviation. The 80- to 5,000-Hz range is significant because it extends only one-third octave lower than traditional measurements and would require only minor changes to current measurement standards. The statistics for the 100- to 5,000-Hz range are not acceptable for the aircraft noise source; however, the range could be used temporarily until 80-Hz data become available. OITC is still a significant improvement over STC or R_w.

TABLE 1 CORRELATION OF A-WEIGHTED SOUND LEVEL REDUCTION (80–5,000 Hz) WITH LOUDNESS REDUCTION (50–5,000 Hz)

Spectrum	Slope	*Y*-Intercept	Correlation	Standard Deviation of Slope
Railroad	0.871	6.6	1.00	0.8
Freeway	1.118	2.6	0.95	2.6
Aircraft	1.001	3.9	0.94	2.9
Speech	0.995	4.7	0.98	1.8

TABLE 2 CORRELATION OF OITC WITH LOUDNESS REDUCTION (50–5,000 Hz)

	50–5,000 Hz				80–5,000 Hz				100–5,000 Hz			
Spectrum	Slope	*Y*-Intercept	Correlation	Standard Deviation of Slope	Slope	*Y*-Intercept	Correlation	Standard Deviation of Slope	Slope	*Y*-Intercept	Correlation	Standard Deviation of Slope
Railroad	0.871	2.9	0.96	2.1	0.999	0.8	0.99	1.1	1.007	2.4	0.99	1.0
Freeway	1.051	0.4	0.99	0.9	1.120	1.0	0.95	2.6	1.081	4.2	0.91	3.4
Aircraft	1.078	4.3	0.98	1.6	1.113	6.2	0.91	3.5	1.050	10.1	0.85	4.4
Speech	0.603	7.2	0.82	4.3	0.727	4.0	0.90	3.8	0.766	3.8	0.94	2.9

CONCLUSIONS

STC and (by implication) R_w ratings are not effective for characterizing the effectiveness of walls in providing protection from transportation noise. Calculation of loudness reduction in phons is complex, requiring graphic interpretation or a computer program. Use of frequency band limited A-weighted sound reduction based on a fixed spectrum shows promise. The calculation of A-weighted reduction is simple and the rating is relatively easy to explain to the layman. Until transmission loss data in the 80-Hz one-third octave band are available, the method could temporarily use the 100- to 5,000-Hz range. Further limitation to 3,150 Hz would result in little change in the OITC value. Because OITC has not been verified with sounds other than those described in this paper, its use should be limited to transportation noise until further statistical work is performed. This study has dealt only with loudness; no correlation between OITC and speech interference from transportation noises has been established.

REFERENCES

1. American Society for Testing and Materials. Classification for Rating Sound Insulation. In *Annual Book of ASTM Standards*, Vol. 04.06, ASTM E413-87, Philadelphia, Pa., 1989.
2. International Organization for Standardization. *Rating of Sound Insulation in Buildings and of Building Elements.* ISO 717-1, Geneva, Switzerland, 1982.
3. K. W. Walker. Single Number Ratings for Sound Transmission Loss. *Sound and Vibration*, Vol. 22, No. 7, 1988, pp. 20–26.
4. International Organization for Standardization. *Acoustics—Method for Calculating Loudness Level.* ISO 532–1975E, Geneva, Switzerland, 1975.
5. E. Scholes et al. Barriers and Traffic Noise Peaks. *Applied Acoustics*, Vol. 5, No. 3, 1972, pp. 205–222.
6. J. P. Raney and J. M. Cawthorn. Aircraft Noise. In *Handbook of Noise Control* (2nd ed.), McGraw-Hill, New York, 1979, pp. 34–35.
7. S. Pearsons et al. *Speech Levels in Various Noise Environments.* Office of Health and Ecological Effects, U.S. Environmental Protection Agency, 1977.
8. Wyle Laboratories. *Study of Soundproofing Public Buildings Near Airports.* Report DOT-FAA-AEQ-77-9, Office of Environmental Quality, FAA, U.S. Department of Transportation, Washington, D.C., 1977.
9. *Recommendations for Sound Level Meters.* IEC–123, Bureau Central de la Commission, Electrotechnique Internationale, 1, rue de Varembe, Geneva, Switzerland, 1961.

Publication of this paper sponsored by Committee on Transportation-Related Noise and Vibration.

Control of Wheel Squeal Noise in Rail Transit Cars

M. A. STAIANO AND G. SASTRY

Because of community annoyance near a Washington, D.C., Metro rail transit car maintenance yard, a comprehensive noise measurement and analysis program was implemented for the Washington Metropolitan Area Transit Authority (WMATA) to examine the wheel squeal generated as transit cars traveled around small-radius curves. Sound levels were measured near the track as well as at locations in the neighborhood near the subject maintenance yard. Comparative measurements were also performed in two other nearly identical yards. In the absence of wheel squeal, train movements were almost undetectable outside the yard; hence, squeal elimination would satisfy community complaints and allow removal of an operations curfew. Water lubrication of the rails, found to be effective in eliminating squeal, was considered impractical for winter operations. Rail facing (a proprietary rail-head treatment) was selected by WMATA as an experimental squeal control. Testing of the rail facing within 1 week of installation yielded a 23-dBA sound level reduction and the complete elimination of squeal. However, after about 3 months' service, a 14-dBA reduction with some squeal was observed; and after 6 months' service chronic squeal reappeared. This loss of effectiveness was ascribed to rapid contact point wear of the facing treatment.

Wheel squeal is a tonal noise heard when railcars travel around curves of small radii. Washington Metro transit car movements in a maintenance yard produced wheel squeal and aroused complaints from neighbors. In response, the Washington Metropolitan Area Transit Authority (WMATA) implemented a number of noise abatement measures, including the installation of a prototype water rail lubrication system. Rail lubrication by water, although effective in eliminating squeal, presented significant operational problems. The other actions reduced wheel squeal sound levels, but—because of its distinctive character—squeal was still perceptible and some neighbors remained dissatisfied.

To ensure that no viable option was overlooked, a comprehensive measurement and analysis program was developed and implemented. Sound levels were measured in the subject maintenance yard and in two nearly identical yards under controlled conditions at locations near the track. At the subject yard, sound levels were also measured at locations in the community outside of the yard. Squeal at nighttime, with low background noise, was clearly audible. The squeal frequency spectra from the three maintenance yards appeared to exhibit characteristic differences. The overall A-weighted sound levels from the yards showed more variation than explainable by train speed and railcar/track geometry influences—possibly a result of restraining rail conditions. In the absence of squeal, train movements were almost undetectable outside the yard. Thus, squeal elimination would probably provide community satisfaction and permit removal of an operations curfew. Therefore, noise controls that essentially eliminated squeal were sought.

Rail facing, the application of a proprietary alloy filler to a specially ground groove in the rail head, was selected by WMATA for prototype testing. The prototype rail-facing treatment was completed in January 1989. Within a week of the installation, sound level measurements showed a 23-dBA sound level reduction and the complete elimination of squeal. However, measurements after about 3 months' service showed only a 14-dBA sound level reduction and occasional squeal, and after 6 months' service, chronic squeal had reappeared.

M. A. Staiano, Staiano Engineering, Inc., 1923 Stanley Ave., Rockville, Md. 20851–2225. G. Sastry, Deleuw, Cather & Co., 600 5th St., N.W., Washington, D.C. 20001.

SQUEAL GENERATION

Railcars are supported on each end and guided through curves by a swiveling truck consisting of two pairs of wheels with parallel axles. Because the axles are held rigidly by the truck frame, they cannot take up radial positions as the car traverses a curve. Consequently, the wheels must slide sideways across the rail top as well as roll along its length. The lateral sliding of the wheel over the rail head creates rubbing forces on the wheel, which, if conditions are suitable, will cause its vibration to grow until a stable amplitude is reached (*1*). The wheel vibration is radiated as squeal noise characterized by one or more intense, high-pitched tones at the natural vibration frequencies of the wheel. The vibration excitation by the rail and the sound radiation by the wheel is analogous to a bow exciting a violin string.

The sliding of the wheel over the rail head is described by lateral creep, $c = v/V$, where v is the lateral velocity of the wheel at the wheel-rail interface and V is the rolling velocity of the wheel. Lateral creep is determined to the first order by the geometry of the truck and curve, as shown in Figure 1. The average creep, c_a, is proportional to W/R, where W is the truck wheelbase and R is the curve radius.

The intense squeal sound levels are an outgrowth of the high vibration levels induced by negative damping. The magnitude of the damping is proportional to the slope of the friction-creep curve shown in Figure 2. The slope of the friction-creep curve (hence the negative damping) has three significant ranges of behavior:

- *No squeal*—c_a is less than c_0 (the lateral creep corresponding to μ_0, the maximum occurring coefficient of friction),

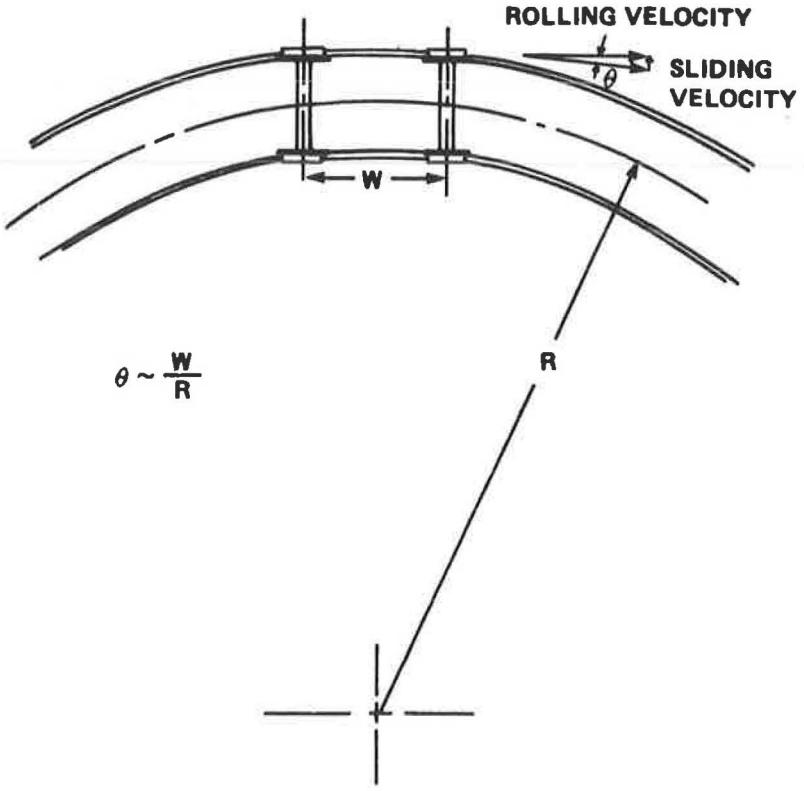

FIGURE 1 Wheel squeal excitation geometry (*2*).

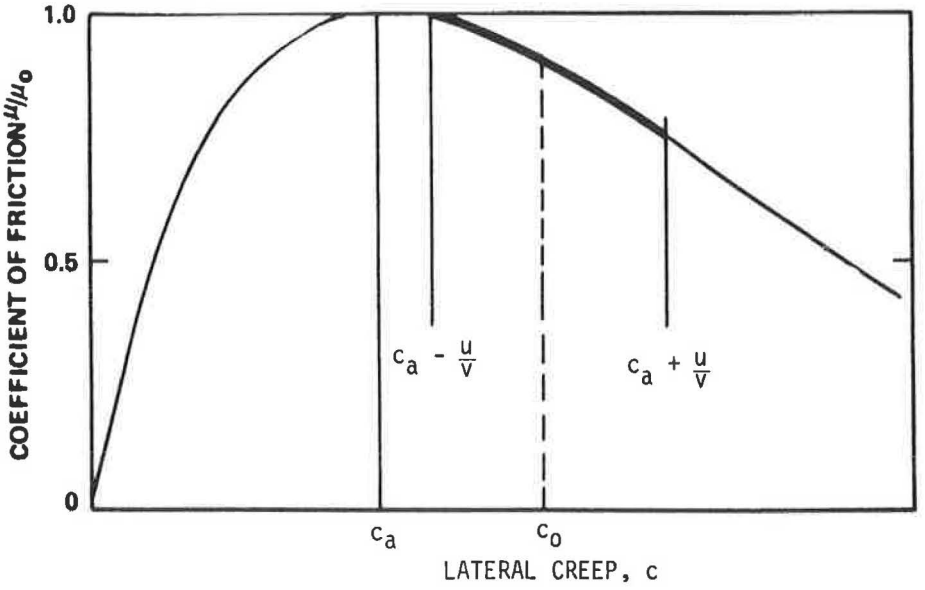

FIGURE 2 Friction-creep curve (*2*).

- *Intermediate squeal*—c_a is greater than c_0 but less than $3c_0$, and
- *Severe squeal*—c_a is greater than $3c_0$.

For the intermediate squeal condition, the generated squeal sound power can be shown to be proportional to

$$u = V^2 c_0^2 \{(8/3)[(c_a - c_0)/(3c_0 - c_a)]\}$$

Thus, the squeal noise magnitude is a function of V, W, and R—because $c_a \cong W/R$.

Approximate values for c_a and c_0 are (*1*, *2*)

$$c_a \cong 0.7W/R$$

$$c_0 \cong 0.007$$

Consequently, the boundaries for the squeal regimes are about $W/R > 0.01$ for intermediate squeal and $W/R > 0.03$ for severe squeal. For the geometries occurring in the WMATA railcars and maintenance yards ($0.02 < W/R < 0.03$), the intermediate squeal condition is predicted.

These relationships suggest that severe squeal will occur with WMATA railcars for curve radii less than 240 ft and that the minimum radius for no squeal will be greater than 755 ft. In actual practice, increasing curve radius initially causes a transition of squeal behavior from continuous to intermittent, with considerably larger radii necessary to ensure that even intermittent squeal will not occur (*2*). For WMATA railcars, preventing intermittent squeal would require a curve radius of 1 mi or greater.

The preceding analysis is predicated on a wheel-rail sliding motion that consists of the wheel tread moving laterally across the rail head. Other rubbing mechanisms are possible: the wheel flange against the side of the running rail head, and for curves fitted with a restraining rail, the flange against the restraining rail—as shown in Figure 3 (*3*). (A restraining rail is an auxiliary rail located adjacent to the inner rail. It relieves the leading outside wheel flange of lateral curving forces and transfers them to the back of the inner leading wheel flange, reducing wear and a tendency to derail.) The squeal contri-

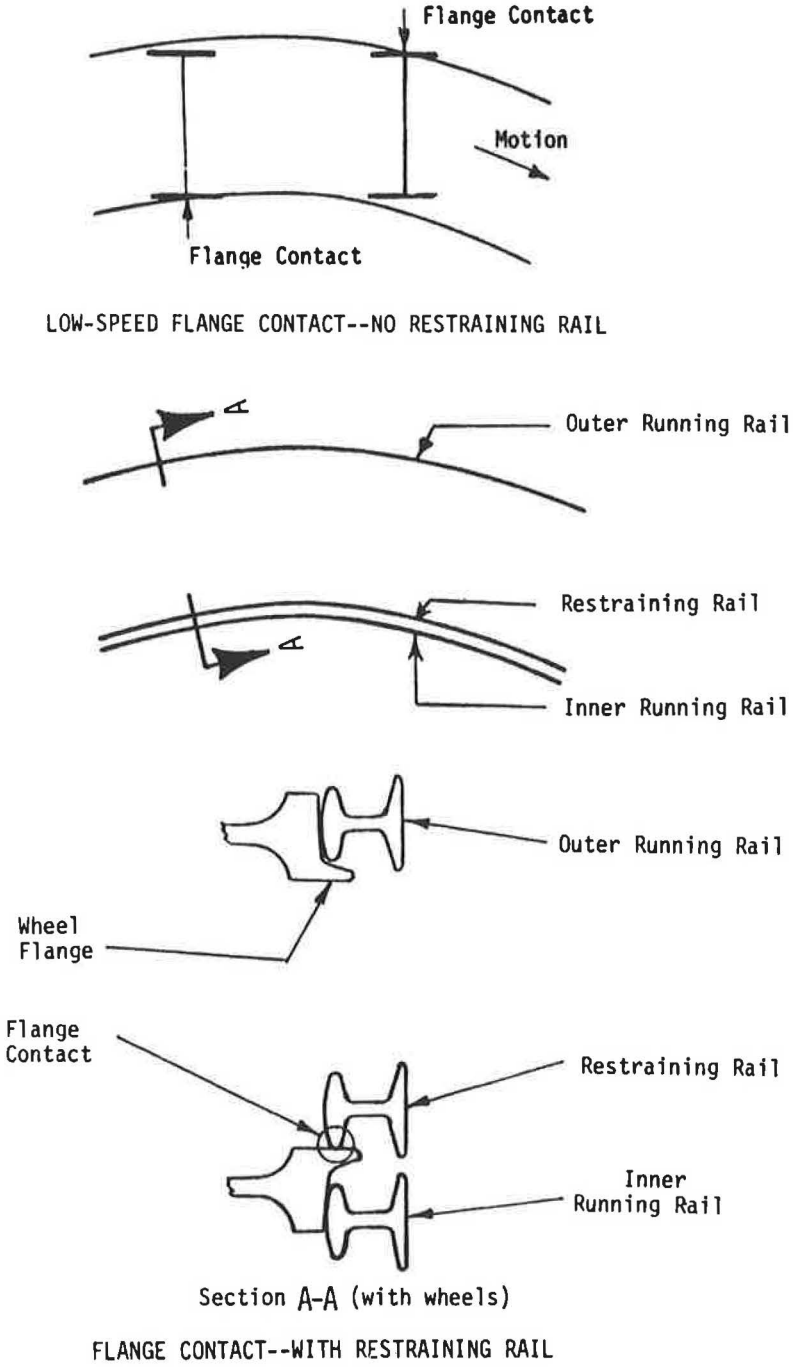

FIGURE 3 Flange rubbing locations (*3*).

butions of the various rubbing surfaces have been determined in experiments involving lubrication of the surfaces to temporarily reduce the friction forces. These experiments have shown that flange rubbing alone is not a sufficient mechanism for squeal (*1*), and that "in all tests where lubrication occurred on the top of the rail, squeal was reduced or eliminated" (*4*). Although the restraining rail introduces an additional surface for flange contact, it does reduce some contact forces, and some data suggest that the restraining rail actually reduces wheel squeal (*4*).

WMATA SQUEAL NOISE

Train operation sound levels were measured at locations around and inside the subject facility, the West Falls Church maintenance yard, and also at locations inside the two other similar yards, the Alexandria and Shady Grove maintenance yards. The purpose of these measurements was to define the community squeal exposure with controlled train operations and to compare squeal generation at West Falls Church with other similar facilities.

Community Noise Exposures

Two locations were selected as representative for the measurement of the squeal noise exposure in the community. Both locations were approximately 400 ft from the track—one each near the east and west loops of the yard. To avoid background noise interference (due to vehicles and insects), measurements were performed after midnight and after the onset of freezing weather. In the nighttime tests, the measured squeal sound levels for the east loop were close to the background noise levels but squeal was clearly perceptible. With a 48-dBA background sound level, the estimated squeal-only mean maximum sound level was 49 dBA at this location. For the west loop measurements, wheel squeal was prominent and clearly perceptible. With a background sound level of 46 dBA, the estimated squeal-only sound level was 56 dBA. Third-octave band spectra measured in the community are given in Figure 4. The prominent peak at 630 Hz is wheel squeal.

Comparison of Maintenance Yards

Sound levels within the maintenance yards were measured 15 ft inside the centerline of the track curve with a 2.5-ft microphone height (roughly axle high). Four-car test trains with a 7.6-ft wheelbase were operated at 5- and 10-mph speeds for the measurements. (At the Alexandria yard, trains with a 7.3-ft wheelbase were used; the microphone height was 5 ft; and some measurements were performed outside the track curve due to access constraints.) Average maximum A-weighted sound levels obtained in the yards are presented in Table 1.

Of interest is the apparent effect of the restraining rail. Restraining rails had been removed from all curves at West Falls Church in an effort to reduce wheel squeal. At Alexandria and Shady Grove, the restraining rails were in place—with grease lubricators for the restraining rails operative at Shady Grove but not at Alexandria. Removal of the restraining rails does not appear to have had any significant benefit—the West Falls Church yard is comparable to the Alexandria yard with restraining rail. On the other hand, the Shady Grove

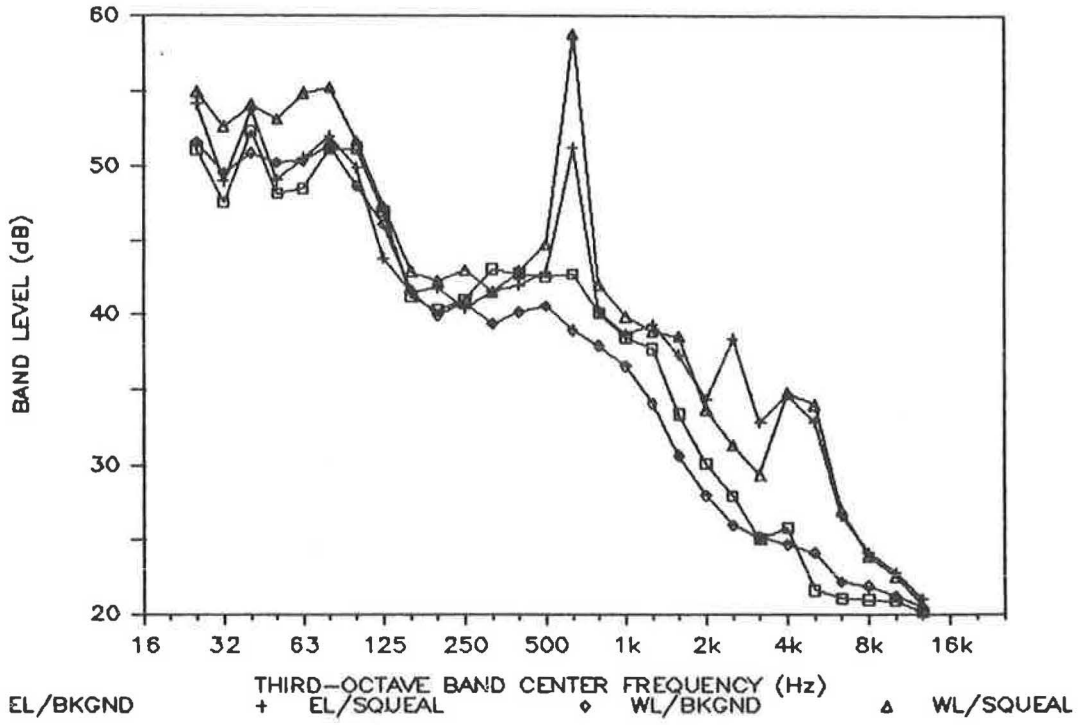

FIGURE 4 Measured wheel squeal in-community sound levels, West Falls Church, December 1, 1987 (EL, east loop; WL, west loop; BKGND, background noise; SQUEAL, squeal and background noise).

TABLE 1 SUMMARY OF MEAN MAXIMUM A-WEIGHTED SOUND LEVELS MEASURED 15 FT INSIDE TRACK CENTERLINE (FOUR-CAR TEST TRAINS WITH 7.6-FT WHEELBASE AT 5 MPH)

YARD	DATE	TRACK RADIUS (ft)	RESTRAINING RAIL INSTL.	RESTRAINING RAIL LUB.	MEAN L_{Amax} (dBA)	NUM. EVENTS
WEST FALLS CHURCH						
--East Loop	23-Oct-87	305	No	--	95.2	4
	23-Oct-87	290	No	--	100.1	4
	01-Dec-87	290	No	--	98.8	5
--West Loop	01-Dec-87	300	No	--	103.7	6
ALEXANDRIA *	20-Oct-87	320	Yes	No	101.6	4
SHADY GROVE	28-Oct-87	330	Yes	Yes	85.9	4
	28-Oct-87	315	Yes	Yes	85.3	4
	28-Oct-87	300	Yes	Yes	95.8+	4

* 7.3-ft-truck-wheelbase cars; mic. height: 5 ft instead of 2.5 ft

\+ +1-dBA adjustment for calibration drift

yard with the restraining rail and operative lubricators was relatively quiet. This may be the result of

- A vibration-damping effect induced by the lubricated restraining rail, or
- A more even distribution of flange loads or wheel slip among the wheels of a truck.

As discussed, squeal sound levels are expected to be proportional to a function of train velocity V, curve radius R, and train truck wheelbase length W. When the daytime in-yard A-weighted sound levels were normalized and plotted with this relationship, the results are as shown in Figure 5. The expected variation for intermediate squeal is shown by the straight line. This plot includes 5- and 10-mph events, where the 10-mph events are at $-26 < f(V, W, R) < -22$. The measured levels exhibit considerable deviation from the predicted sound levels, with the Shady Grove yard appearing to be somewhat quieter. These differences may be explained

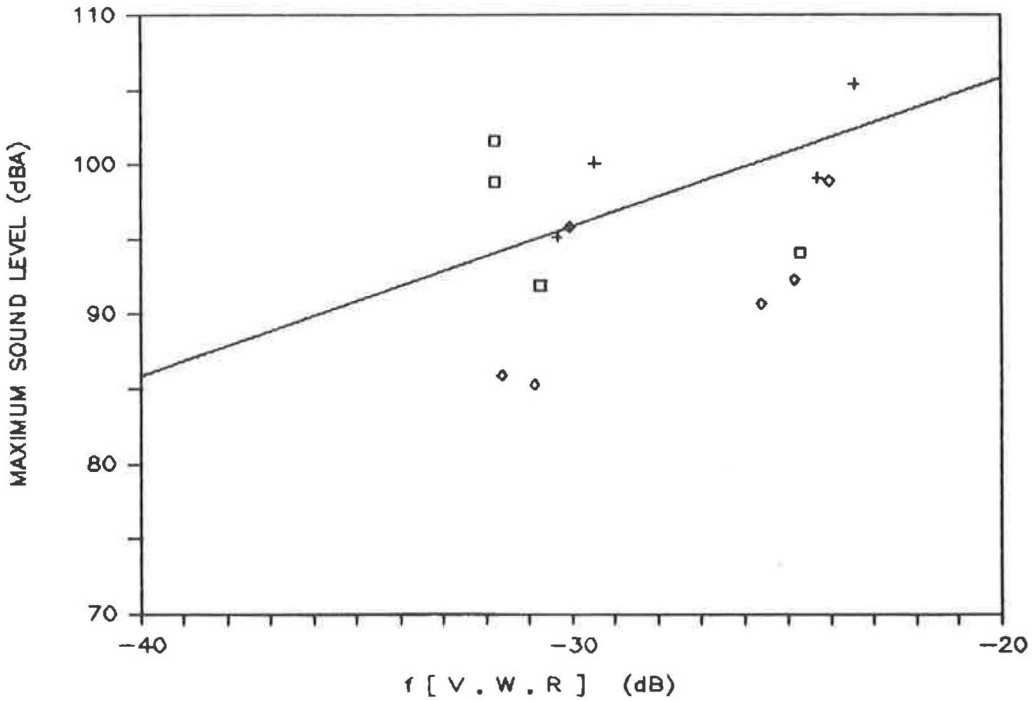

FIGURE 5 Mean maximum A-weighted squeal sound levels measured 15 ft from track centerline, October 1987 (□ = Alexandria yard, + = West Falls Church yard, ◇ = Shady Grove yard).

by the varying restraining rail conditions summarized in Table 1.

Third octave-band spectra obtained in the three maintenance yards are shown in Figure 6. The West Falls Church yard has a very prominent first-order wheel mode along with the high-frequency, higher-order wheel modes. The Alexandria yard is dominated by higher-order wheel modes. The Shady Grove yard exhibited an almost nonexistent first-order wheel mode and relatively subdued higher-order modes as well.

WHEEL SQUEAL CONTROL

Actions by WMATA

WMATA had taken a number of actions to abate the squeal noise exposure in the community. These actions included reduction of in-yard train speeds, elimination of train operations after midnight, removal of restraining rails, construction of acoustical barrier walls, and installation of a prototype rail lubrication system.

Train-Speed Reduction

The reduction of train speed from standard WMATA practice of 10 mph in maintenance yards to 5 mph is likely to have caused about a 6-dBA squeal sound level reduction, as can be seen in Figure 5.

Operations Curfew

The implementation of a curfew on in-yard operations, so that no train movements are permitted under normal circumstances after midnight, prevents late-night disturbances but does not affect noise exposures during noncurfew hours.

Restraining Rail Removal

The restraining rail was removed in an effort to reduce the number of possible squeal-exciting track surfaces. Comparison of sound levels in Table 1 and in Figure 5 does not indicate any clear benefit from this action. In fact, the Shady Grove

(a)

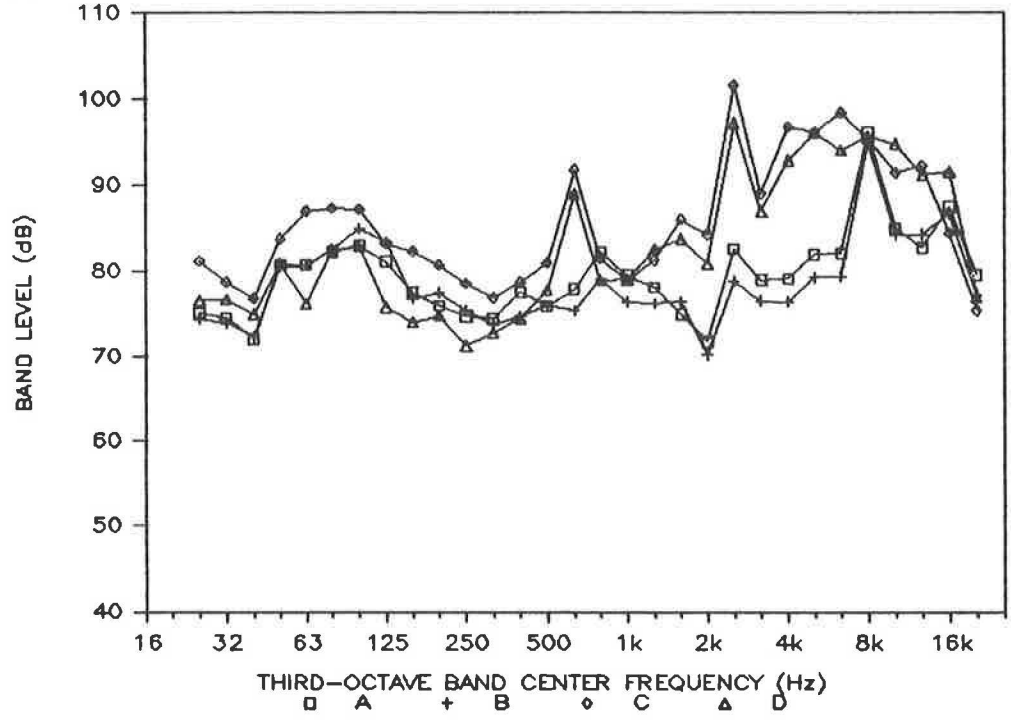

YARD	MEAS. SERIES	TRAIN SPEED	TRACK	MIC. LOC.*	TRACK COND.
ALEXANDRIA	A	5	inner	outside	dry
	B	10	inner	outside	dry
	C	5	outer	inside	dry
	D	5	outer	outside	dry

* re track curvature

FIGURE 6 Wheel squeal measurements: a, Alexandria yard; b, West Falls Church yard, east loop; c, Shady Grove yard. ***(continued on next page)***

(b)

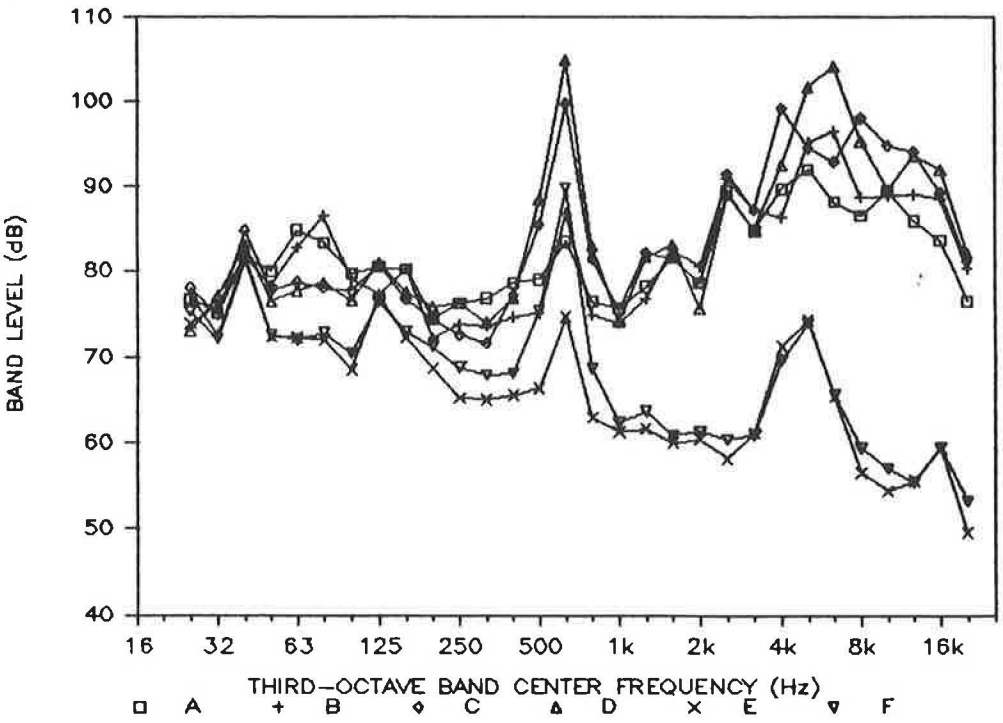

YARD	MEAS. SERIES	TRAIN SPEED	TRACK	MIC. LOC.*	TRACK COND.
WEST FALLS CHURCH	A	5	outer	inside	dry
	B	10	outer	inside	dry
	C	5	inner	inside	dry
	D	10	inner	inside	dry
	E	5	inner	inside	wet
	F	10	inner	inside	wet

* re track curvature

FIGURE 6 (*continued on next page*)

yard with its grease-lubricated restraining rail is relatively quiet and more broadband in character.

Acoustical Barrier Walls

Walls were constructed as high as 17 ft near the west loop property line and as high as 10 ft adjacent to the east loop track. The barrier benefit of the walls was estimated by comparing in-yard measured squeal sound levels to background-corrected in-community measured sound levels after accounting for sound propagation attenuation. Source spectra were derived from the third-octave band sound levels obtained inside the West Falls Church yard. The source locations were taken at the positions along the curves that were expected to have resulted in the maximum in-community squeal sound levels. The barrier benefits are the reductions in sound levels with the barriers relative to the sound levels estimated at the same locations without the barriers—about 5 dBA for the east loop and 3 dBA for the west loop.

Water Lubrication

A prototype water rail-lubrication system was installed at the inner track of the east loop at West Falls Church. Controlled measurements both in the yard and in the community were obtained. This system is highly effective in reducing wheel squeal. The average maximum A-weighted in-yard sound levels measured with and without water lubrication presented in Table 2 show reductions in excess of 18 dBA. The effect of the system on the frequency spectra can be seen in Figure 6b, where the high-frequency squeal tones are virtually eliminated and the first-mode wheel squeal tone at 630 Hz is substantially reduced. The train noise with a well-wetted track is essentially wheel-rail rolling noise and propulsion-system noise. In the

(c)

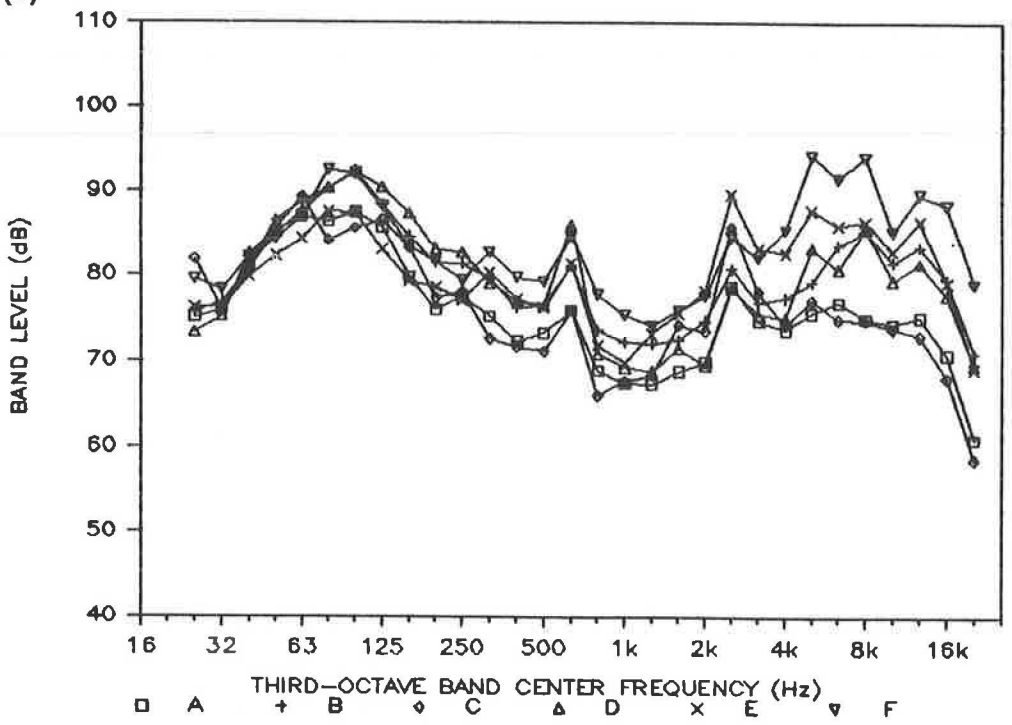

YARD	MEAS. SERIES	TRAIN SPEED	TRACK	MIC. LOC.*	TRACK COND.
SHADY GROVE	A	5	outer	inside	dry
	B	10	outer	inside	dry
	C	5	middle	inside	dry
	D	10	middle	inside	dry
	E	5	inner	inside	dry
	F	10	inner	inside	dry

* re track curvature

FIGURE 6 (*continued from previous page*)

TABLE 2 EFFECT OF WATER LUBRICATION (EAST LOOP, INNER TRACK, AT 15 FT INSIDE TRACK CENTERLINE, FOUR-CAR BREDA TEST TRAINS)

MEASUREMENT DATE	SPEED (MPH)	CONDITION	L_{Amax}* (dBA)	LR+ (dBA)
23-Oct-87	5	Dry	100.1	--
		Wet	81.4	18.7
	10	Dry	105.4	--
		Wet	86.6	18.8
01-Dec-87	5	Dry	98.8	--
		Wet	76.3	22.5

* Mean of test series
\+ Dry-wet sound level reduction

community, train operations with the track wet were virtually imperceptible.

Options for Effective Squeal Control

A number of the actions taken by WMATA achieved reductions in squeal sound levels. However, because of the distinctive character of the squeal signal, squeal is clearly perceptible in the community and quite pervasive during low-background-noise conditions. Even noticeable reductions of the squeal levels are unlikely to achieve community satisfaction if the squeal remains perceptible. Consequently, effective controls must essentially eliminate the generation of squeal. Water lubrication, as has already been demonstrated, is an example of such a control. Potentially effective squeal controls include rail lubrication, wheel or rail damping, rail facing, and track (tunnel) enclosures.

Wheel Damping

Wheel squeal increases in magnitude until the negative damping of the excitation is counterbalanced by the positive internal damping of the system. A number of approaches have been taken to increase wheel damping in practice. The simplest and most successful approach is the use of ring dampers. Ring-damped wheels have metal rings that are snapped into a semicylindrical groove cut into the inner diameter of the wheel rim. The rings are usually steel and are sprung into the groove such that the ring is free to vibrate (*4*). Damping is apparently provided by the frictional forces arising from the relative movement of the damping ring and the wheel. Ring dampers are used operationally by Chicago, Lindenwold (PATCO), New York City, and the Port Authority of New York and New Jersey (PATH) and are generally considered quite effective in reducing wheel squeal. Wayside sound level reductions due to ring dampers in curved track, reported by a number of different transit properties, have ranged up to 32 dBA (*4*).

Rail Damping

Another means for adding damping to the wheel-rail system is to increase the internal damping of the rail. However, the vibration magnitude of the rail is generally much less than that of the wheel. Thus, the effectiveness of rail damping is limited. Damping materials have been placed either on the bottom or sides of rails with "erratic and unpredictable" squeal reductions (*4*). Research indicates that damping of the rail is beneficial only if the rail vibration levels are sufficiently large, that is, greater than about 3 *g* (*5*).

Bolt-on tuned-damper assemblies can be secured to rails if diagnostic tests indicate high rail-vibration levels and if damper effectiveness is verified by prototype tests.

Rail Facing

Altering the metallurgy of the rail head is a means of eliminating wheel squeal—possibly by reducing the friction coefficient at the wheel-rail contact point. This approach has been marketed as a commercial process consisting of

- Grinding a groove in the rail head,
- Depositing a proprietary alloy filler,
- Grinding the weld so that the alloy surface is no higher than the rail surface, and
- Straightening the finished rail (*6*).

This treatment is shown in Figure 7.

The antisqueal process has been used by a number of transit properties in Europe, primarily on light rail systems (G. J. Mulder, Orgo-Thermit, Inc., unpublished data). In North America, use of the antisqueal treatment has been limited to light rail installations by Philadelphia and Toronto. The Philadelphia installation has yielded inconclusive results (G. Heines, Orgo-Thermit, Inc., unpublished data). After extended service, Toronto reported that treated curves were "clearly quieter" than identical untreated curves, no reliability problems were encountered, and rail wear was as good as standard rail (T. Whibbs, Toronto Transit Commission, unpublished data).

Rail Lubrication

As noted previously, when the tops of rails are lubricated, squeal is reduced or eliminated. Illustrative of this effect are the extensive tests performed by PATH with various combinations of grease-and-water-lubricated, steam-cleaned, and in-service-lubricated rail (*7*). The measurements used train-truck-mounted microphones on each side of a train close to the wheels. Sound levels were recorded while traversing various segments of an underground curve of very small radius (W/R = 0.06). Table 3 presents the resulting sound-level reductions with respect to track with 8 days of revenue service without the usual grease lubrication. The results are ranked by average sound-level reduction in track section. Squeal

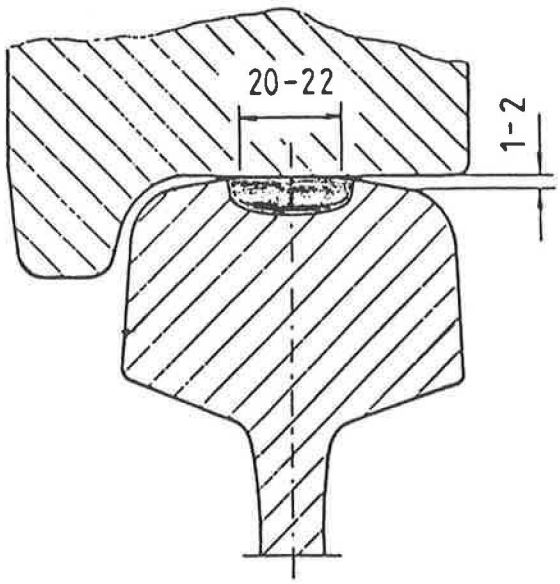

FIGURE 7 Antisqueal rail head treatment.

TABLE 3 PATH RAIL LUBRICATION TESTS (7)

--RAIL COND.--					TRACK SECTION										
-Out-		-In--		RR	At Outer Rail						At Inner Rail					
T	S	T	S	S	A	B	C	D	MEAN	SD	A'	B'	C'	D'	MEAN	SD
					AVG. SOUND LEVEL (dB) IN SECTION											
D	D	D	D	D	116.0	125.0	124.0	112.0	119.3	6.3	113.0	114.0	113.0	111.0	112.8	1.3
					AVG. LEVEL REDUCTION (dB) IN SECTION											
W?	WG	W	W	WG	12.0	22.0	21.0	7.0	15.5	7.2	11.0	12.0	11.0	6.0	10.0	2.7
W?	WG	W	W	W	11.0	20.0	20.0	5.0	14.0	7.3	9.0	10.0	9.0	4.0	8.0	2.7
G	G	G	G	G	13.0	20.0	19.0	4.0	14.0	7.3	10.0	10.0	8.0	4.0	8.0	2.8
W	W	W	W	W	11.0	18.0	18.0	3.0	12.5	7.1	9.0	9.0	8.0	3.0	7.3	2.9
C	C	C	G	G	9.0	16.0	14.0	3.0	10.5	5.8	8.0	5.0	6.0	4.0	5.8	1.7
C	C	G	G	G	10.0	19.0	10.0	1.0	10.0	7.3	9.0	5.0	2.0	3.0	4.8	3.1
?	G	?	?	G*	2.0	15.0	11.0	1.0	7.3	6.8	7.0	8.0	7.0	4.0	6.5	1.7
C	G	C	C	C	10.0	-2.0	17.0	3.0	7.0	8.3	5.0	4.0	8.0	3.0	5.0	2.2
?	G'	?	?	G'*	4.0	1.0	11.0	4.0	5.0	4.2	5.0	6.0	4.0	3.0	4.5	1.3
?	G	C	C	G	4.0	-1.0	2.0	2.0	1.8	2.1	7.0	6.0	5.0	2.0	5.0	2.2
C	C	C	C	C	-6.0	-2.0	4.0	-4.0	-2.0	4.3	5.0	5.0	5.0	2.0	4.3	1.5

LEGEND: In = inner rail of curve T = condition of rail top
Out = outer rail of curve S = condition of rail side
RR = restraining rail
* usual in-service lubricant application
D = 8 da. w/o lubrication G = standard grease lubricant
C = steam clean G' = MoS_2 grease lubricant
W = water lubricant ? = possible grease migration

reduction was greatest for combined water-grease lubrication with grease lubrication and water lubrication to all rails also effective.

Major users of grease lubrication are Chicago, New York City, and Boston. Chicago reported that lubrication reduces squeal levels but never completely for any turn (R. Smith, Chicago Transit Authority, unpublished data). New York City routinely uses lubrication in both yards and on revenue track, but finds that constant maintenance is required to retain effectiveness (W. Jehle, New York Transit Authority, unpublished data). The Boston (MBTA) lubrication practice is to apply grease to both the running and restraining rails and allow the grease to migrate to the rail head (J. I. Williams, Massachusetts Bay Transit Authority, unpublished data). This approach has been effective in squeal quieting. Figure 8 shows the results of a test for MBTA of train pass-by sound levels with and without manually applied grease lubrication (*8*). The effect of lubrication on average train pass-by spectra is shown in Figure 9. A major concern with greasing of running rails is the potential for traction problems. Although MBTA makes no effort to prevent grease migration to the rail head, no traction problems have been encountered after 3 years of revenue service experience (J. I. Williams, MBTA, unpublished data). The key to avoiding traction problems appears to be proper adjustment of the grease application system to prevent discharge of excessive lubricant (V. J. Petrucelly, Port Authority of New York and New Jersey, and T. D. Smith, Toronto Transit Commission, unpublished data).

The only North American rail transit properties that have operationally implemented water lubrication are Toronto and PATH. The PATH installation was an underground revenue line, free of freezing temperatures. It was used operationally

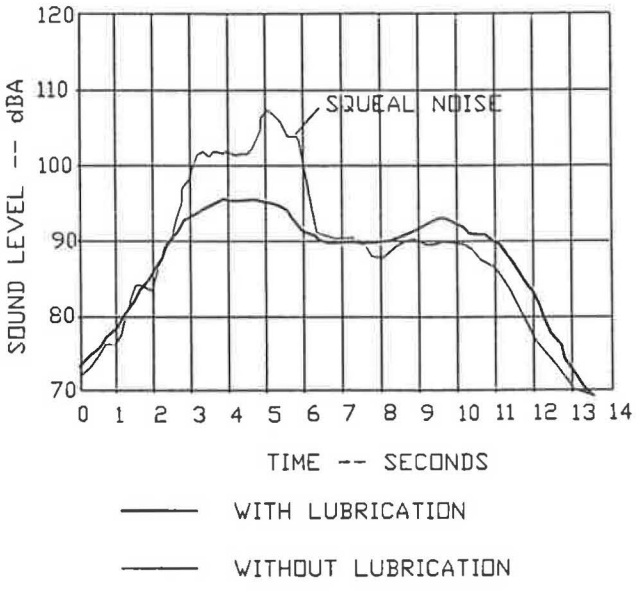

FIGURE 8 MBTA grease lubrication tests—pass-by time histories (*8*).

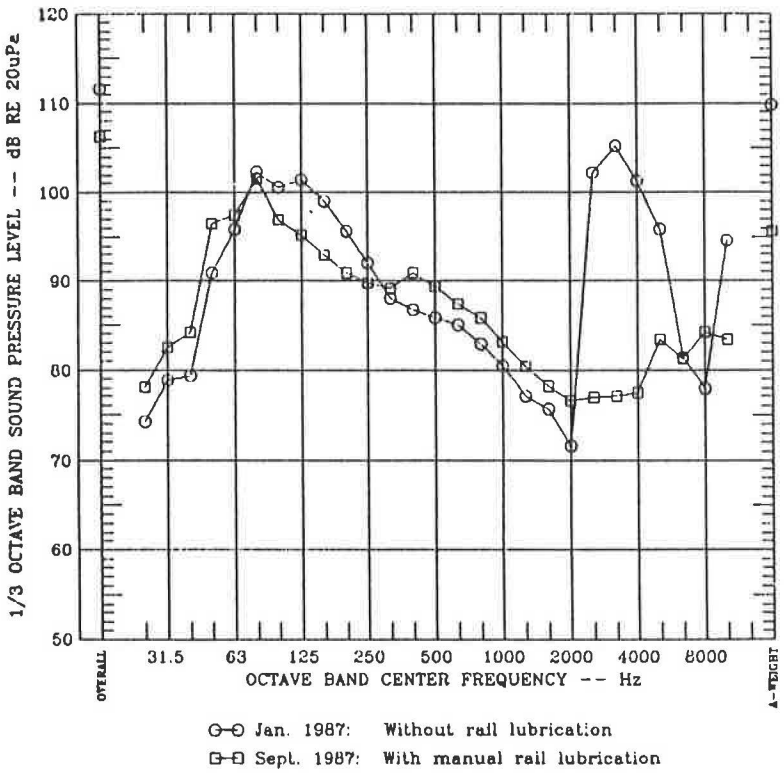

FIGURE 9 MBTA grease lubrication tests—average frequency spectra (*8*).

and successfully for a number of years but is currently inactive (G. Figueredo, Port Authority Trans-Hudson Corp., unpublished data). The Toronto system has been used at a maintenance yard since 1974. It is shut down in freezing-weather months, at which time grease lubrication is manually applied once daily.

Tunnel Enclosures

Three-sided enclosures covering the inner and outer tracks of each loop must be composed of walls with high sound transmission loss and with sound-absorptive interior lining. The tunnels would have to extend sufficiently beyond the ends of the loops to minimize sound radiation from the enclosure apertures. However, even a relatively long tunnel may permit perceptible sound levels to escape.

Recommendations

In summary, the six potentially effective squeal-control options are

- Water lubrication (with manual winter greasing),
- Automatic all-rail grease lubrication,
- Rail facing,
- Tunnel enclosures,
- Wheel dampers, and
- Rail dampers.

The advantages and disadvantages of these options are presented in Table 4. (Note that the comments in Table 4 regarding cost are not based on quantitative investigation.)

RAIL-FACING TREATMENT EXPERIENCE

The rail-facing squeal-control option was chosen by WMATA because

- Water lubrication requires the use of grease lubrication in wintertime,
- Grease lubrication evokes fears of traction problems,
- Tunnel enclosures are expensive and impractical,
- Wheel dampers necessitate retrofit of the entire Metro car fleet, and
- Rail dampers have shown little promise in previous experiments.

The prototype rail-facing treatment was applied to approximately 800 ft of rail on the curve of 290-ft radius of the inner track of the east loop at West Falls Church in January 1989.

Sound-level measurements were made shortly after the installation of the treatment and periodically thereafter. The initial measurements showed that train pass-by sound levels were reduced to 75 dBA at 30 ft (height 5.5 ft) with the complete elimination of squeal (versus 98 dBA measured in August 1987 typically with six 5- to 6-sec squeal occurrences per pass-by). However, subsequent tests conducted in April to July 1989 showed the return of squeal, and in spite of experiments involving adjusting the restraining rail gap and grinding of the inside rail, squeal has persisted. A summary of the measurements is presented in Table 5.

TABLE 4 POTENTIALLY EFFECTIVE SQUEAL-CONTROL OPTIONS

NOISE CONTROL	ADVANTAGES	DISADVANTAGES
WATER LUBRICATION	Demonstrated effective at West Falls Church Yard, prototype system in place, moderate(?) installation costs.	Freezing weather problems, relatively high(?) operating cost, relatively high(?) maintenance requirements.
ALL-RAIL GREASE LUBRICATION	Demonstrated effective on other systems, reduced wheel and rail wear, easily evaluated by manual application, moderate(?) installation cost for automatic system.	Potential wheel slip problem, very high maintenance requirement, requires very stringent in-use monitoring.
RAIL FACING	Low maintenance, possible improved(?) rail wear.	Requires replacement of track, not yet demonstrated effective in U.S. on heavy-rail system.
TUNNEL ENCLOSURE	No maintenance, more suitable for more severe West Loop.	Very expensive installation--probably prohibitive for East Loop, West Loop length limited by yard layout.
WHEEL DAMPERS	Demonstrated effective and used operationally on number of U.S. systems.	Requires modification to entire car fleet, may not sufficiently attenuate first wheel vibration mode, relatively expensive(?) to implement.
RAIL DAMPERS	Possible low(?) installation cost, usefulness easily tested.	Little in-service experience, often not suitable.

? = unquantified judgment

TABLE 5 RAIL-FACING TREATMENT EXPERIENCE

DATE	L_{Amax}* (dBA)	SQUEAL EXTENT+	DESCRIPTION**
Aug 87	98	6	No rail facing
3 Feb 89	75	None	Immediately after rail-facing installation
21 Apr 89	87	3	
19 May 89	86	3-4	
12 Jun 89	78	1	With restraining-rail gap increased by 0.25 in.
29 Jun 89	85	2	With normal restraining-rail gap restored
7 Jul 89	90	6	After grinding inside rail

* average over 5-6 passbys, measured 30 ft inside centerline of inner loop track

\+ squeal occurrences per passby

** all tests with restraining rail

A preliminary evaluation suggests that, because the rail-facing material is much softer than the adjacent rail head and has a tendency to adhere to the wheel tread, its initial effectiveness is lost due to rapid contact point wear caused by a peeling-off of the facing treatment.

REFERENCES

1. M. J. Rudd. Wheel/Rail Noise—Part II: Wheel Squeal. *Journal of Sound and Vibration*, Vol. 46, No. 3, Elsevier, Oxford, England, 1976, p. 381.
2. P. J. Remington et al. *Control of Wheel/Rail Noise and Vibration*, Report MA-06-0099-82-5, UMTA, U.S. Department of Transportation, Cambridge, Mass., Apr. 1983.
3. *Reduction of Wheel Wear and Wheel Noise Study: Phase I—Exploratory Research, Vol. 3: Wheel Squeal.* Report A541, The Port Authority Trans-Hudson Corporation, Jersey City, N.J., Oct. 1978.
4. L. G. Kurzweil and L. E. Wittig. *Wheel/Rail Noise Control—A Critical Evaluation.* Report UMTA-MA-06-0099-81-1, UMTA, U.S. Department of Transportation, Cambridge, Mass., Jan. 1981.
5. *Test to Reduce the Noise During Breaking and Running Around a Sharp Curve: Results of Tests and Conclusions.* Report 7, Office of Research and Experiments of the International Union of Railways, ORE Question C137, Oct. 1977.
6. Technology News—Riflex Rail Comes to North America. *Modern Railroads*, July 1985.
7. A. R. Patel. *Reduction of PATH Wheel Wear and Wheel Noise. Phase II—Analysis and Test, Task 3—Rail Lubrication Tests (Volumes 1 and 2).* The Port Authority of New York and New Jersey, Reports 81-15 and 81-17, Jersey City, Oct. 1981.
8. C. E. Hanson. Red Line Lubricator Noise Tests. Report 260362-1, Harris, Miller, Miller, and Hanson Inc., Lexington, Mass., Oct. 1987.

Publication of this paper sponsored by Committee on Transportation-Related Noise and Vibration.

Knowledge-Based Preprocessor for Traffic Noise Prediction

HUNG-MING SUNG AND WILLIAM BOWLBY

A knowledge-based preprocessor system has been developed to assist the engineer in creating data input files for the STAMINA 2.0 traffic noise prediction program. The preprocessor uses rule-based heuristic knowledge for certain decisions, algorithmic routines to provide data to the rules and to help automate the file creation process, and linkages to editing routines for manual manipulation. The system is used as the engineer works with a design project's plans. The system requests certain data from the user, and ultimately creates two STAMINA input files. The first file contains the baseline noise barriers as starting points for final barrier design with a companion program called OPTIMA, and the second file contains only the ground-line elevations for accurate assessment of no-barrier levels. System performance was tested on two major analysis areas on each of two design projects previously done by human experts. In all cases, the system created syntactically correct STAMINA input files that resembled those of the experts and produced meaningful sound level results when run. In some cases, these STAMINA files resulted in barrier insertion loss predictions very similar to those produced by the experts using the OPTIMA program. Although it was not the intent of this work to replace use of OPTIMA, the files produced by the system should reduce time spent using OPTIMA, as well as time typically spent making modifications to the STAMINA files. Although fully functioning, the system should be considered an operational prototype until further testing and refinement.

Highway traffic noise is a major public concern with the construction of noise barriers being the most common method for control used by state departments of transportation. Noise barrier analysis and design is typically done using the barrier cost reduction (BCR) procedure (*1*) that involves sequential use of two computer programs, STAMINA 2.0 and OPTIMA (*2*).

STAMINA 2.0 mathematically models the noise levels from a highway project on the basis of user-defined geometric coordinates (x,y,z) of the sound receptor points (receivers), roadway, and proposed barriers, as well as traffic volumes and speeds, ground cover conditions (alpha factors), and level reductions due to shielding from buildings and terrain. To produce the needed barrier design information for OPTIMA, a baseline barrier height is specified in STAMINA for each barrier segment, as well as desired perturbations of this height. STAMINA 2.0 then calculates the sound energy at each receiver that passes over each of the multiple barrier heights for each barrier segment. STAMINA 2.0 generates an acoustics file that contains these sound energy data, which are required by OPTIMA as input. The designer then uses OPTIMA in an iterative fashion to test various designs, working toward a goal of selecting the lowest-cost barrier for a given amount of noise control. The most efficient design for barrier height can only be obtained if the STAMINA input data have the optimal lateral location of each barrier and the proper range in heights above and below the baseline height for each barrier segment. In many cases, the input data can only be developed properly through a time-consuming process of changing the STAMINA input file and rerunning STAMINA before rerunning OPTIMA.

Several years ago, the knowledge-based system Computerized HIghway Noise Analyst (CHINA) (*3*) was developed. This system ran the OPTIMA program to produce a good noise barrier design after the human engineer had separately created the STAMINA 2.0 input file and had run STAMINA. However, that barrier design would only be as good as the original site modeling permitted it to be. If the engineer did a poor job locating the barrier in plan view, choosing baseline barrier segment heights, or choosing receivers, then it would be unlikely that the human engineer or CHINA could accomplish a satisfactory design.

This paper presents an overview of the results of research on the development of a knowledge-based system to assist in highway noise modeling (*4–6*). The major objective of the research was to develop a tool to help an inexperienced designer in the difficult task of building a good input file for STAMINA 2.0. Additionally, an experienced designer can take advantage of the computing ability of the system to speed file creation and to reduce the number of iterations in the noise analysis, thus saving time.

The resultant final product when one uses the system is actually two input data files for STAMINA 2.0 that contain the needed data for receivers, roadways, barriers, ground-covering factors, and shielding factors. The first file contains the initial barrier design, and is used by STAMINA to produce the acoustics file for OPTIMA. The second file, with ground-line barriers only (no-barrier or without barriers), may be used to determine impacts without noise abatement features.

PROBLEM IDENTIFICATION

The major problem areas in the creation of input files for STAMINA 2.0 for most highway noise analysis projects include (a) selecting representative receivers, (b) modeling highway systems to correctly represent the noise sources, (c) determining the best lateral locations to build noise barriers and a good set of initial heights aimed at reaching a design goal, (d) choosing proper alpha factors for ground effects on noise propagation, and (e) choosing proper building shielding values.

H.-M. Sung, Trinity Consultants, Inc., 12801 N. Central Expressway, Ste. 1200, Dallas, Tex. 75243. W. Bowlby, Vanderbilt Engineering Center for Transportation Operations and Research, Vanderbilt University, Box 96–B, Nashville, Tenn. 37235.

These types of problems must be considered regardless of the highway noise prediction method selected, but they are critical when using STAMINA 2.0. In addition, the sheer volume of (x,y,z) coordinate data required to create a file calls for ways to automate the process as much as possible.

KNOWLEDGE ACQUISITION

Although some simple rules are provided in reports or manuals, the solutions to most of the problems require human experience, which is primarily heuristic knowledge. Thus, it is very important to ensure that the quality of the rules used in the expert system is consistent and well accepted by other experts. In this research, the resources employed for knowledge acquisition included the following:

1. Learning from a short course: The lead author attended a short course for highway noise barrier design, taught by three leading domain experts (including the coauthor).
2. Analyzing public domain knowledge: Four major design manuals (*3*, *7–9*) were carefully analyzed to examine the applicability of the rules cited in those manuals.
3. Conducting a survey: A survey consisting of 32 questions was answered by three engineers with extensive state department of transportation (DOT) experience in barrier design.
4. Studying the experts' performance: Previous projects done by the domain experts were analyzed and actual designs were done on state DOT projects in cooperation with a domain expert.

TOOL EVALUATION

Selecting a proper knowledge-based system developmental tool is important for programming and for maintenance of the system. The basic requirements for this research were rule-based knowledge representation, flexible problem-solving mechanism, integrated development environment, easy interface with procedural languages, compatibility with existing microcomputers, ease of learning and use, and low cost of the software.

Among all types of knowledge representation schemes, the rule-based scheme has been used most often because of its discrete nature, which is simple and flexible for most engineering designs. This research has already organized more than 100 rules to represent knowledge and experience. Also, for real-world applications of this knowledge-based system, the program must be able to call computer programs in other languages, such as computational routines in FORTRAN that process data for use by the rules. Additionally, software development is a repetitive and time-consuming process; an integrated development environment can help decrease programming time.

When this research began, tool evaluations showed that most commercial software was generally quite expensive or did not offer good interfacing capabilities. However, the low price and powerful interface of the knowledge-based developmental tool VP-Expert (*10*) led to its testing for suitability for this study. Implementing a small prototype on an IBM-compatible system led to the conclusion that this software was acceptable for this study. After completion of the project, it was concluded that use of a microcomputer with expanded memory capabilities was desirable.

PROGRAMMING THE KNOWLEDGE-BASED SYSTEM

The first stage in constructing the system was to design a framework that emulated the human expert's thought process. After that, numerous rules were organized and programmed into this design frame to accomplish the required functions. The rules were built into the system either implicitly as logical expressions or mathematical functions, or explicitly as guidance to help the user. The system was expected to be capable not only of executing the program correctly, but also of meeting two important concerns: (a) user-friendly interface, and (b) ease of future modification and maintenance. Thus, the program structure was divided into two parts. Figure 1 shows an overview of the structure of the system. The upper part of the figure is the knowledge base (or rule base) that was developed under VP-Expert. The lower part contains several data manipulation processes that were written in FORTRAN. The results generated from the knowledge base of each module need to be rearranged by an associated data manipulator before those data can be accessed by the next module.

A total of 14 rule-based routines and 16 FORTRAN routines were developed to form the major modules shown in Figure 1. System execution begins with a title block and then goes to a control block that is designed as a shell for the system. This shell links each design module to provide a more flexible design process for the user. Using the shell, the designer may make changes in a certain module without repeating the entire design process.

Centerline Module

The centerline module was designed to simplify the data representation scheme. Because the major task in file creation is to determine the receiver, roadway, and barrier points in three-dimensional coordinates, a simplified data representation scheme reduces the chance of accidental error input and saves analysis time. In this system, the user only needs to define (x,y) coordinates for designated stations of the roadway centerline. Points on the same plan may then be specified by station numbers with offsets, which are then converted to (x,y) coordinates based on the centerline data. This scheme is much more convenient than reading the coordinates of each point from design plans and is flexible for future enhancements such as interface with a digitizing table or a roadway computer-aided design (CAD) program. The required length of the centerline depends on the project requirements and the distribution of the noise receivers. To determine the length of the centerline, the user must first identify the receiver at each end with the longest offset distance. The centerline is then extended as follows:

1. If the offset is less than or equal to 250 ft, then extend the centerline by 4 times the offset.
2. If the offset is between 250 and 500 ft, then extend the centerline by 1,000 ft.

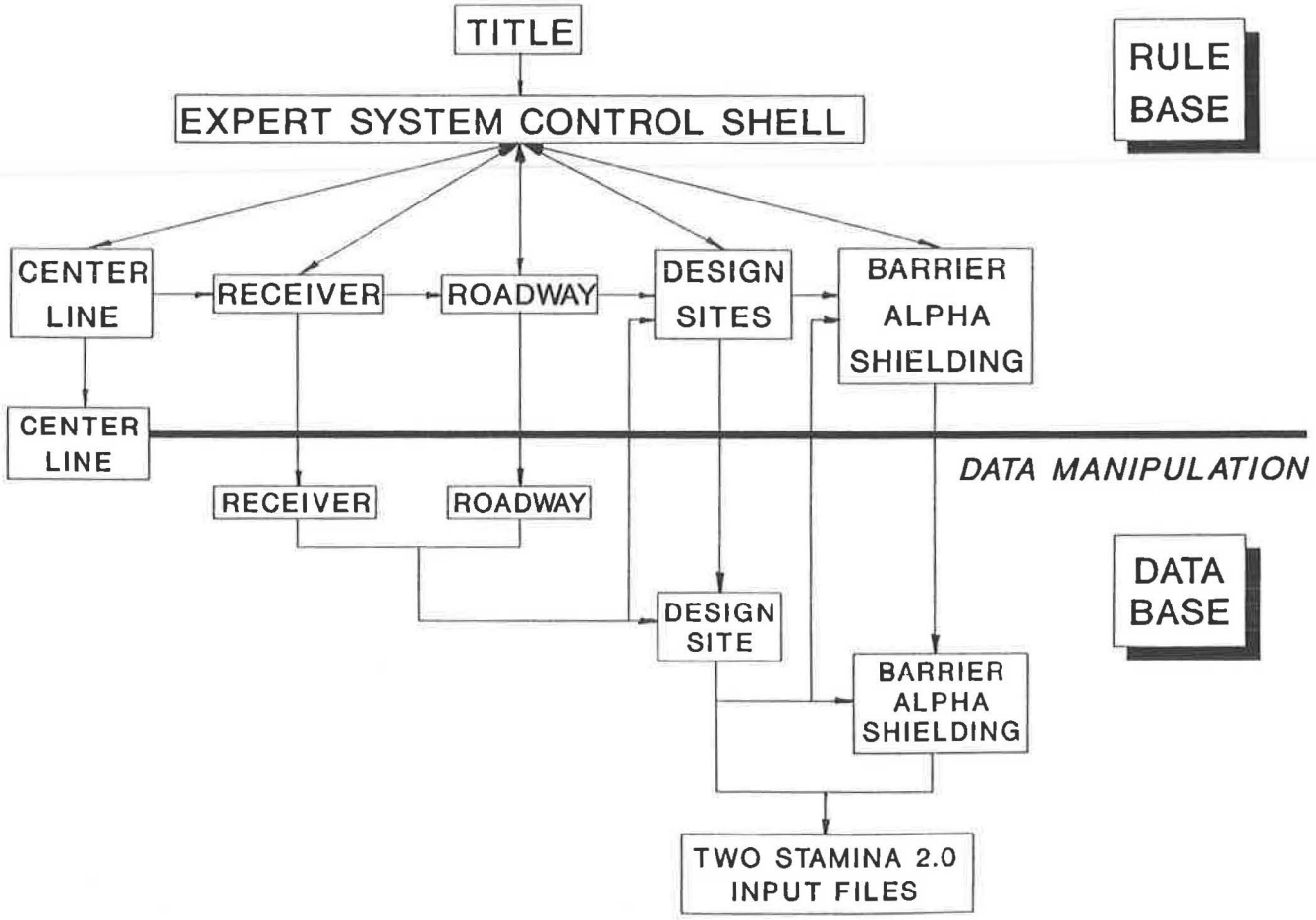

FIGURE 1 The knowledge-based system structure.

3. If the offset is greater than 500 ft, then extend the centerline by twice the offset.

The multipliers were determined during knowledge acquisition based on sound propagation characteristics and guidance from the experts.

The major requirement of this scheme is to express the centerline by both the station numbers and the (x,y) coordinates at the minimum number of points that can still provide the required accuracy. For instance, a straight roadway centerline can be expressed by just the two end points and the user needs to provide (x,y) coordinates for these two points to the system. For a more complicated highway plan, the required points are determined by the horizontal alignment of the centerline. Horizontal curves can be approximated by several straight lines. After testing the system with several design cases, the maximum offset of each straight line to the arc of the curve was determined to be 5 ft to avoid cumulative errors.

Receivers Module

This module presents the option of creating receiver data for the input file either manually or automatically. If the receiver distribution is fairly uniform, the receiver data can be generated automatically by the system with only a few input parameters: the desired distance between receivers, and one offset distance and one z-coordinate for each group of receivers. The system will then generate receiver title, station number, offset distance, and (x,y,z) coordinates for each receiver. As with the centerline module, this scheme is amenable to future interface with a digitizer or a CAD system.

If the user chooses to enter the receiver points manually, the system will call either a word processor or a spreadsheet program at the user's request. In this option, the user needs to define the receiver title, station number, offset, and z-coordinate for each receiver, and the program computes the (x,y) coordinates. A series of textual rules is provided as a guideline for the inexperienced designer for manual selection of meaningful receivers. These rules include the following:

1. For a row of houses, if the distance from one house to the next is less than 200 ft, then select the two end houses and every third house as the receiver points.
2. For a row of houses, if the distance from one house to the next is greater than 200 ft and less than 500 ft, then select the two end houses and every second house as receiver points.
3. For houses separated by more than 500 ft, select each house as a receiver point.
4. If the terrain of one receiver location is different from the surrounding area (e.g., top of a hill), then this location should be selected as a receiver point.

Roadways Module

This module assists the designer in dividing a highway system into representative noise sources called "roadways" in STAMINA. The first parameter considered for breaking a highway down into roadways is the number of lanes. Generally, each modeled roadway represents two or three real lanes and each ramp is considered as a single roadway for noise analysis.

In addition, the user is told to longitudinally divide the highway into separate roadways for changes in traffic parameters. The user must define the traffic volumes and speeds for each roadway. However, a set of rules was built to define the traffic speed on ramps. The speed is determined on the basis of AASHTO guidelines (*11*) by the shape of ramp (directional, semidirectional, or loop), the type of ramp (on, off, or interchange), and the presence of traffic control devices at the end of the ramp.

The system also provides advice to assist the user in further breaking down the highway system into more roadways on the basis of ground cover conditions. For instance, the system suggests to the user to divide a modeled roadway into two or more shorter roadways when the surface covering conditions between this roadway and the receivers vary more than 25 percent, such as at a large paved area or at a large water-covered site surrounded by a grass-covered surface. The use of shorter roadways permits the ground absorption factors (alpha factors) to be defined more accurately.

Additionally, each roadway needs to be broken into a number of segments. A 400-ft length for each roadway segment is typically used as a default by the experts consulted during knowledge acquisition and is therefore initially suggested to the user by the system. The user may also specify other segment lengths. These lengths are then used as starting points by the module as it begins the process of dividing the roadways into segments and computing (x,y) coordinates for all endpoints. The system uses the information from the centerline module and also inquires about vertical curves using a maximum allowable offset elevation of 2 ft between the actual curve and the STAMINA roadway segment in its decisions.

Design Sites Module

One philosophy incorporated into the knowledge base is that each side of the highway should be analyzed as a separate design site. Basically, the rules used in this module are determined by the restrictions or limitations of the STAMINA 2.0 program. If the proposed numbers of receivers or roadways in a data file are greater than the upper limits of STAMINA 2.0, the system will help the user to divide the data file into smaller files.

Other reasons to divide a noise analysis site into several design sites are (a) to save computation time for each STAMINA run and (b) to simplify noise barrier design and alpha and shielding factors selection. The system has a set of rules to help the user to define the range of main roadway system (length of roadways beyond the end receivers) and to determine if any ramps that may be present should be included in the file for a design site (essentially on the basis of ratios of ramp traffic to mainline traffic).

Barriers Submodule

After the design sites are defined, barrier locations and baseline heights are determined. Figure 2 indicates the process for both barrier design and alpha and shielding identification. Although these two tasks are conducted in one module, their rules will be discussed separately. The system offers a capability beyond the simple creation of properly formatted barrier data for the input file. It actually performs an initial barrier location and height analysis. This analysis was not meant to replace the design process using OPTIMA but to provide the user with an intelligently determined starting point.

Longitudinal Location

The first step followed by this module is to determine the longitudinal location of the endpoints of all barrier segments relative to the roadways. The second step, discussed in the next section, is to determine the lateral (cross-sectional) location of the barrier points. The barriers are initialized to match with the endpoints of the defined roadways. In many cases, the roadways and barriers are parallel to each other. If the endpoints of each roadway are matched by barrier endpoints, there is a reduction in the chances of making errors such as creating an unrealistic low point in the barrier top on a crest vertical curve or crossing a barrier over a roadway. However, in most cases, it is useful to define the length of a barrier segment to be shorter than that of a roadway segment. Shorter segments allow the user to fine-tune the barrier height during the OPTIMA design process. A common length applied by human experts is 100 ft. The system also checks with the user to see if highway bridges are present in the analysis area. Because a barrier wall built on a bridge may require special structural support or use of lighter-weight materials, it is useful to delineate these areas in the definition of the noise barriers. Therefore, the user has the opportunity to insert new barrier section points for bridges.

The program then automatically generates the longitudinal location of each barrier section point using the 100-ft default value or different user-supplied value. Extra barriers may also be generated if overlapped barriers are needed for locations such as an interchange area with barriers along the ramp as well as in the gore area between the mainline and the ramp. The rules used for calculating the endpoint location of a barrier between a ramp and a main roadway are based on the merging sight distance requirements cited by AASHTO (*11*).

Lateral Location

The second barrier endpoint determination problem relates to the best lateral offset location from the road for a given barrier point. The decision on the location of this point is related to the needed attenuation, and as a result, the needed barrier height above existing ground. The first step in this process is for the user to supply an insertion loss (IL) design goal. For receivers located more than 200 ft from a noise source, the user-supplied IL is revised downward by the system because, in practice, the more distant receivers will experience less noise reduction for a given barrier design than the

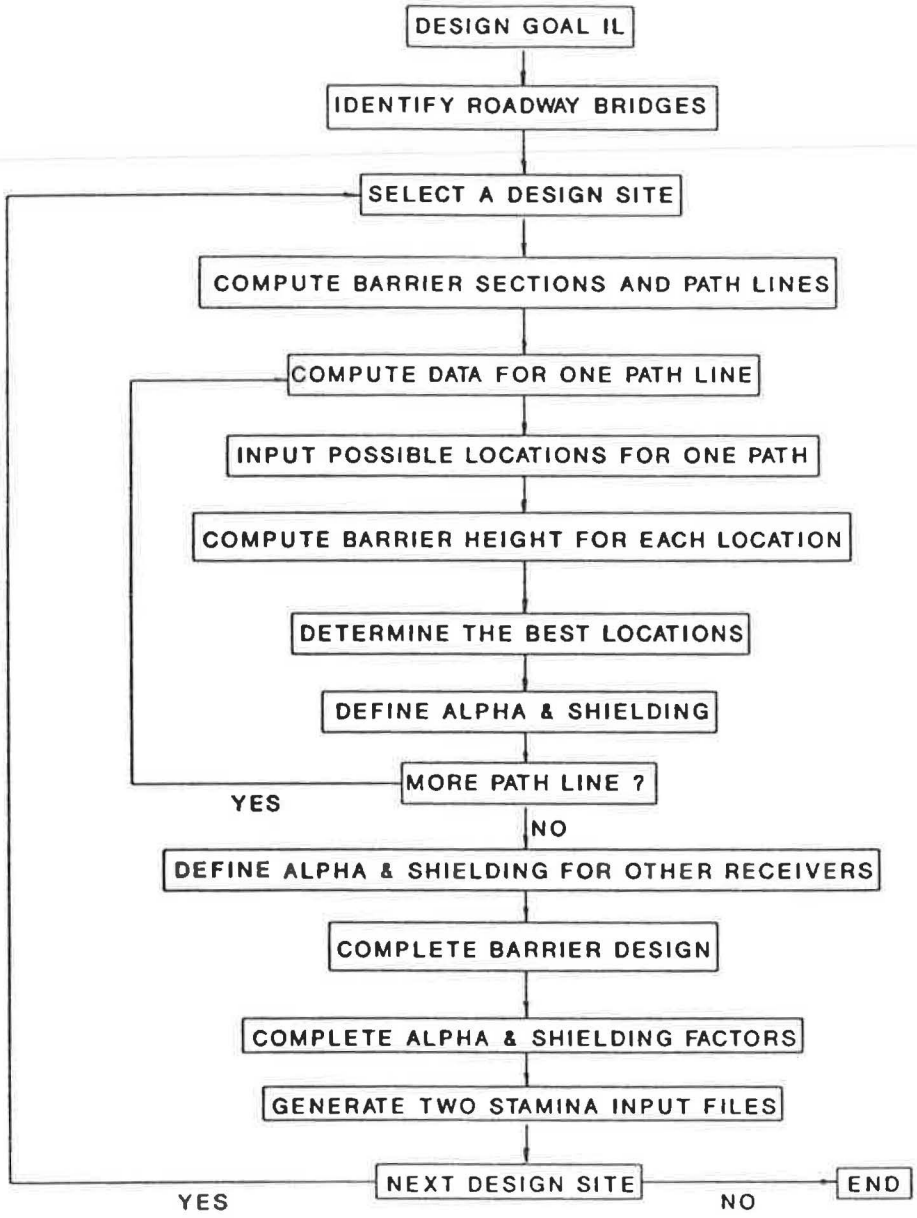

FIGURE 2 Barrier analysis procedure used by system.

closer receivers (for which the design is generally being done). The purpose in choosing a design goal during STAMINA input file creation is to give the system information to use in selecting an initial barrier location and baseline height.

The system then determines a number of paths representing receiver-source pairs, as shown in Figure 3. For all but the end receivers, a path is the perpendicular offset line from one of the first row receivers to the centerline. However, for both ends of a design site, several extra paths are generated to extend the barrier design to the end of the modeled roadways. The path of the first (and last) receiver-source pair runs from the nearest end of the centerline in the design site to the end receiver with the longest offset distance as shown in Figure 3. This receiver may not be in the first row. If not, an additional path is generated by connecting the end receiver of the first row with the corresponding centerline endpoint.

For each receiver-source pair, the offsets and elevations of the receiver and the sources, which include near lane, far lane, and ramp lane (if existing), are extracted from the previously created data base. The designer is asked to examine the highway plans to input the offsets and z coordinates for all potential barrier locations along each path. Some guidelines are provided for this assignment. Again, this procedure was established with the thought of ultimate transition to automated interface with a CAD system.

Based on an algorithm developed in this research, the system then calculates the barrier baseline heights for all the barrier locations entered by the user for each path. The basic concept of this algorithm is to determine the required break height at each barrier location for the needed barrier attenuation (on the basis of a heavy truck source), which is determined by the IL entered by the user, as explained next.

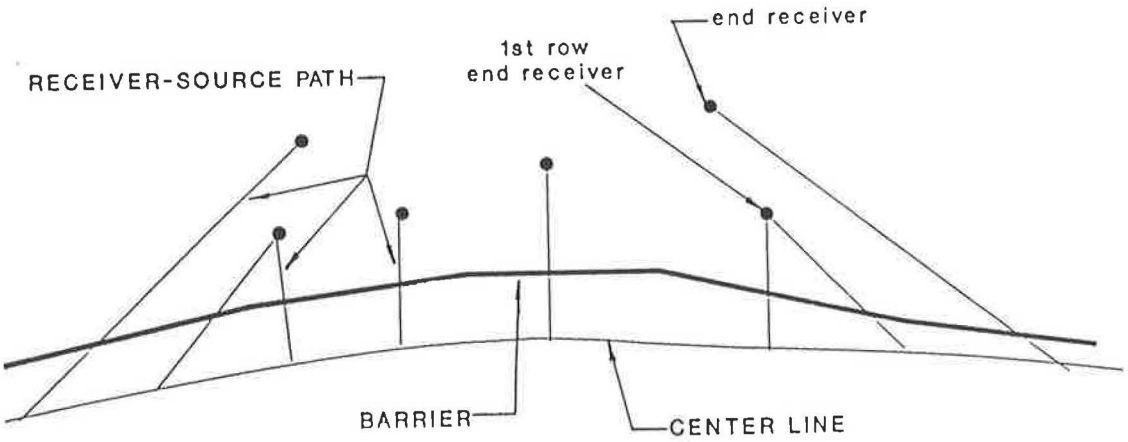

FIGURE 3 Plan view of paths used in determining initial barrier location and height.

The first step is to compute two line-of-sight (L/S) functions, one from the near lane and one from the far lane, and their distances (C) to the receiver (see Figure 4). Then the barrier attenuation for each L/S is determined. Because the attenuation caused by soft ground covering may be lost due to the insertion of a barrier, the barrier attenuation used in this analysis is set to be 2 dB higher than the IL goal if the receiver is located up to 200 ft from a noise source (*9*). The effects of distance in reducing attenuation are then introduced to adjust the IL for the receivers located more than 200 ft from a noise source. The barrier attenuation used for barrier break height calculation is determined by the following equations:

For $C < 200$ ft,

$$A_0 = \text{IL} + 2 \tag{1}$$

For $200 < C < 500$ ft,

$$A = A_0 + 10 \log [100/(C - 100)] \tag{2}$$

For $C > 500$ ft and $A_0 \leq 12$ dB,

$$A = 4 \tag{3}$$

For $C > 500$ ft and $A_0 > 12$ dB,

$$A = A_0 - 8 \tag{4}$$

where A_0 is the barrier attenuation in decibels for a path length less than or equal to 200 ft and A is the barrier attenuation in decibels for a path length longer than 200 ft.

It needs to be emphasized that these attenuations are not being recommended for use in barrier design. Rather, they are being used by the program to determine a reasonable set of baseline barrier heights in the STAMINA file for subsequent design by the user.

The needed path length difference δ for a desired barrier attenuation may be approximated as follows:

For $A < 5$ dB,

$$\delta = 0 \tag{5}$$

For $5 \leq A \leq 9$ dB,

$$\delta = 10^{(-2.6154 + 0.2564A)} \tag{6}$$

For $9 < A \leq 15$ dB,

$$\delta = 10^{(-1.6536 + 0.162A)} \tag{7}$$

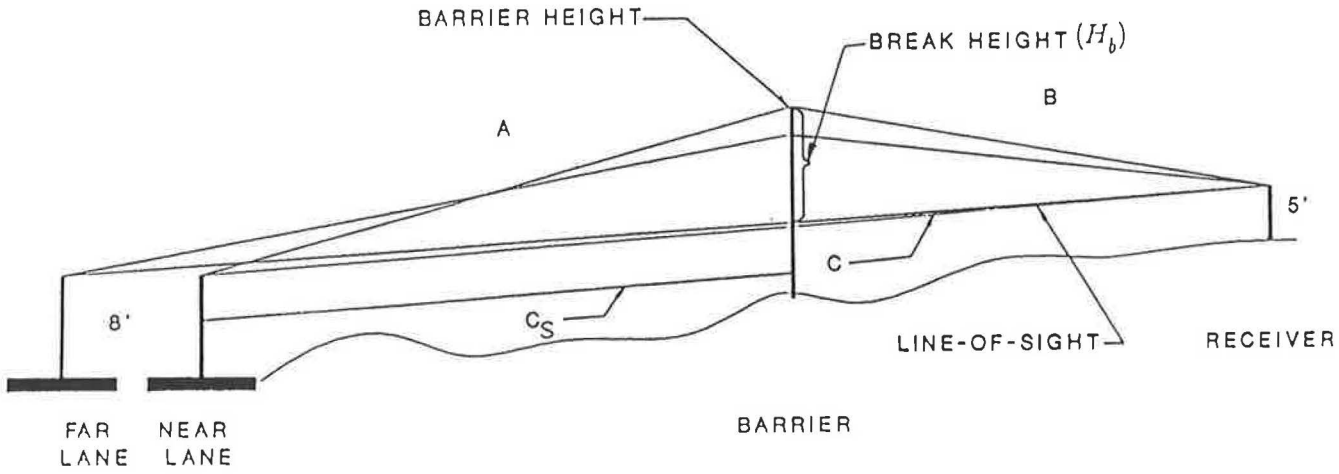

FIGURE 4 Section view for source-barrier-receiver paths.

In barrier analysis for a flat (at-grade) site, the location that provides the least path length difference for a given barrier height is the midpoint of the path. Therefore, the midpoint was used as a reference point for calculating the required break height $(H_b)_r$ which is the barrier height above the L/S line (see Figure 4). Because δ (equal to $A + B - C$ in Figure 4) can be calculated by Equations 5 to 7, the break height may be approximated as

$$(H_b)_r \approx [(\delta C)/2]^{1/2} \quad (8)$$

The break height for any barrier location other than at the midpoint that results in the same path length difference as the midpoint can be approximated by the following equation (*12*):

$$H_b = 2\,(H_b)_r\,[(C_s/C)(1 - C_s/C)]^{1/2} \quad (9)$$

where C_s is the distance between barrier and source (see Figure 4). After testing this approximation method with various C_s/C ratios, it was found that Equation 9 was only good for a C_s/C ratio from 0.1 to 0.9. If the ratio was less than 0.1 or greater than 0.9, a good approximation for the break height would be produced by using the value associated with a C_s/C ratio of 0.1 or 0.9, respectively. Through this procedure, the system determines the needed break height for a given barrier location and ground elevation. Then, the baseline barrier height and top elevation are calculated using the break height, the L/S height, and the ground elevation of each location.

For each barrier location, the calculations are performed separately for both near and far lanes, as they represent different sources. The final barrier height for a given barrier location is determined by comparing the results for the two sources. In terms of acoustical performance, for a given path the best location for a noise barrier is the location with the lowest barrier height that provides the needed attenuation. Nevertheless, some modifications in that location may be necessary to ensure barrier continuity in transition areas (e.g., going from a cut section to a fill section) or to address other concerns such as drainage or special construction requirements. Thus, for each path, the barrier results calculated by the system for the other lateral locations are also stored in a data base.

The process is repeated for all the paths determined by the system. After this initial barrier analysis is completed, the best barrier heights for all paths determined by the system are summarized in a file. The user may verify this baseline barrier design by a printout of this data file. The user may also modify the design manually by following the guidelines provided by the system.

Height Adjustment

After the verification, a data manipulation process is used to adjust the heights resulting from the analysis. For each barrier, the number of paths and resultant barrier heights generated by the system are usually greater than one. Thus, the first step in adjusting the barrier heights is to coordinate the baseline height for each barrier. This is the initial baseline height for the STAMINA 2.0 input file. A first simple rule of thumb by which to determine the baseline height for each barrier is to use the tallest barrier height required by one of the paths for this barrier. For more complicated cases, if the difference in baseline heights between two consecutive path lines is greater than 6 ft, the barrier is divided into two separate barriers.

After this adjustment of the baseline heights, a second set of adjustments is made by the rules presented in Table 1 to give a more standardized look to the heights. In addition to the baseline height, associated height increments for the STAMINA file are also presented in this table. The number of increments and the increment sizes listed in the table allow the user to have maximum changes for barrier heights. These values are also commonly used by the human experts as the initial values in their designs.

Two data files are produced by this data manipulation process, one containing no noise barriers other than the natural

TABLE 1 RULES FOR REFINING BARRIER HEIGHTS AND DEFINING HEIGHT INCREMENT

Computed Baseline Height (ft)	Refined Baseline Height (ft)	Number of Increments	Increment Height (ft)
0	0	0	0
0-6	6	3	1
6-15	6,9,12,15	3	2
15-20	15,18,20	3	3
20-30	20	3	3
30 or more	30	3	4

terrain (i.e., ground line barrier), and the other containing the results of the initial barrier height analysis, namely the baseline barriers with height increments for production of the acoustics file for use by OPTIMA.

Alpha and Shielding Factors Submodule

Figure 2 shows that alpha and shielding factors are assigned by the same module that does the barrier analysis. The rules presented in the FHWA traffic noise prediction model report (*7*) for determining alpha and shielding factors are applied by the system as general guidelines. To apply these rules, the user first defines a series of paths for certain receiver-source pairs. The pairs include each receiver and the roadway directly in front of it; some extra paths are defined for the end receivers for extending the design to the end of the design site, as was done in the barrier analysis. The designer then only has to assign alpha and shielding values for this subset of all possible receiver-source pairs. Rules are built in to enable the system to generate a complete alpha or shielding matrix with this relatively limited information.

Figure 5 indicates by solid lines the paths for which the user must supply factors. The dashed lines (which are shown for Receiver 2 only) indicate the other receiver-source pairs that will have their factors automatically generated by the program. These factors are assigned by the program through an examination of the factors for the user-specified path lines that cross the path line of interest. The results of this submodule are then combined with all the data generated in the preceding steps to create a STAMINA 2.0 input file for one or more design sites.

TESTING AND EVALUATION OF THE SYSTEM

As mentioned earlier, the major goal of this study is to provide a good input file with which to begin the noise analysis. The final design results using a program like OPTIMA will be strongly dependent on the quality of this initial file. A good initial input file should at least contain all correct information to run STAMINA and to start a noise analysis, reducing iterative modifications of the STAMINA input data. As it turned out, the initial barrier heights produced by the system could be close to the final design using OPTIMA, especially for at-grade sites, an unexpected benefit of the results of this research.

During programming, the system was verified and evaluated step by step in order to ensure that the information was complete and accurate for further development. Verification cannot be accomplished, however, by using a case with a simple geometric configuration. Thus, the overall performance of the system was tested against two full-scale design projects that were completed by two domain experts at Vanderbilt University. A full presentation, discussion, and documentation of the results of the evaluations are available for study (*4*).

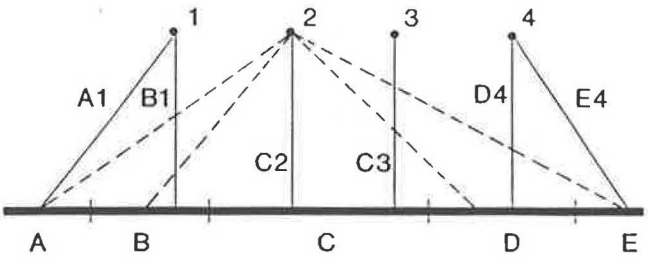

FIGURE 5 Plan view of roadway-receiver pairs for alpha and shielding factor identification.

The first project was a 1.5-mi section of the planned six-lane I-68 in Bowie, Md. Two design sites—the north and south sides of the project—were modeled by both the experts and the system. The second design project was the existing 10-lane I-95 in northern New Jersey, where the goal was to design noise barriers to be added alongside the existing highway. Four design sites were modeled for this project: two adjacent areas to the south and two adjacent areas to the north. The two northern areas were chosen for system evaluation (*4*). The design sites were neither simple nor straightforward. Collectively, they included such features as ramps, cut, fill and at-grade sections, fairly steep roadway grades, and a mixture of hard and soft ground cover. In order to compare the results of the system's files to those of human experts, virtually the same receiver and traffic data used by the experts were used when running the system. All the other results were determined according to the guidelines provided in the system or generated by the system directly.

In the testing and evaluation, the design accomplished by the human experts represented the final results arising from a series of iterations, which include modifying the STAMINA input files as well as running the OPTIMA design program. The results of the knowledge-based system, on the other hand, were generated directly by the system without any subsequent modification to the STAMINA input file and prior to any final design with OPTIMA. The usefulness as well as the limitations of the knowledge-based system can be illustrated through the comparison of the human experts' final OPTIMA design with the system's initial STAMINA design.

It is very difficult to specify quantitative benchmarks to evaluate system performance. In all cases, the system produced syntactically correct files that could be directly run with STAMINA. On a second level of evaluation, the STAMINA files produced by the system were very much like those produced by the experts. Similar numbers of roadways and barriers were defined and the locations of these features were comparable. This similarity was expected because, assuming correct programming, the heuristics used were the same. However, the system has not yet been compared to designs of other experts. The similarity of the files would depend very much on the similarity of the heuristics used by each set of experts. Different experts often do create STAMINA input files in different manners using different rules. These files should, however, lead to similar sound level results. The experts just approach the goals in different ways.

When differences between the system files and the experts' files existed, they involved the barrier heights for the most part. In one case, the user working with the system read a different set of ground line elevations from the contour mapping than did the experts. Until a fully integrated CAD system interface is developed to automatically read elevation data, this specific problem will plague any method of creating STAMINA files, including all existing digitizer preprocessors.

In a second case, the experts had taken their final acoustically optimized results and increased barrier heights in certain areas beyond what was needed to give the top of the wall a smooth transition profile.

In a third case, the road was on a grade and changed from fill to a deep cut, with the houses on an even steeper grade along the top of the cut. The height selection rules in the system for all but the end sections of a barrier are based on perpendicular paths between the source and receiver. On grades, the user needs to be concerned about sound leaks over the barrier top from oblique angles. Revision of the barrier height selection mechanism would be needed to cover these situations. However, even these differences need not be viewed as fatal because the resultant file could indeed be run by STAMINA 2.0 to produce the acoustics output file for subsequent use with the OPTIMA design program.

To illustrate the performance of the system, the results for one of the design sites (the south side of I-68) will be discussed. Figure 6 is a map of the site. This project area included the main lanes of I-68 with ramps for an interchange at the west end. The road passed through rolling terrain, such that it was depressed for certain sections, at grade for others, and on fill elsewhere. Figure 7 provides two plan view plots of the STAMINA files for this site. The lower plot was generated from the file created by the system (and its human user), whereas the upper plot was created from the file developed by the human experts. The upper plot illustrates that two possible barrier lines were assigned by the human experts for the west (left) end of the site. The experts included both lines because they could not tell, a priori, which would be better. However, in the knowledge-based system, various barrier locations were evaluated according to the user-supplied IL goal, and only one was chosen by the system for the input file. Evaluation of the STAMINA results confirmed that this barrier location was indeed the correct choice. As a result, only one barrier line needed to be added to the STAMINA input file when using the system.

Figure 8 compares elevations of the ground line barriers produced by the human experts and the system (Lines C and D, respectively), and the barrier top elevations for each (Lines A and B, respectively). The first difference to note deals with the ground line elevations between Stations 18 and 28. The contour mapping in this area was read differently by the user of the system and the experts. No system can deal with this type of human error: judging the correctness of what otherwise would seem to be reasonable elevations. An enhancement to allow the system to read CAD roadway design files would eliminate this particular type of problem. Because the system then selected barrier heights based on IL goals, the difference in ground elevations was largely responsible for the resulting difference in barrier top elevations.

The data presented in Table 2 help to illustrate system performance. The first five columns show STAMINA 2.0 results for each receiver based on the two input data files created by the system [ground line barriers only (WITHOUT BARR) and baseline noise barriers (WITH BARR)]. The difference in the predictions is shown in the IL column. The next four columns show the OPTIMA results for the human experts' design. The last three columns of the table compare each set of results for the three quantities.

Because of the ground line and barrier top elevation differences caused by the human data entry error between Stations 18 and 28, both the without-barrier and with-barrier noise levels of the receivers located in this range (RS18 through RS28 and S1820 through S2760) were predicted to be higher by the system than by the human experts. Note, however, in the last column of Table 2, that despite the problem with the correct ground elevation, there were only small differences in IL for most of the receivers between Stations 18 and 28.

Because different barrier ground elevations were used in certain areas by the two designs, as shown in Figure 8, it is not entirely appropriate to evaluate the results in terms of the actual wall heights. However, the overall comparison of ILs indicates that the system achieved good agreement with the human experts' design. As presented in Table 2, the IL differences of all the receivers, except for the first three, were 1.5 dB or less. The IL differences of the first three receivers were caused by different barrier designs. The system analyzed the need to extend a barrier along the roadway to Station 11 in an attempt to meet the design goal IL at the first three receivers. However, there was a creek between Stations 14 and 18 and the human experts designed the barrier to stop at

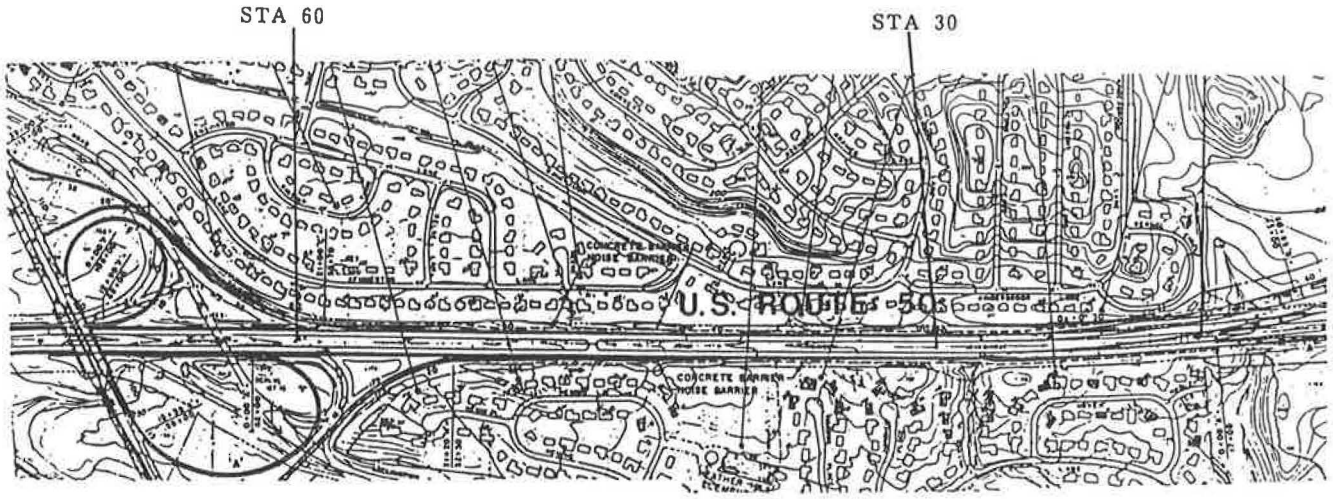

FIGURE 6 I-68 between Maryland Routes 197 and 301.

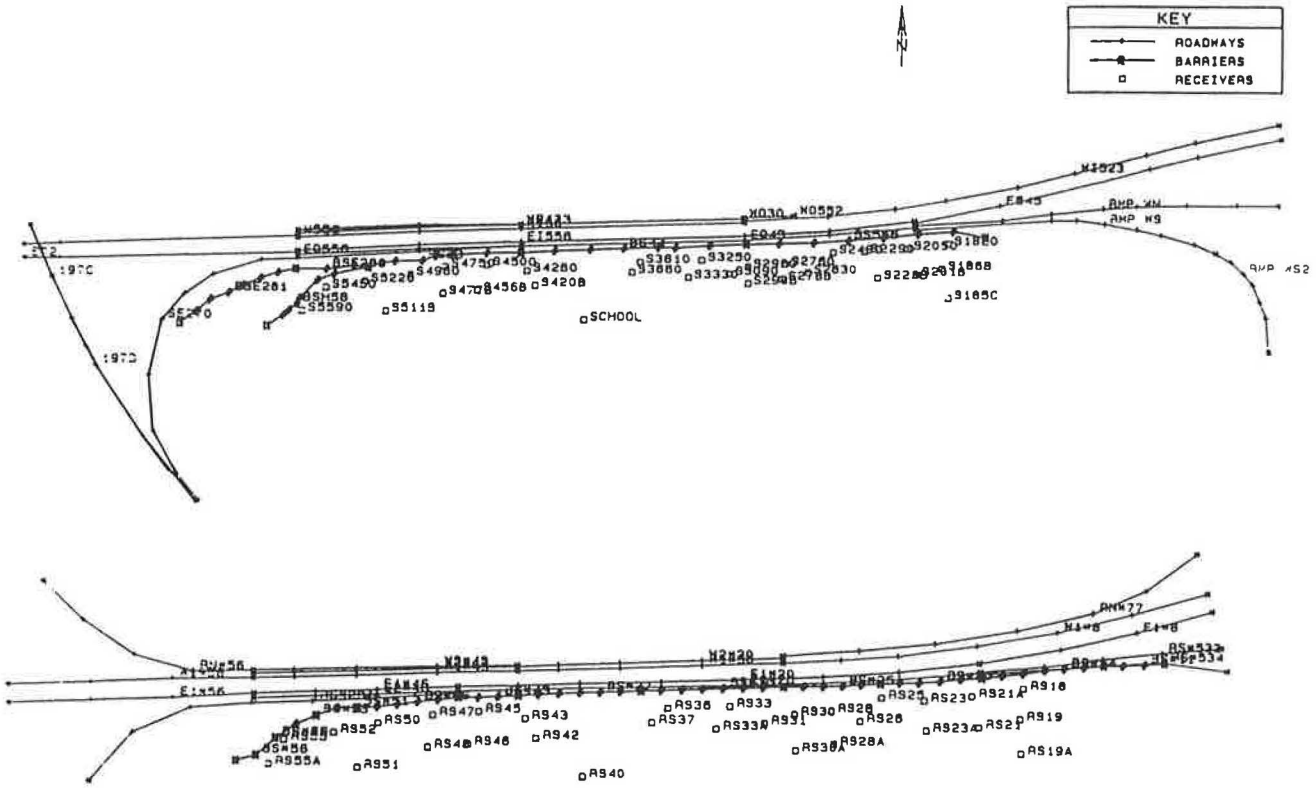

FIGURE 7 I-68S plan view plots of files created by human experts (*top*) and by knowledge-based system (*bottom*).

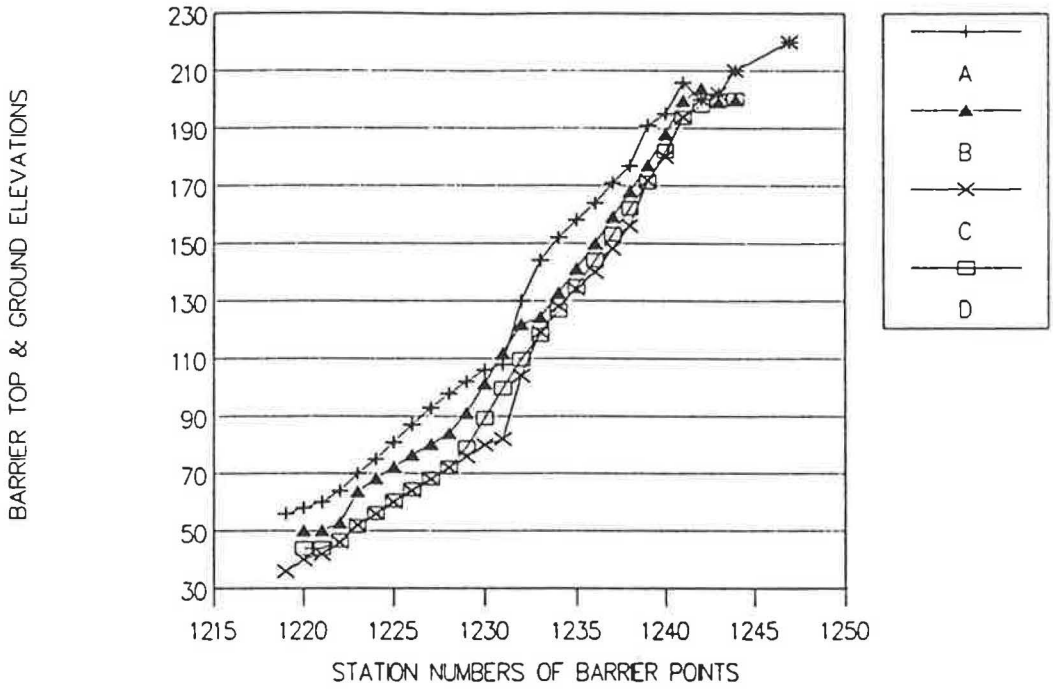

A: Barrier top elevations designed by human experts

B: Barrier top elevations designed by expert system

C: Ground elevations defined by human experts

D: Ground elevations defined by expert system

FIGURE 8 Profile of initial barrier selected by system for STAMINA and final OPTIMA barrier designed by human experts.

TABLE 2 COMPARISON OF SYSTEM AND HUMAN EXPERT RESULTS FOR I-68S CASE

(A) EXPERT SYSTEM'S DESIGN					(B) HUMAN EXPERT'S DESIGN				DIFFERENCES BETWEEN A & B		
RECEIVER ID	OFFSET (FT)	WITHOUT BARR (dB)	WITH BARR (dB)	IL (dB)	RECEIVER ID	WITHOUT BARR (dB)	WITH BARR (dB)	IL (dB)	WITHOUT NO-BARR (dB)	WITH W/BARR (dB)	IL (dB)
RS18	200	71.7	61.1	10.6	S1820	68.2	59.9	8.3	3.5	1.2	2.3
RS19	350	65.7	58.5	7.2	S186B	65.5	60.1	5.4	0.2	-1.6	1.8
RS19A	520	61.5	55.8	5.7	S185C	62.5	58.9	3.6	-1.0	-3.1	2.1
RS21	360	64.0	56.7	7.3	S201B	63.0	56.4	6.6	1.0	0.3	0.7
RS21A	200	71.9	62.4	9.5	S2050	70.3	60.5	9.8	1.6	1.9	-0.3
RS23	190	72.1	61.7	10.4	S2290	70.8	60.1	10.7	1.3	1.6	-0.3
RS23A	340	64.3	56.0	8.3	S223B	63.0	55.3	7.7	1.3	0.7	0.6
RS25	160	73.7	62.9	10.8	S2480	71.7	61.2	10.5	2.0	1.7	0.3
RS26	270	69.1	60.7	8.4	S2630	67.9	59.5	8.4	1.2	1.2	0
RS28	210	70.5	60.4	10.1	S2760	68.5	59.1	9.4	2.0	1.3	0.7
RS28A	375	61.3	52.8	8.5							
					S278B	63.5	54.8	8.7			
					S298B	63.8	55.4	8.4			
RS30	220	70.2	61.0	9.2	S2980	69.6	59.9	9.7	0.6	1.1	-0.5
RS30A	400	61.0	53.2	7.8							
RS31	260	66.1	58.3	7.8	S3090	68.5	60.3	8.2	-2.4	-2.0	-0.4
RS33	170	72.4	63.7	8.7	S3250	71.4	61.8	9.6	1.0	1.9	-0.9
RS33A	280	65.2	56.6	8.6	S3330	67.9	58.8	9.1	-2.7	-2.2	-0.5
RS36	170	71.8	61.3	10.5	S3610	72.2	60.4	11.8	-0.4	0.9	-1.3
RS37	240	66.6	57.5	9.1	S3660	70.3	60.2	10.1	-3.7	-2.7	-1
RS40	500	64.7	57.2	7.5	SCHOOL	61.6	53.9	7.7	3.1	3.3	-0.2
RS42	300	65.3	56.9	8.4	S420B	65.2	56.1	9.1	0.1	0.8	-0.7
RS43	200	70.9	61.0	9.9	S4260	70.3	59.8	10.5	0.6	1.2	-0.6
RS45	160	72.2	61.9	10.3	S4500	71.6	59.8	11.8	0.6	2.1	-1.5
RS46	320	64.4	56.4	8.0	S456B	64.1	55.0	9.1	0.3	1.4	-1.1
RS47	170	71.7	61.9	9.8	S4750	70.5	60.1	10.4	1.2	1.8	-0.6
RS48	330	63.9	56.3	7.6	S477B	62.7	55.0	7.7	1.2	1.3	-0.1
RS50	200	66.9	62.0	4.9	S4960	66.5	60.2	6.3	0.4	1.8	-1.4
RS51	420	62.7	55.9	6.8	S511B	61.2	54.8	6.4	1.5	1.1	0.4
RS52	240	67.5	59.2	8.3	S5220	66.9	57.9	9.0	0.6	1.3	-0.7
RS55	270	69.1	60.8	8.3	S5450	69.0	62.0	7.0	0.1	-1.2	1.3
RS55A	390	66.3	62.9	3.4	S5590	66.1	62.9	3.2	0.2	0.0	0.2

the creek at Station 18 for nonacoustical reasons. This nonacoustical concern could have been taken care of by a user of the system during a subsequent OPTIMA design session.

Two other receivers with significant differences in the predicted without-barrier noise levels are RS37 and RS40. In the system's design, RS37 was defined as a second row receiver and a 3-dB building shielding factor was introduced. The human experts, however, did not assign shielding to this receiver in their design. Conversely, for RS40 the human experts considered building shielding whereas the system did not. The situation of a partially shielded second-row receiver needs more consideration in future rule refinement with the system.

It is again important to note that the human expert design is the result of using the OPTIMA program whereas the knowledge-based system has only run the STAMINA program. It was not the objective of this work to have the system eliminate the use of OPTIMA, but to provide a good starting point for an engineer to use OPTIMA. The fact that the system gave initial results comparable to the humans' final OPTIMA results is an interesting and important side benefit of this work and supports the conclusion that the system is providing good results.

It is also important that the results of the knowledge-based system are obtained on the basis of the inputs provided by the user in response to the requests from the system. Thus, the user of the system, as it currently stands, is an integral part of the design system, and the accuracy of the responses is important for good performance of the system. The user must be able to react to the system's messages to read certain data from the plans and enter the data into the computer. This relatively extensive user interaction is a current weakness, but the system is still a substantial improvement over a person working without any type of input enhancement tool.

In general, comparison of the results presented in these figures and the table indicates that the knowledge-based system was able to create a good input file for a case as com-

plicated as this I-68 case. Both files consisted of approximately 350 lines of data. With the system, the STAMINA files were completed by one of the authors in about 8 hr. Producing this same file without the help of a preprocessor (or a digitizer) would easily take 2 person-days or more. With certain exceptions, the data produced by the system were accurate. Moreover, the insertion losses provided by the initial barrier heights determined by the system were comparable in some instances to the human experts' final design, which was accomplished using OPTIMA.

FINDINGS

The following findings are summarized from all the cases studied in this research:

1. The centerline module handled all cases without any conversion errors and provided the user a much more convenient scheme for data acquisition (i.e., station number coupled with offset).
2. For a fairly uniform site, it was found that the receivers could be generated automatically by the system. Obviously, for a large-scale project, this function could save a great deal of time in data input. This function was tested in one of the cases to ensure its accuracy.
3. The roadway configurations determined by the system were found to be as good as those modeled by the human experts. This finding was tested by the existing conditions of all the cases.
4. In general, the good agreement of the no-barrier predicted levels indicates that the system was properly choosing the best lateral location for the ground line barrier. Moreover, if more than one ground barrier exists in a receiver-source path (i.e., rolling terrain), the system could detect the location that would provide most nonbarrier shielding for the no-barrier model case, which is important in accurately predicting the no-barrier levels. However, the system has no means of judging the accuracy of a user-specified elevation.
5. For cases with complicated surface absorption conditions or building shielding, it was found that the system could generate the alpha and shielding matrices with limited information in a much shorter time than the human experts, and provide acceptable results in nearly all cases.
6. For a modeling area without steep roadway grades, the barriers designed by the system were found to be good enough not only to be used for a starting point for the STAMINA program but also to be comparable with the final designs accomplished by the human experts using OPTIMA. Thus, with the site as modeled by the system, the iterative design steps using OPTIMA could be reduced significantly.
7. For a site with steep roadway grades, the initial barrier specified by the system will not be as good as one specified for a roadway on a slight grade; however, the system still created a valid STAMINA input file. The rules used in choosing source-receiver pairs for the barrier attenuation analysis would have to be expanded to cover oblique angles to address this problem.
8. For sites with all receivers beyond 500 ft from the noise source, it was found that the design goal strategy for selecting an initial barrier height may not be suitable. However, in general, these receivers are rarely the controlling factor in highway noise control projects, and trying to accommodate this situation probably should have been beyond the scope of the system. Nonetheless, the system still produced an executable STAMINA file.
9. The memory size of the 80286 machine used in system development is a limiting factor for future enhancements. Useful future work probably should be done on an 80386 machine with expanded memory.

CONCLUSION

The system described in this research was developed to assess the potential for a knowledge-based approach for automating file creation for traffic noise modeling. The specific goal was to assist a user in creating a good initial input data file for the STAMINA 2.0 traffic noise prediction program in less time than without use of an input enhancement tool. The results have demonstrated that the system and its user can indeed produce large input files for relatively complex situations.

However, the system should still be considered in an operational prototype stage and some improvements would be helpful. These include (a) an expanded barrier height algorithm to use oblique analysis paths in addition to perpendicular paths, (b) more rules for identifying the factors for shielding and ground absorption, and (c) an expanded interactive environment that might include a graphic display feature for data presentation and more help information for the inexperienced designer.

Additionally, the full time-saving benefits of a knowledge-based approach to assistance in file creation will probably not be obtained until the system is interfaced at least with a digitizing system. Even then, the possibility of human error remains in entering elevation data, a problem faced by all current preprocessors. Ultimately, interface with a CAD-based roadway design system would eliminate many of the situations where human error could occur. Nonetheless, the system does not, will not, and should not eliminate human participation in the highway noise analysis or noise barrier design process.

REFERENCES

1. G. E. Anderson, E. Cuoco, and C. W. Menge. The Barrier Cost Reduction Program: A New Tool to Reduce Highway Noise Barrier Costs. In *Proc., Conference on Highway Traffic Noise Mitigation*, TRB, National Research Council, Washington, D.C., 1978.
2. W. Bowlby, J. Higgins, and J. Reagan (eds). *Noise Barrier Cost Reduction Procedure, STAMINA 2.0/OPTIMA, User's Manual.* FHWA-DP-58-1, FHA, U.S. Department of Transportation, 1982. (Based on C. W. Menge. *User's Manual: Barrier Cost Reduction Procedure, STAMINA 2.0 and OPTIMA.* Report No. 4686, Bolt, Beranek, and Newman, Cambridge, Mass., 1981.)
3. R. A. Harris, L. F. Cohn, and W. Bowlby. Designing Noise Barriers Using the Expert System CHINA. *Journal of Transportation Engineering*, Vol. 113, No. 2, ASCE, New York, 1987.
4. H. M. Sung. *An Expert System for Highway Noise Analysis.* Doctoral Dissertation, Vanderbilt University, Department of Environmental and Water Resources Engineering, Nashville, Tenn., 1989, 290 pp.
5. H. M. Sung. *An Expert System for Traffic Noise Modeling.* Pre-

sented at the Annual Meeting of the Air and Waste Management Association, Anaheim, Calif., 1989.
6. W. Bowlby. *Expert Systems for Traffic Noise Analysis*. Invited lecture at the International Seminar on Road Traffic Noise, Centre Scientifique et Technique du Batiment, Grenoble, France, 1988.
7. T. M. Barry and J. A. Reagan. *FHWA Highway Traffic Noise Prediction Model*. FHWA-RD-77-108, FHWA, U.S. Department of Transportation, Washington, D.C., 1978.
8. B. A. Kugler, A. G. Commins, and W. J. Galloway. *NCHRP Report 174: Highway Noise: A Design Guide for Prediction and Control*. TRB, National Research Council, Washington, D.C., 1976.
9. M. A. Simpson. *Noise Barrier Design Handbook*. FHWA-RD-76-58, FHWA, U.S. Department of Transportation, Washington, D.C., 1976.
10. *VP-Expert, Rule-Based Expert System Development Tool*. Paperback Software International, Berkeley, Calif., 1987.
11. *A Policy on Geometric Design of Highways and Streets*, AASHTO, Washington, D.C., 1984.
12. K. M. Eldred et al. *Noise From Traffic and Noise Barrier Performance: A Prediction Technique*. Construction Engineering Research Laboratory, U.S. Army Corps of Engineers, Technical Report N-178, Champaign, Ill., 1984.

Publication of this paper sponsored by Committee on Transportation-Related Noise and Vibration.

Barrier Overlap Analysis Procedure

V. LEE, S. SLUTSKY, E. KEN, R. MICHALOVE AND W. MCCOLL

Situations arise in which noise barriers are overlapped to accommodate highway entrance or exit ramps, service roads, local access roadways, underground utilities, or community desires regarding placement within the right-of-way. This arrangement of two parallel vertical barriers with an opening in between gives rise to the overlap noise barrier problem. The need to protect residential or institutional properties near the barrier opening led to the development of an analytical procedure to investigate the reflection-diffraction effects of overlapping barrier designs.

In many highway noise barrier designs, breaks are introduced in otherwise continuous noise barriers to accommodate entrance or exit ramps. Typically, a noise barrier along the highway is terminated at the ramp and then resumes on the service roadside, as shown in Figure 1. A break may be necessitated because of underground utilities or to provide access to shielded portions of the right-of-way. The presence of the break in an otherwise continuous noise barrier degrades barrier performance at receivers in the immediate neighborhood of the gap. To restore the integrity of the barrier, an overlap may be introduced to compensate for the presence of the gap. Problems that arise include how long the overlap should be and the amount of degradation due to the multiple reflection effect created between the overlapping barrier sections. The barrier overlap analysis procedure (BOAP) was developed to answer these questions.

A ray acoustics approach adopted to deal with the multiple reflection problem was combined with Maekawa's simple diffraction treatment for appropriate paths. Simplifying assumptions were made to provide an approximate solution of the problem. A FORTRAN version of BOAP was implemented on a PC for use as a supplemental noise barrier design tool in conjunction with STAMINA 2.0/OPTIMA (*1*) to achieve the most cost-effective barrier design.

ANALYSIS OF PROBLEM

To simplify the solution, the following assumptions have been made:

1. Barriers are vertical, parallel to each other and to the roadway,
2. Barriers are of equal height, and
3. Barrier edge diffraction arising during reflection is ignored.

V. Lee and E. Ken, Analysis & Computing, Inc., 82 N. Broadway, Suite 205, Hicksville, N.Y. 11801. S. Slutsky, 1611 George Road, Wantagh, N.Y. 11793. R. Michalove, Frederic R. Harris, Inc., 300 E. 42nd St., New York, N.Y. 10017. W. McColl, Environmental Analysis Bureau, New York State Department of Transportation, 1220 Washington Ave., Albany, N.Y. 12226.

It should be noted that these assumptions may be dropped if more comprehensive procedures (*2*) are used, but at the cost of considerably greater effort. In addition, the double diffraction effect of barriers can be ignored and replaced by the most effective barrier assumption (*3*) as is done in STAMINA 2.0.

As in the simple barrier case, the sound level at a receiver due to a roadway segment is the sum of contributions from the direct rays (if any) passing through the gap and the diffracted rays passing over the most effective barrier. For overlapping barriers, however, an additional contribution resulting from multiple reflections in between the barriers must be accounted for. This is done by using the method of images and rectified rays. The contribution due to multiple reflection can be calculated by summing over the contributions of the roadway segments to each of the image receivers in the rectified geometry. The summation process is carried out until a prescribed convergence criterion is met. The reachable paths from a roadway segment to an nth-order image receiver after n reflections in between the overlapping barriers or diffracted over the nth image barrier after $n - 1$ reflections may be classified into four ray path categories or cases.

Figure 2a shows the first category (Case A) of diffracted ray paths with $n - 1$ multiple reflections; the corresponding roadway configuration, with left and right semi-infinite overlap barriers, is shown schematically. The first image of the left barrier and the second ($n = 2$) image of the right barrier and the receiver are also shown. The angle to the normal from the nth image receiver to the lip of the nth right barrier is denoted by N. Similarly, the angle to the lip of the first image of the left barrier is denoted by U, and the angle to the lip of the left barrier is denoted by L. In this case, $L > N$, and those rays originating from the roadway segment opposite the angle D ($D = U - L$) would reach the nth image receiver after $n - 1$ multiple reflections and a diffraction over the nth image barrier.

In the bottom half of Figure 2a, both the physical and rectified (virtual image) paths are presented for a typical ray, for $n = 2$. Every crossing of an image barrier by the image ray corresponds to a reflection of the real ray by a real barrier, except for the final crossing, which may be a diffraction by the (upper) barrier edge.

Case B, the second category, is characterized by paths that not only involve multiple reflection followed by diffraction as in Case A, but also by paths that involve no diffraction, as shown in Figure 2b. In this mixed case, when $U > N$ and $N > L$, those rays originating from the roadway segment opposite the angle D ($D = U - L$) would reach the nth image receiver after $n - 1$ multiple reflections and a diffraction over the nth image barrier, and those rays originating from the roadway segment opposite the angle R ($R = N - L$) would reach

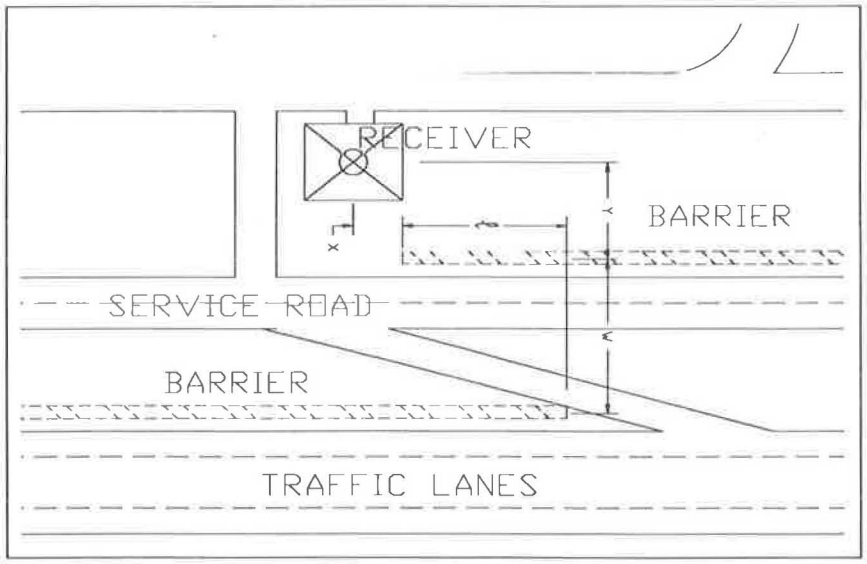

FIGURE 1 Overlap barrier at service road.

the nth image receiver after n multiple reflections in the rectified geometry, as shown in Figure 2b.

As the overlap shortens (Figure 2c), angle U is less than angle N, but greater than the vertex angle M to the lip of the $(n - 1)$th image of the right barrier (and $L > M$), pure multiple reflections occur (Case C2). Those paths originating from the roadway segment opposite the angle R ($R = U - L$) would reach the nth image receiver after n complete reflections. As the overlap shortens further, when $U > M$ and $L < M$, a partial multiple reflection category (Case C1) results (Figure 2d). Only that part of the roadway segment opposite the angle R ($R = U - M$) would have paths reaching the nth image receiver through n multiple reflections. No other reachable paths exist for multiple reflected rays.

It is easily seen that an overlap configuration consisting of a right bottom barrier and a left top barrier is but a reverse image of the problem shown. The preceding analysis and classification of the ray path construction led to the development of the following computational procedure.

PROCEDURE

Given a specific roadway-barrier-receiver geometry, the sound pressure level (SPL) at the receiver is computed by summing over the range of SPL values computed for the receiver and each of its images. For each receiver or its image receiver, the roadway contributions may consist of

1. The direct line-of-sight rays through the gap,
2. The simple diffracted rays over the left and the right barriers,
3. The multiple reflected rays from the overlapping barriers, and
4. The diffracted multiple reflected rays from the overlapping barriers.

Computation of the first two contributions is straightforward and can be modeled readily using STAMINA; computation of the last two contributions from the overlapping barrier sections may be greatly facilitated by applying the following formulation to the rectified geometry.

Let

x = horizontal distance from the receiver to the lip of the top right barrier,
y = perpendicular distance from receiver to the top right barrier,
w = width of the gap separating the barriers, and
l = length of the overlap section of the barrier (see Figure 1).

Then the ray classification angles N, M, U, and L may be readily computed for each image ($n \geq 1$) as follows:

$$\tan N = x/y$$

$$\tan M = x/(y + w)$$

$$\tan U = (x + l)/[y + (2n - 1)w]$$

$$\tan L = (x + l)/[y + (2n + 1)w].$$

The ray paths may be classified as

Case A:	$L > N$	$D = U - L$
Case B:	$U > N, N > L$	$D = U - N, R = N - L$
Case C2:	$L > M, U > M$	$R = U - L$
Case C1:	$U > M, M > L$	$R = U - M$

The computations for diffracted and reflected paths are based on the modified algorithms developed in the *FHWA Highway Traffic Noise Prediction Model* (*4*) as follows:

$$L_D = L'_{0i} + 10 \log \frac{N_i D_0}{S_i} + 10 (1 + \alpha) \log \frac{D_i}{D_0}$$

$$+ 10 \log \frac{D}{\pi} + \Delta_{\text{barrier}} - 25$$

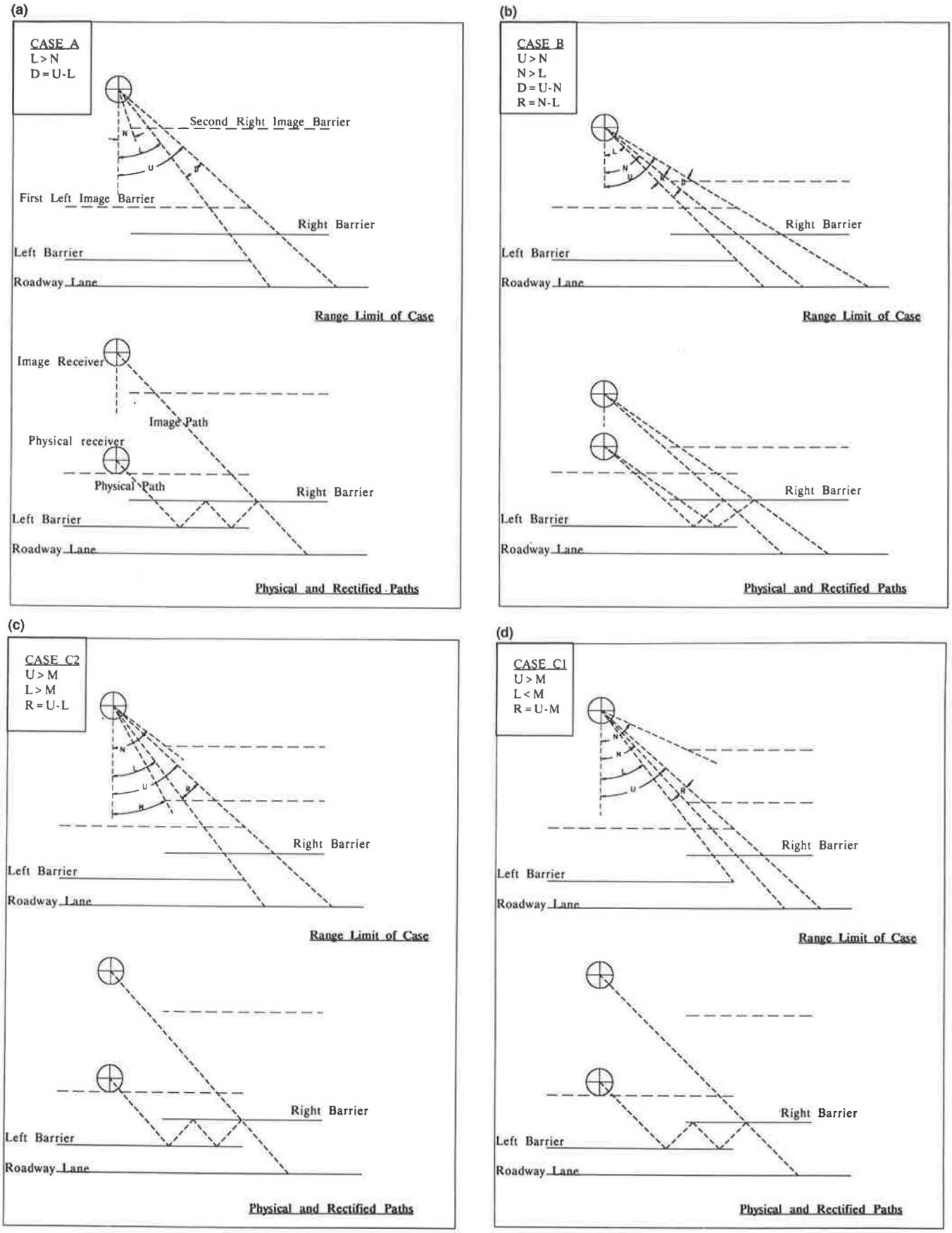

FIGURE 2 Ray geometries: a, diffracted multiple reflected rays; b, mixed multiple reflected rays; c, multiple reflected rays; d, partial multiple reflected rays.

$$L_R = L'_{0i} + 10 \log \frac{N_i D_0}{S_i} + 10 (1 + \alpha) \log \frac{D_i}{D_0} + 10 \log \frac{R}{\pi} - 25$$

respectively, for diffracted multiple reflected ray paths and multiple reflected ray paths without diffraction as categorized above, in which Subscript i denotes the ith vehicle type, L'_0 is the reference emission level at $D_0 = 50$ ft, the second term on the right hand sides is the traffic adjustment term for a vehicle type, the third term on the right hand sides is the distance adjustment term, the fourth term on the right hand sides is the modified finite roadway adjustment term, and $\Delta_{barrier}$ is a barrier attenuation term in the diffracted case.

The computations are carried out in the rectified geometry (i.e., all geometric parameters such as receiver-barrier distances are in reference to the nth image receiver and nth image left and right barriers). Provision for consideration of absorptive barriers is incorporated by replacing the reference emission level by a reflection-dependent term, and the atmospheric absorption effect is incorporated by adding an additional attenuation term to the distance-adjustment term.

COMPUTER IMPLEMENTATION

BOAP was implemented in two versions as an MS-FORTRAN program compiled and executed on an IBM–PC (and compatibles) with a math coprocessor. In the first version, SPL values are calculated for a grid of receivers, as shown in Figure 3, and noise level contours are plotted. In the second version, SPL values are calculated as a function of barrier overlap length for a single site-specific receiver. BOAP is programmed to start without any overlap, to increment the overlap by integral multiples of the width w between barriers, and to stop when no reachable multiple reflected paths exist. The convergence criterion for computation at each receiver is set as an increase in SPL of less than 0.1 dB over the previous calculation. As presently programmed, the grid version of BOAP may handle up to an 11-by-11 array of receivers.

The program also incorporates a small FORTRAN subroutine for computing octave-band atmospheric absorption coefficients under a given set of atmospheric conditions (pressure, temperature, and relative humidity). This subroutine implements American National Standards Institute S1.26 (*5*) for the calculation of the absorption of sound by the atmosphere.

SAMPLE APPLICATIONS

The development of BOAP is an outgrowth of New York State Department of Transportation (NYSDOT) project PIN 0227.86, Long Island Expressway Service Roads, Half Hollow Road to Commack Road, Suffolk County. This project involves completion of missing service roads and construction of mainline and service road noise barriers along a 5-mi section of I-495 through a residential neighborhood in Dix Hills, N.Y. Breaks in the noise barriers were necessitated by underground utilities, ramp-service road configurations, and community input regarding placement within the right-of-way.

An illustration of geometric input data required for the grid version of BOAP is shown in Figure 3. The nearest roadway is approximately 60 ft away from the left barrier. There is a gap of 15 ft between barriers, and an 11-by-11 grid (with only 5 rows and 8 columns shown) of receivers at intervals of 1

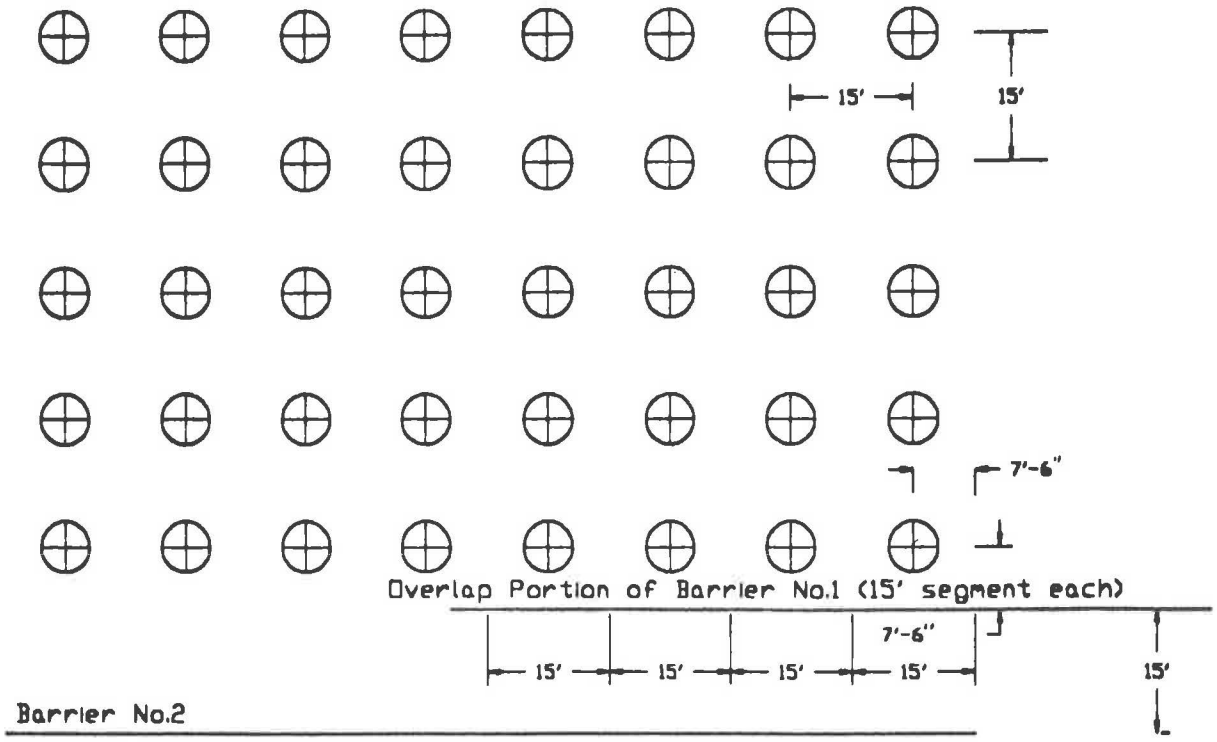

FIGURE 3 Geometry of grid sample application.

width apart starts at a half-width down and away from the tip of the right barrier without overlap (zero-width overlap). The traffic volume on the roadway is 5,650 veh/hr with a mix of 83 percent automobiles, 9 percent heavy trucks, and 8 percent medium trucks, and the average speed is 54 mph.

Figures 4 to 6 show the resulting noise level (in dBA) contour output plots obtained using the grid version of BOAP (with the 8-by-8 array shown in Figure 4 and with the 9-by-9 array shown in Figures 5 and 6) as the right barrier is extended from zero-width overlap to one-width overlap and to four-width overlap. Both X-axis and Y-axis in Figures 4 to 9 are measured in units of gap width between the barriers. In Figure 4, the gap between the barriers results in increases in noise levels in the immediate area adjacent to the opening in the form of a ripple, as would be expected. The ridge of the ripple is along the line-of-sight transmission path (as shown in the three-dimensional views in Figure 7) and decreases further from the opening. As the barrier overlap increases, the effects of the opening become more localized and diminish in magnitude as shown in Figures 5 to 7; the ripple effect due to the line-of-sight transmission through the gap is replaced by the ripple effect resulting from multiple reflection as shown in Figures 8 and 9. Figure 10 is a sample computer output at a single grid point (receiver at third row and second column of Figure 3); the output L_{eq} for the no-barrier and simple-barrier cases agree well with STAMINA 2.0 results to the nearest decibel.

Figure 11 shows the resulting output from a sample application of the single site-specific receiver version of BOAP. The receiver is located at $X = 120$ ft and $Y = 30$ ft from the edge of the right barrier, 230 ft from the roadway. The gap width between the barriers is 50 ft. The barriers are 25 ft in height, and the receiver elevation is 15 ft above ground with the same traffic conditions as the previous example. Figure 11 shows the localized multiple reflection effect (the difference between the upper curve and the lower curve in dBA) as the overlap is extended at 50-ft increments (one barrier gap width) towards the receiver. Without the barriers, the noise level at this particular receiver was estimated at 74 dBA. With the barriers (as configured without any overlap), the noise level would be reduced to 62.8 dBA. Extending the right barrier (the closer barrier) by 100 ft would reduce the noise level to 60.8 dBA if it were not for the multiple reflection effect (+2.4 dBA) between the overlapping barriers. The multiple reflection effect disappears as the right barrier is extended past the receiver, in which case no reflected ray would reach the receiver. For this particular receiver, then, barrier overlap would result in the degradation of barrier performance.

CONCLUSION

A procedure to analyze the effect of overlapping noise barriers has been developed and implemented on a NYSDOT project. It is shown that the gap between noise barriers results in increased noise levels in a localized region along a line-of-sight transmission path through the gap. Overlapped barrier sections used to compensate for the gap would introduce localized increases resulting from multiple reflections. The effect, however, is very dependent on the receiver-barrier-roadway geometry and must be analyzed on a case-by-case basis as illustrated by the sample applications discussed. In a site-specific situation in which the distribution of receivers near the gap is fixed, the procedures presented permit an optimal design of a barrier overlap configuration to provide the pro-

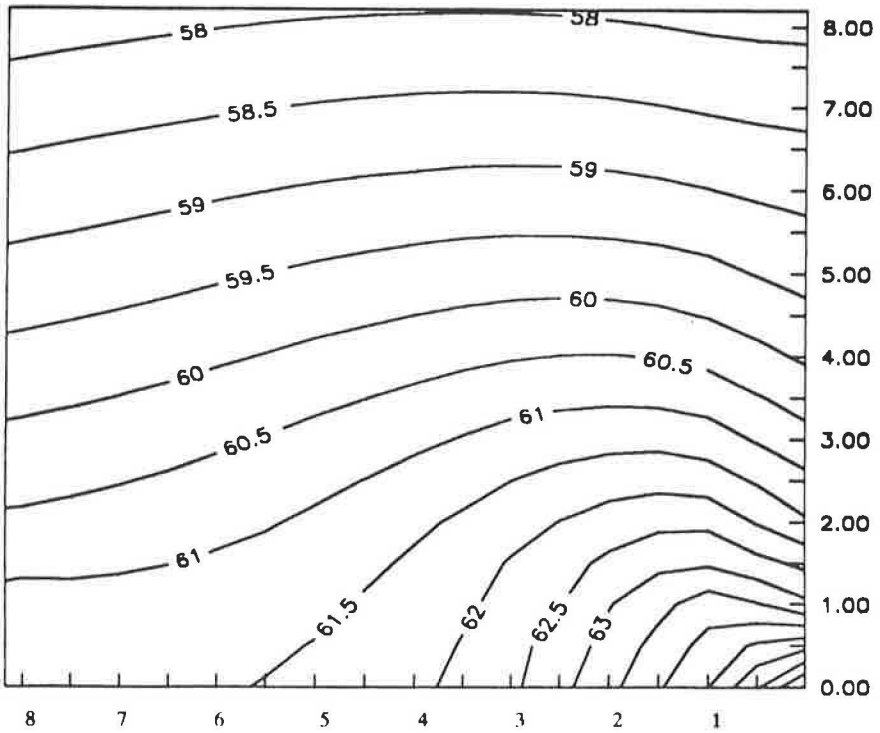

FIGURE 4 Noise level contours—zero-width overlap.

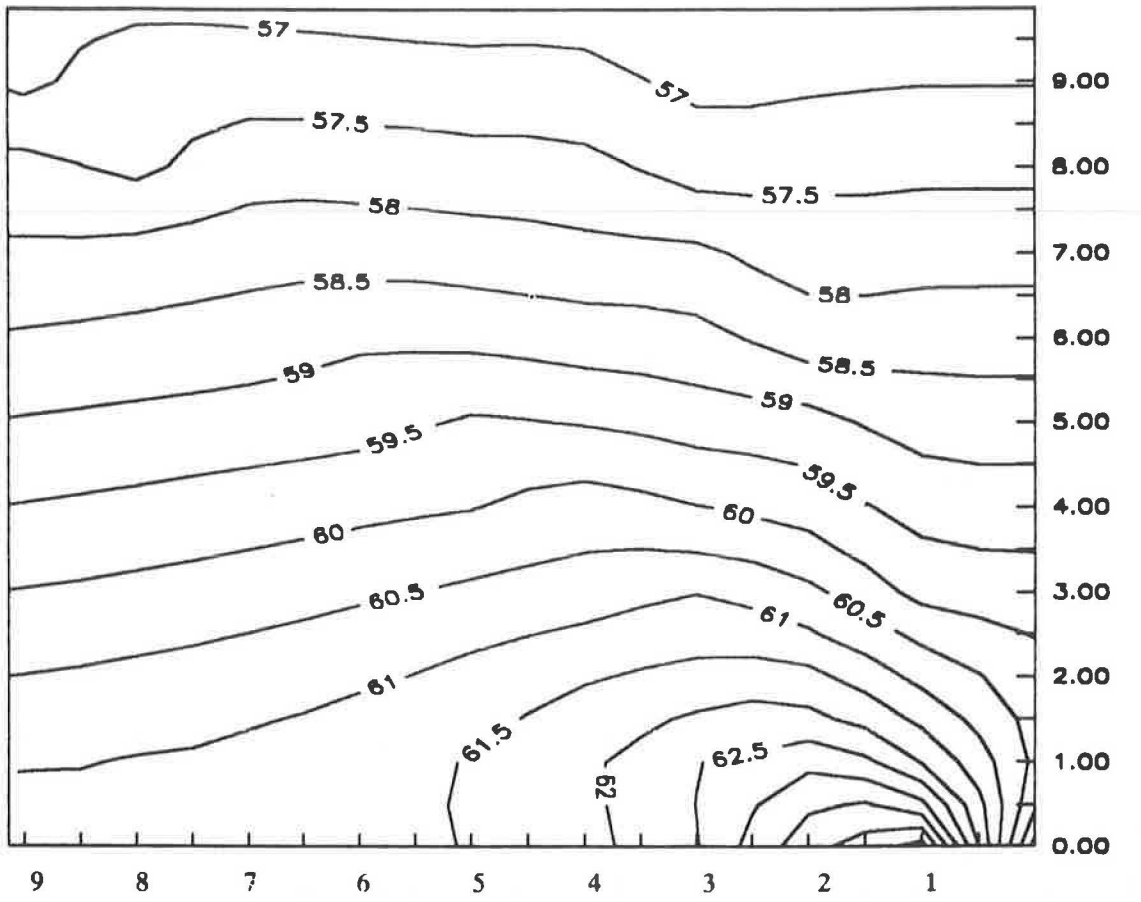

FIGURE 5 Noise level contours—one-width overlap.

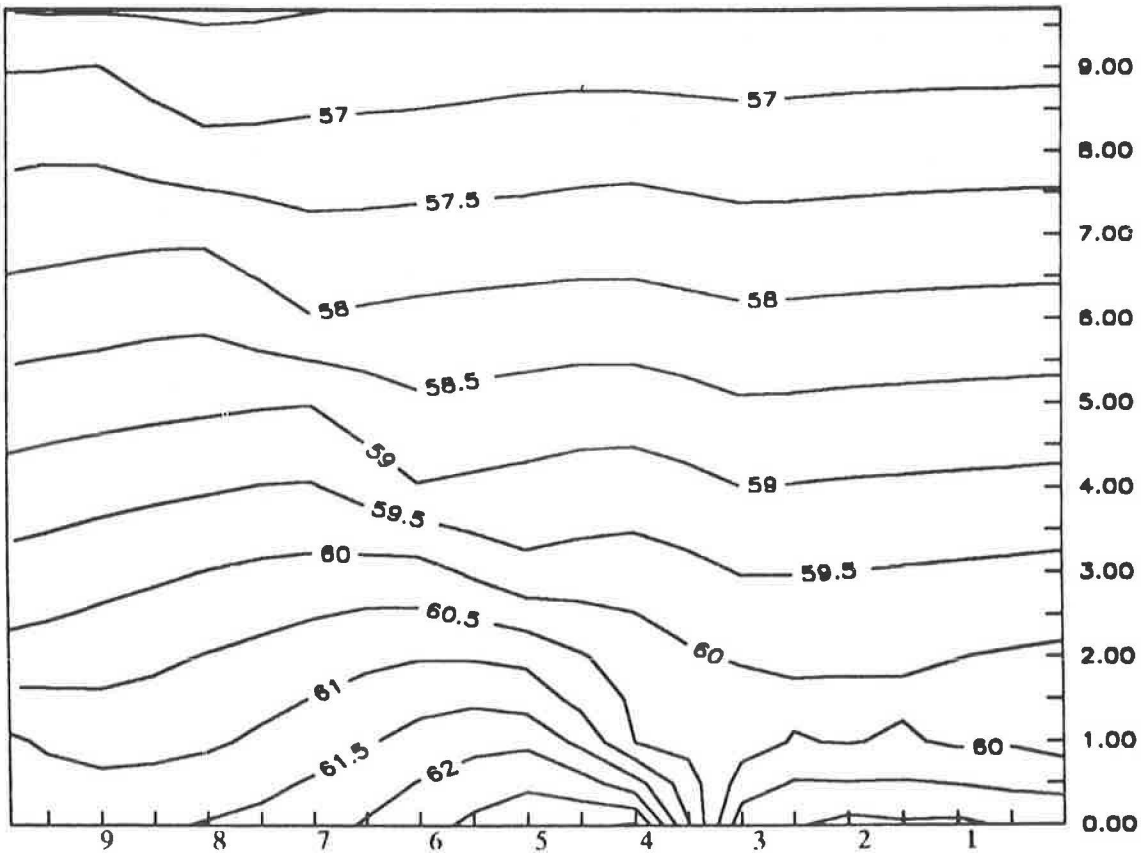

FIGURE 6 Noise level contours—four-width overlap.

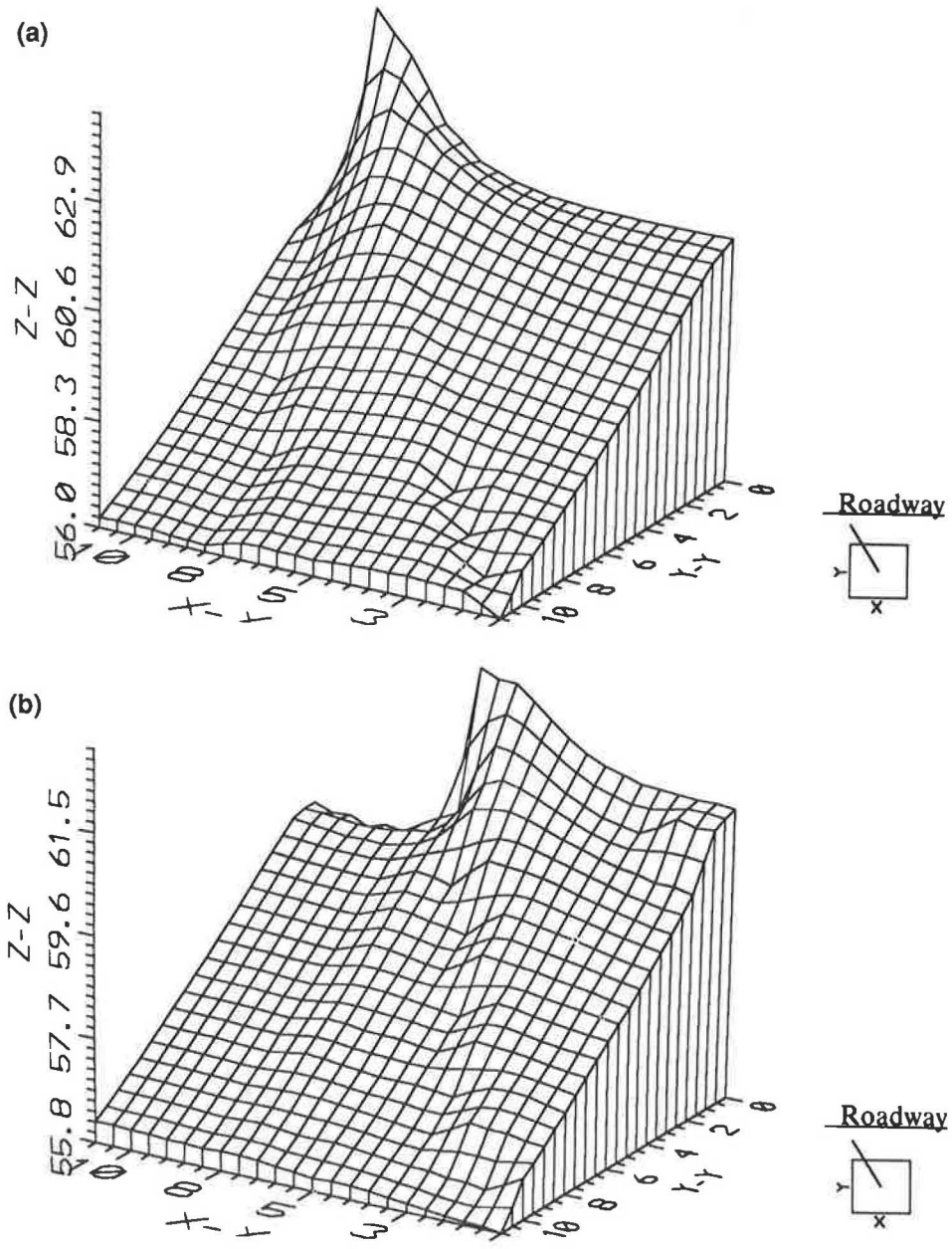

FIGURE 7 Three-dimensional noise level display: a, one-width overlap; b, four-width overlap.

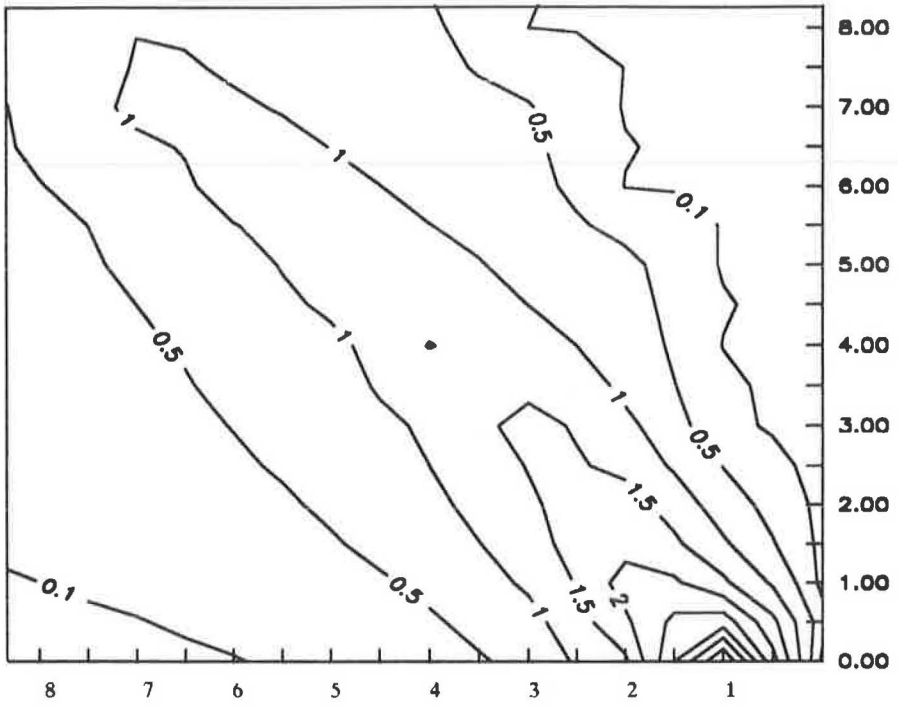

FIGURE 8 Multiple reflection effect—one-width overlap.

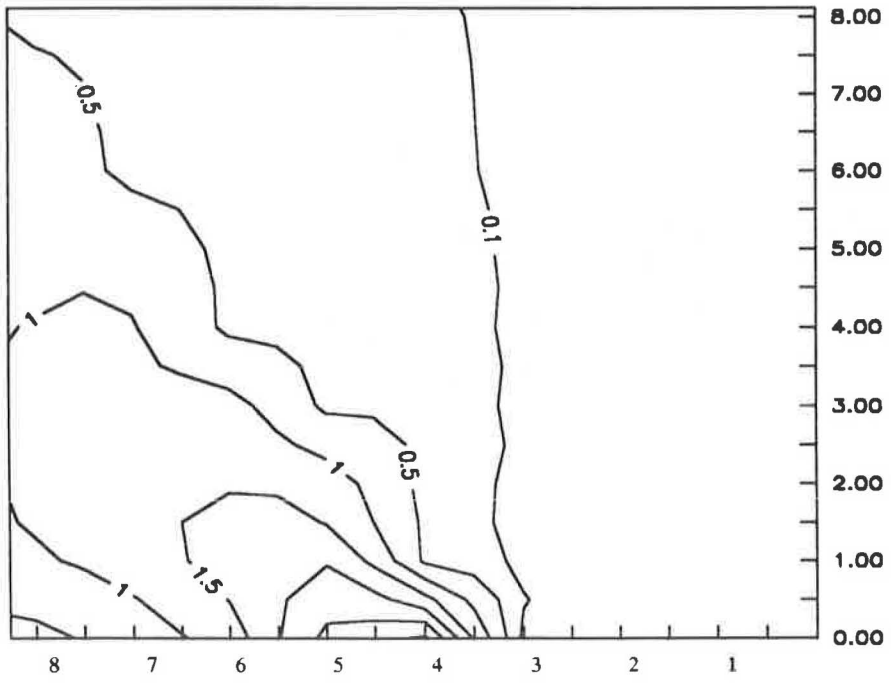

FIGURE 9 Multiple reflection effect—four-width overlap.

Receiver at 3rd Row 2nd Column from 15' Gap

X1= 22.5 Y1= 37.5
X2= 22.5 Y2= 52.5
Distance to Rdwy. 105.0

Barrier Elevation =15.0
Receiver Elevation =5.0
Roadway Elevation =0.0

NO BARRIER LEQ= 77.996170
********** Receiver may see gap , Leq = 63.525240
ORIGINAL Leq=67.523680
CASE A: ALEQD=47.839630
1TH IMAGE TERM LEQ=47.839700
NEW Leq =67.570140

For overlaping length = 15.0 ft

ORIGINAL Leq=65.296620
CASE A: ALEQD=50.823090
1TH IMAGE TERM LEQ=50.823120
CASE B: ALEQR=52.016870 ALEQD=45.661850
2TH IMAGE TERM LEQ=52.921120
CASE C2: ALEQR=54.627750
3TH IMAGE TERM LEQ=54.627770
CASE C1: ALEQR=40.527630
4TH IMAGE TERM LEQ=40.528020
NEW Leq =66.025110

FIGURE 10 Sample output from BOAP at a single receiver.

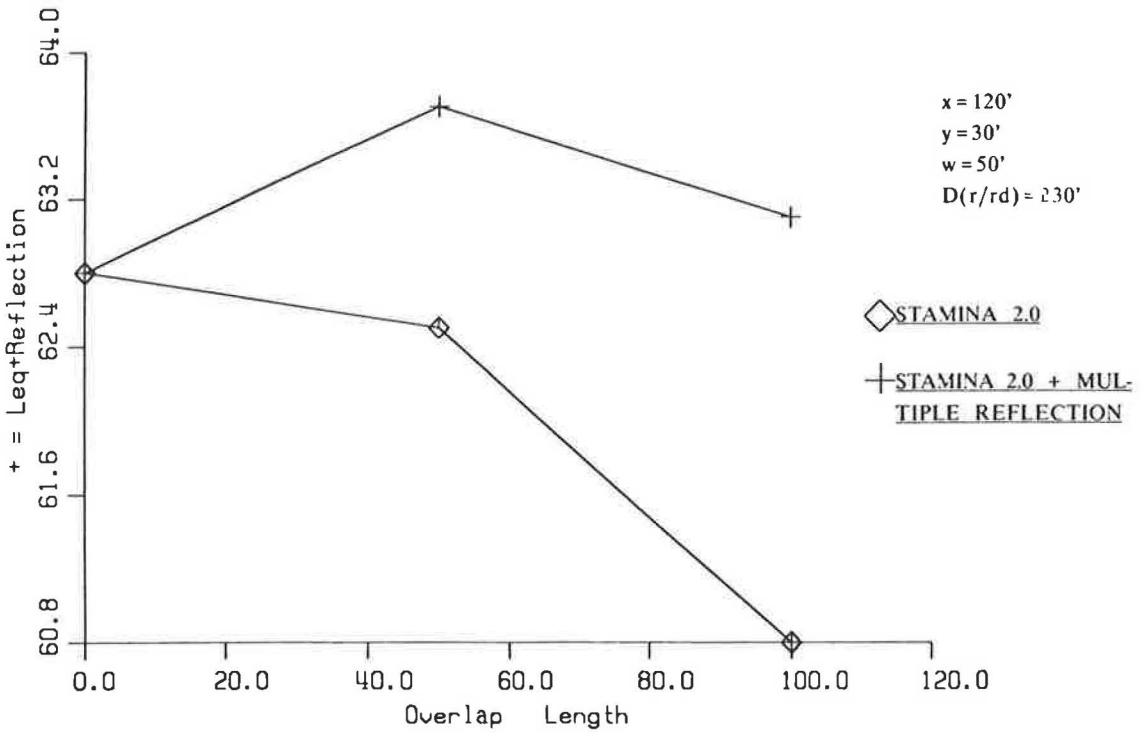

FIGURE 11 Effect of multiple reflection versus barrier overlap.

tection needed against the break in the barriers while avoiding the effect of multiple reflections on specific receivers.

REFERENCES

1. W. Bowlby, J. Higgins, and J. Reagan. *Noise Barrier Cost Reduction Procedure STAMINA 2.0/OPTIMA: Users Manual.* FHWA-DP-58-1, FHWA, U.S. Department of Transportation, Washington, D.C., revised March 1983.
2. S. Slutsky and H. Bertoni. Analysis and Programs for Assessment of Absorptive and Tilted Parallel Barriers. *Transportation Research Record 1176*, TRB, National Research Council, Washington, D.C., 1988, pp. 13–22.
3. P. Zimmerman and J. Higgins. *Noise Barrier Cost Reduction Procedure STAMINA 2.0/OPTIMA: Program Maintenance Manual.* FHWA-DP-58-2, FHWA, U.S. Department of Transportation, Washington, D.C., June 1982.
4. T. M. Barry and J. A. Reagan. *FHWA Highway Traffic Noise Prediction Model.* FHWA-RD-77-108, FHWA, U.S. Department of Transportation, Washington, D.C., 1978.
5. *Method for the Calculation of the Absorption of Sound by the Atmosphere.* American National Standards Institute, S1.26, New York, 1978.

Publication of this paper sponsored by Committee on Transportation-Related Noise and Vibration.

Atmospheric Effects on Traffic Noise Propagation

ROGER L. WAYSON AND WILLIAM BOWLBY

Atmospheric effects on traffic noise propagation have largely been ignored during measurements and modeling, even though it has generally been accepted that the effects may produce large changes in receiver noise levels. Measurement of traffic noise at multiple locations concurrently with measurement of meteorological data is described. Statistical methods were used to evaluate the data. Atmospheric effects on traffic noise levels were shown to be significant, even at very short distances; parallel components of the wind (which are usually ignored) were important at second row receivers; turbulent scattering increased noise levels near the ground more than refractive ray bending for short-distance propagation; and temperature lapse rates were not as important as wind shear very near the highway. A statistical model was developed to predict excess attenuations due to atmospheric effects.

Outdoor noise propagation has been studied since the time of the Greek philosopher Chrysippus (240 B.C.). Modern prediction models have become accurate, and the advent of computers has increased the capabilities of models. However, primarily because of their dynamic nature, atmospheric effects on traffic noise propagation have not been predicted well.

A research effort involving quantitative analysis of data and correlation of measured meteorological effects on traffic noise propagation at relatively short distances common to first and second row homes along heavily traveled roadways is described. Project planning and the collection, reduction, and analysis of data are described.

METHOD OF RESEARCH

The problem, simply stated, is to determine the physical mechanisms that cause atmospheric (weather) effects on traffic noise levels and to predict these levels accurately. The solution is complicated by the interacting effects of geometric spreading, shielding (diffraction), reflection, ground impedance, atmospheric absorption, and atmospheric refraction, all of which must be considered in the modeling process.

These effects may be considered to act separately on the noise levels received by an observer as reported by many sources including the well-read text by Beranek (*1*) and the FHWA methodology (*2*). Using this concept, the receiver noise level may be defined as

$$L_x = L_0 + A_{geo} + A_b + L_r + A_e \quad (1)$$

where

L_x = time-averaged sound level at some distance x (in dB),
L_0 = sound level at a reference distance,
A_{geo} = attenuation due to geometric spreading,
A_b = insertion loss due to diffraction,
L_r = level increases due to reflection, and
A_e = attenuation due to ground characteristics and environmental effects.

It should be noted that all levels in dB in this paper are referenced to 2×10^{-5} N/m^2.

The last term on the right side of Equation 1, A_e, consists of three parameters: ground attenuation, attenuation due to atmospheric absorption, and attenuation due to atmospheric refraction.

$$A_e = A_{grd} + A_{abs} + A_{ref} \quad (2)$$

where

A_{grd} = attenuation due to ground interference,
A_{abs} = attenuation due to atmospheric absorption, and
A_{ref} = attenuation due to refraction.

The effects of rain, sleet, snow, and fog are not considered here. With the careful site selection used for this research, L_r and A_b were considered negligible, so Equation 1 could be written

$$L_x = L_0 + A_{geo} + A_{grd} + A_{abs} + A_{ref} \quad (3)$$

To evaluate the relationship between L_x and A_{ref}, the other variables needed to be known; this was done by normalizing the data for refractive effects. After all terms in Equation 3 except A_{ref} were determined in various ways, allowing the data to be normalized, excess attenuation from atmospheric refraction was calculated. Once sample data were on a common basis, comparison of each sample period for changes in excess attenuation due to atmospheric variables could be determined. These relationships were then evaluated to determine statistical correlation.

Once data were normalized, the statistical approaches presented a realistic way to correlate the effects of random atmospheric motion. Statistical methods used were regression analysis, Gaussian statistics, and hypothesis testing.

DATA COLLECTION

Data were collected in March and April 1987 along I-10 in Houston, Tex. I-10 at this location consisted of three main lanes in each direction, two frontage roads in each direction, and a center, high-occupancy vehicle (HOV) lane, all at grade.

Vanderbilt Engineering Center for Transportation Operations and Research, Vanderbilt University, Box 1625, Station B, Nashville, Tenn. 37235.

The frontage roads were separated by a small grassy median from the main lanes, whereas the HOV lane was separated by Jersey crash barriers. The south side of the highway facility, where sampling was done, consisted of a large open field with mown grass. Figure 1 shows general site layout and the measurement site locations in regards to I-10. Table 1 presents a complete listing of the data collected.

During data collection, specific sets of atmospheric conditions were desired. A total of 29 periods of data were finally collected, ranging in duration from 4.2 to 24.7 min (28 to 148 10-sec averages). Table 2 presents the average weather conditions for each sample period. Weather data were collected concurrently; in this way, a comprehensive spatial data base was developed. Periods 24 and 29 were deleted due to incompleteness of data.

An on-site mobile laboratory housed required instrumentation and provided shelter and convenience. Meteorological sensors and microphones were connected by long shielded cables to the mobile laboratory. All cables were carefully checked, and calibrations were conducted with the cables in place. Recording was done on studio quality tapes using a precision RACAL tape recorder at a speed of 15 in./sec to ensure high-quality recording. Proper, careful calibrations were recorded on each tape. Precise calibrations were repeated for each instrument. To quantify the noise data, the tapes were analyzed using a Norwegian Electronics real-time analyzer. The selected output of this noise analyzer was in one-third octave bands from 16 to 10,000 Hz for each microphone. A data-averaging time of 10 sec was used because the atmospheric changes and effects on noise data are minimized on

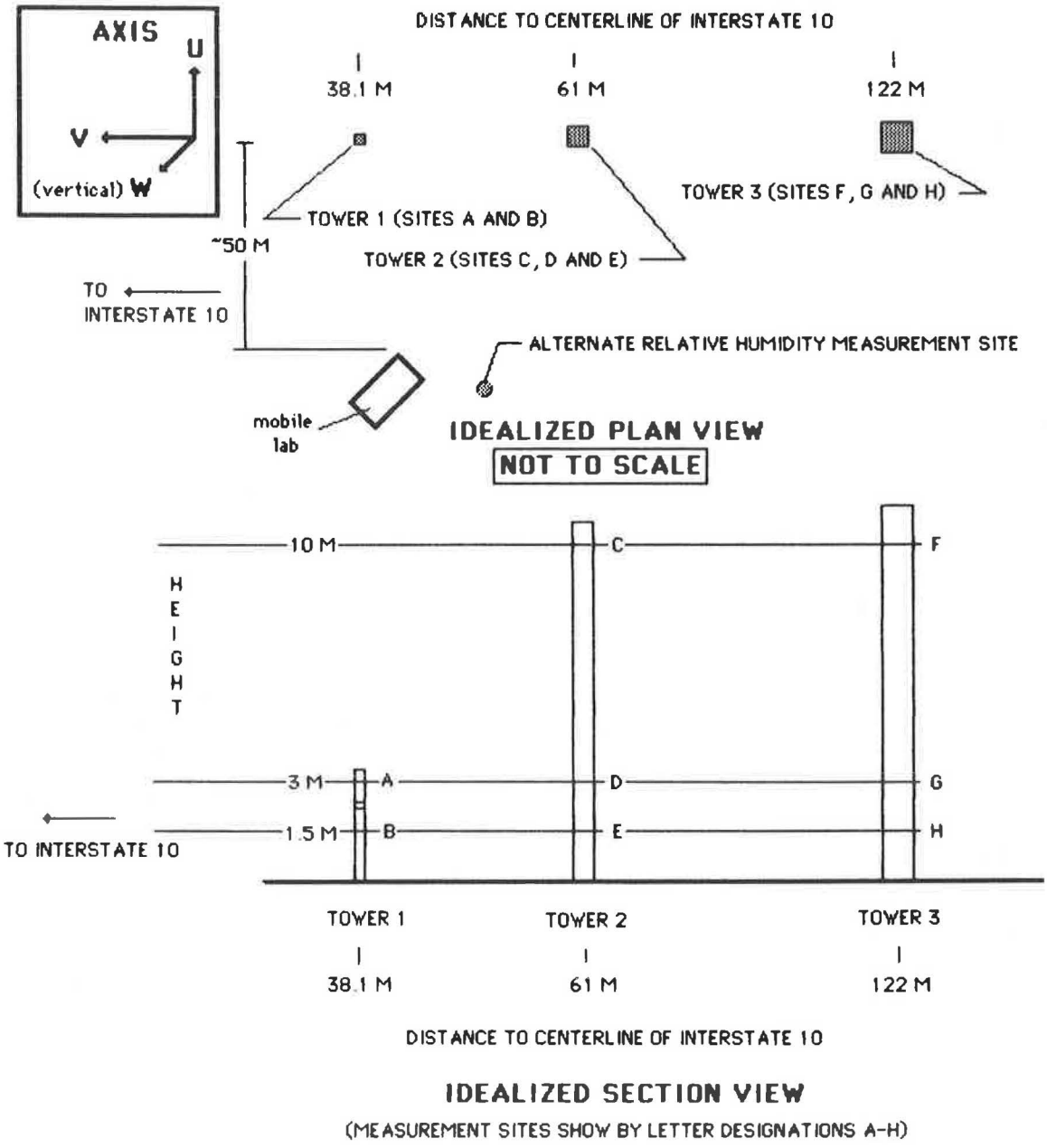

FIGURE 1 Highway and site detail.

TABLE 1 DATA COLLECTED BY LOCATION

Measurement Station	Traffic Noise	u-v-w Wind Speed	Asperated Temp.	Shielded Temp.	Relative Humidity
A	x				
B	x				
C	x	x	x		
D	x	x		x	x
E	x	x			
E**			x	x	
F	x	x		x	
G	x	x			
H	x	x			
H**				x	
MEL III					x

A,B: Tower 1

C,D,E,E**: Tower 2 (E** at 0.5 meters)

F,G,H,H**: Tower 3 (H** at 0.5 meters)

*Also collected manually were:

- soil type and relative moisture content
- traffic data
  - vehicle counts (by lane classification)
  - vehicle average speeds
  - vehicle types
- cloud cover
- relative humidity (sling psychometer)
- unusual noises

this time scale. Weather data were collected using a Balconies minicomputer with half-sec recording intervals of all weather data and output to nine-track computer tapes.

Each data file was reviewed for accuracy and completeness. A series of FORTRAN computer programs was written, tested, and run for each sample period to format these VAX-compatible, ASCII data files. Indirectly measured parameters were calculated such as lapse rate γ, vertical wind gradient du/dz, turbulent intensities i_u, i_v, i_w, standard deviations, Richardson number Ri (*3*), and Tatarski's refractive index function (*4*). A mathematical description of Ri and Tatarski's refractive index function is given in the appendix at the end of this paper. The meteorological data were averaged in 10-sec intervals to match the noise data averaging procedure.

From the final meteorological and noise data files, various data combinations were sorted and combined. These files were manipulated to contain specific information of interest for correlation analysis. Statistical testing, as well as correlation analysis, was done using a commercial software statistical testing package (*5*). Figure 2 displays graphically the series of events needed to combine and analyze the data.

ANALYSIS

After formatting was accomplished, data were mathematically adjusted to normalize for traffic, distance, ground interference, atmospheric absorption, and the reference microphone. Formatting also allowed combinations of various data sets for statistical testing. Logarithmic averaging was done for each sample period. The following discussion explains how each term in Equation 3 was determined or calculated.

Reference Level (L_0)

Noise levels measured at Site B were used as the reference levels L_0 for data normalization. Site B presented a measured

TABLE 2 AVERAGE WEATHER CONDITIONS BY SAMPLE PERIOD

Sample Period	Avg. RH (%)	Avg. Temp. (C)	Avg. V 10 M (m/s)	Cloud Cover	P/G Class	Lapse Rate (C/m)	Wind Shear (m/s/m)	RI#
1	78	23	2.10	0.4	B	-0.036	0.031	-1.64
2	80	23	2.42	0.4	B	-0.030	0.049	-0.56
3	79	23	2.21	0.4	B	-0.044	0.056	-0.57
4	49	14	2.80	0.2	A	-0.140	-0.017	-17.60
5	47	14	2.93	0.2	A	-0.137	-0.054	-1.71
6	37	19	1.29	0.9	B	-0.010	-0.019	-1.75
7	37	19	2.37	0.5	B	-0.145	-0.048	-2.24
8	32	22	2.70	0.8	C	-0.094	-0.044	-1.83
9	41	20	0.29	0.8	B	0.035	0.027	1.15
10	45	20	0.44	0.8	E	0.052	0.028	1.75
11	49	19	3.30	0.9	C	-0.080	-0.086	-0.40
12	48	20	4.10	0.9	C	-0.095	-0.092	-0.41
13	44	21	1.66	0.1	A	-0.026	-0.073	-0.23
14	31	22	2.93	0.0	B	-0.123	-0.024	-7.59
15	33	22	0.37	0.0	A	0.007	0.018	-0.26
16	50	19	0.23	0.0	A	0.261	0.002	2708.10
17	28	26	1.38	0.0	A	-0.107	0.059	-1.09
18	27	26	1.47	0.3	B	-0.032	0.069	-0.29
19	28	24	1.79	0.3	B	0.018	0.060	0.08
20	29	24	1.10	0.4	B	0.027	0.041	0.33
21	31	20	3.64	0.0	B	-0.142	-0.045	-2.48
22	31	20	3.59	0.0	B	-0.108	-0.046	-1.83
23	31	20	3.50	0.0	B	-0.096	-0.046	-1.69
25	62	12	2.23	0.0	B	-0.035	0.078	-0.26
26	30	23	2.92	0.0	B	-0.125	0.088	-0.58
27	29	23	3.40	0.0	B	-0.041	0.126	-0.11
28	58	21	3.35	0.0	B	-0.159	0.002	-1020.89

reference level at a known distance for each sample period that could be used to normalize each of the other microphone levels. Use of Site B as a reference level is similar in concept to energy-mean emission levels developed for STAMINA (*6*), except an overall traffic noise level was developed rather than extrapolating for a single-vehicle pass-by. The normalization process was necessary to allow for traffic variations in each sample period.

Site B was evaluated to determine if it was affected by meteorology by first comparing modeled to measured values for each sample period using sample-period-specific traffic data. During the modeling runs, the atmospheric absorption algorithm in STAMINA 2.0 was bypassed with comment indicators and no ground attenuation was assumed. The results of the computer model were then compared to the measured data. Differences in the values were expected because of the averaged national emission levels used in the model. If only the emission levels were in error, relatively constant differences should have occurred. However, differences ranged from −3.3 to 0.4 dB. Figure 3 shows the differences for each sample period. The changes in these differences indicated that perhaps some other changing phenomenon was influencing the measured noise levels at the reference microphone.

To identify the interference phenomenon, statistical correlations using the least squares analysis method were used along with testing of the null hypothesis. The null hypothesis, simply stated, is that traffic noise levels are not affected by atmospheric phenomena.

To prove the null hypothesis at a 95 percent level of confidence, a correlation coefficient r of less than 0.374 would be expected for a two-variable correlation, here an atmospheric phenomenon compared with excess attenuations. For a multiple regression correlation that contained three variables, in this case noise levels, wind shear, and lapse rate, a value of less than 0.454 would be expected for r. These values are for testing absolute values of correlation coefficients, to prove or disprove the null hypothesis, from standard index tables supplied in texts (*7*).

When the reference location (Site B) was evaluated, the null hypothesis could not be proven. The results could be interpreted to mean that even at this small distance from the traffic source, noise levels are affected by atmospheric phenomena. This does not necessarily mean noise levels are affected but that it cannot be proven that they are not affected. However, the probability that they are affected is high because the other effects were carefully eliminated from consideration during the normalization process.

Geometric Spreading (A_{geo})

In order to normalize for energy loss due to geometric spreading, the amount of attenuation for each microphone had to be evaluated. Use of the STAMINA program provided an easy way to accurately allow for geometric spreading, with the atmospheric absorption algorithm being bypassed and no

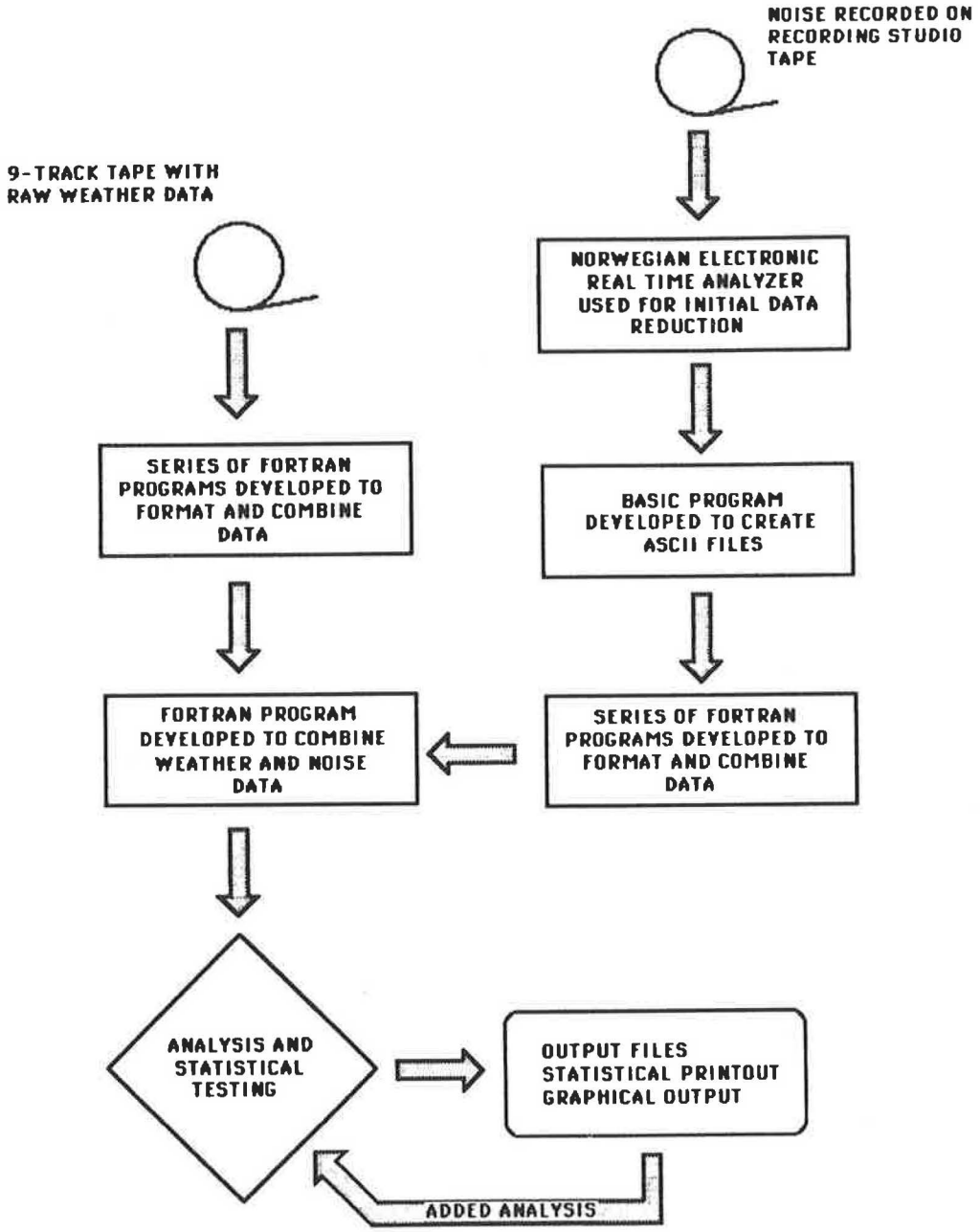

FIGURE 2 Data reduction flow chart.

allowance being made for ground interference. Using STAMINA in this way, correction factors (in dB) could be determined for geometric spreading.

Ground Attenuation (A_{grd})

Modeling was considered as a method to correct each site for ground interference, especially by using the Penn State Model (*8*). However, any increased accuracy of these methods above actual measured levels was doubtful.

During data collection, considerable effort was spent trying to measure a base-case sample period. Ideally, the base-case period would contain no wind or temperature gradient. Although a quiescent atmosphere never really occurs, conditions were very favorable for a base case to be developed in two of the periods, 6 and 15, in which the wind shear and lapse rate were both small. In these cases, convective mixing dominated, but again, winds were slight. Small amounts of refraction would be expected from these weather conditions. Each of these sample periods had the same difference (-1.5 dB) from the modeled STAMINA level at the reference site. Similar differences occurred at the other sites. Accordingly, an average of Sample Periods 6 and 15 without atmospheric influence other than absorption was used as a reference datum point to determine ground attenuation.

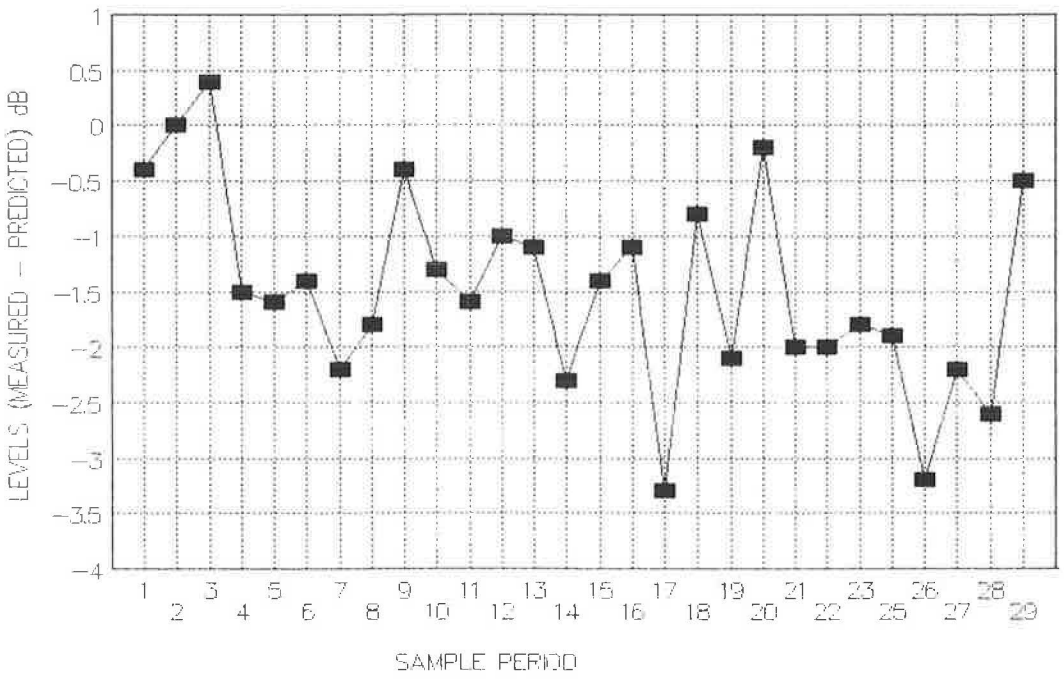

FIGURE 3 Level differences—measured minus predicted at reference microphone at Site B.

Atmospheric Absorption (A_{abs})

The American National Standards Institute (ANSI) standard method (*9*) was used to determine correction values for each sample period, microphone, and one-third octave frequency band. This process allowed a normalization of data for varying weather conditions and propagation path lengths, because atmospheric absorption is a linear function of path length.

Final Combinations of Normalized Data

Once all terms of Equation 3 were determined (as previously discussed), the measured noise data were adjusted to solve for refractive excess attenuation (A_{ref}). The first step in this process was to adjust each frequency band for atmospheric absorption. Once corrected, the one-third octave band values were combined logarithmically to develop A-weighted L_{eq} values, representative of each sample period. The final product was normalized, time-averaged, A-weighted refractive excess attenuations. From the reduced data values, A_{ref} was determined for each 10-sec interval in each sample period by evaluating Equation 3. Table 3 presents these values for refraction only, whereas Table 4 includes ground interference.

REFRACTIVE EXCESS ATTENUATION OBSERVATIONS

After derivation of the refractive excess attenuations, Tables 3 and 4 were reviewed to distinguish trends in the data. The data presented in Table 3 show that when averaged for all sample periods, no effect is seen at Site A or E. However, individual sample periods show strong effects. At Site A, values range from −2.9 to 3.7 dB. At Site E, values range from −1.2 to 1.8 dB. Likewise, Sites C and D show small effects in the aggregate but wide variances from sample to sample, with Site C values ranging from −0.9 to 3.4 dB and Site D values from −0.9 to 2.3 dB. Sites F and G show slightly greater ranges. Because these represent normalized values, it can be assumed that these ranges are the result of varying weather conditions

One theory (*10–12*) hypothesizes that a primary mechanism for causing increased noise levels near the ground is the scattering of the skywave by turbulence. In this paper, skywave is used in the acoustical sense (as the referenced literature does) to mean a sound wave propagating at or above 5 degrees from horizontal. If this mechanism is significant, decreased refractive excess attenuations should result at sites nearer the ground than for the sites at higher elevation because of decreased effect with distance from the skywave propagation path. This relation is indeed the case as shown in Table 3 in general for individual sample periods. Accordingly, scattering of the skywave from turbulence is a strong mechanism that increases noise levels near the earth's surface.

Ray bending due to refraction has also been considered a process that could change noise levels near the ground (*13,14*). Whether this phenomenon can occur with enough bending to affect receivers typical of first and second row residences, which are usually less than 150 m from the roadway, was investigated. Established equations were evaluated for these short distances using an arbitrary worst case scenario (chosen on the basis of experience), with lapse rate equal to 0.3 degrees/m and wind shear equal to 0.98 (m/s)/m. A chord of 150 m (used to simulate a distance typical of second-row residences) would mean the horizontal wave front would be displaced by approximately 2 m. Consequently, even in unusual cases, only a 2-m displacement could be expected at 150 m from the source. For typical conditions and shorter distances, a much smaller effect on traffic noise levels would be expected, except

TABLE 3 REFRACTIVE EXCESS ATTENUATION LEVELS—REFRACTION ONLY

Sample No.	Refractive Excess Attenuations (dB)						
	Mic A	Mic C	Mic D	Mic E	Mic F	Mic G	Mic H
1	0.7	0.3	0.5	0.9	0.5	-1.1	-1.7
2	-2.7	0.9	0.2	1.3	-0.0	-0.7	-1.9
3	-2.9	-0.3	0.1	0.4	4.7	-0.1	-1.5
4	-0.4	0.5	-0.4	-0.4	2.1	1.0	-0.6
5	-0.2	0.6	-0.5	-0.7	1.6	0.9	1.1
7	0.2	0.6	-0.5	-1.2	1.7	2.0	0.3
8	-0.4	0.2	-0.9	-0.9	2.5	4.5	4.1
9	0.2	-0.2	-0.9	0.8	-0.1	-1.2	-2.2
10	0.4	0.1	-0.5	0.8	-0.0	-0.6	-1.7
11	0.1	-0.5	-0.1	-0.2	-0.1	0.2	-0.8
12	0.2	-0.9	-0.0	-0.5	-0.4	-0.2	-1.9
13	0.8	1.3	0.2	1.3	2.0	2.9	1.7
14	0.5	1.5	0.4	0.3	3.5	5.3	5.2
16	-0.3	-0.9	0.2	0.8	-0.7	0.5	-1.0
17	0.7	2.6	1.4	1.8	4.9	3.4	3.1
18	-0.8	0.4	-0.2	-1.2	1.1	1.3	1.0
19	-0.6	0.7	2.3	-0.4	0.8	-0.1	-0.8
20	-1.2	0.2	0.2	-0.1	-0.2	-0.6	-1.2
21	-1.3	0.9	0.3	0.4	1.9	3.0	1.9
22	-1.1	0.9	0.7	0.5	1.4	2.6	1.9
23	-1.3	0.1	0.7	0.1	1.0	1.8	0.5
25	2.7	0.2	0.4	-1.2	-1.0	6.5	-1.4
26	3.7	3.4	1.0	-0.3	2.8	0.5	-0.1
27	1.8	2.3	0.2	-1.0	1.2	-0.5	-1.2
28	0.1	1.9	0.5	-0.0	2.1	0.9	-1.5
MAX	3.7	3.4	2.3	1.8	4.9	6.5	5.2
MIN	-2.9	-0.9	-0.9	-1.2	-1.0	-1.2	-2.2
AVG	0.0	0.7	-0.2	0.0	1.3	1.3	0.0
STD	1.4	1.0	0.7	0.8	1.5	2.0	2.0

perhaps for changes in ground interference, because the angle of the wave striking the ground would change.

To further evaluate the effects of ray bending, refractive excess attenuations were reviewed. One would expect levels of refractive attenuation to be similar at sites along the projected curved ray path. The data in Table 3 do not support this theory. Therefore, turbulent scattering appeared to have a greater effect on receiver noise levels near the highway than ray bending.

Quite noticeable (see Table 4) was the effect that ground interference had on the 1.5-m-high sites (E and H). As expected, ground interference became less prominent with increasing height. A review of Table 4 shows similar refractive excess attenuation trends at Sites C and F, which were both 10 m high. Also apparent are the larger attenuations with decreasing height at each tower.

Also of interest in Table 4 are the similar values that occur for microphones of similar height, with the exception of Site A. Site A, being within 10 m of the edge of the pavement, would appear to behave differently from the atmospheric effects, because the values are between those derived for the 3-m and 10-m sites. However, if the angles from the roadway surface to the microphones are considered, Site A follows the pattern established at the other sites. Accordingly, the results at Site A are not different but would appear to be following the same pattern as Sites C and D most of the time (but not always) if the angle to the roadway centerline is considered. The proximity to the highway for Site A most probably causes the irregularities in the pattern because the propagation path is much shorter and less affected by the changing atmospheric phenomena. This is reinforced when an irregularity occurs, because during most of these cases the Richardson number has a large absolute value. Accordingly, sites of similar height away from the roadway display similar refractive excess attenuation when ground effects are included.

SIGNIFICANCE OF VARIABLES

In order to model any phenomenon, it must be assumed that the event is repeatable and dependent on key variables. To establish the significance of each variable, correlation analysis and null-hypothesis testing were used. To test for the significance of variables, microphone locations were assumed to be independent and evaluated singularly. In this way, no overall bias would occur at any sample site. In all testing, the traffic refractive excess attenuations were considered to be the dependent variable. The null hypothesis was as stated before.

TABLE 4 REFRACTIVE EXCESS ATTENUATION LEVELS—GROUND INTERFERENCE INCLUDED

Sample No.	Refractive Excess Attenuations (dB)						
	Mic A	Mic C	Mic D	Mic E	Mic F	Mic G	Mic H
1	1.9	2.9	1.0	2.8	2.6	-0.9	-0.7
2	-1.5	3.5	0.7	3.2	2.1	-0.5	-0.9
3	-1.7	2.3	0.6	2.3	6.8	0.1	-0.5
4	0.8	3.1	0.1	1.5	4.2	1.2	0.4
5	1.0	3.2	0.1	1.2	3.7	1.1	-0.1
6	1.4	2.7	0.4	1.7	1.8	-0.7	-1.5
7	1.4	3.2	0.0	0.7	3.8	2.2	1.3
8	0.8	2.8	-0.4	1.0	4.6	4.7	5.1
9	1.4	2.4	-0.4	2.7	2.0	-1.0	-1.2
10	1.6	2.7	0.0	2.7	2.1	-0.4	-0.7
11	1.3	2.1	0.4	1.7	2.0	0.4	0.2
12	1.4	1.7	0.5	1.4	1.7	0.0	-0.9
13	2.0	3.9	0.7	3.2	4.1	3.1	2.7
14	1.7	4.1	0.9	2.2	5.6	5.5	6.2
15	1.0	2.5	0.6	2.1	2.4	0.2	-0.5
16	0.9	1.7	0.7	2.7	1.4	0.7	0.0
17	1.9	5.2	1.9	3.7	7.0	3.6	4.1
18	0.4	3.0	0.3	0.7	3.2	1.5	2.0
19	0.6	3.3	2.8	1.5	2.9	0.1	0.2
20	0.0	2.8	0.7	1.8	1.9	-0.4	-0.2
21	-0.1	3.5	0.8	2.3	4.0	3.2	2.9
22	0.1	3.5	1.2	2.4	3.5	2.8	2.9
23	-0.1	2.7	1.2	2.0	3.1	2.0	1.5
25	3.9	2.8	0.9	0.7	1.1	6.7	-0.4
26	4.9	6.0	1.5	1.6	4.9	0.7	0.9
27	3.0	4.9	0.7	0.9	3.3	-0.3	-0.2
28	1.3	4.5	1.0	1.9	4.2	1.1	-0.5
MAX	4.9	6.0	2.8	3.7	7.0	6.7	6.2
MIN	-1.7	1.7	-0.4	0.7	1.1	-1.0	-1.5
AVG	1.2	3.2	0.7	1.9	3.3	1.4	0.8
STD	1.4	1.0	0.7	0.8	1.5	2.0	2.0

Wind Effects

The effects of the wind were examined for statistical significance at each measurement location. These variables included the average wind speed vector for the orthogonal coordinates, with the x-axis along the centerline of I-10 and the positive direction to the east. In meteorology, the x-, y-, and z-axes are commonly referred to as u, v, and w, respectively, the convention used in this paper (see Figure 1). Also examined was the wind shear at Towers 2 and 3.

Correlation coefficients (r) ranged from 0.003 to 0.797. To disprove the null hypothesis for 25 samples and 2 variables, a value exceeding 0.381 was required for r as previously discussed (7). Sample Periods 6 and 15 were not included because they were used to normalize for ground effects. Again, it must be noted that if the null hypothesis is not proven, it does not necessarily mean that the variables are correlated. However, because the data have been normalized to eliminate all other variables except for refraction from wind, temperature, and turbulence, it can be assumed that there is a significant correlation if r exceeds the critical value.

Of importance in the analysis was the inclusion of the u and w components of the wind. From a point source, only the v components of the wind would be expected to affect the noise propagation because wind effects on receiver noise levels are related to the angle of propagation, from the source to the receiver. However, the traffic stream propagates noise at various angles to the receiver depending on the location of the vehicle as it travels on the roadway. To ensure that the results were not biased, the u components of the wind were included in testing. Also, because the microphone arrays were at various heights, to maintain the scientific method and not prejudice results, the w coordinate vector components of the wind were also evaluated. However, none of the evaluations for any u or w wind vector component proved significant, with the exception of those for Tower 3. This finding is significant. If it is assumed that there is indeed a correlation, then the u vector component of the wind is not an important factor at 61 m from the roadway, at which the null hypothesis was proven, but does begin to play an important role as distances increase to 122 m, at which the null hypothesis was disproven.

As expected, all v vector components of the wind, as well as the v wind shear, proved to be statistically valid for at least one microphone location, with many correlating at multiple microphone locations. The greatest frequency of significant correlations occurred at the first two towers, which is impor-

tant because wind plays a significant part in influencing noise levels at relatively close distances to the highway.

The v vector components of the wind also correlated with measurements at Tower 3, but to a lesser degree. A probable cause is that the wind is not constant at all towers and the further tower is affected somewhat differently. To further test this probable cause, wind parameters at both towers were analyzed using autocorrelation. A close following of the pattern of each suggests that the use of Taylor's frozen turbulence hypothesis (*15*) is valid for the wind field. However, wind parameters were sometimes quite different. For example, in Sample Periods 4 and 16, the magnitudes are opposite. The varying wind field could cause Tower 3 to sometimes behave in a fashion dependent on more than a measurement at a single point, and reduce the amount of correlation. Regardless, the number of significant hits (correlation values above the null hypothesis level) strongly shows the importance of the v wind component parameters.

Further testing was also done for the v wind components. A review of statistical plots showed that in many cases two distributions actually occurred when the v wind components were correlated to noise levels, because of the positive and negative wind vectors. This effect is substantial because it shows that for locations near the highway, perhaps two regression analyses are required, one for the positive and one for the negative wind vectors. Further statistical testing showed this to be true as correlation coefficients increased and the numbers of hits at sample locations also increased. For example, the testing of the v component of the wind at Site C hit with an r value of 0.421. Testing for only the positive wind vector (of v) increased r to 0.585 and also had hits at Sites A, E, and G, at which the r values were 0.775, 0.534, and 0.540, respectively. The high correlation value (0.775) at Site A shows the strong influence the v component of wind has on traffic noise levels close to the highway. The negative component also had correlation values of 0.719, 0.678, and 0.553 at Sites C, F, and G, respectively. Because the number of sample periods for each correlation decreased, the critical value required to disprove the null hypothesis increased to 0.532 for positive values and 0.514 for negative values. Because r^2 increased significantly, a stronger linear relationship was shown between the independent and dependent variable. Accordingly, a significant finding is that the positive and negative wind vectors should be modeled separately.

Temperature Effects

Data in this classification included lapse rate, thermal intensity fluctuations, and standard deviation of the temperature averages. Although the intensity fluctuations and standard deviations of the temperature averages are actually turbulence characteristics, they are included here to help eliminate confusion. As with the wind parameters, correlations were made between the measured temperature parameters (the independent variables) and refractive excess attenuations (the dependent variable).

As before, statistical testing of the null hypothesis for all temperature parameters was conducted. Two-thirds (14 of 21) of the tested parameters disproved the null hypothesis or were assumed statistically valid, for at least one location. So, although the rate of significant correlation was less than the 100 percent rate shown for the v components of wind, the matches were still highly significant. In some cases, r values were greater than those calculated for the v components of the wind. An interesting finding is that the wind speed tended to correlate better at the front towers, whereas the temperature became more important with distance.

One interesting result occurred in Sample Period 16. A very strong inversion occurred and noise levels measured at the top microphones (10 m high) showed an increase. Noise levels at the lower microphones were relatively unaffected. These data indicate that levels at greater heights may be affected more by inversions than those near the earth's plane close to the highway. This finding coincides with the finding of Larsson (*16*). Accordingly, inversions probably show increased effects at distances greater than those of concern here due to ray bending, which was shown earlier to be not as important as turbulent scattering near the roadway.

Turbulence Effects

To eliminate effects of any preconceived biases of the researcher, many different turbulence parameters were evaluated. These parameters included the standard deviation of each wind vector at each measurement location, the intensity of turbulence for each wind vector at each measurement location, the standard deviation of each wind measurement location, the Pasquill-Gifford stability class estimations (*17*), the Richardson number, and Tatarski's refractive index structure function.

Statistical hits occurred with nearly equal frequency at all three towers. The significance at all three towers points out the importance of turbulence on traffic noise levels near roadways. The evaluation of Tatarski's turbulence index function showed a correlation at only one site, whereas the Pasquill-Gifford stability classes showed no significant correlation.

The Richardson number showed significance at Tower 3, Sites G and H. However, some absolute values of the Richardson number during evaluation proved to be quite large. Because the area of importance for the Richardson number is small values around zero, the decision was made to limit the values to the range -10 to $+10$. Using this scenario, correlation at more measurement locations disproved the null hypothesis.

The standard deviation of the wind and turbulent intensity also correlated with many statistical hits. An important trend of these correlations was that the significance close to the roadway was offset by decreased significance at the rear towers. This trend indicates that turbulent intensities are more important than other phenomena near the roadway than would be expected from data at greater distances. Indeed, it appears that the wind speed and the resulting fluctuations are the most important meteorological effects on sound levels very near roadways.

In summary, v components of the wind, temperature parameters, and turbulence are the significant parameters that should be considered in any model. Figure 4 tabulates the number of significant weather parameters tested for each of these three general weather classifications by location. Multiple correlation appears to be appropriate and would help compensate for reduced wind correlations at distances such as those associated with Tower 3, which was 122 m from the

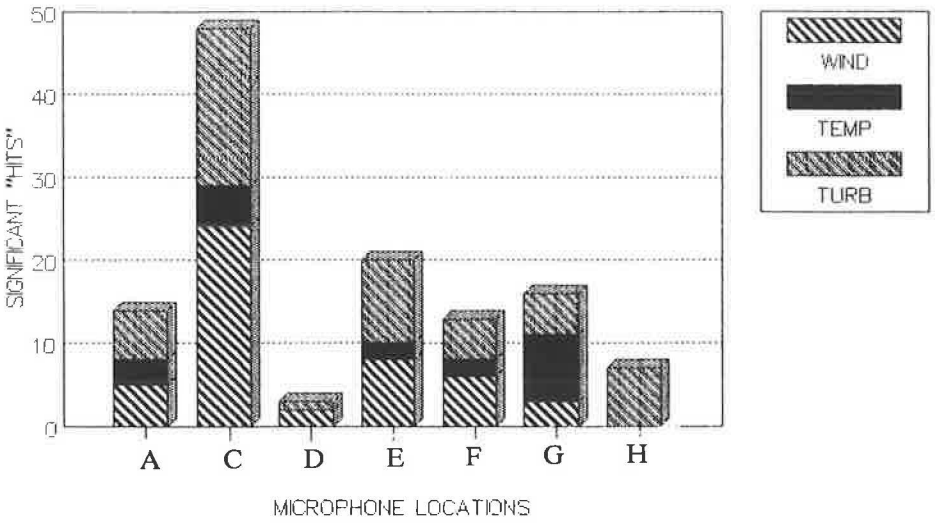

FIGURE 4 Statistical hits by location and general weather classification.

highway centerline. Multiple correlation may also compensate for reduced temperature correlation at distances less than those demonstrated at Tower 2, which was 61 m from the highway centerline.

MULTIPLE CORRELATION

The next part of the analysis centered on selection of variables for multiple correlation. Each of the three general defined classes of variables previously discussed (wind, temperature, and turbulence) were evaluated for significance. Criteria used during evaluation were significant correlation at the most locations, the largest r values, and increased predictive accuracy at all locations.

That the average wind speed is the best parameter available to characterize the wind is obvious. The selection for temperature was less obvious and included more evaluation. The lapse rate, which was significant at Towers 2 and 3, is more easily determined than the other parameters. Accordingly, the lapse rate was selected for the temperature parameter. The selection of the turbulence parameters was also difficult. Turbulent intensities were shown to be valid for the v component of the wind near the roadway, but at distances away from the roadway (i.e., at Tower 3) this could be a shortcoming. The limited Richardson number proved to be valid at all sites on Tower 3. Accordingly, statistical testing was used to determine which parameter should be selected.

When only wind components of standard deviation were included in multiple correlation testing, there were no significant correlations; r was less than 0.506. This result meant that the null hypothesis was proven at all sites. However, when the Richardson number was included as an independent variable, three locations became significant ($r \geq 0.545$). These locations were E, F, and H, with r values of 0.625, 0.550, and 0.583, respectively. Further testing by eliminating vector standard deviation components one at a time reduced the values of the correlation coefficients. Accordingly, it was determined that all three vector components of standard deviation values along with the Richardson number, lapse rate, and the average v vector wind speed should be correlated to provide the best estimate of refractive excess attenuation. For completeness, and because u components of the wind were shown to be significant with distance, all three axis components of the standard deviation of the wind were used.

Table 5 presents the results of testing with various independent variables. Terms used to describe variables tested in Tables 5 and 6 are standard deviation of wind speed perpendicular to roadway (VSTD); standard deviation of wind speed parallel to roadway (USTD); standard deviation of the vertical wind speed (WSTD); the Richardson number (RI#); thermal, vertical lapse rate (GAMMA); and average wind speed perpendicular to roadway (VAVG).

As presented in Table 5, Test 1, the r values proved to be significant ($r \geq 0.608$) at Sites C and F. To further increase the correlation, the sample periods were divided into positive and negative wind speeds as before. After separation, the correlation coefficients tended to increase and be statistically valid at more sites. For example, the positive wind speed case was statistically valid at all sites. Additionally, all correlation coefficients, except at Site G, were greater than 0.8, which is significant because it means that over 64 percent of the variance of the dependent variable can be explained by variations of the independent variables.

MODEL DEVELOPMENT

After significant parameters were identified, an analytic model based on statistical testing was derived. To accomplish this task, all refractive excess attenuations were divided by distance to normalize each measurement site. The variables are assumed to be normalized for distance henceforth. This normalization process for distance is valid because Taylor's frozen turbulence theorem was assumed. Making this assumption was similar in nature to using the ANSI standard for atmospheric absorption (but not quite as valid because of the much greater random nature and small scale of turbulence compared with those of temperature and humidity variations). However, in this work, homogeneous turbulence was assumed

TABLE 5 CORRELATION RESULTS FOR MULTIPLE REGRESSION TESTS

Test No.	Independent Variable Tested	0.95 Sign. Value	Mic A	Mic C	Mic D	Mic E	Mic F	Mic G	Mic H
1	VSTD, USTD, WSTD,RI#, GAMMA, & VAVG	0.608	0.560	0.762	0.560	0.429	0.664	0.501	0.585
2	USTD, WSTD, USTD & RI#	0.545	0.453	0.432	0.516	0.625	0.550	0.484	0.583
3	USTD, WSTD, USTD	0.506	0.361	0.339	0.312	0.483	0.468	0.334	0.457
4	USTD, USTD & RI#	0.506	0.435	0.427	0.507	0.282	0.487	0.477	0.532
5	USTD, WSTD & RI#	0.506	0.453	0.345	0.455	0.538	0.550	0.479	0.583
6	USTD, WSTD, RI#, VAVG & GAMMA (NEG CASE)	0.578	0.461	0.709	0.560	0.700	0.809	0.737	0.694
7	USTD, WSTD, RI#, VAVG & GAMMA (POS CASE)	0.578	0.897	0.764	0.796	0.776	0.788	0.605	0.823
8	USTD, WSTD, RI#, VAVG & GAMMA	0.578	0.560	0.737	0.516	0.591	0.661	0.496	0.585
9	USTD, USTD, WSTD, RI# GAMMA & VAVG (NEG CASE)	0.608	0.488	0.736	0.568	0.700	0.657	0.781	0.729
10	USTD, USTD, WSTD, RI# GAMMA, & VAVG (POS CASE)	0.608	0.907	0.874	0.809	0.843	0.802	0.612	0.823

in the sound propagation path at the relatively short distances of concern. Additionally, because ground attenuation was normalized in the calculation procedure, the effect of height was minimized and not accounted for in model development.

The excess attenuations, now on a consistent basis for distance, were averaged to form a single dependent variable for each sample period. In this way, each sample period was reduced to a single refractive excess attenuation normalized for distance that could be expected for the meteorology values measured during that sample period.

Table 6 presents correlation coefficients calculated using combinations of the variables determined to be significant. If the data are considered collectively, Tests 9 and 10 disprove the null hypothesis. Independent variables of Test 9 included the average wind speed and lapse rate. Test 10 included the standard deviation of the u vector coordinate wind speed, the lapse rate, the limited Richardson number, and the average wind speed.

However, if the data sets are once again divided into positive and negative wind speed vectors, one-half of the selected variable combinations disprove the null hypothesis for the positive case. For the negative case, 6 of the 10 tests disprove the null hypothesis. From a review of Table 6 it can be seen that many of the correlation coefficients exceed 0.7. Correlation values of this magnitude are considered to be quite good on the basis of past experience with air pollution modeling.

The best fit of the data, as expected, occurs when all variables that were determined to be significant are included. For the positive wind speed case, a value for r of 0.807 was calculated. For the negative wind speed case, the r value was calculated to be 0.785. From this evaluation of the data, a model was developed to predict refractive excess attenuations from traffic sources. The derived model is presented in two parts—the positive wind speed case and the negative wind speed case. Accordingly, to use this model, the sign of the wind speed must be determined before proceeding.

For the positive wind speed case,

$$A_{ref} = [-26.4 - 131.3(\gamma) + 23.4(\text{VAVG}) - 1.2(\text{Ri}) - 38.6(\text{WSTD}) - 70.2(\text{VSTD}) + 73.7(\text{USTD})]/1000 \quad (\text{dB/m}) \qquad (4)$$

Variables are as previously defined. The standard error of estimate for this model is 0.019 dB/m. Of note is the left side of Equation 4. The refractive excess attenuation is divided by distance and has the units dB per meter. After Equation 4 is evaluated, the user must multiply by the propagation path distance to determine the absolute refractive excess attenuation. The denominator on the right side of Equation 4 was

TABLE 6 CORRELATION RESULTS OF VARIOUS MODELING SCENARIOS

Case No.	Critical Absolute Value of Significance (0.95 Sign. Level)	Correlation Coefficient
Pos & Neg Wind		
1	0.632	0.574
2	0.506	0.314
3	0.545	0.316
4	0.601	0.467
5	0.601	0.573
6	0.601	0.370
7	0.506	0.496
8	0.454	0.274
9	0.454	0.494
10	0.545	0.559
Neg Wind Only		
1	0.768	0.785
2	0.664	0.400
3	0.703	0.744
4	0.739	0.780
5	0.739	0.680
6	0.739	0.773
7	0.664	0.665
8	0.608	0.659
9	0.608	0.495
10	0.703	0.667
Pos Wind Only		
1	0.787	0.807
2	0.683	0.690
3	0.722	0.697
4	0.758	0.758
5	0.758	0.785
6	0.758	0.768
7	0.683	0.634
8	0.627	0.633
9	0.627	0.501
10	0.722	0.662

Case Descriptions:

1. VARIABLES = RI#, USTD, VSTD, WSTD, VAVG, GAMMA
2. VARIABLES = USTD, VSTD, WSTD
3. VARIABLES = RI#, USTD, VSTD, WSTD
4. VARIABLES = RI#, USTD, VSTD, WSTD, VAVG
5. VARIABLES = USTD, VSTD, WSTD, VAVG, GAMMA
6. VARIABLES = RI#, USTD, VSTD, WSTD, GAMMA
7. VARIABLES = RI#, VAVG, GAMMA
8. VARIABLES = RI#, GAMMA
9. VARIABLES = VAVG, GAMMA
10. VARIABLES = RI#, USTD, VAVG, GAMMA

added for convenience because the calculated variable coefficients were very small numbers.

For the negative wind speed case,

$$A_{ref} = [33.4 + 107.3(\gamma) + 4.6(VAVG) + 3.9(Ri) - 150.5(WSTD) - 15.6(VSTD) - 26.2(USTD)]/1000 \quad (dB/m) \quad (5)$$

As before, variables are as previously defined (VAVG is a negative quantity). The use of this equation is the same as that of the positive wind speed equation; the user must multiply by propagation path distance to obtain an absolute value of the refractive excess attenuation. The standard error of estimate for Equation 5 is 0.015 dB/m.

These models have been developed for short-range propagation typical of first- and second-row homes at the first- and second-floor heights. Additionally, measurements were

taken during free-field propagation and the model validated only from approximately 10 to 100 m from the highway in perpendicular distance. Validation efforts could be done to extend these limits.

These results must also be presented with a word of caution. Although the data base is considered the best developed for short-range traffic noise propagation concurrently with weather data, data have been taken at only a single location. More measurements are needed at additional sites to validate and refine this analysis.

CONCLUSIONS

Specific findings and conclusions reported in this paper are as follows:

- Atmospheric phenomena may affect traffic noise levels even very close to the roadway;
- The components of the wind speed parallel and vertical to the highway may become important at approximately 120 m from the highway, a distance typically associated with second-row receivers;
- Deviations in noise levels due to refraction were measured to be 7.7 dB at 122 m from the centerline of the highway, 4.3 dB at 61 m from the centerline, and 6.6 dB at only 38.1 m from the centerline;
- Turbulent scattering of noise from skywaves appears to be a prominent mechanism in increasing noise levels above that expected close to the earth's plane near the roadway;
- At very close distances to the highway, the angle formed by the receiver location and highway is more important than the elevation of the receiver;
- Ray bending due to wind shear and temperature lapse rates does not appear to be as important as turbulent scattering very near the roadway;
- For distances beyond 38.1 m from the roadway, similar refractive excess attenuations appear to occur at equal heights above the ground plane;
- Regression analysis shows that negative and positive perpendicular components of the wind should be modeled separately for increased accuracy;
- Temperature lapse rates do not exert significant influence on refractive excess attenuations within 61 m of the roadway, but become important with increased distance such as beyond 122 m;
- Strong inversions do not appear to significantly affect refractive excess attenuations within 122 m of the roadway near the earth's plane but become significant with height;
- Turbulence appears to have an effect comparable to that of the combined wind and temperature parameters within 122 m of the roadway; and,
- A combination of all three vector component standard deviations of wind speed, Richardson number, lapse rate, and wind speeds perpendicular to the roadway appear to form an effective model with very good correlation results.

DIRECTIONS FOR FUTURE RESEARCH

Atmospheric effects on traffic noise propagation have not been well researched. While this research effort has added to the topic, much more research is needed. In general, three important areas of research are needed—more measurements, more theoretical development, and better characterization of the turbulence close to roadways.

The data base created by the measurements for this project is the most detailed known for traffic noise and concurrent meteorology very near roadways. However, the data are for a single site and probably contain some site bias. Additionally, the data are for a flat open area and do not include the effects of diffraction that are important to the development of noise walls. Multisite measurements are needed to validate and refine this initial work. The model developed is based on statistical methods. Much more work is needed to incorporate theory into the prediction process. Another area of future research relates to a basic meteorological science. Better methods that apply to air pollution prediction as well as traffic noise are needed to characterize turbulence along roadways.

After validation, the results of the derived mathematical models (Equations 4 and 5) could be used to correct results from prediction models such as STAMINA. To accomplish this, excess attenuation would have to be determined using Equations 4 and 5 and results subtracted from the predicted results of the model used. The weather data collection effort would add some cost to the overall project, including costs for equipment, labor, and time. Cost from project to project would vary, but would be small when compared to the cost of an ineffective barrier. Accordingly, the additional cost would be well worthwhile to help ensure proper design.

ACKNOWLEDGMENT

The authors would like to acknowledge the help and support of the Texas State Department of Highways and Public Transportation, Texas A&M University, and Scantek Electronics, without whose help this research could not have been performed.

REFERENCES

1. L. L. Beranek (ed.). *Noise and Vibration Control, Revised Edition.* Institute of Noise Control Engineering, Washington, D.C., 1988.
2. T. M. Barry and J. A. Reagan. *FHWA Highway Traffic Noise Prediction Model.* FHWA-RD-77-108, FHWA, U.S. Department of Transportation, 1978.
3. L. F. Richardson. Some Measurements of Atmospheric Turbulence. *Philosophical Transactions of the Royal Society*, Series A, Vol. 221, London, 1920, pp. 1–28.
4. V. I. Tatarski. *The Effects of the Turbulent Atmospheric on Wave Propagation.* Keter, Jerusalem, Israel, 1971.
5. SPSS-X Inc. *SPSS-X User Guide, 3rd Ed.* Chicago, Ill., 1988.
6. W. Bowlby, J. Higgins, and J. A. Reagan (eds.). *Noise Barrier Cost Reduction Procedure, STAMINA 2.0/OPTIMA: User's Manual.* FHWA-DP-58-1, FHWA, U.S. Department of Transportation, Arlington, Va., 1982.
7. E. L. Crow, F. A. Davis, and M. W. Maxfield. *Statistics Manual.* Formerly NAVORD Report 3369-NOTS 948, Dover, New York, 1960.
8. S. I. Hayek, J. M. Lawther, R. E. Kendig, and K. T. Simowitz. *Investigation of Selected Noise Barrier Acoustical Parameters.* NCHRP Final Report, Pennsylvania State University, University Park, 1977.
9. American National Standards Institute. *Method for the Calculation of the Absorption of Sound by the Atmosphere.* ANSI S1.26-1978, New York, 1978.

10. K. U. Ingard. The Physics of Outdoor Sound. In *Proc., 4th Annual Noise Abatement Symposium*, 1955, pp. 11–25.
11. P. H. Parkin and W. E. Scholes. The Horizontal Propagation of Sound from a Jet Engine Close to the Ground at Hatfield. *Journal of Sound and Vibration*, Vol. 2, No. 4, 1965, pp. 353–374.
12. E. A. G. Shaw and N. Olson. Theory of Steady-State Urban Noise for an Ideal Homogeneous City. *Journal of the Acoustical Society of America*, Vol. 51, No. 6, 1972, pp. 1781–1793.
13. G. S. Anderson. *Single-Truck, Blue-Route Noise Levels at Swathmore College*. Pennsylvania Department of Transportation Draft Report, Philadelphia, 1986.
14. A. D. Pierce. *Acoustics: An Introduction to Its Physical Principles and Applications*. McGraw Hill, New York, 1981.
15. G. I. Taylor. The Spectrum of Turbulence. *Proc., Royal Society*, Series A, No. 1964, London, 1938, pp. 453–465.
16. C. Larsson, S. Israelsson, and H. Jonasson. *The Effects of Meteorological Parameters on the Propagation of Noise from a Traffic Route*. Report 54, Meteorological Institute of the University of Uppsala, Uppsala, Sweden, 1979.
17. D. B. Turner. *Workbook of Atmospheric Dispersion Estimates*. U.S. Environmental Protection Agency, Washington, D.C., 1970.

APPENDIX

RICHARDSON NUMBER

$$\mathrm{Ri} = (g/T_A)\{(\gamma - \Gamma)/[(du/dZ)^2]\} \quad \text{(A-1)}$$

where

g = gravitational acceleration,
u = average wind speed,
γ = existing (or true) lapse rate,
Γ = adiabatic lapse rate,
T_A = absolute ambient temperature, and
Z = height between measured locations.

TATARSKI'S REFRACTIVE INDEX FUNCTION

$$(C_n)^2 = (C_T)^2/4(T_0)^2 + (C_v)^2/(c_0)^2 \quad \text{(A-2)}$$

where

T_0 = absolute temperature,
c_0 = phase velocity,
$(C_v)^2$ = mechanical turbulence structure, and
$(C_T)^2$ = thermal structure function.

The mechanical turbulence structure is given by

$$(C_v)^2 = (V_1 - V_2)^2(r)^{0.667} \quad \text{(A-3)}$$

The thermal structure function is defined as

$$(C_T)^2 = (T_1 - T_2)^2(r)^{0.667} \quad \text{(A-4)}$$

In these equations,

V_1, V_2 = fluctuating wind velocities at two points separated by a distance r, and
T_1, T_2 = fluctuating temperatures at two points separated by a distance r.

Publication of this paper sponsored by Committee on Transportation-Related Noise and Vibration.

Predicting Stop-and-Go Traffic Noise With STAMINA 2.0

WILLIAM BOWLBY, ROGER L. WAYSON, AND ROBERT E. STAMMER, JR.

The STAMINA 2.0 computer program is the most commonly used method for prediction of traffic noise levels for impact analysis and noise barrier design. However, the program was based on theory for freely flowing vehicles at a constant speed. The work presented in this paper represents development of a methodology to use STAMINA 2.0 in nonconstant speed situations, such as signalized intersections, intersections with Stop signs, tollbooths, and highway loop and slip ramps. Through a review of literature and collection of new emission levels on accelerating, decelerating, and cruising heavy trucks, a data base was established for the methodology. The concept of zone of influence (ZOI) was used to represent stretches of road on which acceleration or deceleration occurs and on which sound levels may vary from cruise condition levels. Two series of equivalent constant speeds (one for acceleration, one for deceleration) were developed, permitting STAMINA 2.0 to calculate the desired difference in noise level relative to cruise on the basis of the findings of the literature review and field data analysis. Validation at two sites containing intersections produced results within 1 dB of predictions at all measurement points after refinement of the preliminary ZOI lengths and after calibration of the cruise predictions.

This paper presents the results of a study for the National Cooperative Highway Research Program (NCHRP) on predicting stop-and-go traffic noise with the STAMINA 2.0 traffic noise prediction computer program. The purpose of the study was to develop a method for using the STAMINA 2.0 program for nonconstant speed situations. There were two major tasks: (a) to study the existing literature and (b) to collect additional data as needed. The scope did not include development of any new computer programs. Also, the method had to be easy to use by the typical noise analyst.

APPLICABLE SITUATIONS

The first task was to define the universe of changing-speed situations and then to narrow that universe down to an acceptable subset for this research. The changing-speed situations can be categorized in six ways:

1. Areas in which there is congestion or unstable flow, such as level-of-service (LOS) F on highways, or LOS E or F for intersections;
2. Urban city street networks in which there are a large number of traffic signals in a highly reverberant area;
3. Highway entrance, exit, and transition ramps;
4. Suburban situations in which there are signalized arterials but no highly reverberant sound fields because of closely spaced buildings;
5. Areas with stop signs, but again no highly reverberant field; and
6. Highway toll booths, at which traffic decelerates to a stop and then accelerates back to cruising speed, similar to the case of the Stop sign.

The first two situations were not within the scope of this work. The first, congested or unstable flow, was not a condition toward which a designer would work. The second, urban street networks with highly reverberant sound fields, was a situation with which the STAMINA 2.0 program is not designed to deal. The last four situations, however, were all appropriate to be included in the scope of this study. After an examination of these four situations, the scope of study focused on three areas: (a) unsignalized (but signed) intersections, (b) signalized intersections, and (c) loop or slip transition ramps. The case of the unsignalized or signalized intersection could include the beginning or end of a ramp between a local highway or street and an arterial highway.

CURRENT FHWA RECOMMENDATIONS

The current FHWA recommendations for dealing with changing-speed or low-speed situations are contained in Appendix I of the *FHWA Highway Traffic Noise Prediction Model* (*1*). When speeds are below 30 mph, FHWA recommends that the analyst use a constant automobile noise emission level equal to the level at 30 mph. However, the FHWA model includes speed in a negative logarithmic function for the traffic flow adjustment calculation as well as in a positive logarithmic function for the noise emission level calculation. The result is that use of a constant noise emission level and these adjustments will actually cause the 1-hr equivalent sound level [L_{eq}(1h)] to increase as the average operating speed decreases.

For medium trucks, FHWA recommends the same strategy—to use the noise emission level at 30 mph. This procedure results in the same effect as for automobiles—an increasing L_{eq}(1h) as speed drops below 30 mph. For heavy trucks, FHWA recommends using the 87-dB emission level at approximately 62 mph when speeds drop below 30 mph. In terms of the effects on L_{eq}(1h) this use represents a 7-dB stepped increase in the levels as the speed drops below 30 mph and then a further increase in the hourly L_{eq}(1h) as the speeds drop lower. The result of the recommendation is that the L_{eq}(1h) for trucks below 30 mph is higher than the L_{eq}(1h) for trucks traveling 60 mph.

Vanderbilt Engineering Center for Transportation Operations and Research, Vanderbilt University, Box 96, Station B, Nashville, Tenn. 37235.

RELEVANT LITERATURE

The first task in this work was to study existing literature. Most U.S. literature has focused on constant speed situations (*2*). Several useful European studies were found, including work by Lewis and James in 1980 (*3*). These researchers measured individual vehicle sound level changes at various distances from a traffic circle (roundabout) along the approach (deceleration) and departure (acceleration) roads. Three sites were studied with data for both trucks and cars. For the approach situation, the authors found that in all cases the levels dropped off smoothly as the distance to the roundabout decreased. However, for the departure cases, they found a fluctuation in the levels with increasing distance away from the roundabout. Generally, the levels first decreased and then increased, and finally either decreased or continued to increase, depending on the final speed.

Work in foreign countries has also focused on simulating traffic flow toward and away from a signal. In 1978, Favre (*4*) published the results of a simulation study of the effect on L_1 and L_{eq} for a mix of traffic approaching a signal, stopping, and then accelerating away from the signal. His results showed that the noise levels decreased during deceleration to a low point at about 160 ft behind the signal, which accounted for the queuing of vehicles waiting for the signal to change. He also found that the noise levels then increased as traffic accelerated away from the traffic signal, and then finally decreased before settling out to a constant level. Limited field data supported these simulation results.

As noted, most of the U.S. data focused on constant speed situations. However, a good data base for this study was developed for the U.S. Environmental Protection Agency (EPA) for its National Traffic Noise Exposure Model (*5*). Data were presented for a number of vehicle types for four operating modes: cruise, acceleration, deceleration, and idle. However, the noise emission levels were presented as average levels over the entire acceleration or deceleration event for an observer moving alongside the vehicle at a reference offset distance of 50 ft. This assumption greatly simplified the EPA model for predicting national exposure to traffic noise, but posed complications for a site-specific analysis such as those done with STAMINA 2.0.

Nevertheless, the data were still able to be used in this study after some manipulation and additional analysis. The EPA report presented emission levels averaged separately for events with the following speed ranges: 0 to 20, 0 to 30, 0 to 40, 0 to 50, and 0 to 60 mph. However, noise emission levels averaged over entire events would not be as useful for this work as noise emission levels that were more related to specific speeds. Using standard AASHTO vehicle acceleration rates (*6*), the times for a vehicle to go from 0 mph to various final speeds could be computed. Given these times and the average levels for acceleration from stopped to two different final speeds, average levels for the intermediate speed range between those two final speeds could be approximated as follows:

$$L_{(x-y)} = 10\log\{[1/(t_y - t_x)]\,[(t_y)(10^{0.1L_y}) - (t_x)(10^{0.1L_x})]\} \quad (1)$$

where

$L_{(x-y)}$ = averaged level while the vehicle accelerates from x to y mph,
L_x = averaged level while the vehicle accelerates from 0 to x mph,
L_y = averaged level while the vehicle accelerates from 0 to y mph,
t_x = time to accelerate from 0 to x mph, and
t_y = time to accelerate from 0 to y mph.

For example, the average automobile noise emission level for a 0- to 40-mph acceleration event, according to EPA, was 64.1 dB. The average level for a 0- to 60-mph event was 67.4 dB. The time to accelerate from a stop may be computed as 18 sec for a final speed of 40 mph and 27 sec for a final speed of 60 mph. By Equation 1, the average level during the 30- to 60-mph acceleration is 70.5 dB. Similarly, the average levels can be computed for speed changes of 20 to 30 mph, 30 to 40 mph, 40 to 50 mph, and 50 to 60 mph, giving a stepwise speed profile for automobile acceleration. The EPA deceleration data were analyzed in a similar manner.

STUDYING THE ACCELERATION PHENOMENON

The next step was to gain a better understanding of the effect of the acceleration phenomenon on traffic noise levels. A small-timestep simulator was devised (using conventional spreadsheet software) for computation of the sound level at any given second during a vehicle passby event and subsequent plotting of the results.

Shown in Figure 1 are plots for an automobile cruise event at 60 mph and for an acceleration event (from 0 to 30 mph) for a receiver located 100 ft downstream from a Stop sign. In both cases, the receiver is located at an offset distance of 50 ft from the centerline of travel. For the cruise event, the vehicle is assumed to pass the receiver at time $t = 0$ sec. Note the symmetrical shape of the sound level profile time history. The computed sound exposure level (SEL) for this event was 76 dB. For the acceleration event, note the asymmetrical time history. The event begins at an arbitrarily assigned time of $t = -20$ sec and passes the receiver at a time of $t = -11$ sec; in other words, it takes 9 sec for the vehicle to accelerate from a stopped position to a position 100 ft downstream. The SEL value for this acceleration event was 70 dB, or 6 dB below the 60-mph cruise event.

Use of the simulator allowed the distance downstream for the receiver position to be varied to gain a better understanding of the effects. In general, as the receiver moved further downstream from the starting point, the sound level profile became more symmetrical.

Through use of the automatic calculation features of the spreadsheet, the SEL could be generated at a sequence of distances from the start for a particular event and then plotted. Figure 2 shows such an event for an automobile accelerating to 30 mph (open boxes on the graph), compared with the SEL from an automobile traveling at a constant 30 mph (solid boxes). Note the similarity in shape to the measured data shown earlier by Lewis and James (*3*)—a decrease in the levels, then an increase, and finally another decrease. Through

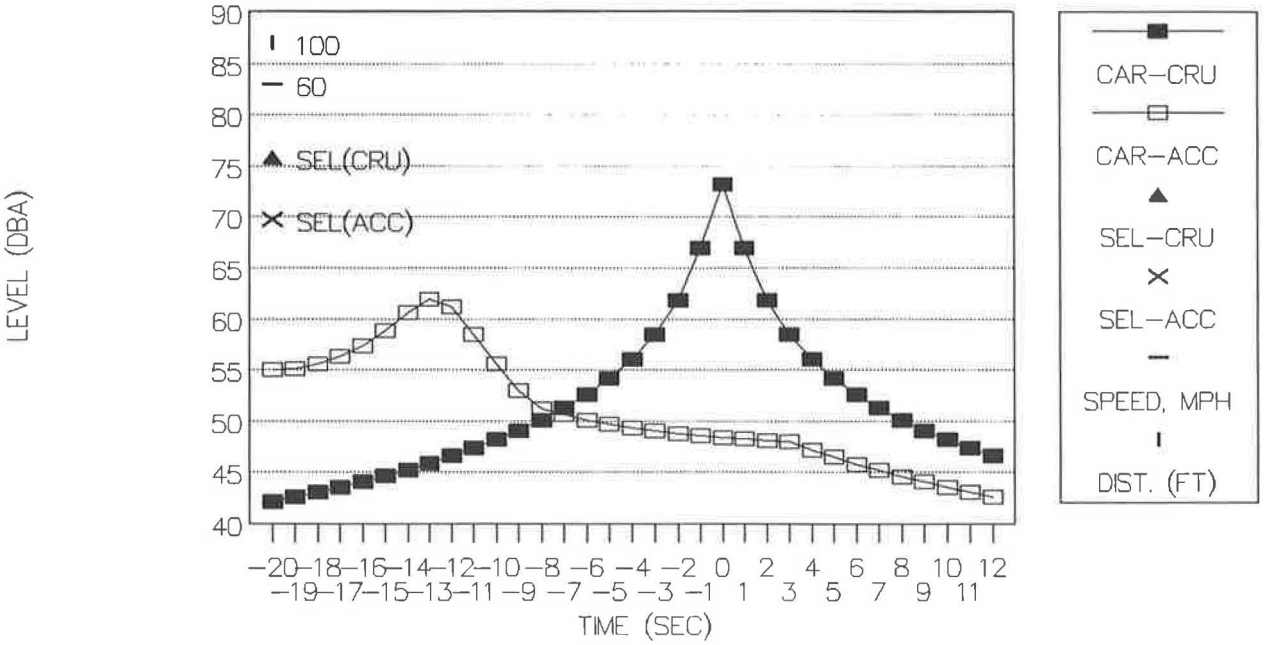

FIGURE 1 Predicted sound level time histories at a 50-ft offset distance for an individual car (a) cruising at 60 mph and (b) accelerating to 60 mph at a longitudinal distance of 100 ft from the start of acceleration.

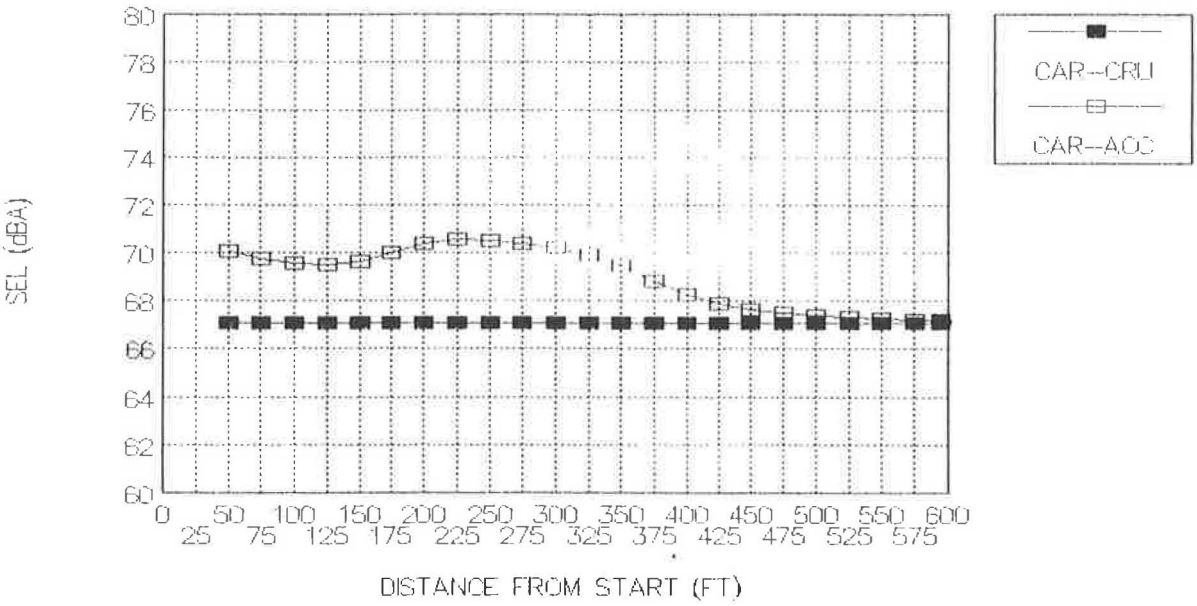

FIGURE 2 Predicted SEL at a 50-ft offset distance (a) at various distances from start for a car accelerating to 30 mph per EPA data and (b) cruising at 30 mph.

the use of the timestep simulation programs, tests could be run on the effects of the FHWA model assumptions, the EPA data base, and this study's measured data for heavy trucks.

FIELD-MEASURED DATA

Although some medium truck and automobile levels were measured, most of the data collection for this study focused on heavy trucks because of the importance of their contribution to overall received sound levels. The measurement sites were at two truck weigh stations on I-65 north of Nashville, Tenn. These sites were relatively flat and level, allowing analyzers to be set at a series of distances along the acceleration and deceleration lanes as well as downstream where the trucks were cruising at full speed. Trucks were measured simultaneously, three or four points at a time, allowing individual events at the different sites to be paired for analysis.

Care was taken to collect clean passbys, unaffected by other trucks at the weigh station or by automobile noise on the highway.

Time-Averaged Noise Levels

One of the first steps was to simply measure the L_{eq} for a series of 4-min periods simultaneously, at the cruise site, on the acceleration ramp, and on the deceleration ramp of one of the weigh stations, at an offset distance of 50 ft from the center of the travel lane. These data, shown in Figure 3, gave information on the effects of the various operating modes on the time-averaged level. The deceleration data were typically 6 to 9 dB below the cruise data at 60 mph, whereas the acceleration data were 0 to 4 dB below the cruise data. Note that these samples do not precisely represent the same vehicle populations because several minutes was required for a truck to decelerate, be weighed, accelerate, and finally pass the cruise site. Nonetheless, the trends are apparent. A similar series of 10-min L_{eq} measurements (not shown) at the cruise site and at three points along the acceleration ramp indicated that the L_{eq} values increased with increasing distance from the stopline. In all cases, the acceleration levels were less than the cruise levels when the vehicles were traveling at about 60 mph.

Noise Emission Level Data

With this better understanding of the anticipated effects, the noise emission level measurements were conducted. Both maximum level (L_{max}) and SEL data were collected on individual trucks. Figure 4 shows histograms of the sampled cruise events for both parameters. There is a fairly broad distribution and slight skew to the L_{max} data. However, the SEL data are more narrowly distributed, and in more of a Gaussian-shaped curve, with a mean of approximately 88 dB.

Figure 5 shows the aggregate results at the acceleration sites. The downstream distances range from 75 to 875 ft, all at a 50-ft offset distance. The mean SEL value was about 85 dB, or 2 to 3 dB below that of the trucks cruising at 60 mph. The tightness of the distribution suggests that a constant-acceleration SEL could be used, at least over the measured distance ranges (with a standard deviation very similar to that for the cruise data).

Figure 6 shows the deceleration data, aggregated over distances ranging from 175 to 475 ft before the stopline. Again, there is a broader, more skewed distribution for L_{max} values and a tighter, more symmetrical distribution for SEL values. The mean SEL value is about 79 dB or about 8 to 9 dB below that for the cruise condition.

The next step was to try to disaggregate the data by distance from the stopline. The distance dependence of both SEL and L_{max} is shown in Figure 7, but the relatively small variation for SEL is less than 2 dB between 75 and 875 ft. Figure 8 shows similar data for the deceleration sites. Again, the variation in mean SEL, at least to the 255-ft site, is only about 2 dB. The mean SEL at 175 ft, however, is 3 dB below that at 255 ft. This sharp decrease in the final stages of deceleration matches other results in the literature. The deceleration data are far below the data values for the cruise site.

ZONES OF INFLUENCES

On the basis of the findings from data collection and the literature review, it was decided to adopt the concept of zone of influence (ZOI) for modeling purposes. A ZOI is defined as an area in which the sound level changes because of acceleration or deceleration events. To create a methodology for

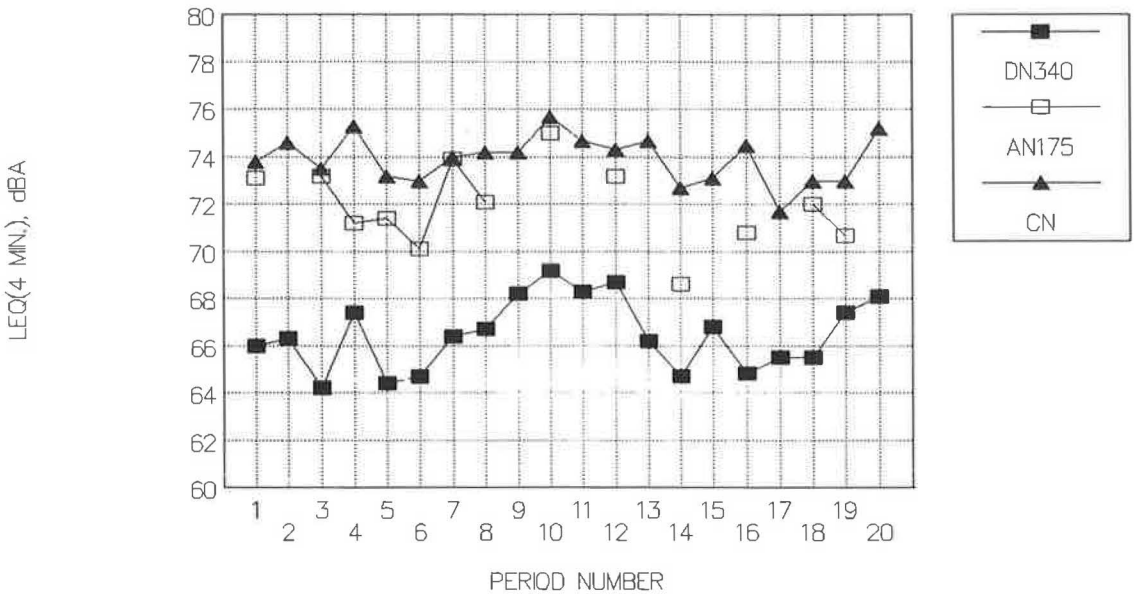

FIGURE 3 L_{eq}(4-min) samples at I-65NB weigh station at deceleration (DN340), acceleration (AN175), and cruise (CN) sites, June 1, 1988.

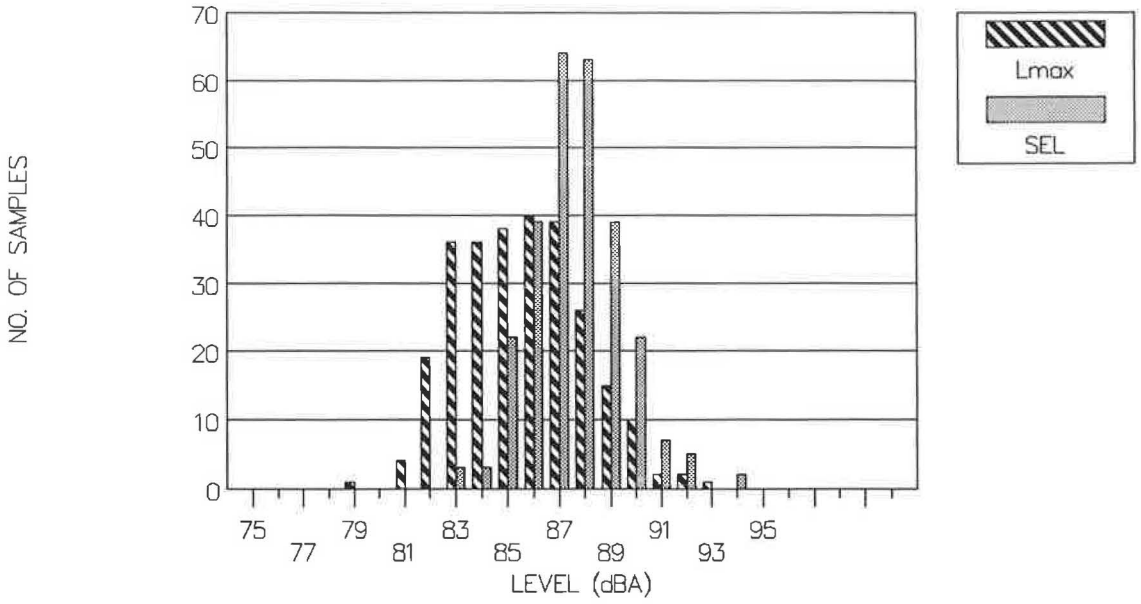

FIGURE 4 Distribution of sampled heavy truck emission level data for cruise site (55 to 65 mph, 50-ft offset).

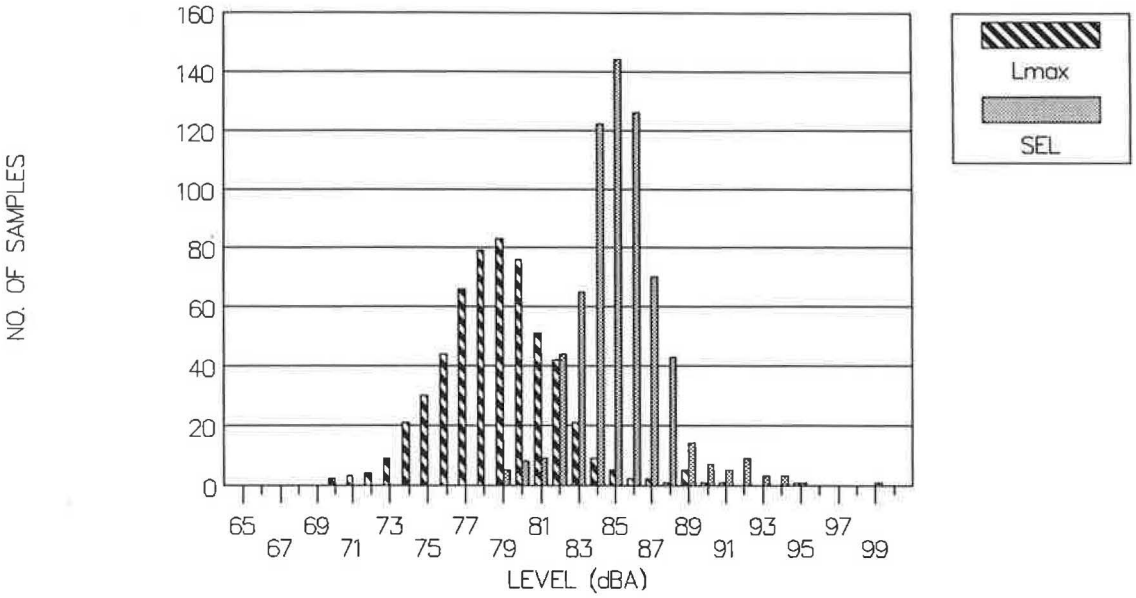

FIGURE 5 Distribution of sampled heavy truck emission level data along acceleration lane at 75 to 875 ft from stopline (50-ft offset).

the STAMINA 2.0 program, it was important to minimize the number of ZOIs that an analyst would be required to code as roadways for STAMINA 2.0. The data suggested that the number of ZOIs could be limited to two each for acceleration and deceleration with little loss in accuracy. Figure 9 shows these ZOIs.

After substantial analysis and validation, with the goal of minimizing predicted error, two tables, one for acceleration and one for deceleration, were developed that gave the recommended lengths for ZOIs. If the effects on SEL values observed in the field data were simulated, then the same effect on the predicted L_{eq} would be predicted, on the basis of the definitions for SEL and L_{eq}.

Tables 1 and 2 present a series of acceleration or deceleration ranges in terms of initial and final speeds and the recommended lengths for the first and second ZOI for each operating mode. In some cases, only one ZOI was needed to approximate a particular speed range. By using these tables as part of a step-by-step design guide presented in the final report for the project, an analyst could model signalized inter-

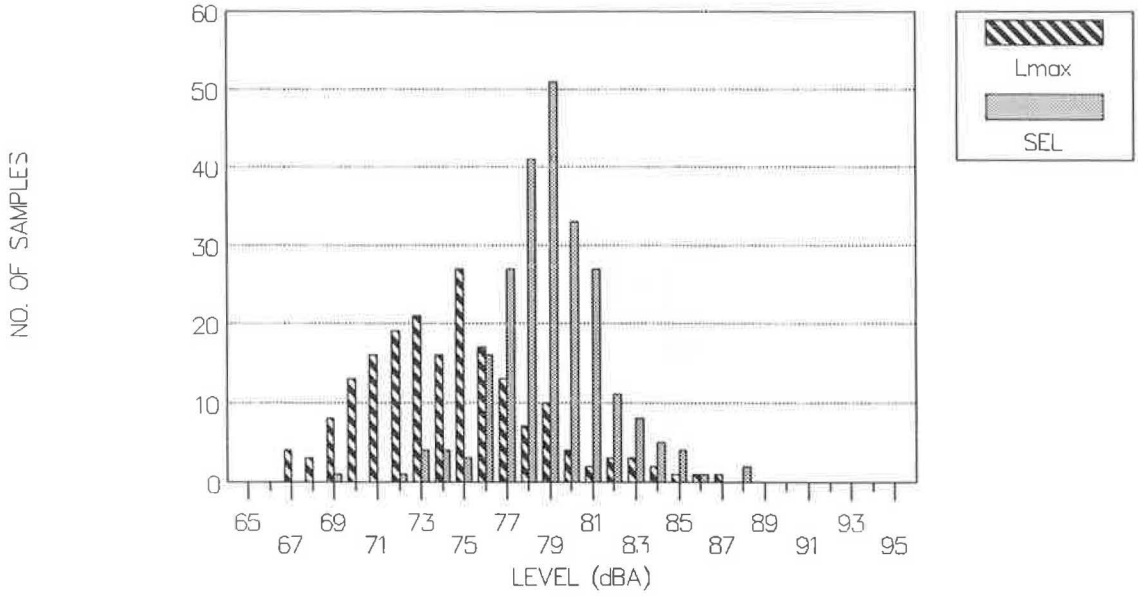

FIGURE 6 Distribution of sampled heavy truck emission level data along deceleration lane at 175 to 475 ft before stopline (50-ft offset).

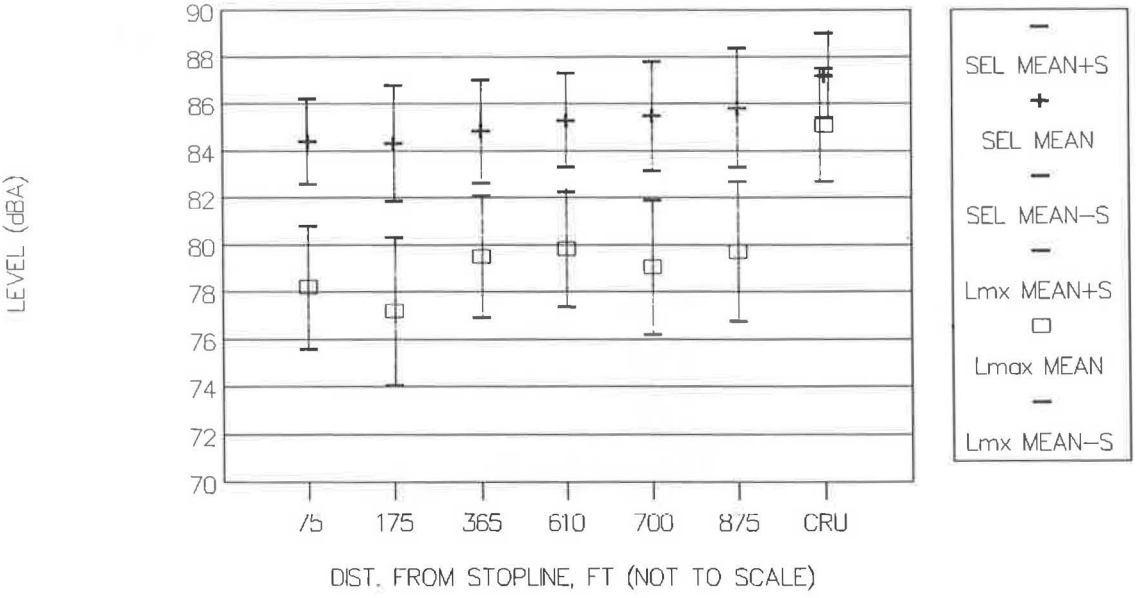

FIGURE 7 Mean and standard error of heavy truck emission level data for acceleration as function of distance from the stopline.

sections, unsignalized intersections, and highway ramps as a series of STAMINA 2.0 roadways.

The speeds given in these tables are not average operating speeds, but equivalent speeds that would produce the desired effect on the SEL values and hence the L_{eq} values at incremental distances on either side of a stopping point.

SENSITIVITY ANALYSIS

As part of the methodology development, a sensitivity analysis of parameters such as speed, distance, and percent of interrupted flow was performed. Figure 10 shows an example of L_{eq} profiles for a flow of 1,000 automobiles, 50 medium trucks, and 100 heavy trucks with a cruise speed before and after the stopping zone of 60 mph (flow is from left to right with the stopping point at 0 ft). Total L_{eq} values as well as the L_{eq} values for each vehicle type are shown. A decrease in L_{eq} of up to 6 dB relative to cruise occurs at a point somewhat behind the stopping line (which is located in the second of the deceleration zones).

Shown in Figure 11 is the same type of acoustical profile (L_{eq} as a function of receiver distance upstream or downstream) for cruise speeds of 30, 40, 50, and 60 mph. For all

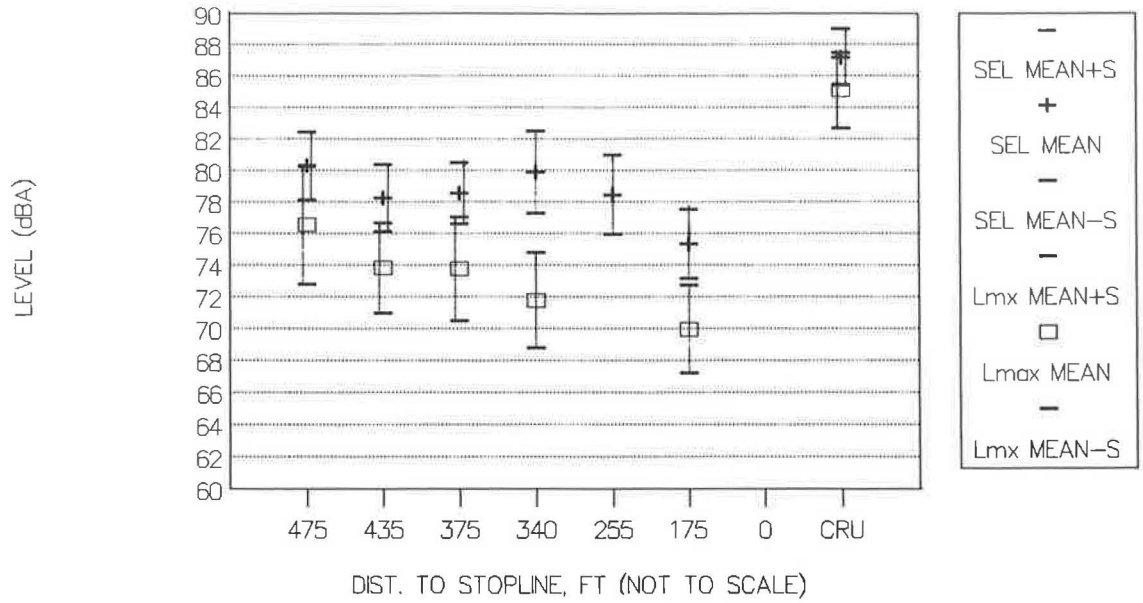

FIGURE 8 Mean and standard error of heavy truck emission level data for deceleration as function of distance from stopline.

cases, the deceleration levels are less than the cruise levels, but the acceleration levels are either greater or less than the cruise levels, depending on the final cruise speed.

Figure 12 shows the effects of introducing a percentage of nonslowing traffic through the stopline, as might happen at a signalized intersection. Once the proportion of cruise-through traffic exceeds 50 percent, the difference in levels relative to 100 percent cruise-through is less than 2 dB.

Finally, the sensitivity analysis examined the effect of increasing the receiver distance away from the modeled roadways. In Figure 13, the effect, which exceeds 6 dB for an offset distance of 50 ft, decreases to less than 2 dB by the time the receiver is offset 1,600 ft from the center of the travel lane. Also, the effect tends to broaden (while decreasing in magnitude) because of contributions from adjoining cruise speed roadway segments.

VALIDATION

As part of the method development, a limited validation was called for in the project scope. Two signalized intersection sites were chosen, one in a suburban area with two intersecting two-lane roads, and one in a slightly more urbanized area where a four-lane arterial with turning lanes intersected a two-lane local street.

Site 1

At the first site, monitors were set at two points on the deceleration side of the southbound lane and at five points on the acceleration side, as well as at a cruise speed position. Measurements were made for different periods over a 2-day span, with not all points being monitored at the same time. However, there were common points between sets of measurements, allowing comparison of all of these points.

Figure 14 shows a comparison of the measured and predicted levels for one of the measured hourly periods at Site 1. The lower curve (solid boxes) showed the measured hourly L_{eq} at each site. Notable were the lower levels in the deceleration range, the effects of the cross-street traffic near the intersection, and the increased level during acceleration.

The first attempt to predict the levels at this site used a 55-45 percent split between the stopping and the cruise-through traffic based on the observed signal cycle splits. The initial predicted results were 2.5 to 4 dB higher than measured. A return visit to the site and detailed observation of the actual number of vehicles stopping showed that fewer than 25 percent were able to cruise through at the posted speed of 50 mph on the north side of the intersection and 55 mph on the south side of the site.

When all traffic was modeled as stopping, the agreement between the measured and predicted levels was very good in the acceleration sites but still about 1.5 dB high in the deceleration sites. The original technique for modeling the ZOIs was then examined, using a detailed five-zone representation to model the changing deceleration levels more precisely. The results showed that by increasing the length of the deceleration zone nearest the signal by an additional 100 ft, the predicted levels at all points were within 1 dB of the measured levels and within 0.5 dB for the acceleration sites.

Site 2

Data were collected at the second validation site at one deceleration point, three acceleration points, and a cruise site. Figure 15 shows the measured (open boxes) and predicted levels at those points. An increased level occurred at the site that was 360 ft from the stopline. A closer examination in the field revealed that a solid wooden fence was located on the opposite side of the road from this microphone and that a reflection of the traffic noise was observable.

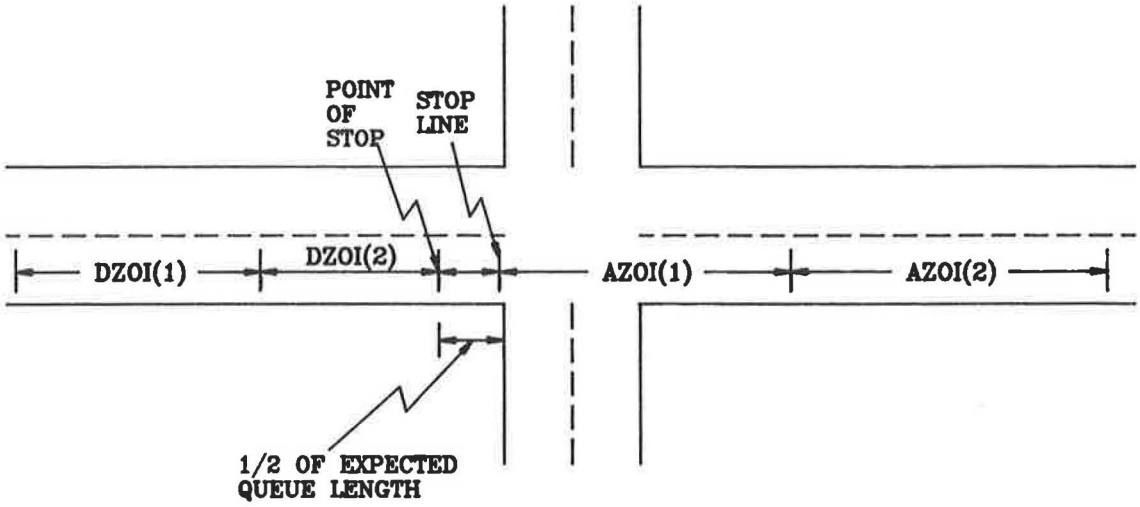

SIGNALIZED

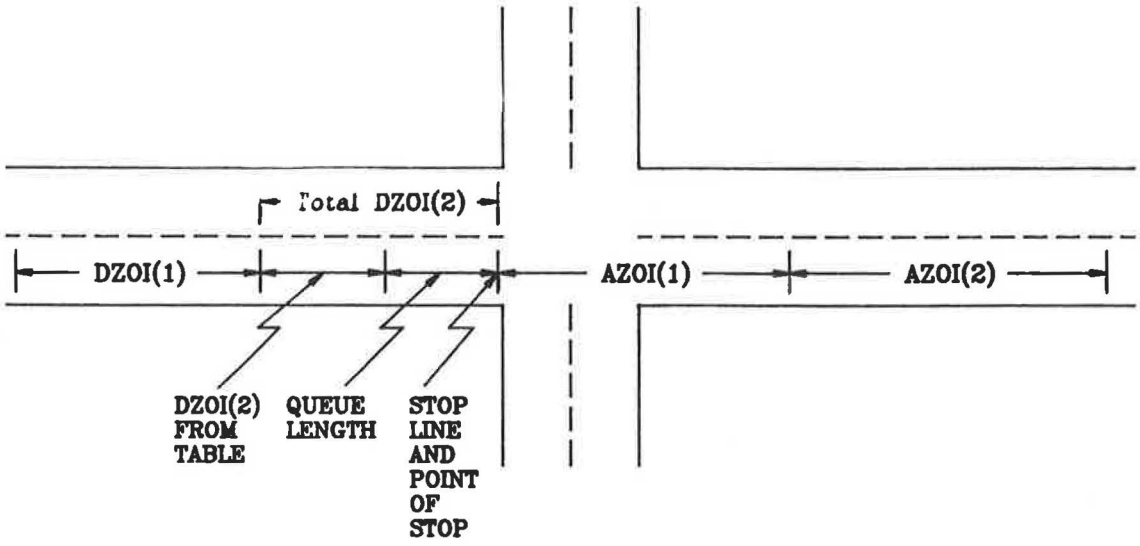

UNSIGNALIZED

FIGURE 9 Definitions of zones of influence for signalized and unsignalized intersections.

TABLE 1 COMBINED ACCELERATION ZOIs AND CORRESPONDING EQUIVALENT SPEEDS FOR THREE VEHICLE TYPES

Accel. Range (mph)		Length(ft)		Speed, ZOI(1)(mph)			Speed, ZOI(2)(mph)		
$S_{INITIAL}$	S_{FINAL}	ZOI(1)[a]	ZOI(2)[b]	Autos	MT	HT	Autos	MT	HT
0	30	500	300	38	43	43	30	43	43
0	35	600	650	39	43	43	35	43	43
0	40	1000	none	40	43	43	n/a[c]	n/a	n/a
0	45	1000	none	42	43	43	n/a	n/a	n/a
0	50	1000	800	42	43	43	50	47	47
0	55	1000	800	42	43	43	50	40	49
0	60	1000	800	42	43	43	50	52	52
30	40	400	none	40	43	43	n/a	n/a	n/a
30	50	1000	none	42	43	43	n/a	n/a	n/a
30	60	1900	none	51	52	53	n/a	n/a	n/a
40	50	600	none	45	43	43	n/a	n/a	n/a
40	60	1500	none	50	52	53	n/a	n/a	n/a
50	60	any	none	60	60	60	n/a	n/a	n/a

[a] Starting from point of stop (or the end of queue for unsignalized intersections) and proceeding in direction of flow (see Figure 9).

[b] Starting from end of ZOI(1) (see Figure 9).

[c] n/a = not applicable

TABLE 2 COMBINED DECELERATION ZOIs AND CORRESPONDING EQUIVALENT SPEEDS FOR THREE VEHICLE TYPES

Decel. Range (mph)		Length(ft)		Speed, ZOI(1)(mph)			Speed, ZOI(2)(mph)		
$S_{INITIAL}$	S_{FINAL}	ZOI(1)[a]	ZOI(2)[b]	Autos	MT	HT	Autos	MT	HT
30	0	150	100	29	26	24	18	13	10
40	0	250	100	34	30	28	18	13	10
50	0	200	200	38	34	31	18	13	10
60	0	300	200	41	36	33	18	13	10
40	30	220	none	37	32	30	n/a[c]	n/a	n/a
50	30	375	none	42	37	36	n/a	n/a	n/a
50	40	270	none	46	41	42	n/a	n/a	n/a
60	30	530	none	46	41	42	n/a	n/a	n/a
60	40	430	none	51	46	47	n/a	n/a	n/a

[a] Starting from point of stop (or the end of queue for unsignalized intersections) and proceeding in direction of flow (see Figure 9).

[b] Starting from end of ZOI(1) (see Figure 9).

[c] n/a = not applicable

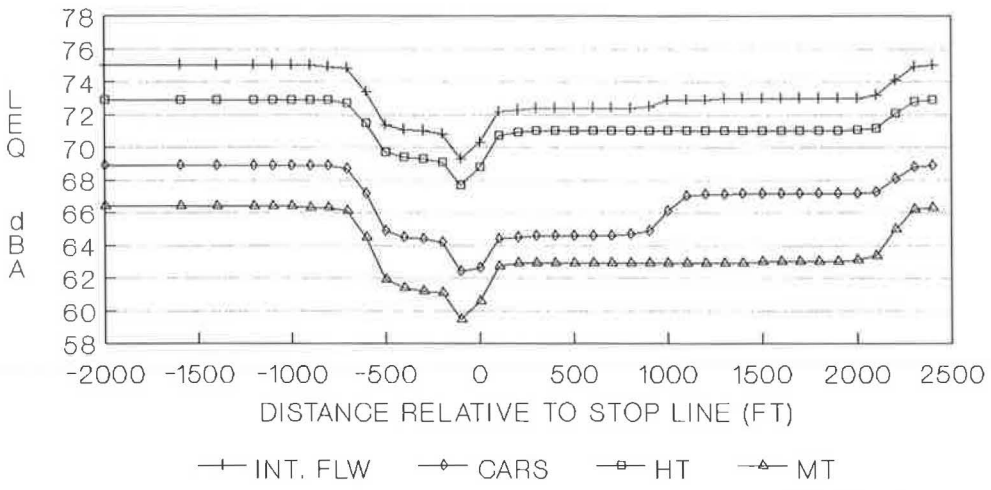

FIGURE 10 Predicted L_{eq}(1h) sound level contributions by vehicle type at a 50-ft offset distance for one-way traffic with 100 percent interrupted flow (hourly flow of 1,000 automobiles, 50 medium trucks, and 100 heavy trucks; cruise speed of 60 mph).

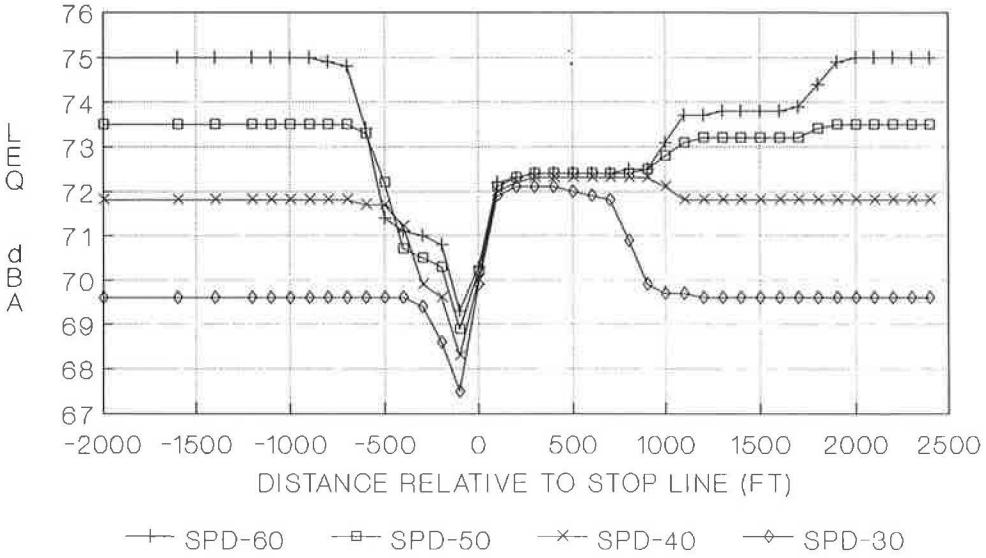

FIGURE 11 Predicted L_{eq}(1h) based on initial speeds of 30 to 60 mph for one-way traffic with 100 percent interrupted flow at a 50-ft offset distance (hourly flow of 1,000 automobiles, 50 medium trucks, and 100 heavy trucks).

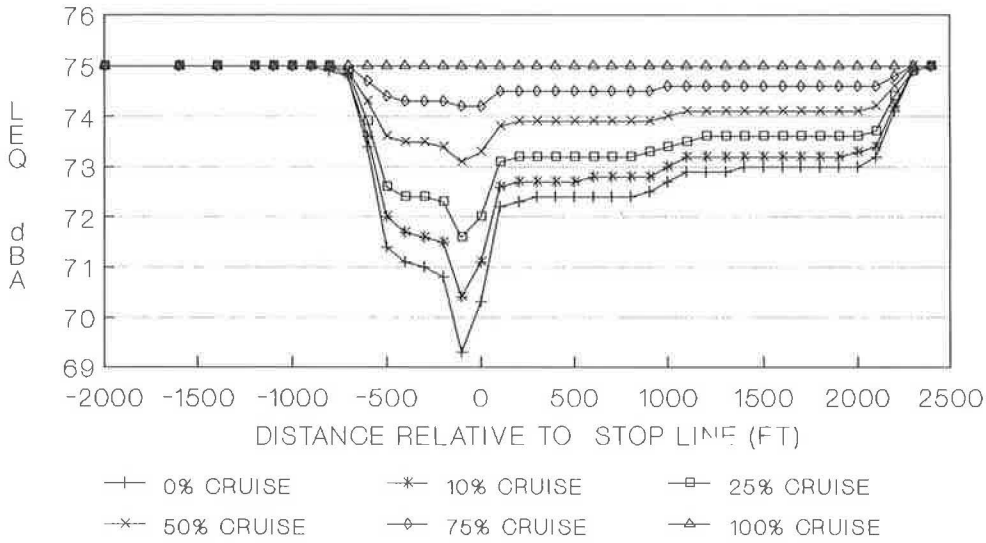

FIGURE 12 Predicted L_{eq}(1h) as a function of percentage of cruise traffic based on a cruise speed of 60 mph and a 50-ft offset distance (hourly flow of 1,000 automobiles, 50 medium trucks, and 100 heavy trucks).

In the first attempt to model this site, a pattern very similar to the measurements was achieved, with the exception of a point near the reflecting wall. However, all of the other predicted levels were about 2 dB higher than measured, including those at the cruise site. The differences were attributed to the vehicle noise emission levels, because the measured cruise site levels were also 2 dB lower than predicted. By calibrating the predictions with the measurements, excellent agreement was achieved (within 0.5 dB at all points except the point opposite the wooden wall).

GENERALIZED EXPRESSION

The data in Tables 1 and 2 are based on the use of the national reference energy mean noise emission levels (*1*). Several state departments of transportation have determined their own noise emission levels. In these cases, an agency must develop its own set of equivalent speeds to produce the needed difference between cruise levels and acceleration or deceleration levels. The generalized equation for computing those speeds is

$$S_{equiv} = \{\text{antilog}[(L_0)_{E,60} - 19.82 - a - \Delta_c]/(b - 10)\} \quad (2)$$

where

S_{equiv} = equivalent speed (km/hr),
$(L_0)_{E,60}$ = state reference energy mean noise emission level $[(L_0)_E]$ at 60 mph,
a = Y-intercept from state $(L_0)_E$ equation,

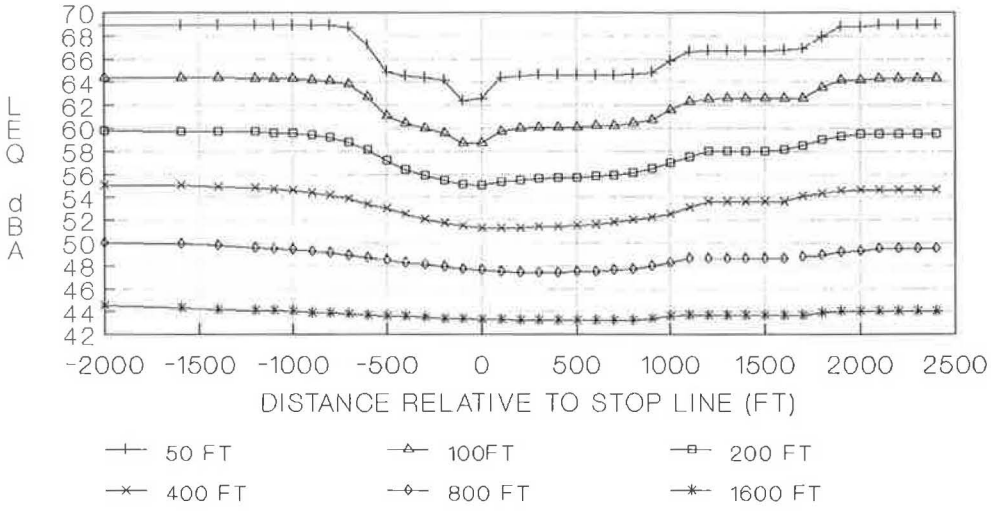

FIGURE 13 Predicted L_{eq}(1h) as function of receiver offset distance based on one-way hourly flow of 1,000 cars (100 percent interrupted flow; cruise speed of 60 mph).

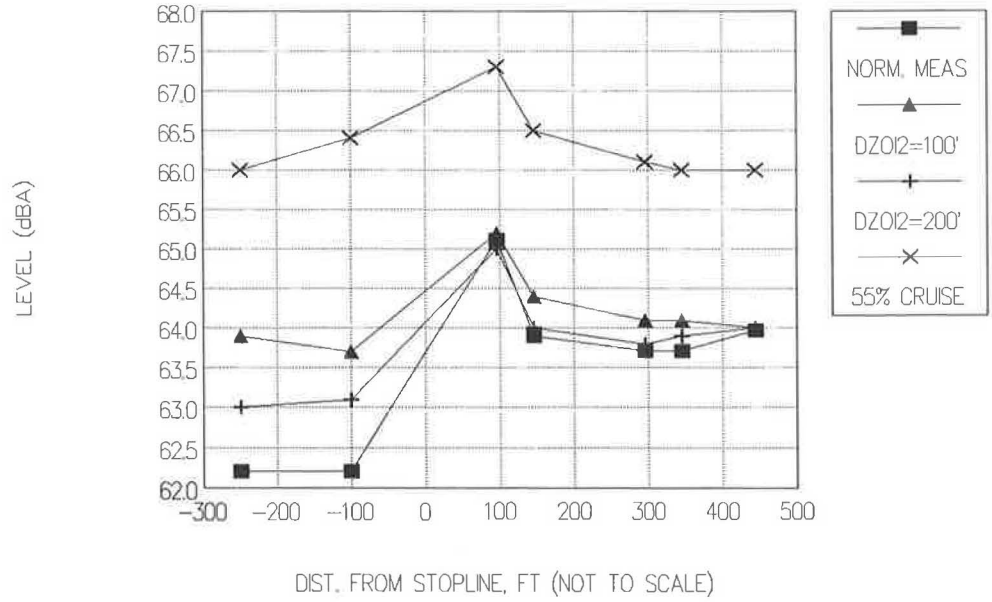

FIGURE 14 Validation results at Site 1 (Hillsboro Road), based on measurements normalized to the October 12, 1988, data, 1:00 to 2:00 p.m.

Δ_c = desired change in SEL value for cruise at 60 mph, and
b = slope from state $(L_0)_E$ equation.

Values for Δ_c are presented in Tables 3 and 4.

SUMMARY

To summarize, a detailed analysis of the levels associated with accelerating and decelerating vehicles was performed for three major situations: the signalized arterial or end of a highway ramp; the unsignalized, but signed, intersection such as a Stop sign on an arterial highway or at the end of a highway ramp, or at a toll booth; and the loop or slip transition ramp on a freeway. Two tables (one for acceleration and one for deceleration) were developed as part of a design guide. The tables presented the lengths to be used to model the site as STAMINA 2.0 roadways, and the equivalent speeds to be used for each vehicle type on these roadways. Levels in a deceleration zone decreased below cruise levels by 2 to 6 dB, depending on the initial cruise speed. In the acceleration zones, levels increased over the deceleration levels, but whether or not these increases exceeded the cruise levels depended on the final cruise speed. For example, if the final speed was 30 mph, the acceleration noise level was about 2 dB higher than the cruise level. However, if the final speed was 60 mph, the

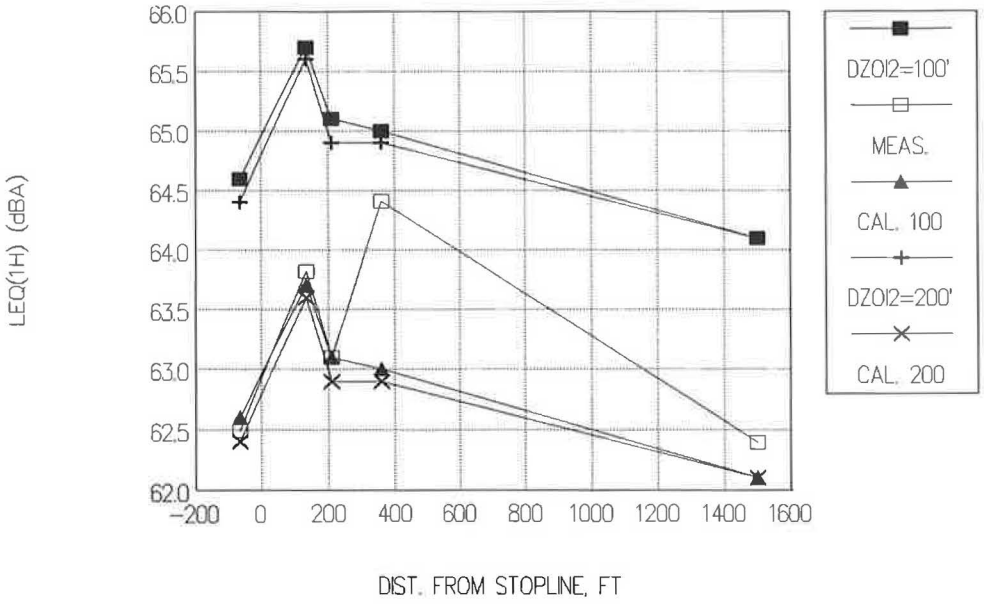

FIGURE 15 Validation results at Site 2 (Blakemore Avenue), based on measurements normalized to the October 14, 1988, data, 2:00 to 3:00 p.m.

TABLE 3 CHANGE IN SEL VALUES IN ACCELERATION ZOIs FOR THREE VEHICLE TYPES

Accel. Range (mph)		Change in SEL for ZOI(1) (dBA)			Change in SEL for ZOI(2) (dBA)		
$S_{INITIAL}$	S_{FINAL}	Autos	MT	HT	Autos	MT	HT
0	30	5.6	3.5	2.1	8.5	3.5	2.1
0	35	5.3	3.5	2.1	6.6	3.5	2.1
0	40	4.9	3.5	2.1	n/a*	n/a	n/a
0	45	4.4	3.5	2.1	n/a	n/a	n/a
0	50	4.4	3.5	2.1	2.2	2.5	1.5
0	55	4.4	3.5	2.1	2.2	2.1	1.3
0	60	4.4	3.5	2.1	2.2	1.5	0.9
30	40	4.9	3.5	2.1	n/a	n/a	n/a
30	50	4.4	3.5	2.1	n/a	n/a	n/a
30	60	2.0	1.3	0.8	n/a	n/a	n/a
40	50	3.5	3.5	2.1	n/a	n/a	n/a
40	60	2.2	1.5	0.8	n/a	n/a	n/a
50	60	0.0	0.0	0.0	n/a	n/a	n/a

*n/a = not applicable

TABLE 4 CHANGE IN SEL VALUES IN DECELERATION ZOIs FOR THREE VEHICLE TYPES

Decel. Range (mph)		Change in SEL for ZOI(1) (dBA)			Change in SEL for ZOI(2) (dBA)		
$S_{INITIAL}$	S_{FINAL}	Autos	MT	HT	Autos	MT	HT
30	0	8.9	8.7	5.8	14.7	15.9	11.4
40	0	6.9	7.2	4.8	14.7	15.9	11.4
50	0	5.6	5.9	4.2	14.7	15.9	11.4
60	0	4.6	5.3	3.8	14.7	15.9	11.4
40	30	5.9	6.5	4.4	n/a[a]	n/a	n/a
50	30	4.4	5.0	3.2	n/a	n/a	n/a
50	40	3.2	4.0	2.3	n/a	n/a	n/a
60	30	3.2	4.0	2.3	n/a	n/a	n/a
60	40	2.0	2.8	1.5	n/a	n/a	n/a

[a]n/a = not applicable

acceleration time-averaged noise level was about 2 dB lower than the cruise level.

CONCLUSION

There is certainly a need for more validation of the technique and for collection of more car and medium truck noise emission level data. It may also be desirable to build these results into the STAMINA 2.0 code or to modify the way in which STAMINA 2.0 computes the noise emission levels for its various roadway subsections. For now, however, the developed procedure will allow the STAMINA 2.0 model to be used with relative ease in changing speed situations with an improved level of accuracy relative to previously recommended methods.

ACKNOWLEDGMENTS

The authors gratefully acknowledge the support of the National Cooperative Highway Research Program (NCHRP), which funded this work. Special thanks go to the members of Project Panel 25–2 and NCHRP program staff. The work has been published as *NCHRP Report 311* (2).

REFERENCES

1. T. M. Barry and J. A. Reagan. *FHWA Highway Traffic Noise Prediction Model.* FHWA-RD-77-108, FHWA, U.S. Department of Transportation, July 1978, 272 pp.
2. W. Bowlby, R. L. Wayson, and R. E. Stammer, Jr. *NCHRP Report 311: Predicting Stop-and-Go Traffic Noise Levels.* TRB, National Research Council, Washington, D.C., 1989, 97 pp.
3. P. T. Lewis and A. James. Noise Levels in the Vicinity of Traffic Roundabouts. *Journal of Sound and Vibration*, Vol. 72, No. 1, 1980, pp. 51–69.
4. B. Favre. Noise at the Approach to Traffic Lights: Result of a Simulation Program. *Journal of Sound and Vibration*, Vol. 58, No. 4, 1978, pp. 563–578.
5. F. F. Rudder, Jr., L. Ronk, and B. Hutcheson. *National Roadway Traffic Noise Exposure Model.* Office of Noise Abatement and Control, U.S. Environmental Protection Agency, Nov. 1979, 395 pp.
6. *A Policy on Geometric Design of Highways and Streets.* AASHTO, Washington, D.C., 1984, 1,087 pp.

Publication of this paper sponsored by Committee on Transportation-Related Noise and Vibration.

Feasibility of Transparent Noise Barriers

SARAH E. ROCCHI AND SOREN PEDERSEN

The preliminary investigations by the Ministry of Transportation of Ontario into the possibility of using transparent sheet glazing products made of glass or plastic in noise barriers are documented. The political issues and principles of using these types of barriers are not addressed. The concerns of the Design Development and Application Section with regard to the ability of various substances to meet current standards for noise barrier materials are discussed, providing a substantial foundation for establishing standards with regard to properties unique to glass or plastic such as transparency, flammability, safety under impact, and design considerations.

The Ministry of Transportation of Ontario (MTO, originally the Ministry of Transportation and Communications) has been actively involved in decreasing the impact of highway noise since 1971 when the first barrier was constructed. The Ministry's concern and involvement have grown with the increase in traffic volume, development along freeways, and public awareness and expressed concern about highway noise. Although freeway noise generation is not completely under MTO control, the Ministry nevertheless accepts some responsibility for it. In 1977 a retrofit program was established that identified existing residential sites in need of barriers and ranked them in order of priority. Under this program, funding was allocated to construct a number of these sites every year until all sites had been addressed. Transparent noise barriers, in general, have been considered for aesthetic reasons for many years. However, the MTO had not conducted any feasibility studies until a proposal was made to construct such a barrier along a portion of the Queen Elizabeth Way, west of Toronto. Representatives of a shopping mall and service station at that location expressed concern that the construction of a concrete or steel noise barrier at the site would obstruct the view of their operations from the roadway, cutting off a free source of advertising for them. Because a transparent barrier at this site might solve this problem, this site was suggested as a test area for this system. Although it would have entailed only a short stretch of barrier, the MTO did not want to test transparent products on such a scale without having done some background work on a smaller scale. It was feared that the proposed test area might also set a precedent that would result in more demands by other enterprises for visual access from major roadways (*1–4*).

CONSULTATION WITH INDUSTRY AND PUBLIC ORGANIZATIONS

As part of the investigation into the use of transparent barriers for noise control, the initial task was to consult others with experience in related areas. Organizations consulted included

Ministry of Transportation of Ontario, Highway Design Office, Design Development Section, 1201 Wilson Ave., West Building, Downsview, Ontario M3M 1J8, Canada.

- The French Ministries of the Environment and Quality of Life and of Transportation,
- Glass and plastics manufacturers,
- Two state highway departments (Maryland and Massachusetts) in the United States that had previous experience with transparent noise barriers, and
- The City of Toronto.

This section contains background information on the organizations consulted and the projects they pursued. The information on various aspects of transparent noise barriers that was received is summarized in a later section.

A report (*5*) obtained from the French Ministries of the Environment and Quality of Life and of Transportation contains guidelines for the construction of glass noise barriers based on experiences of the ministries. This report covered such topics as

- Safety—strength and shatter tests,
- Implications of the sizing of glass plates,
- Technical arrangements to avoid glare from opposing traffic,
- Vandalism,
- Vibrations,
- Installation,
- Maintenance, and
- Repair.

Representatives of the Plastics Divisions of Canadian General Electric (J. N. Coutu, private communication) and of Dupont Canada (G. W. Haywood, private communication), were contacted. Although Dupont does not manufacture sheet glazing products, it does manufacture ethylene copolymer laminates such as Butacite, a polyvinyl butaryl film, and Surlyn ionomer resin. These products are used by the glass fabricating industry as a laminate material between sheets of glass. Companies using them are Advanced Glass Systems (N. P. Bolton, private communication), which uses Surlyn Film, and Lamilite Ltd. (*6*), which uses Butacite.

Laminated glass consists of a layer of a plastic product, such as one of the preceding, bonded between layers of either tempered or annealed glass to improve the strength, safety, sound control, and penetration resistance characteristics of the glass. Tempered glass requires high impact energy to break; however, it shatters completely upon impact. Annealed glass is more easily fractured and produces long, sharp-edged splinters, but is less expensive.

After extensive discussions with various glass companies, it was found that the Monsanto product Butacite is similar to Surlyn and is used interchangeably with Surlyn.

Canadian General Electric manufactures Lexan, which is a sheet glazing product made of high-strength polycarbonate

(*7*). It is more resistant to impact than glass, but less resistant to abrasion, heat, and ultraviolet rays.

Promotional material from the plastics and glass manufacturers describes various installation, strength, sound attenuation, and safety properties of their products. Samples of all types are available from the companies contacted that could be used to test their claims.

American Experience with Lexan Noise Barriers

Canadian General Electric was able to provide information regarding Fanwall Corporation (E. W. Angove, private communication), a noise barrier fabricating company, that had already constructed noise barriers of Lexan for two American State Highway Departments, the Massachusetts Department of Public Works (B. Reynolds, private communication) and the Maryland State Highway Administration (R. Douglas, private communication).

In 1980 the Maryland State Highway Administration had chosen a limited length of roadway along I-95 as the site for experimental transparent noise walls. A report published in 1981 (*8*) detailed the selection process that led to the choice of Lexan and evaluated the project at that time in terms of construction details, aesthetics, and acoustics, drawing positive conclusions with respect to all aspects. The administration, contacted in February 1987, described a favorable public response to the Lexan walls when they were first constructed but reported that after 6 years' experience, some of their conclusions were not as favorable.

The Massachusetts Department of Public Works, under extenuating circumstances, offered transparent material as an option at a public meeting for a project. The report on its use dealt mainly with the acoustic properties of the project (*9*).

Glass Applications in the Toronto Area

The City of Toronto is involved in two projects in which large pieces of glass are used along the roadway. The first is a glass-enclosed walkway along Bay Street; the second is the system of bus shelters throughout the city. A city representative (K. Greenberg, private communication) was able to provide detailed information about the walkway. Mediacom, a company contracted with to be responsible for the construction and maintenance of these bus shelters, uses them to display advertising for their clients.

The walkway along Bay Street consists of sheets of glass mounted on concrete traffic barriers. Located immediately adjacent to the roadway in an area of high traffic volume, it was constructed in 1984 of tempered laminated glass to reduce the effects of vehicle exhaust fumes and roadway runoff that was being splashed on pedestrians walking under a viaduct. The City of Toronto is very pleased with the results of this project.

EXAMINING THE CONCERNS OF THE MTO

MTO-preapproved manufacturers' noise barrier designs must meet the standards set by the Ministry (*10,11*). Glass and plastic products would have to meet these standards for the materials currently used in noise barriers—namely, concrete, steel, and wood—in order to be considered at all. The standards include requirements for sound transmission loss and structural design. Also, because of the nature of these materials, new standards would have to be developed for properties such as transparency and shatterability. The different types of laminated glass and Lexan should be evaluated on these counts to see whether any are usable, and if so, which are best suited for this type of application.

Aesthetics

The major advantage of transparent materials over traditional materials in noise barriers is aesthetics. Residents living next to visually imposing walls of concrete or steel liken it to living next to the Berlin Wall. With the use of transparent materials, the motorists' view of the roadside and the sunlight penetration to the highway would not be blocked. With these advantages, the highway and barrier appear less imposing. Maryland and Massachusetts both report a positive public response to the appearance of their transparent noise walls (*8*, *9*).

The MTO's aesthetic requirements are limited to visual and physical relief at uniform intervals, which is required on both the residential and freeway sides of the barrier. The current guidelines recommend that false posts be used to break up an otherwise repetitive pattern, that alignments and heights be varied, and that barrier texture and surface treatments such as painting be used to a limited extent. Such devices would not be necessary with transparent barriers. Restrictions of manufacturing of both plastic and glass limit the size of the actual panels, so there will be enough real posts that false posts would be superfluous. Also, the variation of the landscape beyond the barriers would provide sufficient relief from monotony.

Safety

Flammability

Currently, neither the MTO nor any other government agency has set any restriction on the flammability of structures along the highways. However, the plastic in Lexan and laminated glass is much more flammable than the materials most often used in conventional noise walls. The MTO is therefore concerned with developing standards to protect itself from liability in the event that a barrier should be exposed to open flame. The American Society for Testing and Materials (ASTM) has a number of tests to gauge the fire properties of clear stiff plastics. It does not, however, set any minimum standard, and takes pains to inform readers that none of the tests can stand alone as a fire standard. It was agreed that the MTO might be held liable if it were possible for the wall to exacerbate damage in the event of a fire. For example, if the wall caught fire because of brush, grass, or vehicle fires, the smoke might be so thick as to cause loss of visibility along the highway. If there were a fire near the barrier, the barrier might cause the fire to spread more than if there had been a wood barrier or no barrier in place. It was decided that the factors

most likely to cause damage could be determined through a burn rate test (ASTM D-635) and a smoke density test (ASTM D-643). As a minimum standard, the transparent materials must be compared with wood (pine), the material with the highest burn rate and smoke density of all approved barrier materials.

Laminated glass offers an advantage over Lexan in this respect. The glass must be broken and the laminate material almost entirely exposed before the flame can spread. Breakage is not, however, an improbable scenario and therefore should be investigated further.

Behavior on Impact

Because of the peculiar nature of glazing products and possible risk of injury to third parties, it is necessary to verify that the glass or plastic splinters produced during fragmentation are not harmful and that the glazing has a high resistance to perforation. The various organizations contacted used different impact acceptance testing method.

Maryland (*8*) subjected polycarbon sheets to pellet guns, 0.22 longs, and 0.38 police missiles, and found that there was no shattering in any of the tests; only the 0.22 longs penetrated, leaving tiny holes of inconsequential acoustic concern.

The City of Toronto also required bulletproof glass for its glass-enclosed walkway, and as a result, laminated tempered glass was used. The bus shelters used throughout Metropolitan Toronto are required to be shatterproof as well. To be able to withstand the force of a thrown rock, they are made of ½-in. tempered glass.

The French have a ball test to evaluate the resistance of the glass to perforation and a hammer test to verify that the glass splinters produced during fragmentation are small enough not to cause serious or fatal injuries. Both of these tests are explained in their report (*5*). The Canadian Standards Association standard for automobile glass (CSA D263) could also be used. The MTO could choose any one of these standards for its own use. It is likely that annealed (nonlaminated) glass would not meet any of these standards because of the large slender shards it produces on impact.

Reflection of Light

The French report (*5*) probed the dangers of temporary blindness from the glare caused by reflection of vehicle light by the glass or the confusion produced by seeing the reflection of a phantom vehicle's image. These problems arise, in particular, in the case of curved roadways because of the low angle of incidence of the light. When the sun is low on the horizon, it may dazzle a driver on the highway or a service road. At night the main source of reflection is vehicle headlights, whose rays generally strike the baffles at a low angle of incidence. Several solutions are proposed.

- Inclination of the barriers up to 12 degrees toward the roadways makes it possible to deflect the reflected rays down to a preferred area of the road surface. This also solves the problem of reflection of the sun.
- If glass plates are mounted behind posts, the posts act as obstacles to the propagation of light beams with a low angle of incidence.
- The use of transparent glass specially designed to be nonreflecting is not recommended, because the costs involved are largely prohibitive. Nonreflecting, or even opaque, materials like concrete or painted, corrugated steel can be used for the lower part of the baffle, to a height of at least 4 ft above the surface of the roadway. This may be quite acceptable because most noise barriers are mounted on or behind traffic barriers.
- Glare caused by the headlights of opposing traffic may be diminished by installing an antiglare screen on the median barrier. Care must be taken that this screen does not alter the acoustic characteristics of the roadway, that is, does not reflect sound.

When determining a standard for transparent noise barriers, these suggestions must be taken into consideration and perhaps they should be reevaluated after barriers have been in place for a while.

Neither Maryland nor Massachusetts state departments of transportation using Lexan reported complaints about reflection of light. However, their test sites were of limited length and on tangent sections of roadway.

Structural Design Requirements

MTO's noise barrier design requirements (*10*) state that, except where otherwise noted, the noise barrier should be designed in accordance with the *Ontario Highway Bridge Design Code* (*12*) as a slender structure, not unusually sensitive to wind action. Design loads and ice accretion loads should be prescribed as for sign panels. The reference wind pressure for a 25-year return period should be used for each specific site as described in the Bridge Code. The Maryland State Highway Administration had the Lexan panels tested at an independent testing laboratory and found that they could withstand a loading of 8,142 Pa with no failure or pullout from the posts. Although this more than meets the Ministry requirements, it is, of course, peculiar to their mounting system. The French report (*5*) states that glass products can withstand these pressures, but it depends on the mounting system, the thickness of the glass, and the dimensions of the glass plate. Therefore, it is the duty of the noise barrier manufacturer to ensure that the proposed barrier designs meet the MTO standard.

Acoustic Qualities

The MTO requires that the random incidence sound transmission losses of the noise barrier system, when tested in accordance with ASTM E 90–87, should have an effective sound transmission loss of T greater than or equal to 20 dB. Glazing materials have no difficulty in meeting the MTO's minimum requirements (see Table 1).

Glass and plastic are considered to be totally sound-reflective materials. These materials could not be used for a close parallel barrier situation or for a barrier located between a highway and service road. In these situations, it has been shown that the use of barriers made of sound-reflective materials actually increases the noise levels on adjacent property

TABLE 1 COMPARISON OF SOUND TRANSMISSION CLASS OF VARIOUS MATERIALS

Material	Thickness (mm)	Sound Transmission Class (dB)
Concrete	132	32
Steel	0.91	20
Lexan	6.35	31
Lexan	12.7	34
Laminated glass	7.24	35
Laminated glass	12.25	39

(*13*). Either the service road noise is reflected back toward the community or, in the case of parallel barriers, the reflection and diffraction of sound reduce the effectiveness of the barrier. This, however, would limit the general use of glass and plastic as a noise barrier material. It is believed that some of this reflection can be relieved by tilting the panels slightly so that the noise is reflected upward. More research is required into this theory for both transparent and opaque barriers.

Costs

Costs of transparent materials could prohibit their use as usable noise barrier materials, especially when the added lifetime costs of maintenance are taken into account. Table 2 presents the approximate costs of transparent and opaque materials.

All of the glazing products are comparable when it comes to acoustic and aesthetic qualities; however, in general, as the strength of the product increases, the price increases. Except for annealed laminated glass, which is suspected of not meeting MTO safety standards, all of the glazing products are substantially more expensive than the traditional materials of concrete and steel. Because no mounting system has been discussed yet, it is not known how the price of installed transparent barriers will compare to the cost of installed opaque barriers.

TABLE 2 COMPARISON OF COSTS OF VARIOUS MATERIALS

Material	Thickness of Laminate (mm)	Total Thickness (mm)	Cost per Square Meter ($ Can)
Mar-resistant Lexan	—	12.25	205.00
Mar-resistant Lexan	—	6.63	118.00
Standard Lexan	—	12.25	160.00
Standard Lexan	—	6.63	71.00
Laminated tempered glass	0.06	12.31	113.00
Laminated tempered glass	0.03	12.28	97.00
Laminated tempered glass	0.03	6.66	75.00
Laminated annealed glass	0.03	12.28	43.00
Laminated annealed glass	0.03	6.66	37.60
Concrete (reflective and absorptive)	—	132.00	60.00
Steel (reflective)	—	0.91	36.00

NOTE: All costs are for panel material only. They do not include posts, mounting hardware, or installation.

Maintenance

One of the MTO's requirements for noise barriers is that all materials be durable, with a predicted maintenance-free life expectancy of 20 years. Taking into account some of the special qualities of glass and plastic, it can be seen that this life expectancy will not be possible for these materials. They are also more susceptible to breakage than steel or concrete.

Washing

One of the major concerns when evaluating transparent materials for use in noise barriers is the ability of the material to maintain transparency. Unfortunately, the transparency of glass may be reduced, or even eliminated, as a result of heavy traffic on the roadways. One solution may be to design the panels with an inward inclination, making it possible for the glass to be washed somewhat by rain. The residential side, away from the traffic, is less likely to become dirty. Therefore, it does not have to be cleaned as frequently, if at all.

In 1987 the MTO initiated a field testing program to monitor the buildup of dust and its effect on visibility. From this, the MTO hopes to determine how frequently transparent barriers will need to be cleaned when they are located on Ontario highways and whether there is any difference in the rate of buildup of dirt on the various samples. This project will be discussed later in this paper.

Permanent Degradation of Transparency

It is hoped that the field test mentioned above would also detect any degradation of visibility due to abrasion or exposure to ultraviolet rays. This field test for abrasion would be in addition to comparing the performance of glass and plastic in ASTM D-1044.

As mentioned, the Maryland State Highway Administration attributes the degradation of the transparency of their Lexan barriers to exposure to ultraviolet rays. Of the four materials that were tested (three being plastic and one tempered glass), under accelerated and natural weathering conditions, the tempered glass was favored because of its ability to better withstand abrasion and discoloring (*14*). Under the same conditions, it was found that polycarbonate materials were more susceptible to abrasion and loss of transparency than were acrylics. The manufacturers of Lexan now market products treated with more ultraviolet ray and abrasion-resistant coatings, Lexan XL and Margard. However, there are three disadvantages to these products:

- They are significantly more expensive than the regular Lexan product,
- The performance of the coating in maintaining clarity is only guaranteed for 3 years, and
- Because they cannot be cleaned with petroleum-based products, their suitability for roadside use is questionable.

Breakage

Apart from the concerns regarding safety under impact already noted, the MTO would like to use a high-strength sheet glaz-

ing product in order to minimize this aspect of maintenance. The ability for some of the panels to remain integral would be an asset. This feature would allow the noise barrier to continue to function at least to some extent until the maintenance crews are prepared to make repairs. A standard for minimum strength under impact will have to be set.

Comparing the breakage histories of the other organizations reveals the performance of the various products. Neither of the two state highway departments using Lexan reported any breakage in the collective 8 years that their barriers were in place. The French—who use a variety of glass products, laminated and nonlaminated, tempered, and annealed—recommend putting aside 10 percent of the glass that is needed to construct the original barrier, because that much breakage can be expected. They also suggest that easy remounting of broken panes be taken into consideration in design. In the 4 years that the Toronto walkway has been in place, however, there has been no breakage.

Design and Installation

The use of new materials such as laminated glass and Lexan brings new concerns in design and installation. Advice from the organizations consulted permits avoidance of the problems that they encountered.

Maryland reported that Lexan had a very good anchoring system. Because of the low melting point of the Lexan panels (275°F), the hot asphalt could not be allowed to contact the panels directly. This condition resulted in a 13- to 51-mm gap between the panel and the asphalt, which had to be filled with highway joint sealers. The Massachusetts Department of Public Works reported many problems with the construction of their Lexan barrier. Some panels broke during construction. Also, the panels were left in the sun, and the protective paper backing melted onto the plastic and was hard to peel off. The contractor used linseed oil in an attempt to remove the paper, which had a harmful effect on the panels.

From the laminated glass manufacturers and the French report (*5*), some insight was gained into the design and installation of laminated glass as well. For example, a sealant should be used between the laminated glass and the mounting bracket; this protects the laminate core from water vapor. Any materials that come into contact, such as polycarbonate and metal and the laminate core and the sealant, should be chemically compatible to avoid deterioration. Care should be taken not to break the edges, which helps avoid breakage due to thermal differences.

Some of the design considerations apply to both laminated glass and Lexan. To enhance visibility, it is better to have large pieces of glazing and to limit the number of brackets. The size of the panel is limited by the manufacturers. In the case of Lexan, the maximum size of the sheet is 12 by 10 ft (3.66 by 3.05 m). The dimensions of the laminated glass panels are limited to 12 by 6 ft (3.66 by 1.82 m). The French report (*5*) recommended that wind pressures be taken into consideration. The thickness should be determined by sound attenuation, mechanical study, and shock resistance.

Some concern was raised about vibrations. The Lexan material is strong but flexible. The Maryland State Highway Administration reports that their panels tend to vibrate when heavy trucks drive by. This has caused no problems structurally; however, it does produce an unsettling rattle. The French report (*5*) stated that glass baffles are subject to vibrations from wind as well as highway traffic, especially the backwash of trucks. Studies have shown that these effects produce stresses that are not dangerous and are not likely to lead to breakage of the panels.

Summary of Concerns

Transparent materials thicker than 6.35 mm meet many of the standards for the materials currently used in noise barriers. They are far superior to opaque materials when noise barrier aesthetics are considered. If properly designed, they can meet the necessary structural design requirements. However, there is still work to be done in setting the standards for properties such as transparency and shatterability. The glass and polycarbonate products should be tested to see whether they meet these standards, and their flammability should be compared with that of wood for burn rate and smoke density. The Ministry should choose which of the many shatter standards to use. Glare should be considered in design.

It might be necessary to test these designs on a larger scale once specific sheet glazing products have been approved for use. The cost becomes higher when the lifetime cost of cleaning and replacing broken panes is taken into consideration. Because these materials are sound reflective, their range of use will be limited unless investigation shows that tilt-mounting is a workable way of reducing the negative effect of noise reflections.

MONITORING VISIBILITY DEGRADATION OF SAMPLES AT A ROADSIDE TEST SITE

The MTO has initiated a program to field test samples of tempered glass, annealed glass, and various Lexan products. The buildup of dust and its effect on visibility will be monitored. From this information, it will be determined how frequently transparent barriers should be cleaned. Any difference in the rate of buildup of dirt on the various samples will be noted. A test site that met the following criteria was chosen:

- Ability to mount samples low to the ground and near the driving edge of the road to maximize effects of airborne dirt and grime,
- Sufficient exposure to the sun,
- Protection of the samples from traffic and the traffic from the mounting system, and
- Location near the technical resources of the MTO Head Office.

Description of Project Location

The location chosen for the installation of the test samples generally meets all of these requirements. The mounting system is attached to the steel posts of an existing noise barrier on the east side of Highway 427, approximately 0.2 mi north of the Rathburn Road interchange. Highway 427 at this loca-

tion is 16 lanes wide with a 1987 annual average daily traffic of 223,350 (20 percent trucks). The posted speed in this area is 100 km/hr. The samples face WSW, permitting the sun's rays to strike them at approximately 10:00 a.m., and are unobstructed until sunset. The samples are mounted 1.75 m above the roadway and 4 m back from the driving edge of the pavement. The site is protected by a steel beam and a channel traffic barrier.

Mounting of Samples

The samples were mounted at an angle of 10 degrees to get the full washing benefit of rain. The cut edges of the samples were covered with waterproof tape to protect them from the environment.

Method of Testing

The prime criterion for any interim testing of the samples must be that it be done in the field to avoid disturbing any buildup of dirt. Other criteria were that the testing be reasonably accurate and easy to perform, and that it conform to financial constraints without recourse to an independent laboratory. After investigating most of the methods used by various experts in the field, the MTO settled on one that used a simple photometer and a single light source.

Apparatus

After trial and error, a reasonably accurate and easy-to-use testing device was developed on the principle that the amount of light emitted from a constant light source can be measured accurately if all ambient light is eliminated. If an object is introduced between the light source and the receiver, the amount of light reaching the receiver is reduced in varying degrees. As a light source, a standard automotive brake light bulb was used. The receiver consists of an array of five cadmium selenide photoconductive cells wired in series. The power source for the light bulb was obtained from the vehicle used by the testing crew. The voltage was regulated to 10.5 Vdc. To measure the resistance of the photoconductive cells, a standard multimeter was used with a range of 0 to 2 MΩ. To prevent ambient light from interfering with the measurements, the source and sensors were mounted in separate cases designed to create a light seal around the entire 1-ft-square samples. The equipment was mounted in two separate casings to permit easy movement of the testing apparatus behind and in front of the mounted samples without disturbing the surface of the samples.

After initially adjusting the values of various components, it was possible to measure any degradation as slight as 0.5 percent. This sensitivity was considered to be acceptable for any field testing, considering the accuracy of the voltage regulator (±5 percent).

Preliminary Results

After 3 years of installation, three tests were conducted, one initial and two followups, with 1 year in between. The results of these tests are presented in Table 3.

Analysis

Although the field testing of the samples indicated that there was some loss of transparency, it is still too premature to draw any definite conclusions as to the individual and comparative performance of these products.

CONCLUSIONS

Valuable information regarding the feasibility of using transparent materials such as laminated glass and plastic sheets in noise barriers was obtained by consulting public and private organizations with expertise in this field.

Transparent materials could be used in the construction of barriers that meet MTO's standards for acoustics and structural strength.

The aesthetics of barriers made of transparent materials are superior to those made of opaque materials.

TABLE 3 PERCENTAGE OF SAMPLE DEGRADATION FOR THREE ANNUAL TESTS

Sample	Initial Reading (8/12/87)	Difference	Second Reading (9/7/88)	Difference	Third Reading (7/5/89)	Accumulated Difference
Lexan						
Clear[a]	10.0	0.5	10.5	1.5	12.0	2.0
Clear[a]	5.5	1.0	6.5	3.5	10.0	4.5
Grey	21.0	1.0	22.0	0.5	22.5	1.5
MRS[a]	7.0	1.0	8.0	1.5	9.5	2.5
XL	7.5	0.5	8.0	2.5	10.5	3.0
Glass	9.5	0.0	9.5	1.5	11.0	1.5
Laminated tempered	10.5	0.0	10.5	4.0	14.5	4.0
Laminated tempered	10.0	0.5	10.5	4.0	14.5	4.5
Laminated tempered	10.5	0.5	11.0	3.5	14.5	4.0
Laminated annealed	9.5	0.5	10.0	3.5	13.5	4.0
Laminated annealed	9.5	0.5	10.0	4.5	14.5	5.0
Laminated tempered[a]	9.5	1.0	10.5	5.0	15.5	6.0

[a]Original samples were discovered missing in December 1987 and were replaced on April 20, 1988.

Materials that could be used in transparent noise barriers have several unique properties such as transparency and high strength under impact. These products do not meet the MTO's requirement that all materials be durable and have a predicted maintenance-free life expectancy of 20 years. The properties mentioned and others such as reflection of light, flammability, and resistance to abrasion are not alike in all transparent materials.

The locations at which transparent materials may be used will be limited by their sound-reflective properties.

The actual design of the noise barrier system is hampered by the various size limitations of each product.

In general, transparent materials cost more than conventional noise barrier materials.

RECOMMENDATIONS

It is recommended that the MTO set material specifications for the unique properties of transparent materials, such as flammability, safety under impact, transparency, and reflection of light. Transparent materials should be compared with wood (pine) with regard to burn rate and smoke density in order to set a standard for flammability. Wood is the material with the highest burn rate of all approved barrier materials. The MTO must devise a standard for safety under impact and for resistance to permanent degradation in transparency due to abrasion and exposure to ultraviolet rays. Precautions to reduce the reflection of light must be taken into consideration in design. The different types of sheet glazing products could then be evaluated on how they met the above standards.

The samples of the different sheet glazing materials must continue to be tested at a roadside location to monitor the degradation of transparency. Any cost analysis of a barrier design must take into consideration the projected lifetime costs of cleaning and replacement of broken panes. Because of the size limitations of the transparent sheets, the design of the noise barrier system must be able to accommodate any transparent product available.

MTO policy regarding future implementation of transparent noise barriers must be developed. Such policy would have to deal with the following topics:

- Establishing criteria for identification and priority ranking of transparent noise barrier locations, and
- Assessing the responsibility for the supplemental costs incurred by erecting a transparent noise barrier instead of an opaque one.

More investigation should be carried out to test the theory that the tilting of sound-reflective barriers will reduce the noise impact on the surrounding community.

REFERENCES

1. D. G. Guibord. *Noise Barriers in Ontario—An Evolution.* Ministry of Transportation, Downsview, Ontario, Canada, 1985.
2. *Guidelines on Noise and New Residential Development Adjacent to Freeways.* Ministry of Housing, Downsview, Ontario, Canada, 1979.
3. *Noise Policy and Acoustic Standards for Freeways.* Directive A-1. Ministry of Transportation and Communications, Downsview, Ontario, Canada, 1983.
4. *Proceedings of Noise Barrier Seminar.* Ministry of Transportation and Communications, Downsview, Ontario, Canada, 1978.
5. *Utilisation du Verre dans la Construction d'Ecrans Acoustiques* (Glass Acoustic Baffles). Ministries of Transportation and of the Environment and Quality of Life, Paris, France, 1980.
6. *Laminated Glass.* Lamilite Limited, undated (brochure).
7. *Lexan Sheet—Architectural Glazing.* General Electric Plastics, undated (brochure).
8. R. D. Douglas and J. K. Drinkwater. Transparent Noise Barriers along I-95 in Baltimore City, Maryland. In *Transportation Research Record 865*, TRB, National Research Council, Washington, D.C., 1982, pp. 16–18.
9. *Noise Barrier Acoustical Performance Evaluation: I-93, Ten Hills, Somerville, MA.* L. G. Copley Associates, 1979.
10. *Noise Barrier Design Requirements and Material Specifications.* Ministry of Transportation and Communications, Downsview, Ontario, Canada, 1985.
11. *The Development of Noise Barrier Specifications for Ontario.* Ministry of Transportation and Communications, Downsview, Ontario, Canada, 1986.
12. *Ontario Highway Bridge Design Code.* Ministry of Transportation and Communications, Downsview, Ontario, Canada, 1983.
13. Bolt, Beranek, and Newman, Inc. *Noise Barrier Design Handbook.* Report FHWA-RD-76-58. FHWA, U.S. Department of Transportation, 1976.
14. Urban Systems Research and Engineering, Inc. *Highway Noise.* Reprint of *The Audible Landscape: A Manual for Highway Noise and Land Use.* FHWA, U.S. Department of Transportation, 1974.

Publication of this paper sponsored by Committee on Transportation-Related Noise and Vibration.

Field Testing of the Effectiveness of Open-Graded Asphalt Pavement in Reducing Tire Noise from Highway Vehicles

KENNETH D. POLCAK

Over the last several years, highway pavement rehabilitation projects have incorporated open-graded asphalt, also referred to as "popcorn pavement" for its skid-resistant properties. Subjective observations have noted a decrease in overall noise levels in areas where popcorn pavement has been used. The results are presented of a field testing program conducted in June 1989 along the Baltimore Beltway (I-695) to determine the difference in the overall noise level from typical highway traffic traveling on concrete versus open-graded asphalt pavement. Noise levels were measured simultaneously adjacent to the concrete and asphalt surfaces to determine the difference in noise level, and classified traffic counts were made to determine the effect of truck percentage in the traffic stream on the overall noise reduction attributable to the open-graded pavement. An analysis of the third-octave band frequency spectrum for traffic on the concrete and open-graded asphalt is also presented. The results showed a consistent 2- to 4-dBA reduction in the overall L_{eq} that could be attributed to the open-graded pavement. In the higher-frequency bands, 1,000 to 5,000 Hz, the third-octave band analysis showed a significant reduction (2 to 4 dB at 1,000 Hz to 6 to 7 dB at 2,000 to 4,000 Hz). Future studies are planned to expand the baseline data to include other ages and types of concrete and asphalt surfaces, as well as to determine whether aging of the pavement affects its noise reduction capacity.

Over the course of the last several years, the Maryland State Highway Administration (MSHA) has found the need to undertake numerous projects for rehabilitation of the aging Interstate highway system. The Interstate highways, many of which have existed since the early to mid-1960s, consist of mostly reinforced concrete slabs with expansion joints. The rehabilitation projects involving this type of road surface have utilized a system of asphalt overlays coupled with rigid joint replacement. The existing concrete road surface is milled or grooved before the overlay of asphalt.

A part of the overall goal of the rehabilitation projects is to improve safety. The type of asphalt surface that has been used in a number of locations is an open-graded asphalt mix, which was originally developed as a skid-resistant surface to reduce hydroplaning of tires on wet pavement. This type of surface has also been referred to as "popcorn pavement." Several layers of impervious asphalt are first laid, with the final course a ¾-in. layer of the porous open-graded mix.

Subjective observations have been received from both the public and agency personnel indicating a decrease in noise levels in areas where popcorn pavement has been used. The observations described comparisons between concrete and asphalt surfaces. Some observations indicated that the overall noise level adjacent to the highway was reduced with the asphalt resurfacing, whereas others described a change in the character of the noise. When it was riding on the asphalt surface, noise levels inside the vehicle also seemed to be reduced.

This report presents the results of a field testing program conducted in June 1989 along the Baltimore Beltway (I-695) to document the differences in the overall characteristics of the noise emissions from typical highway traffic traveling on concrete versus open-graded asphalt pavement.

Maryland State Highway Administration, Landscape Architecture Division, 707 N. Calvert St., Baltimore, Md. 21202.

SITE SELECTION AND CRITERIA

The first task involved in this study was to find suitable sites on which to conduct the comparison of the two pavement types. The goal in the site selection process was to find sites that would allow for the most direct comparison of the field data without the need for computer simulations or adjustments to account for variations in traffic flow (such as volume, speed, and vehicle mix) or terrain features.

The most direct comparison would be accomplished with sites with uncomplicated yet similar geometry adjacent to a straight roadway section with minimal or no grade. To avoid variations in the traffic parameters, sites were sought along the Interstate system where traffic speeds were high and relatively constant and where the pavement transition between the concrete and asphalt surfaces occurred between interchanges.

Site selection criteria were based on acceptable FHWA procedures (*1*).

SITE DESCRIPTION

One area was identified that met the selection criteria. The area is located west of Baltimore, along I-695 between the interchanges for US Route 40 and I-70 (see Figure 1). The present highway consists of a six-lane section with auxiliary lanes in both directions, and is oriented in a north-south direction. Resurfacing with open-graded asphalt pavement was completed in 1984 and ended approximately midway between the two interchanges. The asphalt surface tested was approximately 4½ years old. The remaining section of road has a

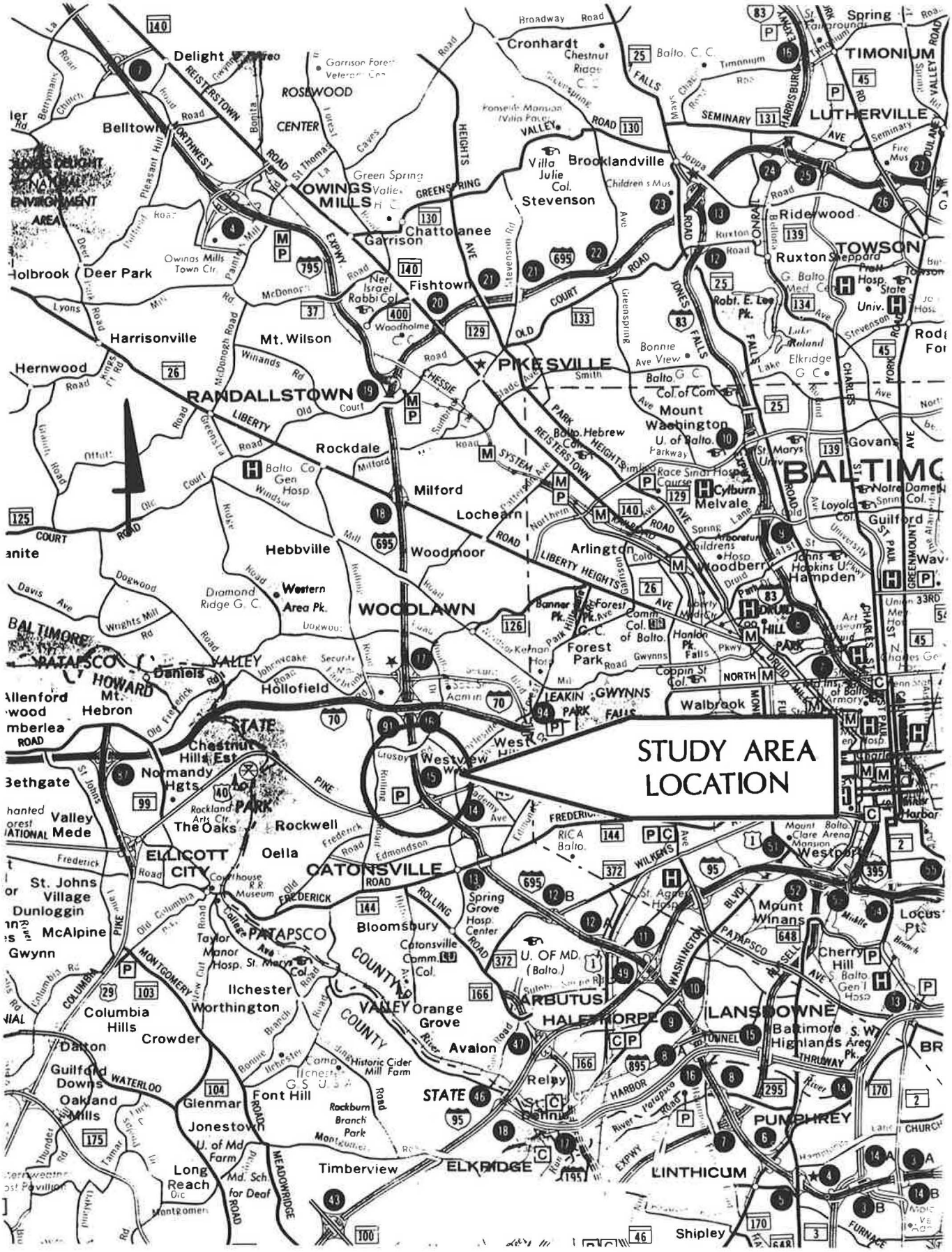

FIGURE 1 Study area location.

reinforced-concrete surface, which was about 25 years old at the time of the study. The road section dates back to 1962 and 1966 (when a lane in each direction was added to the median of the original roadway). A slight upgrade of 1.5 to 2 percent was noted in the southbound direction. The grade as noted was determined to be acceptable on the basis of FHWA criteria (*1*).

The surface of the concrete pavement is severely eroded, with the aggregate readily visible. Although some uneven joints between the pavement slabs were noted, none of the measurement sites was in close proximity to these areas. The asphalt surface was in good condition with no notable surface irregularities.

For the study, four sites were selected, two on each side of the highway. Figure 2 shows the relationship of the various test sites. Sites 1 and 4 are adjacent to the asphalt pavement section, and Sites 2 and 3 are adjacent to the concrete pavement. The reason for selecting sites on both sides of the highway was to determine the effect, if any, of the upgrade on the southbound roadway. Each measurement site was located 50 ft from the centerline of the closest travel lane and a minimum of 470 ft from the pavement transition point. The sites were chosen as far from the pavement transition point as possible to minimize noise influence from the adjacent pavement. Figure 3 shows a cross-sectional view of Sites 1 and 2 (northbound side), and Figure 4 gives a similar view of Sites 3 and 4 (southbound side).

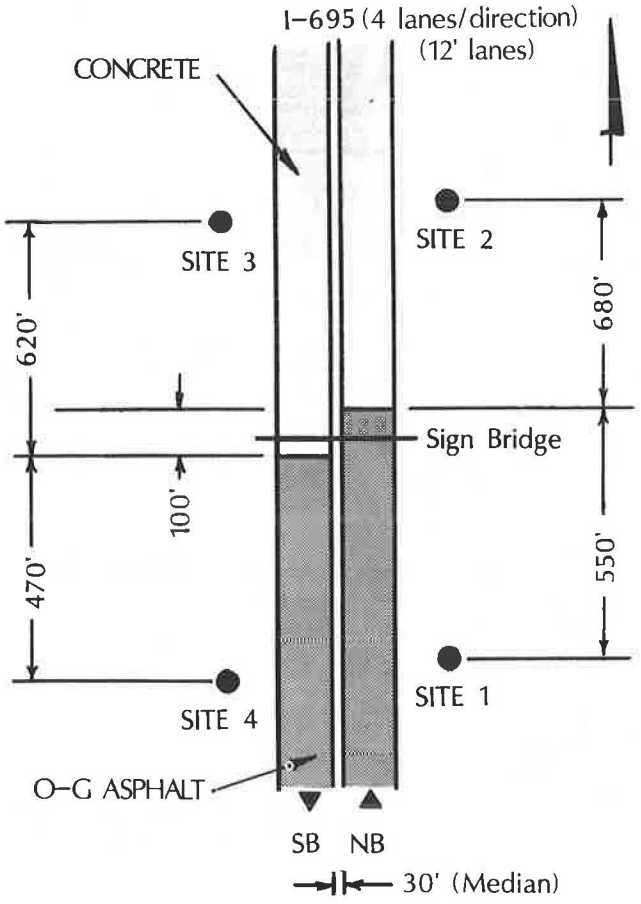

FIGURE 2 Site diagram.

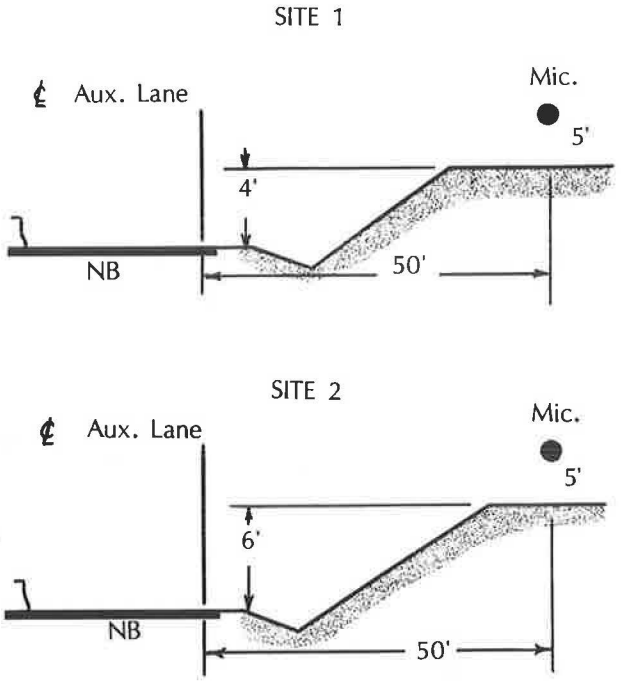

FIGURE 3 Cross sections of measurement Sites 1 and 2 along northbound roadway.

The geometrics between Sites 1 and 2 were considered acceptable on the basis of FHWA criteria (*1*) in that the intervening ground at both sites was grassy and the effective height of the microphones above the pavement elevation was similar, ranging approximately 9 to 11 ft.

The elevation at Sites 3 and 4 was such that the effective microphone height above the pavement elevation was more on the order of about 4 ft. The drainage ditch that runs parallel to the highway (as shown in Figure 4) is present at both sites; however, the ditch is lined with concrete in front of Site 3 and gets progressively deeper toward Site 4. This dissimilarity was considered a possible source of reflections at Site 3, particularly in the third-octave band study. At Site 4, the ditch is depressed sufficiently below the level of the road so that the potential for reflections is minimal. Consistency with the results from Sites 1 and 2 would be examined to validate or discount the data results gathered at Sites 3 and 4.

INSTRUMENTATION

The sound-level meters (SLMs) used in this study were Metrosonics Model dB-308 Metrologgers and meet specifications for Type I SLMs in accordance with ANSI S1.4. Each microphone was located 5 ft (±0.5 ft) above the ground. The tests yielded A-weighted L_{eq} noise levels at each of the four sites. Calibration of each meter was performed before and after each monitoring session.

In addition to the A-weighted L_{eq} measurements, a third-octave band analysis was also conducted at the same four sites to examine the frequency content of the overall noise emissions from the same traffic on the two pavement types. Output from a Bruel & Kjaer (B&K) Type 2231 modular precision SLM was fed to a B&K Type 2515 vibration analyzer, which

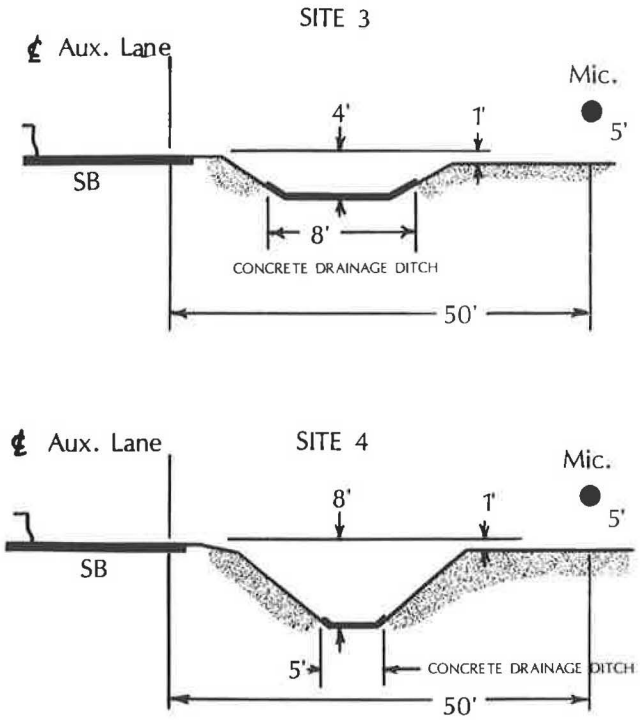

FIGURE 4 Cross sections of measurement Sites 3 and 4 along southbound roadway.

is a single-channel fast Fourier transform analyzer. The L_{eq} for each test was also obtained for comparison with the other data. Microphone heights and locations were identical to those in the A-weighted L_{eq} tests. Calibration was also conducted before and after the test session.

FIELD MEASUREMENTS

The study was conducted in two parts. The first part involved simultaneous measurement of the A-weighted sound levels at all four sites. In the second part of the study a third-octave band spectrum of noise emissions from traffic was obtained for the asphalt versus the concrete pavement.

L_{eq} noise level data were gathered for consecutive 5-min intervals for a total period of 1 hr on two different days. Simultaneously with each measurement interval, classified traffic counts were made identifying automobile, medium trucks, and heavy-duty trucks as defined by FHWA (*1*) to document the percentage of trucks in the traffic stream. Also, random checks of travel speeds of the overall traffic stream were made during each test.

For the third-octave band analysis, Sites 1 through 4 were monitored at the same locations as in Part 1 of the study. It was decided to use the same 5-min test interval as a starting point to be consistent with Part 1. During the initial test, the various third-octave band levels were observed on the analyzer's CRT screen to determine whether the 5-min test interval would yield a stable third-octave band spectrum. The CRT display stabilized after approximately 3 min. Therefore, the 5-min test interval was deemed acceptable, and was also used for the other three sites. At the end of each test interval, a printout of the third-octave band spectrum and the A-weighted L_{eq} noise level was obtained.

RESULTS

A-Weighted L_{eq}

The results of Part 1 of the study are presented in Table 1, which shows the 5-min L_{eq} noise level for each test interval and the corresponding traffic count (for both directions). In addition, the cumulative 1-hr L_{eq} is also given.

For Sites 1 and 2 (along the northbound side), the L_{eq} noise level for traffic on the asphalt pavement (Site 1) was 2.1 to 4.0 dBA less than the level for the same traffic on the concrete pavement (Site 2). The difference in the 1-hr L_{eq} was 2.8 to 2.9 dBA.

Similarly, at Sites 3 and 4 (southbound side), the L_{eq} level for traffic on the asphalt section was 2.3 to 3.6 dBA less than the same traffic on the concrete section. The difference in the 1-hr L_{eq} was 2.9 to 3.1 dBA.

During these tests, the random speed checks noted that the majority of the vehicles were traveling 55 to 65 mph consistently for all the tests.

There was some concern regarding the distance between the sites and the lag time (the time it takes for each vehicle to pass both sites), and the possibility that lane changes might change the individual vehicle-to-microphone distance. However, the large number of test intervals and the consistency of the data seem to indicate that these factors were not a significant source of potential error.

The traffic data gathered concurrently with the noise measurements were then analyzed to determine whether any correlation existed between the noise reduction between the two pavement sections and a variation in the percentage of trucks. The hypothesis is that because trucks have two other major noise-producing components (engine and exhaust) in addition to tire noise, an increase in the number of trucks in the traffic stream may offset some of the reduction of the tire noise component obtained with the open-graded asphalt pavement, thus making it a less effective option for situations in which large percentages of trucks are found. Figures 5 and 6 show plots of the noise reduction attributable to the open-graded surface against the percentage of trucks counted during each measurement interval. The scattering of the values shows no clear trend supporting the hypothesis. It is suspected that the wide variation in noise emission levels of individual trucks in the general truck population is overriding the effect caused by increases or decreases in the number of vehicles, and that the engine and exhaust noise from the trucks is still a major contributor to the overall level.

Third-Octave Band Analysis

For this part of the study, comparisons of the third-octave band spectra were made between Sites 1 and 2, and between Sites 3 and 4. Figures 7 and 8 present the data. In both cases, significant reductions were noted in the higher-frequency bands (1,000 to 5,000 Hz). At Site 1 adjacent to the asphalt pavement, a reduction of 3 to 4 dB was seen at 1,000 Hz and 6 to 7 dB in the 2,000- to 4,000-Hz range compared with Site

TABLE 1 PAVEMENT NOISE TEST SERIES 1 AND 2 DATA FOR BALTIMORE BELTWAY (I-695) BETWEEN U.S. 40 AND I-70

TIME	TRAFFIC DATA AUTOS	MT	HT	Leq NOISE LEVELS (dBA) - 5 MINUTE INTERVALS SITE 1	SITE 2	DIFF. (1-2)	SITE 3	SITE 4	DIFF. (3-4)
2:00	600	48	64	78.5	82.0	3.5	80.5	77.9	2.6
2:05	581	38	42	77.2	79.9	2.7	78.6	75.0	3.6
2:10	698	32	70	77.7	80.5	2.8	79.2	76.1	3.1
2:15	660	41	57	77.2	79.7	2.5	79.0	75.5	3.5
2:20	677	45	44	77.4	79.5	2.1	78.8	75.3	3.5
2;25	675	35	64	77.5	80.4	2.9	79.7	76.8	2.9
2:30	641	24	48	77.9	80.3	2.4	78.6	75.7	2.9
2:35	748	39	67	78.3	81.4	3.1	78.7	75.7	3.0
2:40	796	45	64	77.7	80.3	2.6	79.0	76.0	3.0
2:45	678	36	38	77.3	79.6	2.3	78.3	75.0	3.3
2:50	853	23	47	78.0	81.3	3.3	78.5	75.3	3.2
2:55	890	43	60	77.6	80.7	3.1	79.5	76.2	3.3
CUMULATIVE Leq(h) -				77.7	80.5	2.8	79.1	76.0	3.1
11:30	580	17	76	77.7	80.2	2.5	77.7	75.2	2.5
11:35	577	33	64	76.4	79.1	2.7	77.7	74.9	2.8
11:40	590	31	65	77.3	80.0	2.7	78.5	75.2	3.3
11:45	632	23	70	77.4	81.4	4.0	78.1	75.2	2.9
11:50	636	34	60	76.7	79.4	2.7	77.3	74.3	3.0
11:55	601	28	58	76.7	79.6	2.9	78.0	74.9	3.1
12:00 N	598	28	60	77.1	79.9	2.8	78.0	75.2	2.8
12:05	620	30	51	77.0	80.4	3.4	77.4	74.1	3.3
12:10	643	23	67	77.1	79.9	2.8	77.0	74.4	2.6
12:15	627	29	46	76.2	78.5	2.3	77.6	74.4	3.2
12:20	599	36	45	76.8	79.6	2.8	77.7	75.4	2.3
12:25	621	17	67	77.1	79.9	2.8	78.2	75.6	2.6
CUMULATIVE Leq(h) -				77.0	79.9	2.9	77.8	74.9	2.9

2 adjacent to the concrete pavement. Similarly, between Sites 3 and 4, a 2-dB reduction at 1,000 Hz and a 7-dB reduction at 2,000 Hz were attributable to the asphalt surface.

Corresponding A-weighted L_{eq} levels for the same tests showed a reduction of 3 to 4 dBA attributable to the asphalt surface.

EVALUATION OF RESULTS AND CONCLUSIONS

The results of the L_{eq} noise level comparison showed a consistent 2- to 4-dBA reduction that could be attributable to the 4½-year-old open-graded asphalt surface in this study location. Table 2 presents a summary of the data from the study.

Earlier studies by FHWA (*2*) involving comparison of various pavement types and different tire tread designs showed a 2-dBA reduction in the average noise level with all types of tire tread designs considered together. The reduction was attributed to the open-graded asphalt surface as compared with portland cement concrete pavement.

A substantial reduction in the high-frequency content of noise from traffic on open-graded asphalt was noted compared with the same traffic on concrete pavement. Given that individuals are more sensitive to high-frequency sound, this may indeed explain the positive responses, which seem to be greater than would be anticipated if one only considered the reduction in the L_{eq} noise level.

For this series of tests, no correlation was found between the variation in truck percentage and the noise reduction effects attributable to the open-graded asphalt surface. The additional components of engine and exhaust noise, which still make the truck noise dominant, and the wide variation in noise emission levels of trucks in the traffic stream seem to offset the effect of changes in the number of trucks. It is suspected that a wider variation in truck percentage than was seen in this study would be needed to establish a correlation.

Additional study that is needed relative to this topic is as follows:

- Expanding the data base to include more sites, and additional testing at the original test sites to cover different seasons of the year (to study site vegetation effects).
- More testing involving only automobiles, or small fractions (1 to 2 percent) of trucks, to more closely identify how much reduction in tire noise can be obtained by using open-graded asphalt pavement.
- Developing more data for a wider range of vehicle speeds, pavement types, and pavements of differing ages.
- Monitoring the effects of aging on the noise reduction capacity of the open-graded pavement.

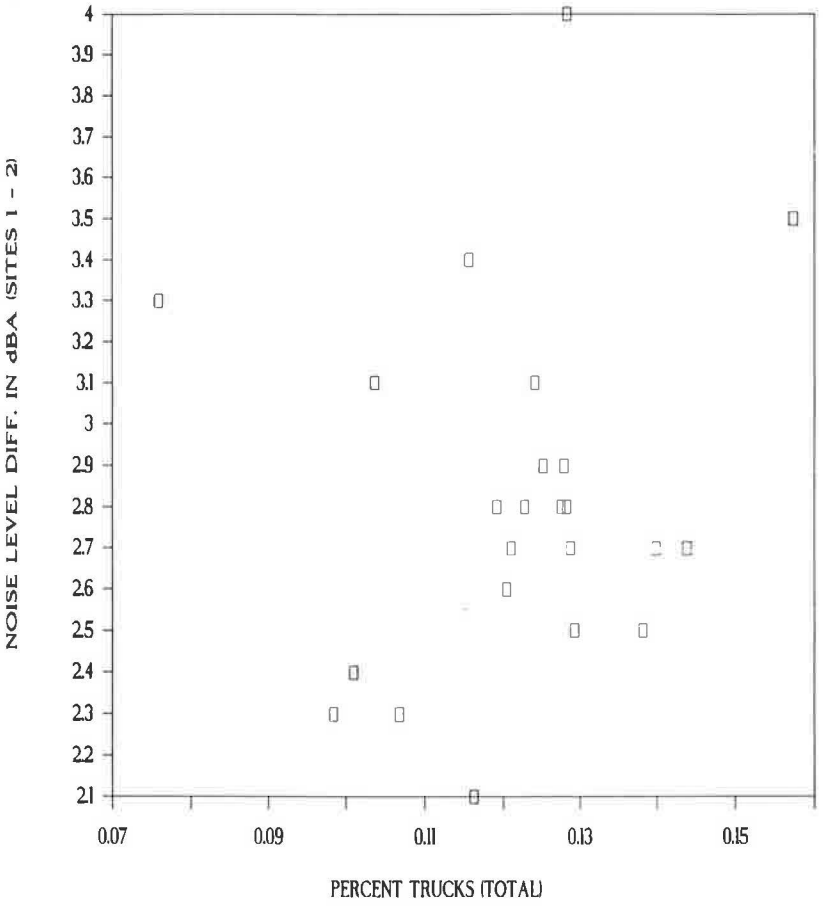

FIGURE 5 Comparison of truck percentage and the measured noise level difference between Sites 1 and 2.

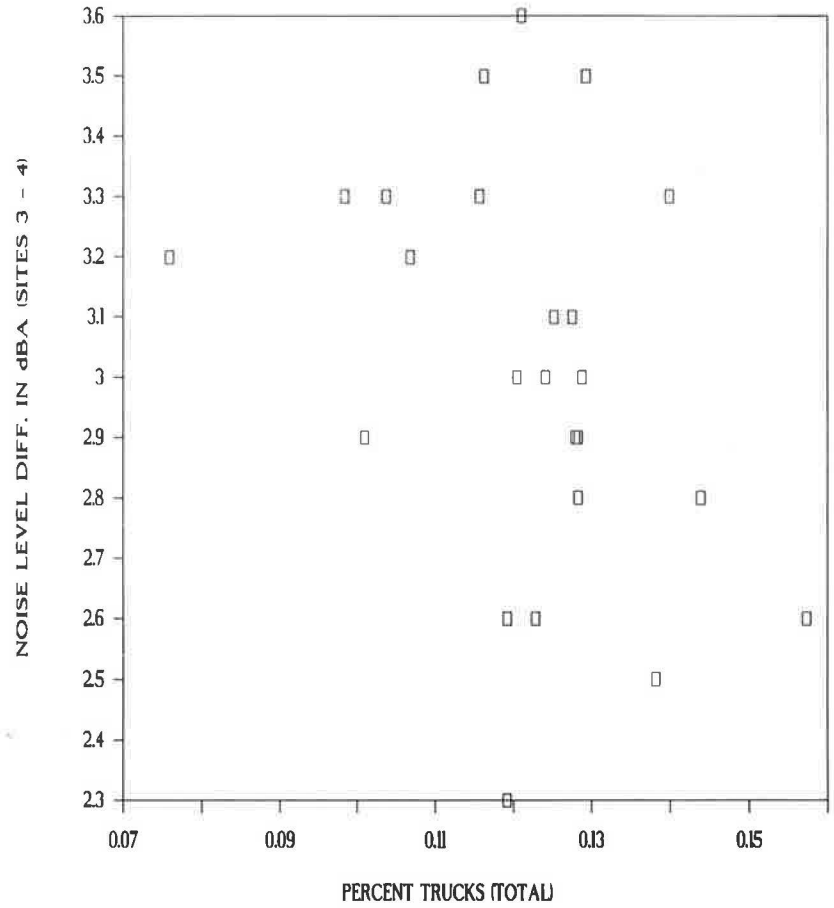

FIGURE 6 Comparison of truck percentage and the measured noise level difference between Sites 3 and 4.

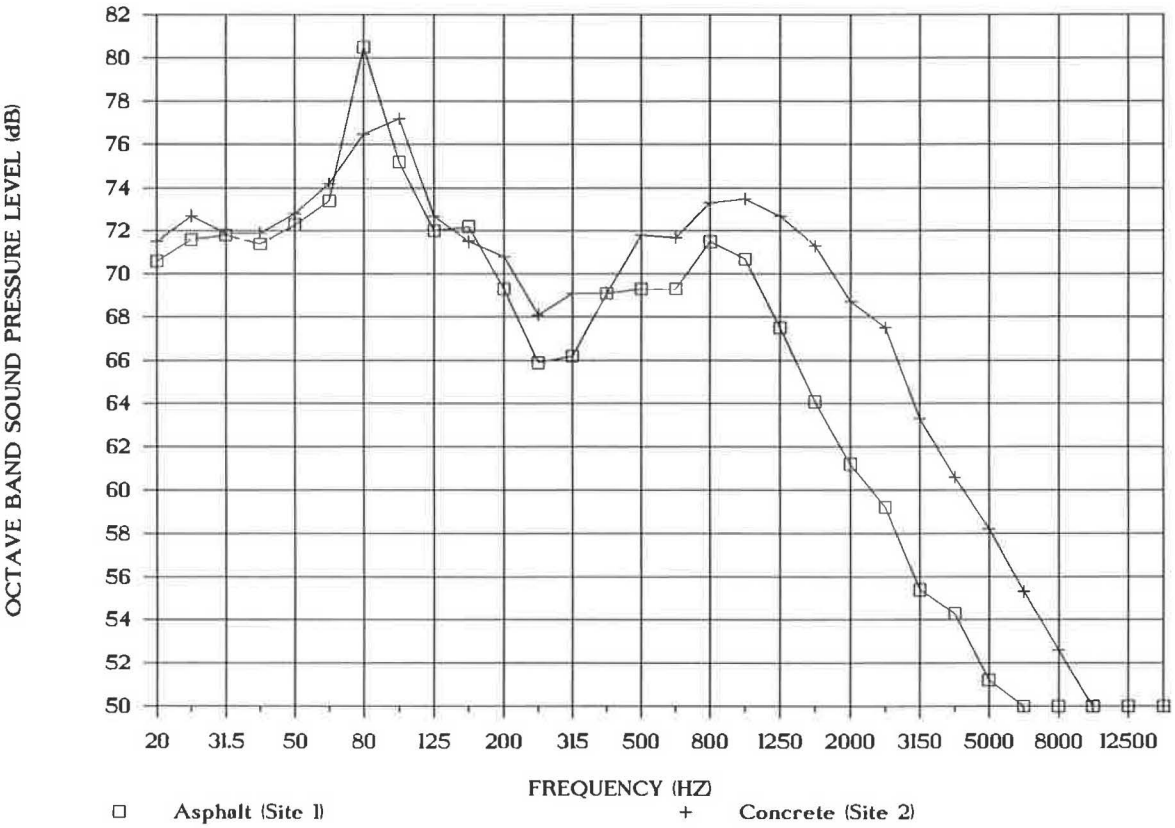

FIGURE 7 Comparison of the third-octave band spectra for Sites 1 and 2.

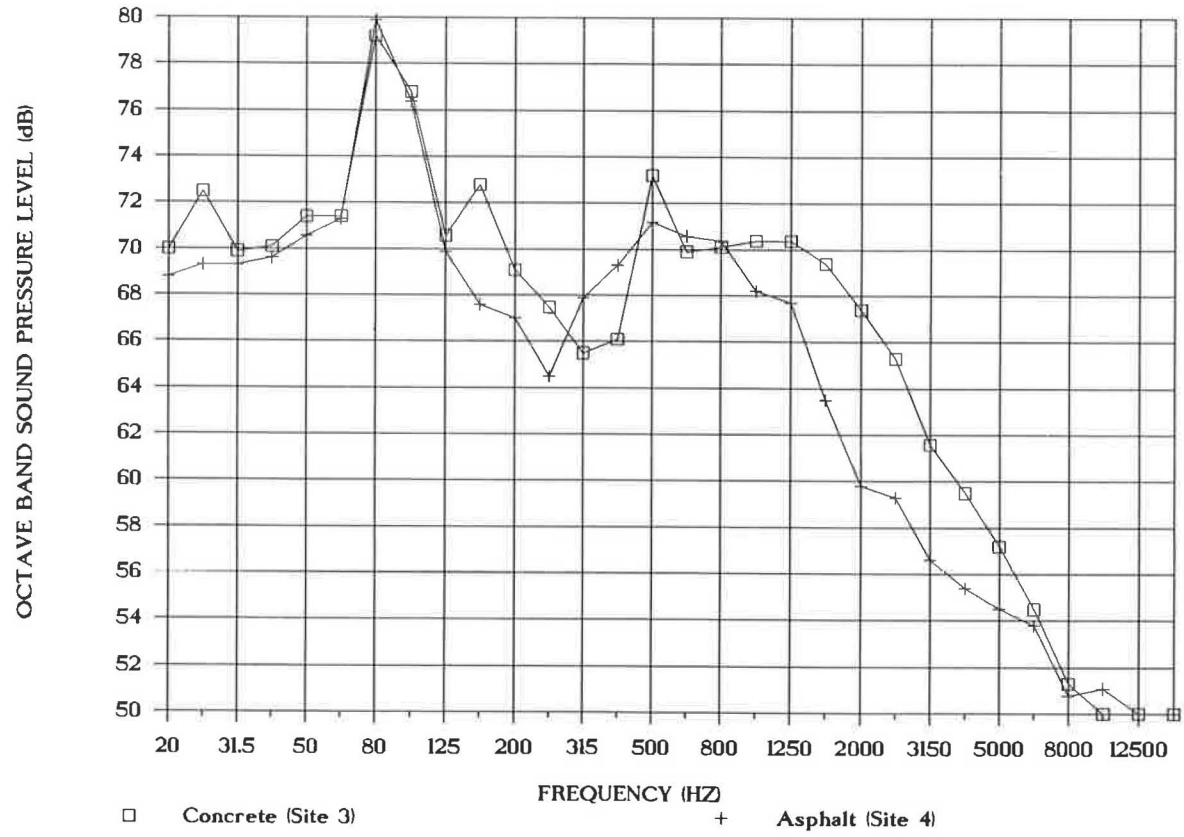

FIGURE 8 Comparison of the third-octave band spectra for Sites 3 and 4.

TABLE 2 SUMMARY OF RESULTS: COMPARATIVE MEASUREMENT OF L_{eq} NOISE LEVEL FROM TRAFFIC ON CONCRETE VERSUS OPEN-GRADED ASPHALT PAVEMENT

Site	$L_{eq}(5)$(dBA)		Cumulative $L_{eq}(h)$(dBA)
	Measured	Calculated[a]	
1—asphalt	76–79	77	77–78
2—concrete	79–82	81	80–81
L_{eq} difference	2–4	4	3
3—concrete	77–81	79	78–79
4—asphalt	74–78	76	75–76
L_{eq} difference	2–4	3	3

[a]Obtained from the third-octave band spectrum analysis data.

- Evaluating the cost-effectiveness of using open-graded pavement as a noise abatement measure.

ACKNOWLEDGMENTS

This study was funded by the Maryland State Highway Administration (MSHA) as a special project under the direction of the Acoustic Analysis Unit of the Landscape Architecture Division. The author expresses special thanks to Bob Matusheski of Bruel & Kjaer Instruments, Inc.; to staff from the consulting firm of Greiner, Inc.; to Tom Nalesnik, staff member for MSHA; and to Shawn Newson, summer student employee for MSHA, for their assistance in the tedious and laborious task of data collection for this project. The author also gratefully acknowledges the anonymous contributions and positive suggestions offered after the review of this paper through TRB Committee A1F04.

REFERENCES

1. W. Bowlby. *Sound Procedures for Measuring Highway Noise: Final Report.* FHWA-DP-45-1R, FHWA, U.S. Department of Transportation, Aug. 1981.
2. R. A. Kay and J. K. Stephens. *Implementation Package 74–11—Porous Friction Courses and Roadway Surface Noise.* FHWA, U.S. Department of Transportation, March 1975.

Publication of this paper sponsored by Committee on Transportation-Related Noise and Vibration.

Cost of Noise Barrier Construction in the United States

LOUIS F. COHN AND ROSWELL A. HARRIS

The results of a study of noise barrier costs in the United States are presented. A survey was made of each state highway agency and the FHWA to codify all barriers constructed through 1987. Costs associated with the construction of the barriers were then made current through the fourth quarter of 1988 using the FHWA quarterly price trends for federal-aid highway construction. New curves correlating cost per linear foot were then developed using standard statistical techniques. The new curves have been incorporated into the OPTIMA code. In addition, other changes to OPTIMA have been made and are described.

In 1982 FHWA distributed the companion computer programs STAMINA 2.0 and OPTIMA (*1*). Together, STAMINA 2.0 and OPTIMA constitute the barrier cost reduction (BCR) technique, which was developed in 1977 by Bolt, Beranek, and Newman (*2*).

OPTIMA contains cost data (Table 1) for noise barriers, allowing the OPTIMA user to develop cost-effective barrier designs based on an effectiveness/cost ratio (*E/C* table). The cost information included in OPTIMA has not been updated since the model was originally distributed and in fact is based on a very limited number of barriers constructed primarily in California in the early to mid-1970s.

Because the cost data currently in OPTIMA are quite old and are based on a limited number of constructed barriers, most users have been unwilling to rely on them for other than purely qualitative comparisons between barrier material types. The unreliability of the cost data has also diminished the use of OPTIMA as a design tool, because users cannot depend on even the relative accuracy of the *E/C* table numbers. Consequently, many barrier designers today use the OPTIMA *E/C* table only as a starting point, and then rely heavily on heuristic judgment to develop final designs.

EXTENT OF THE U.S. BARRIER PROGRAM

To address the problems, a study was undertaken to determine the extent and cost of the barrier construction program in the United States, to develop current base-year cost information for the barriers constructed, and to revise the cost-per-linear-foot curves contained within OPTIMA. Data for this study were received from the states and FHWA in response to a comprehensive survey. Concurrent with this study, another effort was undertaken to improve the usefulness of OPTIMA from a user interface standpoint. Results from both of these studies are discussed in the remainder of this paper.

As mentioned earlier, the costs presented in Table 1 are based on a limited number of barriers constructed in the early to mid-1970s. Since that time, many states have conducted extensive barrier programs; most other states have built at least one barrier. As presented in Table 2, more than 466 linear mi of barriers had been built through 1987 (*3*). This number is in contrast to 189 linear mi of barriers constructed in the United States through 1980 (*4*).

Most of the barriers presented in Table 2 were included in the data supplied by the states in response to the survey mentioned earlier. Distribution of height by material is presented in Table 3; the average height for all the barriers reported in the survey is 11.65 ft.

In summary, several conclusions can be drawn about the extent of the U.S. barrier program to date. Among these are the following:

1. The magnitude of the program has nearly tripled since 1980,
2. Concrete- and masonry-based materials are the most commonly used, and
3. Only a very small percentage of barriers exceed 20 ft in height, with the average barrier being about as tall as a heavy-truck exhaust stack.

COST OF THE U.S. BARRIER PROGRAM

The FHWA quarterly publication *Price Trends for Federal-Aid Highway Construction—1977 Base* (*5*) was used to account for geographic and time differences in construction costs for the barriers presented in Table 2. Factors based on the year of construction and the construction price index for the particular state in which the barrier is located were used to bring all barrier costs to constant 1988 dollars. For example, the cost of a concrete barrier constructed in 1977 in California was brought to 1988 by a factor of 2.26; a concrete barrier constructed in Florida in 1977 was brought to 1988 by a factor of 1.99; last, a concrete barrier constructed in Michigan in 1977 was brought to 1988 by a factor of 1.91. These factors are based on state-by-state cost indices for six indicator items that reflect price trends for all roadway excavation, surfacing, and structures.

This updated cost information was combined with the other information gathered from the state highway agencies in the survey to produce a data base for more than 700 barrier proj-

Department of Civil Engineering, University of Louisville, Louisville, Ky. 40292.

TABLE 1 ORIGINAL BARRIER COSTS IN THE OPTIMA CODE

Barrier Height (ft)	Cost per Linear Foot($)				
	Berm	Concrete	Masonry	Steel	Wood
1	2.40	9.80	5.60	11.20	6.40
5	7.80	41.50	23.90	52.60	28.70
10	23.90	81.50	52.60	124.50	57.50
15	49.50	139.00	95.80	204.40	102.20
20	95.80	183.70	111.80	354.70	175.70
25	142.10	228.30	127.80	505.00	249.20
30	188.40	273.00	143.70	655.20	322.70
35	234.10	311.20	159.70	805.50	396.20

TABLE 2 BARRIERS CONSTRUCTED IN THE UNITED STATES (*3*)

Material Type	Total Length (mi)	Percent
Block/brick	148.1	32
Concrete	91.2	20
Wood	68.9	15
Berm	47.4	10
Metal	22.6	5
Berm/concrete	18.0	4
Berm/wood	9.8	2
Berm/metal	6.7	1
Other	54.2	11
Total	466.9	

TABLE 3 DISTRIBUTION OF BARRIER HEIGHTS BY MATERIAL TYPE

Material Type	Percent Distribution by Height Group (ft)						
	1–5	5–10	10–15	15–20	20–25	25–30	30–35
Concrete	—	32	47	20	1	—	—
Masonry	—	72	18	10	—	—	—
Wood	—	49	18	34	—	—	—
Berm	3	65	17	10	5	—	—
Metal	9	32	31	25	—	3	—
Berm/concrete	—	46	10	32	8	4	—
Berm/wood	—	33	45	22	—	—	—
Berm/metal	—	41	31	28	—	—	—
Other	—	23	26	47	2	2	—
Total	1	42	32	22	1	1	1

ects in 37 states. The data base was prepared for analysis using dBase III Plus, and included the following fields:

State
City
Route
Year of construction
Cost update factor
Length (ft)
Height class (ft)
Actual height (ft)
Material class
Actual material
1988 cost ($/lf)

As Table 1 indicated, the OPTIMA code classifies barrier costs in five material categories: berm, concrete, masonry, steel, and wood. From the more than 700 barrier projects in the data base, 520 were selected for statistical analysis. These 520 were deemed to fit cleanly into one of the five categories. Linear regression was performed on the data in each material category. Cost coordinates were assigned to each of the 520 barriers, with the x-coordinate being height and the y-coordinate being (updated) cost per linear foot. Linear regression fits a straight line in the slope intercept form to produce regression lines. The regression lines developed for the five material categories were then tested for significance using correlation coefficient, t-test, and confidence intervals.

Correlation coefficients (r-values) measure the variation of one variable with respect to the variation of the other. Their values ranged as follows: berm, 0.315; concrete, 0.484; masonry, 0.386; steel, 0.666; wood, 0.524. These r-values indicate a relatively inconsistent relationship between cost per linear foot and height. This is to be expected, given the variety of ways in which the costs of barriers are determined in the construction environment.

In the t-test, the mean of the samples and the standard deviation estimated from the samples are used to make probability statements about the values of observations in the population from which the samples were drawn. A 95 percent level of significance was selected as acceptable for the barrier cost data. The tabulated value of the normal distribution for the 95 percent level of significance is $t = 1.96$. If the calculated t-value for the given material category is greater in absolute value than 1.96, then the null hypothesis is rejected, and the conclusion may be made that the regression line calculated from the actual data is significant. The calculated t-values (absolute values) for the material categories ranged as follows: berm, 3.22; concrete, 7.06; masonry, 4.18; steel, 7.02; wood, 5.88. These values confirm significance.

Table 4 presents the new cost data resulting from this study.

Figures 1 through 5 are plots of the updated cost data, as well as the original cost data found in the OPTIMA code. The figures also indicate the degree of scatter of the actual data for the updated costs.

The data presented in Table 4 may be easily incorporated into the OPTIMA Fortran code. Users with executable microcomputer versions of OPTIMA can seek modification to the cost data section of the Fortran code. Such requests naturally must be made to those with access to the Fortran code.

OTHER IMPROVEMENTS TO OPTIMA

In addition to the updated barrier costs, several improvements have been made to the microcomputer version of OPTIMA that is made available in the short course. Although many of

TABLE 4 UPDATED (1988) BARRIER COSTS FOR USE IN OPTIMA

Barrier Height (ft)	Cost Per Linear Foot ($)				
	Berm	Concrete	Masonry	Steel	Wood
1	25.95	56.42	47.46	14.98	1.00
5	42.19	103.10	84.53	72.95	50.24
10	62.49	161.45	130.86	145.41	117.81
15	82.81	219.79	177.19	217.87	185.38
20	103.11	278.14	223.52	290.32	252.94
25	123.42	336.49	269.86	362.78	320.51
30	143.72	394.83	316.19	434.16	388.07
35	164.00	453.00	363.00	508.00	456.00

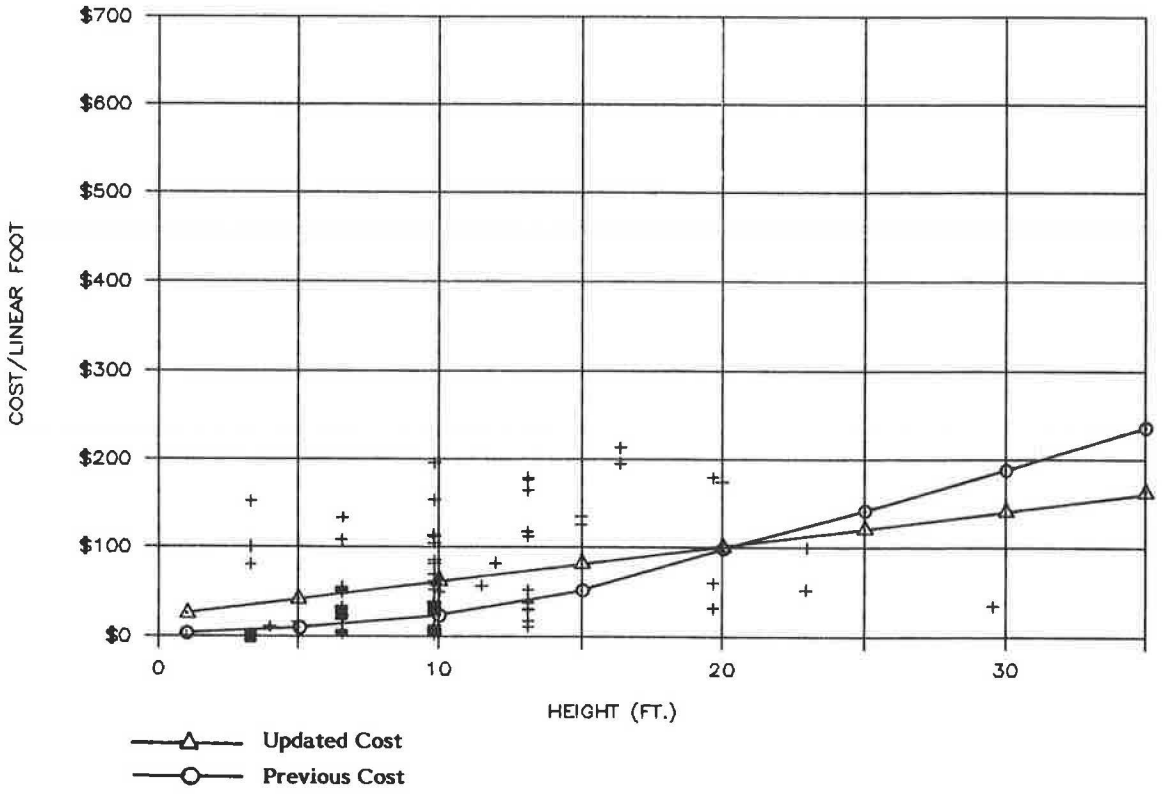

FIGURE 1 Noise barrier cost—berm.

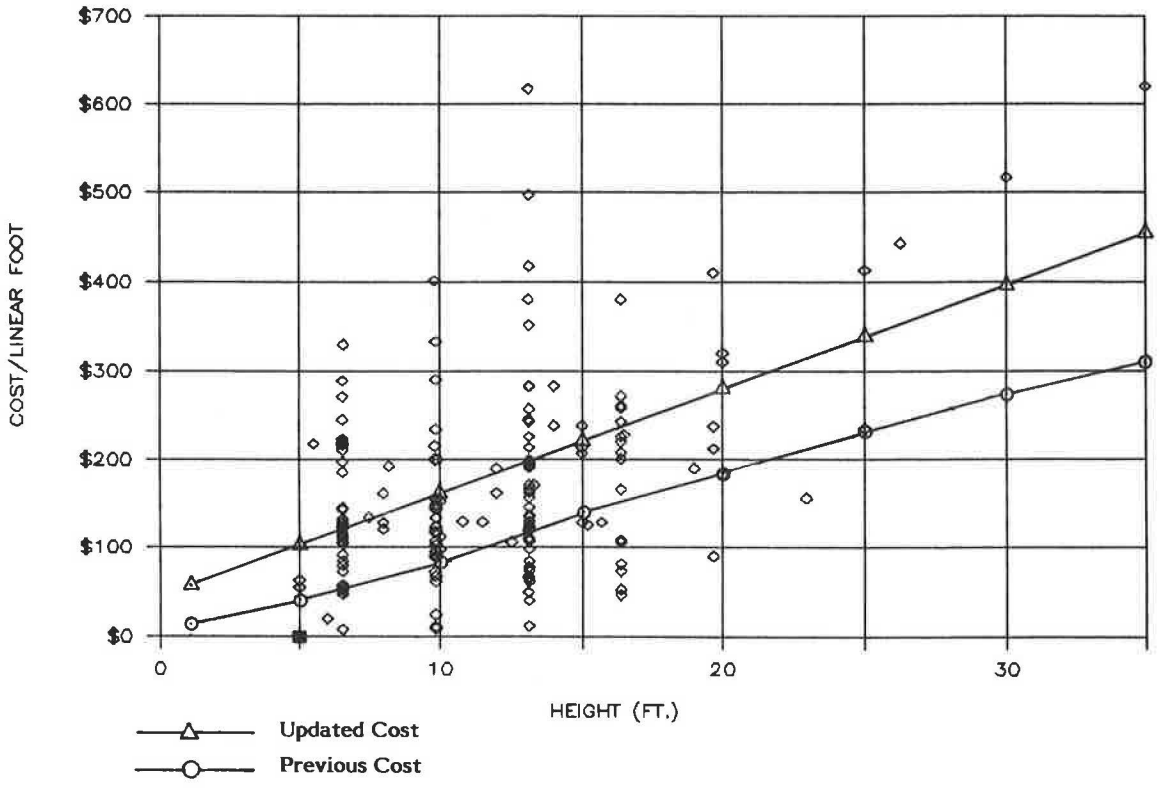

FIGURE 2 Noise barrier cost—concrete.

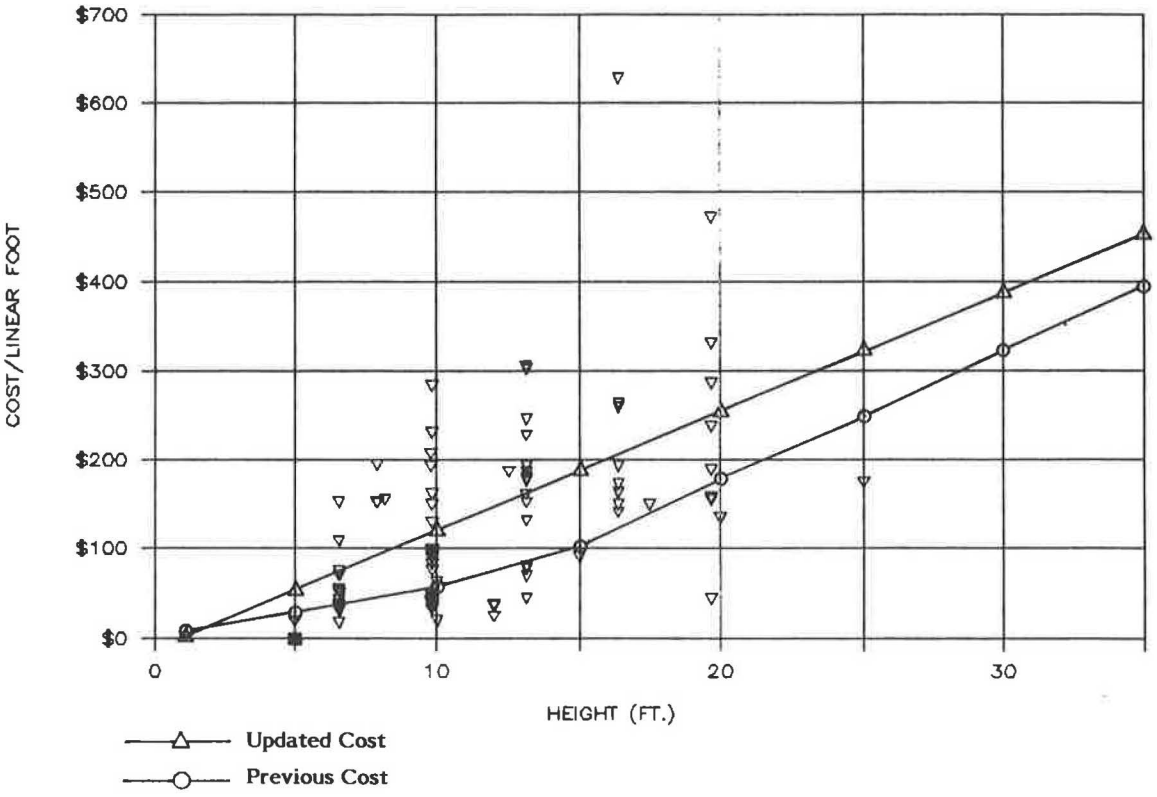

FIGURE 5 Noise barrier cost—wood.

R E S U L T S
****

REC	REC ID	LEQ	LEQ(Z(0))	IL
1	R10	61.5	68.7	7.2
2	R11	60.3	67.8	7.5
3	R12	59.6	67.3	7.7
4	R13	59.8	67.7	7.9
5	R14	59.9	68.0	8.1
6	R15	60.3	68.6	8.2

BARRIER TYPE	COST	AREA (SF)
FH-BERM	35200.	5184.
FH-MASON	118421.	9708.
FH-WOOD	80981.	6731.
FH-CONC	156631.	10743.
FH-STEEL	124985.	8601.

BARRIER COST = $ 516218. TOTAL AREA = 40967.

AREA BREAKDOWN
****

MATERIAL TYPE	BARRIER HEIGHT (FT.) <5	5-10	10-15	15-20	>20
FH-BERM	308.6	2304.6	2571.0	0.0	0.0
FH-MASON	0.0	800.9	3800.9	5105.8	0.0
FH-WOOD	0.0	812.8	4411.8	1506.9	0.0
FH-CONC	0.0	0.0	3641.4	5159.2	0.0
FH-STEEL	0.0	1599.5	3599.2	3402.1	0.0

FIGURE 6 OPTIMA output showing area information.

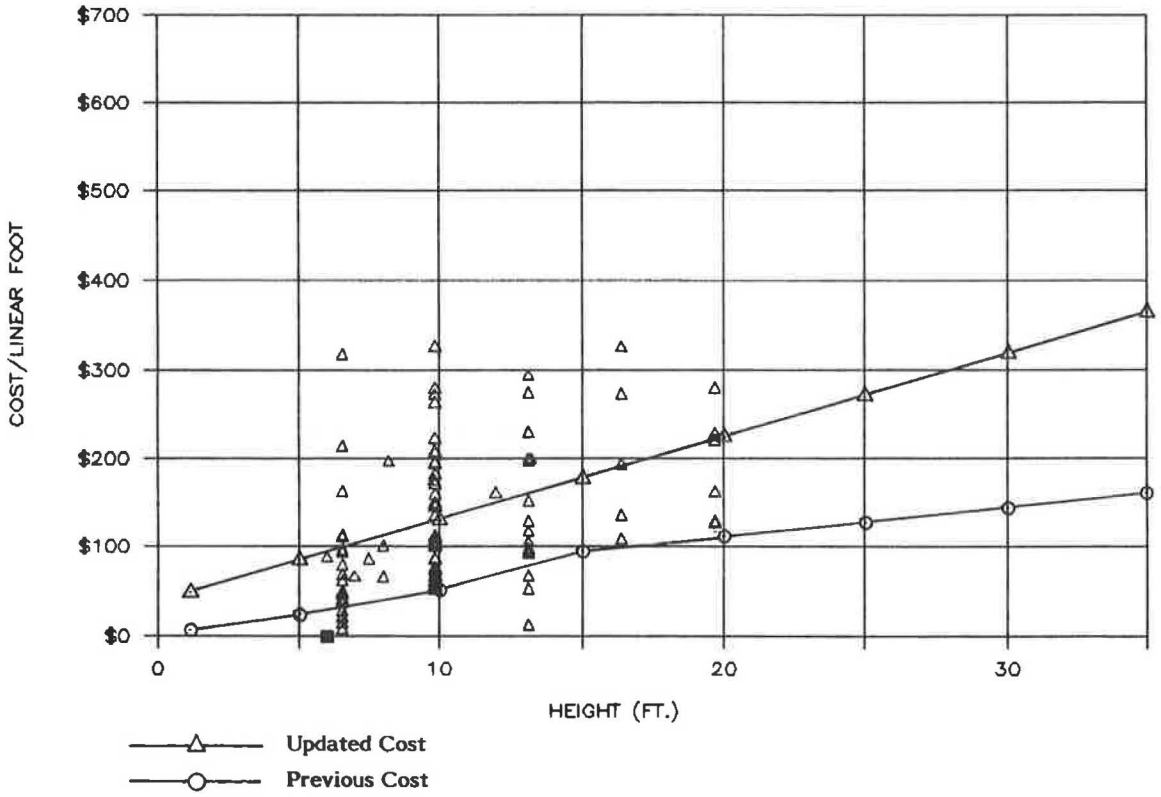

FIGURE 3 Noise barrier cost—masonry.

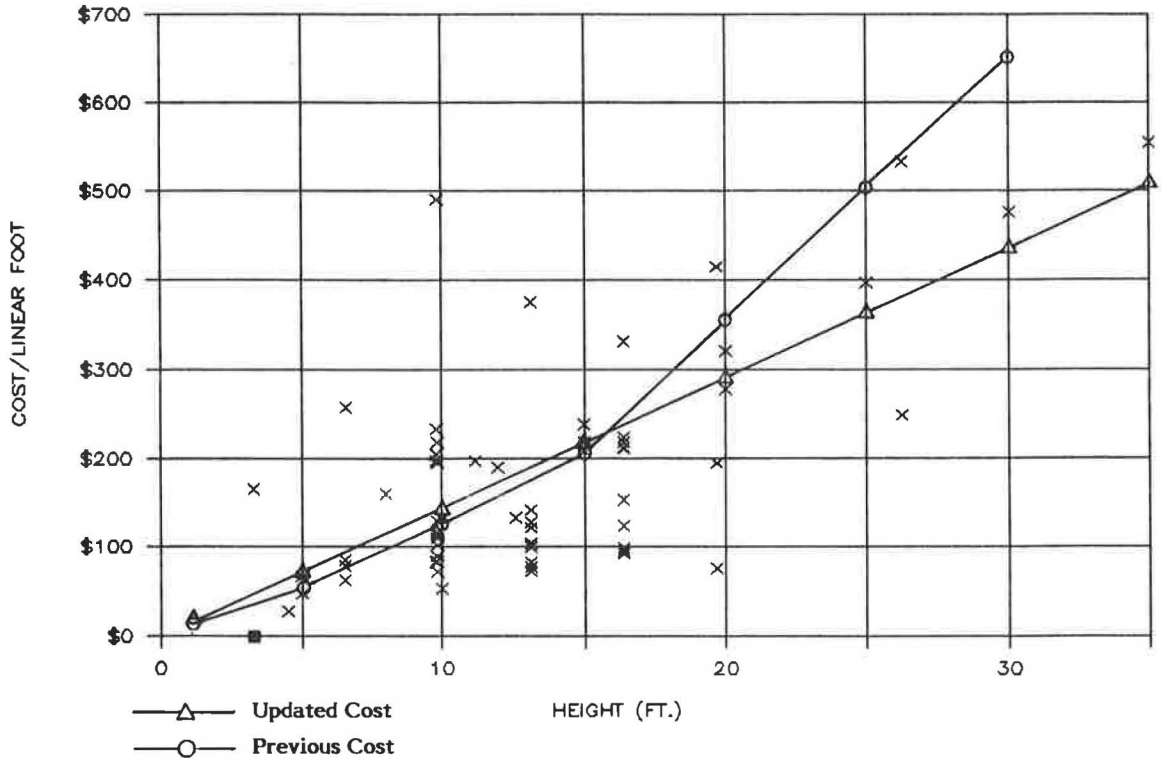

FIGURE 4 Noise barrier cost—steel.

these improvements relate to wording changes in the user interface, two are worth noting. First, it is now possible to reopen an existing OPTIMA output file (.OPT file). Before this change was made, it was necessary to reenter all the initialization information concerning material type for each barrier segment, and population and design noise level for each receiver, each time that OPTIMA was run for a given acoustics output file (.ACO file).

The second change results in the display of area information corresponding to a given set of height indices. This information is in addition to the L_{eq}, insertion loss, cost, and segment contribution data normally associated with OPTIMA output. Figure 6 shows the results portion of a typical OPTIMA output file for a barrier with mixed material types and various heights.

CONCLUSION

The barrier cost reduction (BCR) procedure is of some value in noise barrier design. The usefulness of the procedure has been severely limited by the incomplete and inaccurate nature of the cost data contained within the OPTIMA code for construction cost per linear foot for the various barrier material categories. This study has updated these cost data to 1988 through a comprehensive assessment of actual construction cost information for more than 700 barrier projects around the country.

REFERENCES

1. W. Bowlby, J. Higgins, and J. Reagan (Eds.). *Noise Barrier Cost Reduction Procedure STAMINA 2.0/OPTIMA: User's Manual.* Report FHWA-DP-58-1. FHWA, U.S. Department of Transportation, April 1982.
2. G. S. Anderson, E. Cuoco, and C. W. Menge. The Barrier Cost Reduction Program: A New Tool to Reduce Highway Noise Barrier Costs. In *Proc., TRB/FHWA Conference on Highway Traffic Noise Mitigation*, FHWA, U.S. Department of Transportation, March 1979.
3. *Highway Traffic Noise in the United States: Problem and Response.* FHWA, U.S. Department of Transportation, 1987.
4. L. F. Cohn. *NCHRP Synthesis of Highway Practice 87: Highway Noise Barriers.* TRB, National Research Council, Washington, D.C., 1981.
5. *Price Trends for Federal-Aid Highway Construction—1977 Base.* Report FHWA-ED-89-031. FHWA, U.S. Department of Transportation, 4th quarter 1988.

Publication of this paper sponsored by Committee on Transportation-Related Noise and Vibration.

Comparisons of Emissions of Transit Buses Using Methanol and Diesel Fuel

DANILO J. SANTINI AND JOHN B. RAJAN

The results of several studies on the emission characteristics of methanol- and diesel-fueled buses are summarized. To facilitate comparison, the emissions test data at idle and in various driving cycles are presented on an hourly or per-mile basis and are ordered by the speed of the test. The emissions of specific pollutants from methanol-fueled test vehicles varied greatly with average speed and depended on the engine technology and the emission control devices used. The results suggest that the most likely substitution of methanol-fueled buses for diesel-fueled buses is not likely to result in net air quality improvements for very low-speed bus operations in an urban environment. Under these conditions, the negative effects of increases in carbon monoxide, formaldehyde, and hydrocarbons may offset the positive effects of particulate emissions reduction. In this paper, there is no attempt to weight emissions, estimate air quality, or quantify net emissions effects.

Methanol, the fuel of choice for Indianapolis 500 race cars, is a chemical that, with limited engine modifications, can be burned in engines originally designed to use gasoline or diesel fuel. Methanol is less volatile than these fuels and therefore is less likely to contribute to smog from fugitive emissions during refueling. Its higher octane rating and more complete combustion in spark-ignition engines yield higher engine power output and greater thermal efficiency. However, methanol lacks a cetane rating, indicating that (a) it burns less completely at low engine load than does diesel fuel in compression-ignition (CI) engines, and (b) it provides little change in engine power output. Compared with gasoline, methanol has nearly 50 percent less energy on a unit weight basis, which means that its use involves either more fuel stops or a doubling of the vehicle's fuel tank size. When methanol is compared with diesel fuel, the reduction in energy content exceeds 50 percent.

The U.S. Environmental Protection Agency (EPA) standards for heavy-duty engines are established in grams per brake horsepower-hour (g/bhp-h) on the basis of an engine dynamometer test conducted without regard to vehicle weight. Although this test may be appropriate for trucks, for which it was designed, it will not necessarily give an accurate prediction of emissions patterns from typical bus usage. For a bus engine, this test cycle would be comparable to a driving speed of about 22 mph (*1*), far higher than the typical speed of a bus. This lack of appropriateness has been recognized in tests of the two types of methanol bus engines [two-stroke with glow plug versus four-stroke with spark-ignition (SI) assist] that are candidates for meeting the 1991 standards.

For this paper, buses are assumed to be available to meet the strict 1991 EPA bus engine standards, which call for a reduction of particulate emissions from 0.6 to 0.1 g/bhp-h. At present, only alternative-fuel (natural gas and methanol) bus engines have met this standard (*1*). As of early 1990, the President's proposed Clean Air Act would ease the present bus particulate standard while requiring that transit agencies purchase an increasing share of alternative-fuel buses from 1991 through 1994, requiring 100 percent after 1994. The present regulation might effectively require that only alternative-fuel buses be purchased from 1991 to 1994, because it appears unlikely that diesel-fueled heavy-duty engines capable of meeting the bus standard will be available in 1991. [They are expected to be available in 1994, when trucks have to meet the same standard (*1*)]. Thus, the appropriate question to ask now is whether the new alternative-fuel bus engines will actually improve air quality if they replace diesel engines now in service. This paper summarizes emissions test results to develop some insight on this question; test results for model driving cycles considered representative of typical bus usage are provided (*2–8*).

The test data are examined, and the implications of the tests for net emissions changes are evaluated. The comparisons are complex because the two methanol buses use different combustion cycles (two-stroke versus four-stroke) and different methods of igniting the methanol at low engine load (glow plugs versus SI). As expected, these methanol buses show somewhat different emissions, but certain similarities also exist.

1. The ability of a platinum catalyst to eliminate the relative drawbacks of the methanol engine for such pollutants as carbon monoxide and hydrocarbons;
2. The inability of a used platinum catalyst to provide adequate reductions in high formaldehyde emissions from the methanol engine at idle and low operating speeds;
3. The evidence that there are relatively moderate catalyst effects on NO_x; and
4. The inherent difficulty in igniting methanol at low load and engine speed in a CI engine, leading to generally high emissions at low operating speeds and idle.

CHARACTERISTICS OF VEHICLES AND PREVIOUS TESTING

The significant features of the coach and engine systems tested in various programs (*2*, *6*) include the methanol and diesel versions of the General Motors (GM) coaches and their 277-hp, direct-injection, Detroit Diesel Corporation (DDC) 6V–92TA, two-stroke, unthrottled, turbocharged engines and the

Center for Transportation Research, Argonne National Laboratory, 9700 South Cass Ave., Argonne, Ill. 60439.

200-hp, D2566 MUH-type, four-stroke, unthrottled, naturally aspirated MAN engines used in the MAN SU 240 buses. Comparative testing of a MAN and a DDC methanol bus was done at the Southwest Research Institute (SWRI) using three 6V–92TA diesel buses in service with the Houston Transit Authority as controls (Table 1, columns B–D). One methanol-fueled and one diesel-fueled MAN bus, as well as a regular DDC diesel in revenue service in the Golden Gate area, were also characterized (columns A and E–H) (*6*). Emissions from later models of the DDC methanol vehicles were also examined by Chevron (columns J and K) (*7*). This information was published in conjunction with a retest (column H) of the reengined GM/DDC diesel bus shown in column A and a retest (column I) of the unmodified GM/DDC methanol bus shown in column C (*7*). Both diesel and methanol DDC buses purchased by New York City in 1987, tested in 1988 (*4*), and retested in 1989 (*5*) have 6V–92TA series engines (Table 2, columns 1–9). Most recently, New York

TABLE 1 CHEVRON AND SWRI TEST RESULTS FOR DDC AND MAN DIESEL AND METHANOL ENGINES, 1986–1990

Pollutant Test, speed (mph)	A[a] Unkn.[b,c] DDC/D/82 None Unkn. One	B < May 85 DDC/D/<84 None 107,000 Three	C Jul 85 DDC/M/83 None 18,900 One	D Jun 85 MAN/M/84 Pt/New 28,300 One	E May 88 MAN/M/84 Pt/Used 55,000 One	F Apr 88 MAN/M/84 None 55,000 One	G Jun 88 MAN/D/84 None 58,000 One	H Jun 88 DDC/D/82 None 95,700 One	I May 88 DDC/M/83 None 65,100 One	J Mar 89 DDC/M/88 None 8,400 One	K Apr 89 DDC/M/88 Ag/New 8,700 One
Hydrocarbons[d]											
Cold idle, 0.0 (g/h)	nt[e]	nt	1,185	106	300	326	32	22	1,037[f]	690	580
Hot idle, 0.0 (g/h)	19	29	522	4.7	54	114	14	26	522[f]	160	140
Simulated, 3.9 (g/mi)	4.9	7.5	133	1.5	8.7	38	4.4	7.8	154[f]	80	64
Transient, 8.8 (g/mi)	2.2	3.4	58	0.83	1.0	22	2.4	4.1	79[f]	57	44
Transient, 12.4 (g/mi)	na[g]	3.4	44	0.32	1.7	21	2.1	7.2	81[f]	44	34
Steady-st., 12.4 (g/mi)	2.7	3.4	78	1.2	1.5	14	7.3	3.8	89[f]	67	50
Steady-st., 24.9 (g/mi)	1.6	1.8	84	0.37	0.94	14	2.0	2.3	76[f]	3.1	3.3
Carbon Monoxide											
Cold idle, 0.0 (g/h)	nt	nt	440	56	272	316	59	50	450	330	320
Hot idle, 0.0 (g/h)	21	25	290	2.3	36	177	29	22	280	250	240
Simulated, 3.9 (g/mi)	41	29	167	0.9	6.0	57	10	54	140	69	69
Transient, 8.8 (g/mi)	38	25	126	0.53	0.83	32	6.2	51	100	33	35
Transient, 12.4 (g/mi)	na	22	88	0.77	1.3	28	6.2	59	67	20	22
Steady-st., 12.4 (g/mi)	2.5	3.9	51	0.5	0.75	33	14	4.4	38	38	33
Steady-st., 24.9 (g/mi)	1.5	1.8	43	0.34	0.26	18	5	2.3	17	11	11
Nitrogen oxides											
Cold idle, 0.0 (g/h)	nt	nt	19	47	49	47	31	138	36	11	7
Hot idle, 0.0 (g/h)	202	17.5	3.6	67	65	73	42	137	52	15	13
Simulated, 3.9 (g/mi)	61	29	8	23	20	22	16	48	17	7.3	7.0
Transient, 8.8 (g/mi)	32	27	7.9	13	11	12	10.1	28	9.1	5.2	5.1
Transient, 12.4 (g/mi)	na	27	7.9	14.2	11	12	13	30	11	6.9	7.5
Steady-st., 12.4 (g/mi)	23	19	2.1	5.3	7.8	8.4	8	17	4.1	2	1.5
Steady-st., 24.9 (g/mi)	15	13	2.6	3.9	4.5	4.9	4.9	10	3.8	0.47	0.33
Particulates											
Cold idle, 0.0 (g/h)	nt	nt	6.8	0.6	3.1	0.7	4.9	11	4.3	2.1	1.9
Hot idle, 0.0 (g/h)	5.4	6	3.8	0.8	0.75	0.62	4.6	5.4	2.4	2.5	1.3
Simulated, 3.9 (g/mi)	6.3	5.1	1.2	0.2	0.2	0.2	1.4	3.2	0.7	1.0	0.4
Transient, 8.8 (g/mi)	5.5	4.2	0.63	0.07	0.08	0.12	0.78	2.4	0.32	0.62	0.19
Transient, 12.4 (g/mi)	na	4.5	1.5	0.1	0.06	0.12	1.1	5.6	0.88	1.7	0.5
Steady-st., 12.4 (g/mi)	0.8	1.3	0.5	0.06	0.12	0.12	1	1.5	0.4	0.19	0.15
Steady-st., 24.9 (g/mi)	0.7	0.72	0.3	0.04	0.02	0.04	0.43	0.83	0.2	0.1	0.06
Formaldehyde[h]											
Cold idle, 0.0 (g/h)	nt	nt	35	14	32	28	4.5	2.5	44	28	13
Hot idle, 0.0 (g/h)	0.85	2.2	23	2.1	24	19	2.3	1.5	31	15	6.9
Simulated, 3.9 (g/mi)	0.4	nt	6.0	0.4	4.1	5.6	0.6	0.4	8.8	4.7	2.3
Transient, 8.8 (g/mi)	0.26	nt	2.7	0.14	0.72	2.9	0.32	0.19	4.4	2.6	1.3
Transient, 12.4 (g/mi)	nt	nt	1.9	0.16	0.68	2.6	0.29	0.59	3.5	1.4	0.79
Steady-st., 12.4 (g/mi)	0.09	0.24	3.9	0.29	1	3.5	0.73	0.32	4.4	2.9	1.4
Steady-st., 24.9 (g/mi)	0.06	0.12	1.9	0.06	0.57	2	0.23	0.09	2.5	0.37	0.22

TABLE 1 (*continued on next page*)

TABLE 1 (*continued*)

Pollutant Test, speed (mph)	A[a] Unkn.[b,c] DDC/D/82 None Unkn. One	B < May 85 DDC/D/<84 None 107,000 Three	C Jul 85 DDC/M/83 None 18,900 One	D Jun 85 MAN/M/84 Pt/New 28,300 One	E May 88 MAN/M/84 Pt/Used 55,000 One	F Apr 88 MAN/M/84 None 55,000 One	G Jun 88 MAN/D/84 None 58,000 One	H Jun 88 DDC/D/82 None 95,700 One	I May 88 DDC/M/83 None 65,100 One	J Mar 89 DDC/M/88 None 8,400 One	K Apr 89 DDC/M/88 Ag/New 8,700 One
Diesel equivalant fuel use											
Cold idle, 0.0 (gal/h)	nt	nt	1.9	1	1.2	0.97	0.67	1.1	2.2	1.6	1.5
Hot idle, 0.0 (gal/h)	1.1	1.1	1	1.1	0.89	0.88	0.5	0.9	1.8	1.6	1.6
Simulated, 4 (mi/gal)	2.4	2.4	1.9	2.8	3.2	3.3	4.5	3.0	1.8	2.2	2.1
Transient, 9 (mi/gal)	3.8	3.8	2.7	5	5.4	5.6	6.6	4.8	3.3	4.6	4.2
Transient, 12 (mi/gal)	nt	3.4	3	4.2	5	5	4.9	3.9	2.9	4.9	4.2
Steady-st., 12 (mi/gal	6.5	6.3	5	6.3	5.3	5.6	6.8	6.8	4.6	6.8	7.6
Steady-st., 25 (mi/gal)	8.3	8.1	5.9	9.7	9.6	9.8	12	9.9	7.1	14	14

[a]Column headings include column letter, test date, engine type, catalyst, engine mileage, and number of vehicles tested.

[b]Unkn. = unknown.

[c]Column contains SWRI data (reference unspecified) as reported in Ref. 6 for a 1982 GM/DDC Coach 1016, which was later reengined and retested (see col. H).

[d]All hydrocarbon values are "OMCHE" values except col. B, which is "hydrocarbons."

[e]nt = not tested.

[f]Values from Ref. 6.

[g]na = not applicable.

[h]All columns report values for formaldehyde except col. B, which is "total aldehydes."

Sources: Cols. A and C-G, Ref. 6; col. B, Ref. 3; and cols. H-K, Ref. 7 (but see footnote f).

TABLE 2 NEW YORK CITY TRANSIT BUS TEST RESULTS FOR DDC DIESEL AND METHANOL ENGINES, 1988–1989

Pollutant Test, speed (mph)	1[a] 1988 DDC/D/87 None 28,900 Six	2 1988 DDC/M/87 None 78 Two	3 1989 DDC/M/87 None 22,687 Two	4 1988 DDC/M/87 Pt/New 28 One	5 1989 DDC/M/87 Pt/Used 16,838 One	6 1988 DDC/M/87 Ag/New 65 One	7 1989 DDC/M/87 Ag/Used 23,114 One	8 1988 DDC/M/87 Ag+Pt/New 147 Two	9 1989 DDC/M/87 Ag+Pt/Used 25,053 Two	10 1990 GM/NG/87 O/R[b] 5,639(5,657)[c] One	11 1990 GM/NG/87 O/R 8,213 One
Hydrocarbons											
Transient, 3.9 (g/mi)	5.4	260	250	8.3	61	130	190	150	470	21(15)	33
Transient, 8.8 (g/mi)	2.4	98	130	5.8	42	50	120	50	260	6.0(5.6)	9
Carbon monoxide											
Transient, 3.9 (g/mi)	10	120	150	7	51	110	300	120	130	180(2.7)	0.8
Transient, 8.8 (g/mi)	3.7	61	160	6.9	36	65	170	68	83	65(1.5)	0.6
Nitrogen oxides											
Transient, 3.9 (g/mi)	87	15	12	17	13	11	11	13	14	3.2(32.1)	29.3
Transient, 8.8 (g/mi)	41	8.3	6.6	9	7.3	9	7	8.4	8	3.6(17.4)	16.7
Particulates											
Transient, 3.9 (g/mi)	1.2	nr[d]	1.0	nr	0.29	nr	0.32	nr	0.31	0.16(0.09)	0.13
Transient, 8.8 (g/mi)	0.7	nr	0.46	nr	0.14	nr	0.19	nr	0.16	0.15(0.06)	0.06
Aldehydes											
Transient, 3.9 (g/mi)	0.01	4.3	10	3.3	23.4	0.7	17	2.1	8.2	0.30(0.29)	nt[e]
Transient, 8.8 (g/mi)	0.01	1.8	5.1	2.3	12.1	0.4	9	1.2	5.5	0.13(0.13)	nt
Diesel equivalent fuel use											
Transient, 3.9 (g/mi)	2.5	1.6	1.7	1.8	1.7	1.7	1.6	1.7	1.5	1.7(1.8)	2
Transient, 8.8 (g/mi)	4.7	3.5	3.4	3.7	3.5	3.7	3	3.7	2.9	3.5(3.7)	4

[a]Column headings include column number, test date, engine type, catalyst, engine mileage, and number of vehicles tested.

[b]O/R - oxidation/reduction.

[c]Mileage after tuneup to correct overrich mixture was 5,657.

[d]nr = not reliable.

[e]nt = not tested.

Sources: Cols. 1-9, Ref. 5; Cols. 10-11, Ref. 8.

City has begun testing a compressed natural gas bus (columns 10 and 11) equipped with two converted light-duty spark-ignited engines, a GM Chevrolet 454-in.^{3} engine to provide power to drive the bus, and a Ford 140-in.^{3} engine to provide power for air conditioning (*8*).

Golden Gate Buses

The first experiments with methanol buses were conducted using Golden Gate Transit District methanol buses, allowing comparisons of diesel- and methanol-fueled buses with engines manufactured by MAN and DDC. The 1986 SWRI tests of these two methanol buses (*3*) included comparisons with three diesel-fueled buses, but these were very-high-mileage buses (Table 1, column B). The two GM coaches tested more recently by Chevron were in revenue service from early 1984, and the two MAN buses were put into revenue service approximately 6 months later (*2*).

In June 1985 the MAN methanol vehicle was sent to SWRI in San Antonio, Texas, for chassis dynamometer emissions and fuel-economy testing. The mileage on the engine at that time was 28,300 mi (Table 1, column D). Routine maintenance before the testing included the replacement of a failed catalyst. The following month, the GM methanol bus named "Methanol One," with 18,900 mi and no catalyst, was tested at SWRI (column C). Both buses were returned to service. These SWRI tests used three DDC-engine buses borrowed from the Houston Transit Authority for comparison (*3*). The Houston Transit DDC buses were relatively old, with 90,000 to 230,000 mi (column B).

In early 1988 the two methanol-fueled buses and their diesel-fueled counterparts were transported to the Chevron Research Truck and Bus Dynamometer facility for emissions and fuel-economy testing (*6*). These tests, in California, corrected several flaws in the earlier SWRI tests, including testing of emissions with a used catalyst on the MAN M100 bus (Table 1, column E) and testing of the MAN bus without a catalyst (column F). Further, the testing of the MAN diesel bus (column G) allows a better understanding of how a four-stroke, naturally aspirated, diesel-fueled CI engine with SI assist compares with a two-stroke, turbocharged, methanol-fueled, glow-plug-assisted CI engine. The Chevron tests also give results for a diesel engine at cold idle, which the SWRI tests do not.

Further DDC Engine Developments

Tests on improved DDC methanol-fueled vehicles were performed in early 1989 by Chevron for DDC, and the results from later tests of newer, more advanced DDC methanol engines (Table 1, columns J and K) were published in 1990 (*7*). These results give emissions data on newer versions of the DDC methanol-fueled vehicles with and without a new silver catalyst. These data show that more recent versions of the DDC vehicles with improved technology provide better emissions and fuel-economy characteristics than indicated by previous tests, especially at the steady-state speed of 24.9 mph (compare columns C, I, J, and K). In reading the emission comparisons presented here, it should be remembered that the DDC engine is still under development and that improvements continue to be made. However, some of the information presented may indicate physical attributes of methanol combustion at low engine speeds in CI engines that are intractable problems relative to diesel fuel combustion in engines of essentially the same design.

New York City Tests

New York City (NYC) began its program of evaluating DDC engines modified for methanol use in their urban transit system in early 1988 (*4*, *5*). The emissions of these vehicles were examined without catalysts and with three different types of catalyst: platinum (Table 2, columns 4 and 5), silver (columns 6 and 7), and a combination of platinum and silver (columns 8 and 9). Six diesel buses with 25,000 to 38,000 mi were evaluated as controls without the use of catalysts (column 1). Future diesel engines burning low-sulfur fuel to meet the 1994 heavy-duty engine emissions standards are likely to use catalytic trap oxidizers and may use particulate traps, but none of the diesel buses in these tests was fitted with such devices. Two series of emissions and fuel-economy tests have been conducted on the six NYC methanol buses (*4*, *5*)—one in May 1988, when they had between 28 and 1,786 mi (Table 2, columns 2, 4, 6, and 8) and a second in December 1988, when they had accumulated 16,838 to 26,005 mi (columns 3, 5, 7, and 9). The first round of particulate and formaldehyde emissions estimates from the NYC tests are suspect due to a fault in the tests. The second round eliminated that fault, and the particulate emissions appear to be reasonable in the context of other test results presented here. Although the formaldehyde emissions results for the diesel-fueled buses in NYC tests were considerably less than those estimated by Chevron for the same test speed (Table 1, columns G and H, and Table 2, column 1), the aldehyde emissions for methanol buses in New York City tests were generally comparable with those done by Chevron.

TEST CHARACTERISTICS

Testing at SWRI included two simulated transient driving cycles and steady-state tests at cold idle, hot idle, and speeds of 12.4 and 25.9 mph. The unfiltered bus cycle, a transient test cycle reported by Ullman (*3*) and also used by Chevron (*6*, *7*), covers a distance of 2.9 mi in 19 min 51 sec at an average speed of 8.8 mph and includes the high-frequency components of the simulated bus speed trace (Figure 1). The second transient test cycle used at the SWRI and Chevron test facilities, incorporating stylized changes in speed and load, is a part of the U.S. Department of Transportation (DOT) transient coach-design operating cycle (*9*) and was identified as the central business district cycle. Consisting of a series of full-throttle accelerations to 20 mph and sharp decelerations to halt and idle, it covered a distance of 2 mi in 9 min 20 sec at an average speed of 12.4 mph (Figure 2). These test results are in Table 1.

In contrast, the NYC tests (Table 2) included only two transient driving cycles and no separate idling or steady speed tests. The first cycle, which represented driving in Manhattan, included a series of starts, brief accelerations, stops, and idling.

It covered a distance of 0.65 mi in 10 min at an average speed of 3.9 mph. This is similar in pattern to the first 400 sec of the SWRI unfiltered bus cycle (Figure 1). The second cycle, identified as the NYC composite cycle, covered a distance of 2.51 mi in 17 min 9 sec at an average speed of 8.8 mph and represented citywide travel in a major city (such as a commuter run between Manhattan and the neighboring boroughs). In the analysis, the two transient cycles with average speeds of 8.8 mph are treated as equivalent.

In the tabular and graphical comparisons, the test information is ordered by average speed and engine temperature, from 0 mph and cold idle through 24.9-mph steady-state tests. In order to help compare test results in Tables 1 and 2, a simulated 3.9-mph test was constructed by combining hot idle emission rates for 56 percent of an hour and 8.8-mph transient cycle emissions for 44 percent of the hour, giving an estimate of hourly emissions for a bus averaging 3.9 mph. This hourly emission was divided by 3.9 to obtain the gram-per-mile estimate.

CRITICAL COMPARISON OF EMISSIONS FOR DIFFERENT ENGINES, SPEEDS, AND CATALYST CONFIGURATIONS

In the following analysis, several effects of methanol substitution on the emission characteristics of transit buses are examined, including emissions of four pollutants for which federal emission limits exist, emissions of formaldehyde, catalyst effects, and age effects on diesels. Test results for methanol buses are only for neat (100 percent) methanol, M100. The most promising substitutions in terms of emission reductions are identified.

Carbon Monoxide (CO) Emissions

In general, CO emissions increase when methanol-fueled buses are substituted for diesel-fueled buses. Under all four steady-state conditions, CO emissions from a used, rebuilt 1982 DDC diesel engine with 96,000 mi (Table 1, column H) were well below those from the new 1989 DDC2 methanol-fueled engine with a silver catalyst (column K).

The lowest CO emissions provided by the MAN methanol vehicle (tested in 1986 at SWRI, with the catalyst changed just before testing, column D) are slightly higher at cold idle than those from the DDC diesel-fueled vehicle (column H). Otherwise, however, the 1986 MAN M100 bus with a new platinum catalyst (column D) had lower CO emissions than

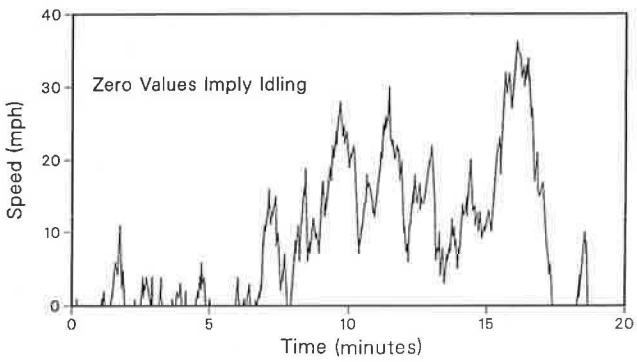

FIGURE 1 Unfiltered bus cycle.

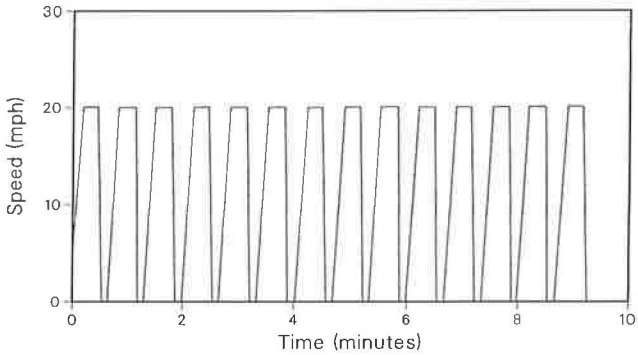

FIGURE 2 Central business district cycle.

the MAN diesel with 58,000 mi (column G) or the DDC diesel with 96,000 mi (column H). Even in the 1989 tests, when the catalyst had been used for 27,000 mi (column E), the MAN four-stroke, spark-assisted engine with platinum catalyst had lower CO emissions in constant-speed operation than either the 96,000-mi DDC diesel or the 58,000-mi MAN diesel. However, at both cold and hot idle, the ability of the MAN platinum catalyst to reduce CO had deteriorated significantly at 27,000 mi (compare columns D and E), so that CO emissions from the MAN M100 bus at idle were higher than those from either diesel bus.

The data presented in Tables 1 and 2 show that the reduction of CO emissions in an M100 transit bus is best achieved through the use of a platinum catalyst. The silver catalyst used in later versions of the DDC methanol buses (compare columns J and K) and in the NYC tests appears to have little effect (compare Table 2, columns 3, 6, and 7), and the silver-platinum combination was also ineffective (columns 3, 8, and 9). The changes with age of the platinum catalyst are significant under both transient and steady-state conditions. Although pronounced age effects on the platinum catalyst are demonstrated at cold and hot idle, these effects appear to become less important once the vehicle is moving (compare Table 1, columns D and E, and Table 2, columns 4 and 5). If this pattern continues in future testing of buses with DDC engines, then the use of an M100 bus with platinum catalyst on routes with higher average speeds and relatively little idling should keep CO emissions reasonably low. The DDC buses tested in New York City were driven at average speeds of less than 10 mph (*4*, *5*); the MAN methanol bus probably averaged higher speeds. The loss of effectiveness of the platinum catalyst appears to have been greater in the NYC DDC methanol bus than in the Golden Gate MAN methanol bus.

In spite of the discouraging CO emissions results for the M100 buses at idle, the evidence for CO emissions at transient cycles of 8.8 mph and above in the M100 buses is rather favorable, but only in comparison with high-mileage diesels. The Chevron tests indicate that the old MAN and new DDC M100 buses without catalysts emit CO at about the same rate at 8.8 and 12.4 mph (compare columns F and J). In either case, this is less than the emissions of DDC buses in current use (96,000 mi) (column H). However, the new NYC diesel buses (column 1) at 8.8 mph emit much less CO than DDC methanol buses. The MAN four-stroke diesel-fueled bus (58,000 mi) emits far less CO than the DDC diesel (96,000 mi) or the MAN M100 bus (55,000 mi) without a catalyst, but more than the MAN M100 bus (55,000 mi) with a platinum catalyst.

At these test speeds, the addition of the used platinum catalyst to the MAN M100 bus reduced CO dramatically, an encouraging result for the use of the platinum catalyst on a DDC bus. New York City first-round tests indicated that a new platinum catalyst could reduce CO emissions from a DDC M100 engine to about the levels from the competing diesel engines when averaged over the two cycles (columns 1 and 4), but catalyst deterioration led to a substantial CO increase in second-round tests (column 5). However, even after the deterioration, the platinum catalyst in the NYC tests clearly controlled CO far better than silver or silver-platinum catalysts. One question that arises from the slightly different results is whether the slow routes in the NYC case, and perhaps the colder East Coast weather, might cause more rapid catalyst deterioration than in California, or whether catalyst reliability might be related to engine attributes.

Particulate Emissions

Both silver and platinum catalysts tend to reduce particulate emissions in a methanol-fueled bus, but the platinum catalyst is not particularly effective at idle (compare columns F with D and J with K). Also, deterioration of the platinum catalyst has a deleterious effect on particulate emissions at cold idle (compare columns D and E). With or without a catalyst, the data in Tables 1 and 2 indicate a sharp reduction in particulates if new methanol buses replace used diesel buses, but compared with new diesels, the gains are far less dramatic (columns 1, 3, 5, 7, and 9).

Oxides of Nitrogen (NO_x) Emissions

Decreases in NO_x emissions through the use of catalysts on methanol buses are observed consistently only at steady-state cruising speeds. The reductions from the silver catalyst on a DDC methanol bus, although evident at cold idle (where the engine temperature is probably below optimal operating limits), gradually decline as the engine warms up and the vehicle operates in the steady-state or transient mode. Compared with effects on other pollutants, the effects of catalysts on NO_x are relatively small.

Hydrocarbon (HC) and Methanol Emissions

Emissions of hydrocarbons and methanol from methanol-fueled vehicles are significantly reduced by a functional platinum catalyst. Emissions of methanol, an oxygenated hydrocarbon, have important air-quality implications.

The methods of counting methanol as a reactive hydrocarbon vary, with the later Chevron tests reporting downward adjustments in estimated hydrocarbon equivalents due to methanol. If reported hydrocarbon emissions from an M100 bus are high, it is reasonable to surmise that almost all of these emissions are unburned methanol. In first-round NYC tests, the mean ratio of hydrocarbon to methanol emissions for M100 buses was 0.96 (*4*). The Chevron tests account for the fact that methanol is not as reactive per unit of molecular weight as are nonoxygenated hydrocarbons emitted by a diesel. In the Chevron tests, the grams of oxygen are subtracted from the methanol emissions to obtain the hydrocarbon equivalence of the methanol emissions. Wherever possible in Table 1, the Chevron estimate of organic material hydrocarbon equivalent (OMHCE) emissions is presented. In the 1989 Chevron tests (*6*), the ratio of OMHCE emissions to methanol emissions was 0.45 when the latter exceeded 50 g/mi (or 100 g/h at idle), and it was 0.54 for the remaining cases, most of which were for the catalyst-equipped MAN bus. The NYC tests (Table 2) do not yield the adjusted value.

The NYC first-round estimates of hydrocarbon emissions from the DDC vehicle with methanol fuel and an effective platinum catalyst are better by an order of magnitude than the closest competitor, a DDC vehicle with methanol fuel and a silver-platinum catalyst (Table 2). All catalysts used in the NYC tests showed substantial deterioration with age in their ability to control hydrocarbons (Table 2). The OMHCE emissions pattern of reduction and effectiveness of the catalyst presented in Table 1 was very similar to the pattern for CO. This similarity included significantly greater deterioration in effectiveness at cold and hot idle as the catalyst aged, with retained effectiveness at speeds of 8.8 mph and faster (*6*, *7*).

Formaldehyde

Formaldehyde (HCHO), a potential carcinogen, is of particular concern with the use of methanol as a transportation fuel. Evidence presented earlier in this paper indicated that CO emissions on bus routes where buses spend a great deal of time at idle would increase if a DDC methanol-fueled bus without a platinum catalyst were substituted for a used diesel-fueled bus. A platinum catalyst was far more effective than a silver catalyst in reducing CO, but the effectiveness was less at idle and decreased with age more rapidly at idle than at speed. When replacing new DDC diesel buses (column 1, Table 2), it does not seem likely that DDC methanol buses can reduce CO at low speeds, and they could increase CO sharply, depending on catalyst type and age. Bus routes on which a great deal of time is spent at idle tend to be in and around central business districts (CBDs), where pedestrian activity is high and potential population exposure is great. Such locations often have high carbon monoxide "concentrations," so the control of CO emissions in such locations is imperative.

Unfortunately, the evidence indicates that a used platinum catalyst actually creates formaldehyde at idle (*6*, *7*). In the Chevron tests, it was estimated that the used platinum catalyst increased the formaldehyde emissions of the MAN bus by about 20 percent at idle, with a greater increase at hot idle (Table 1, columns E and F). The NYC first-round emissions tests indicated that the platinum catalyst had little effect on formaldehyde, but the second-round emissions tests (*5*) indicated that the used platinum catalyst roughly doubled formaldehyde emissions (Table 2, columns 3 and 5). The NYC first-round tests (columns 2 and 6) and the Chevron tests (columns J and K) indicated that a new silver catalyst on a DDC engine reduces formaldehyde sharply, but the second-round tests indicated that the used silver catalyst increased formaldehyde (columns 3 and 7). These poor formaldehyde-control results with used catalysts at idle and low speed represent a serious shortcoming, because the Chevron test results indicated that formaldehyde emissions from M100 engines at cold and hot idle far exceed those from their diesel counterparts.

The Chevron tests did not indicate that the use of a catalyst-equipped M100 bus in place of a diesel bus would inevitably increase formaldehyde at all speeds. For the MAN M100 bus,

some evidence indicates that a platinum catalyst functioning near its optimal capability can, under certain conditions, reduce formaldehyde emissions below those from the competing diesel engine. When the Chevron test results for the 58,000-mi MAN diesel (*6*) are compared with those for the 28,300-mi MAN M100 bus with a new catalyst, the M100 bus has lower formaldehyde emissions than the diesel at 8.8 mph and faster (columns F and D). However, when the 55,000-mi MAN M100 bus with a used catalyst is compared with the diesel engine, the M100 bus consistently has higher formaldehyde emissions, especially at idle (columns F and E). The 28,300-mi MAN M100 bus with a new platinum catalyst (*3*) also exhibited lower formaldehyde emissions than the 96,000-mi DDC diesel tested by Chevron for speeds of 8.8 mph and faster, but not at idle (columns D and H).

These results imply that to get formaldehyde emissions reductions when an M100 MAN bus with a new platinum catalyst replaces an old diesel with no catalyst, two conditions must be satisfied. First, the bus cannot spend a large fraction of its route time idling at stoplights and bus stops. Second, the catalyst must be functioning at or near its optimal capability. For the DDC M100 bus, the evidence indicates that formaldehyde cannot be brought below that of the DDC diesel with catalysts tested thus far. It is possible that catalyst development could ultimately solve this problem. Reportedly, EPA's emissions laboratory has been testing electrically heated catalysts that successfully reduce formaldehyde emissions from methanol-powered cars (*10*). As with the catalysts discussed here, reliable long-term operation of the electrically heated catalysts will be critical.

Other Aldehydes and Ketones

In addition to evaluating formaldehyde, the Chevron tests included measurements of other aldehydes and ketones, including acetaldehyde, acrolein, acetone, propionaldehyde, crotonaldehyde, methylethylketone (MEK), and benzaldehyde. Within the limits of measurement, the MAN M100 bus with a platinum catalyst consistently had emissions of these substances that were equal to or less than those of the MAN diesel (*6*). In about three-fourths of the comparable test cases (for seven pollutants and six test conditions totaling 42 possible combinations), the latest version of the DDC M100 bus with a silver catalyst had emissions of these substances more than or equal to the tested diesel bus (*7*). Emissions of acetaldehyde, acetone, and MEK were generally higher for the M100 engine. In nearly all cases, the MAN M100 bus emissions were less than or equal to those of the DDC M100 bus.

SUMMARIES OF EFFECTS OF METHANOL-FOR-DIESEL SUBSTITUTION OPTIONS

MAN M100 Replacing MAN Diesel

Although the MAN bus is relatively uncommon in the United States, it is in use at a number of locations. Seattle Metro, which has a fleet of MAN M100 and diesel buses, has found the M100 buses to be considerably more expensive to operate (*11*) and has not ordered a second group. Chicago also uses MAN diesel buses. MAN, which once had a U.S. assembly facility, has largely withdrawn from the North American market, but it could return if the potential market were large enough. One reason for MAN's initial entry may be that it offered an opportunity to trade off fuel economy for performance in an environment of high fuel costs. The Chevron tests indicated that at 8.8 mph, the less powerful MAN diesel bus had 38 percent greater fuel economy than the DDC diesel bus; this advantage fell off to 26 percent at 12.4 mph (compare columns G and H). At hot idle, the MAN bus had a significant advantage over the DDC diesel, with a 44 percent lower fuel-flow rate (*6*). Thus, from the fuel-cost point of view, the MAN diesel bus could reemerge and be competitive in downtown areas if diesel fuel prices were to rise sharply relative to those of methanol.

A MAN M100 bus introduced as a replacement for a 1980s MAN diesel bus would reduce particulate emissions dramatically (compare columns D with E and F with G), even if the catalyst failed. Even with a used platinum catalyst, such a substitution should also reduce CO emissions and hydrocarbon emissions if the MAN M100 buses replaced diesel buses on routes where average speed was 8.8 mph or faster; with complete catalyst failure, this would not be true. Even with a functioning used catalyst, if the average speed were lower than 8.8 mph, CO and hydrocarbon emissions might increase.

DDC M100 Replacing DDC Diesel

Detroit Diesel Corporation is the manufacturer of engines most commonly found in buses and has been the most active developer of an alternative-fuel engine for heavy-duty applications, the DDC M100 engine reported on here. The substitution of a new DDC M100 engine for an existing DDC diesel engine is the most likely methanol substitution in the bus market. At transient driving cycle speeds of 8.8 and 12.4 mph, the Chevron tests indicate that the substitution of the DDC2 model M100 engine equipped with a silver catalyst (column K) for a diesel-fueled DDC engine with 96,000 mi (column H) would reduce CO, particulates, and nitrogen oxides (NO_x), although increasing formaldehyde and hydrocarbons. If more time were spent at idle, the substitution would increase CO, as well as hydrocarbons and formaldehyde. This substitution clearly is not so advantageous as the substitution of the MAN M100 equipped with a platinum catalyst engine for the MAN diesel, because far larger increases in formaldehyde and hydrocarbons would result, as well as larger increases in CO at idle (or smaller decreases at 8.8- and 12.4-mph transient cycles).

MAN M100 Replacing DDC Diesel

The substitution of the MAN M100 bus with a used platinum catalyst (column E) for a 96,000-mi DDC diesel bus (column H) would reduce all emissions except formaldehyde at speeds faster than 8.8 mph. With a new catalyst (column D), formaldehyde would also be reduced at those speeds, and other pollutants from the methanol bus would be even lower.

Caveat on Improving Diesels

So far, this comparison has involved new or relatively new methanol buses and relatively high-mileage diesel buses. The

NYC tests compared recent-model diesels with recent-model methanol buses. Because both types of bus are improving, this procedure provides the best comparison between two new buses. Unfortunately, the NYC tests included only one—the 8.8-mph NYC composite transient cycle test—that overlaps the others included here. With that test as a basis of comparison, the data in Tables 1 and 2 imply that new diesels emit CO and particulates at a considerably lower rate than older diesels. The degree to which this is simply a result of newness of the engine rather than the level of technological development is not certain. Hydrocarbon emissions were also slightly lower, whereas NO_x emissions were estimated to be somewhat higher. The differences for hydrocarbons and NO_x could be within the margin of test error. However, the well-known particulate-NO_2 tradeoff is consistent with the noted changes in particulate and NO_x emissions. As combustion temperatures are raised, particulates are reduced and NO_x is increased. According to these test results, the newer diesels have been modified to take advantage of this trade off in order to reduce particulate emissions.

Comparisons of the measured particulate and CO emissions at an average test speed of 8.8 mph (Figures 3 and 4) clearly show that the newer DDC diesels tested in New York City had lower particulate and CO emissions than previous diesels. Figure 3 also shows a degree of consistency in the particulate emissions estimates for DDC M100 buses that implies that in this engine, methanol has no inherent, significant superiority over the diesel. Either a platinum catalyst or a silver catalyst reduces the particulate emissions of the DDC M100 buses, giving the appearance of superiority. However, the diesel technology being developed for 1994 may also use catalytic materials in combination with low-sulfur fuel to reduce particulates, so the apparent particulate emissions superiority of the DDC methanol engine may disappear when like technologies are compared. However, this is a comparison based on weight of particulates emitted and not on the health effects of the substances in the particles.

The MAN diesel (Figure 3, bar 4) had particulate emissions of 0.78 g/mi at 8.8 mph, whereas the MAN methanol bus had 0.12 g/mi without a catalyst (bar 9) and 0.069 to 0.081 g/mi with a catalyst (bars 13 to 14). Thus, for the four-stroke, naturally aspirated engine technology with spark assist, it can be argued that the methanol version of the engine is inherently superior with respect to particulates. In terms of CO emissions, the DDC and MAN M100 buses can be viewed as inherently inferior without a catalyst. However, at 8.8 mph, the MAN M100 bus with a platinum catalyst (new or used) is clearly superior to either a DDC or MAN diesel. These results may indicate an inherent ability to reduce emissions by a larger amount when methanol is introduced into naturally aspirated, four-stroke, spark-assisted engines rather than into turbocharged, two-stroke, glow-plug-assisted engines.

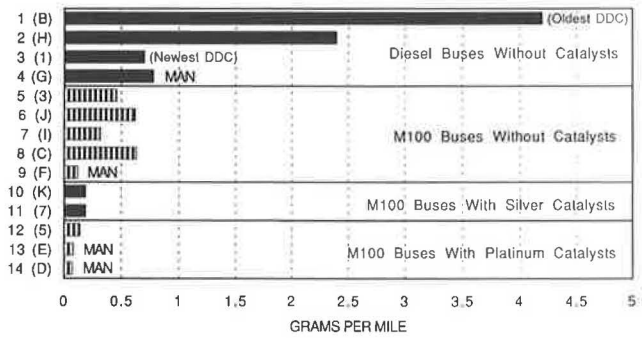

FIGURE 3 Particulate emissions estimates for all tests at 8.8 mph. (Values are for DDC engines except as noted; the corresponding columns in Tables 1 and 2 are shown in parentheses.)

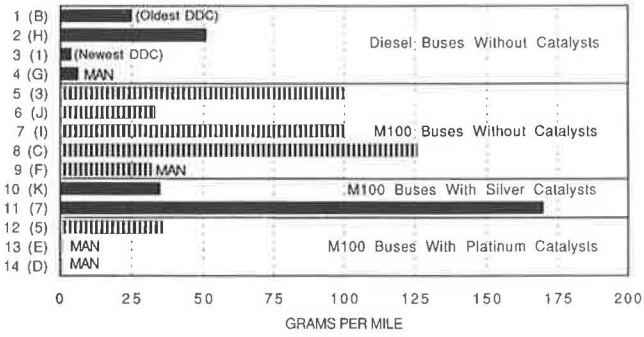

FIGURE 4 Carbon monoxide emissions estimates for all tests at 8.8 mph. (Values are for DDC engines except as noted; the corresponding columns in Tables 1 and 2 are shown in parentheses.)

Fuel Economy

Comparison of energy-equivalent fuel economy is less favorable to the MAN methanol engines as substitutes for MAN diesels than is the comparison for DDC engines. At all but one of the tested speeds (12.4 mph) and idle conditions, the energy-equivalent fuel economy of the MAN M100 engine was less than that of its diesel-fueled counterpart (*6*). However, the latest version of the DDC engine for which there are test results (columns J and K) indicates substantial improvement in energy-equivalent fuel economy at higher average speeds. Compared with an old 96,000-mi DDC diesel, the DDC2 model exhibited improved energy-equivalent fuel economy on the 12.4-mph transient cycle test and at the 12.4- and 24.9-mph steady-state speeds. However, the DDC M100 engine continues to have high fuel consumption at idle, which is consistent with the poor emissions and fuel consumption performance of this engine at low test speeds in New York City. Further, when compared with the fuel economy test results for new diesels in New York (column 1) at 8.8 mph, the new DDC M100 engine had lower energy-equivalent fuel economy. Overall, these fuel economy and earlier emissions results imply that the best initial uses of DDC M100 buses bought in 1991 would be in suburban locations and on express bus routes, where average speeds are relatively high.

Although the MAN M100 bus gets poorer fuel economy than a comparable MAN diesel bus, the MAN engine has less power than the DDC engine and, other things being equal, tends to consume less energy. The low power of this engine, however, makes it less suitable for suburban and express routes, where acceleration can be important. Similarly, the MAN bus may be unsuitable for hilly terrain. However, for the central business districts of large cities with flat terrain, the substi-

tution of a MAN M100 bus for an old DDC bus would result in less energy consumption and lower emissions than would a DDC M100 bus.

RELATED JAPANESE RESEARCH

Like the United States, the Japanese are considering the use of methanol as a substitute for diesel fuel. Tax policy in Japan has encouraged the use of diesel fuel over gasoline, leading to a situation in which diesel-fueled vehicles contribute a relatively greater share of pollutant emissions than in the United States. In Japan, methanol is being touted primarily for its ability to reduce NO_2 emissions and secondarily for particulate reductions. Substitution of methanol-fueled trucks and buses in urban fleets is argued to be a potential solution to both environmental and energy security problems, with the energy security emphasis placed on geographically diverse sources of natural gas as a methanol feedstock (*12*).

It appears that the Japanese are relying on steady-state (six-mode) test results, which imply that NO_x emissions of methanol vehicles will be well below their standards (*12*, *13*). The 12.4- and 24.9-mph steady-state test results in Table 1 imply that the substitution of a new catalyst-equipped methanol engine for a diesel engine will indeed reduce NO_x substantially. However, for the four-stroke, naturally aspirated MAN bus, the results for low-speed transient cycle operation indicate that NO_x emissions could actually be increased. Consistent with the increase in the NO_x emissions of the spark-assisted MAN engine in transient operation versus a decline for the DDC glow-plug-assisted engine, Nakasima et al. (*14*) determined that a spark-assisted M100 test engine had higher NO_x than its diesel counterpart at high fuel flow rates but that the glow plug version had consistently lower NO_x.

Fujita and Ito (*15*) have studied the behavior of various catalyst materials under inlet gas conditions representative of methanol engines at cold start, at idle, and under transient and steady-state conditions, and they have shown that formaldehyde and hydrocarbon emissions from steady-state operation differ greatly from those of cold start and transient operating conditions. For tailpipe emissions, the critical nature of the reaction temperature of the catalyst in conjunction with the exhaust gas temperature and composition at the catalyst inlet was demonstrated. Nishida (*13*) noted that the catalyst used in Komatsu experiments does not function well when the exhaust temperature is below about 200°C, ". . . as occurs at the cold start of the engine."

It is possible that the relatively poor emissions performance of the DDC two-stroke methanol engine equipped with the silver catalyst was a result in part of the characteristically low exhaust temperature of that engine combined with the cooling effect of methanol combustion (relative to diesel fuel combustion). The best emissions performance of this engine was during transient cycle tests, when the engine spent a relatively greater share of its operations under high load, which probably raised the operating temperature. It is also likely that the choice of catalyst material is a contributor to the poor results. Fujita and Ito (*15*) did not even include silver in their tests of five candidate catalysts. Similarly, in U.S. light-duty engine and catalyst experiments, McCabe et al. (*16*) confined their experiments to platinum, palladium, and rhodium, eliminating silver from consideration and emphasizing the particularly great intrinsic activity of platinum and palladium.

Fujita et al. (*17*) found that the presence of nitrous oxide in the exhaust gases tended to increase formaldehyde formation and that positive or negative changes in temperature of the catalyst increased formaldehyde formation. Their finding that formaldehyde formation should be greatest at cold idle is confirmed by the information in Table 1 and by the work of McCabe et al. (*16*), but their expectation that the operation of methanol-fueled vehicles in cold regions could increase formaldehyde emissions on acceleration from idle cannot be confirmed from the currently available U.S. experiments.

Yanigihara et al. (*18*) presented test results for a 2.2-liter, indirect-injection, four-cylinder diesel that showed that hydrocarbon emissions without a catalyst were "almost the same as that of the base diesel at all operating conditions except in the region of low load, low engine speed." Diesel fuel was emulsified with methanol in varying proportions as an ignition enhancer to overcome the problems in igniting methanol at low load and low engine speed. The tendency to emit high amounts of unburned hydrocarbons at low engine load and speed is confirmed by the comparisons in this paper (Tables 1 and 2).

Nishida (*13*), reporting on Komatsu experiments, noted that the oxide catalyst, which was intended to reduce aldehydes, also had the desirable effect of reducing hydrocarbons and CO. Such catalyst-caused emission reductions are also illustrated here. A significant deterioration of a platinum catalyst with respect to CO and hydrocarbon emissions was also reported in the Komatsu tests. This deterioration was measured at about 12,000 mi, whereas the deterioration illustrated in these comparisons occurred after about 20,000 mi (Table 1, columns D and E; Table 2, columns 4 and 5). Nakasima et al. (*14*) showed that both spark-assisted and glow-plug-assisted methanol engines emit larger amounts of CO than a comparable diesel at all fuel injection rates.

The Komatsu tests showed the tendency of the methanol engine to have relatively worse energy equivalent fuel economy at lower speeds on normal roads than in expressway driving. At 12.4 mph the energy equivalent fuel economy of the Komatsu methanol engine was 85 percent of that of the diesel engine, whereas at 50 to 55 mph, the two engines gave essentially identical economy. The improving economy as a function of increasing speed is roughly analogous to the pattern for the latest DDC engine results (compare column H and columns J and K). This pattern also shows up in the NYC tests, where the percentage decline in energy equivalent fuel efficiency is greater at 3.9 mph than at 8.8 mph (Table 2). Nakasima et al. (*14*) showed lower thermal efficiency for methanol engines at low fuel flow rates, whereas Nietz (*19*) noted the tendency to consume more energy "when the performance requirement . . . is relatively low."

The deterioration of the relative merits of methanol versus diesel engines at very low average speed should be of great interest to the Japanese and to those considering the use of alternate fuels in congested cities where transit is more frequently used. According to Boyle (*20*), the average speed in Tokyo is 8 mph and in London, 10 mph.

SELECTED COMPARISONS WITH EMISSIONS TESTS FOR LIGHT-DUTY SPARK-IGNITED ENGINES

The heavy-duty engine conversions from diesel to methanol, as shown in Tables 1 and 2, appear to result in higher engine-out emissions of hydrocarbons and CO at the same engine age without catalysts. In contrast, conversions of light-duty engines from gasoline to methanol tend to reduce these pollutants. For example, emissions tests of like models of a 2.0-liter light-duty, spark-ignited, turbocharged engine using premium gasoline, lead-free regular gasoline, methanol, and liquid petroleum gas (LPG) on the European Community Emissions (ECE-15) urban driving test showed that methanol gave the lowest engine-out emissions of hydrocarbons, CO, and NO_x (*21*). Further, unlike the results presented here for heavy-duty diesel conversions, methanol's advantage in that conversion of a gasoline engine held up during idle and the two steady-state and acceleration components of the ECE-15 test. A recent test of a Ford 3.0-liter flexible-fuel vehicle (FFV) on the U.S. Federal Test Procedure (FTP) showed similar engine-out improvements for hydrocarbons, CO, and NO_x (but almost five times as much formaldehyde) (*16*).

Thus far, however, like the diesels examined in this report, the methanol engines have not shown clear environmental advantages after use of catalysts when formaldehyde is also considered. This is partly the result of the use of catalysts adapted to gasoline. To illustrate, with a platinum catalyst designed for gasoline vehicles, a Ford FFV had very similar catalyst-out average emissions of hydrocarbons, CO, and NO_x over 100,000 mi of simulated use when operated on gasoline and on M85 methanol, but it emitted over three times as much formaldehyde on methanol (*16*). Note the slight relative improvement of formaldehyde emissions with use of a catalyst compared with the tests described in the previous paragraph. The similar average lifetime emissions were due to lower pollutant conversion efficiencies of the gasoline-vehicle catalyst when it was used on a methanol-fueled vehicle. Ideally, after catalyst development and refinement, light-duty methanol engines will show the same advantages downstream of the catalyst as in the engine-out measurements. In view of the apparent increase of some engine-out emissions when heavy-duty CI engines are converted to methanol, the challenge for catalyst technology will be greater.

The development and refinement of catalysts, methanol ignition systems, and air-fuel control systems could result in much more complete and reliable combustion of methanol on cold starts. Such advances could make possible the attainment of levels of hydrocarbons and CO promised in the engine-out emissions in light-duty engines and the control of formaldehyde to acceptable levels. McCabe et al. (*16*) showed that the highest rates of formaldehyde emission occurred in the first 60 sec and that the platinum catalyst did not significantly reduce these emissions until after this time. This implies that catalyst warming could be very effective.

Natural gas is also being evaluated as an alternative fuel for buses by New York City (*8*). The substitution of natural gas engines for diesel engines is in this case a light-duty, spark-ignited, natural gas engine for a more powerful, heavy-duty, CI, DDC diesel with a much higher compression ratio. The emission tests conducted so far indicate that the natural gas engine, when in good operating condition, can reduce hydrocarbons, CO, NO_x, and particulates. However, the problem of ensuring precise control of the air-fuel ratio must be met if these emission reductions are to be ensured (columns 10 and 11, Table 2). The engine tested (column 10) emitted far greater amounts of CO and hydrocarbons than diesel engines when, after about 6,000 mi of service, the air-fuel control system allowed the mixture to become overrich (*8*).

The use of a light-duty natural gas engine in buses raises the question of whether the ultimate solution should involve substituting a lower-compression-ratio, spark-ignited methanol engine for the current high-compression-ratio, CI, diesel-fueled engines. Nishida (*13*) raised the issue of the desirability of a new basic engine for the methanol engine that should replace Komatsu diesels, and Gray and Alson (*22*) have argued that the ideal light-duty methanol engine will be considerably different from today's light-duty gasoline engine.

CONCLUSION

If no diesel buses are available to meet the 1991 heavy-duty bus emissions standard, it appears that methanol buses could be selectively introduced on certain routes to reduce most emissions, as long as catalyst performance was carefully monitored and catalyst replacement was provided as necessary. However, the evidence does not support a conclusion that methanol buses will be environmentally superior to old diesel buses in the places where bus service is most important, the congested central business districts of major U.S. cities. It is even less certain that they would be environmentally superior in the aggregate to new diesel buses, even if those new diesel buses did not meet the 1991 particulate emissions standard. These are weak inferences at best, because they are not supported by air-quality monitoring and health cost and benefit calculations. Nevertheless, the relatively high CO, hydrocarbon, and formaldehyde emissions of methanol buses at idle (a more common condition for buses than for any other vehicle) suggest that great caution should be exercised before the complete substitution of methanol buses for diesel buses in U.S. transit systems is promoted.

As for natural gas, the amount of emissions test information is relatively scanty and is not nearly so detailed as for methanol. Consequently, the authors cannot support the widespread introduction of natural-gas-fueled buses until emissions test information at least as detailed as that presented here becomes available. At this time, the interpretation of the evidence here is that it would be premature to adopt regulations designed to force the complete introduction of alternative fuels into the transit industry on the basis of a presumption of subsequent improvements in overall environmental quality.

Lest this position be misinterpreted, the authors' concern is primarily that adequate research, development, and clear demonstration of the technical viability and relative emissions superiority of alternative fuels be conducted before widespread (i.e., greater than 20 percent of new vehicle sales) introduction of these fuels for environmental reasons is promoted. Either by starting slowly or by thorough advance proof of the technology, the introduction of such fuels will be smoother and more commercially successful, and the possibility of a

widespread consumer or political backlash to unsuccessful technology will be minimized. As the prior section should illustrate, the specific bus comparisons made here should not be interpreted as a broad criticism of the potential environmental benefits of alternative fuels in general or methanol in particular.

ACKNOWLEDGMENT

The authors thank David Moses of the Office of Environmental Analysis, U.S. Department of Energy, and Vincent DeMarco of UMTA for sponsorship of the research discussed in this paper. This work was supported by UMTA, U.S. Department of Transportation, through interagency agreement with the U.S. Department of Energy and by the Office of Policy, Planning, and Analysis, U.S. Department of Energy.

REFERENCES

1. *Alternative Fuels Briefing Report.* Regional Transportation Authority, Chicago, Ill., Jan. 1990.
2. M. D. Jackson, S. Unnasch, and C. Sullivan. *Transit Bus Operation with Methanol Fuel.* SAE Paper 850216. Society of Automotive Engineers, Warrendale, Pa., Feb. 1985.
3. T. L. Ullman, C. T. Hare, and T. M. Baines. *Emissions from Two Methanol-Powered Buses.* SAE Paper 860305. Society of Automotive Engineers, Warrendale, Pa., Feb. 1986.
4. *City of New York Methanol Bus Program Monthly Reports 1–4.* New York City Department of Transportation, July 15, Sept. 29, Nov. 30, and Dec. 13, 1988.
5. *City of New York Methanol Bus Program Annual Report, May 1988–April 1989.* New York City Department of Transportation, Sept. 1989.
6. G. A. Eberhard, M. Ansari, and S. K. Hoekman. *Emissions and Fuel Economy Test Results for Methanol- and Diesel-Fueled Buses.* Presented at the 82nd Annual Meeting and Exhibition of the Air and Waste Management Association, Anaheim, Calif., June 25–30, 1989.
7. G. A. Eberhard, M. Ansari, and S. K. Hockman. *Emissions and Fuel Economy Tests of a Methanol Bus with a 1988 DDC Engine.* SAE Paper 900342. Presented at the SAE International Congress and Exposition, Detroit, Mich., Feb. 1990.
8. C. Speilberg. *New York Department of Transportation Compressed Natural Gas Program, Monthly Report #3, June–Aug. 1989.* Jan. 15, 1990.
9. *Baseline Advanced Design Transit Coach Specification.* UMTA, U.S. Department of Transportation, Nov. 1978.
10. J. Keebler. Electrically Heated Catalyst Tested. *Automotive News*, Oct. 30, 1989, p. 3.
11. A. Turanski. *Technical Report on Methanol Bus Program: First Semiannual Data Analysis Report.* Battelle Columbus Division, Columbus, Ohio, March 1988.
12. H. Nakata. Present State and Future Perspective of Fleet Test of Methanol-Fueled Vehicles. *Proc., International Symposium on Methanol-Fueled Vehicles*, Tokyo, Feb. 7, 1990, pp. 1–10.
13. A. Nishida. The Present State of the Methanol Diesel Engine for Two-Ton Trucks. *Proc., International Symposium on Methanol-Fueled Vehicles*, Tokyo, Feb. 7, 1990, pp. 17–30.
14. N. Nakasima, S. Shiino, S. Shibata, and H. Oikawa. Development of Glow-Assisted Methanol Engine for City Buses. *Proc., 11th International Vienna Motor Symposium*, Vienna, Austria, April 26–27, 1990.
15. O. Fujita and K. Ito. Catalytic Oxidation of Unburned Methanol with the Presence of Engine Exhaust Components from a Methanol-Fueled Engine. *Japanese Society of Mechanical Engineers International Journal*, Vol. 31, No. 2, 1988, pp. 314–319.
16. R. W. McCabe et al. *Laboratory and Vehicle Studies of Aldehyde Emissions from Alcohol Fuels.* SAE Paper 900708. Presented at the SAE International Congress and Exposition, Detroit, Mich., Feb. 1990.
17. O. Fujita, K. Ito, and Y. Sakamoto. Catalytic Oxidation of Unburned Methanol from Methanol-Fueled Engines under Unsteady Operating Conditions. *Proc., 8th International Symposium on Alcohol Fuels*, Tokyo, Nov. 1988, pp. 449–454.
18. H. Yanigihara et al. A New Approach to Methanol Combustion in Direct Injection Diesel Engines. *Proc., 8th International Symposium on Alcohol Fuels*, Tokyo, Nov. 1988, pp. 619–624.
19. A. Nietz. *MAN Methanol Engines for Use in Buses.* SAE Paper P–211. XXII FISITA Congress, Dearborn, Mich., and Washington, D.C., Sept. 25–30, 1988, pp. 2.651–2.657.
20. S. Boyle. Transport and Energy Policies—Only Connect. *Energy Policy*, Jan./Feb. 1990, pp. 34–41.
21. K. D. H. Bob-Manuel and R. J. Crookes. *The Use of Liquified Petroleum Gas, Methanol, and Unleaded Gasoline in a Turbocharged Spark-Ignition Engine Operating on the Simulated ECE-15 Urban Cycle.* SAE Paper 900709. Presented at the SAE International Congress and Exposition, Detroit, Mich., Feb. 1990.
22. C. L. Gray and J. Alson. The Case for Methanol. *Scientific American*, Nov. 1989, pp. 108–114.

Publication of this paper sponsored by Committee on Transportation and Air Quality.

High-Speed Rail System Noise Assessment

CARL E. HANSON

This high-speed rail system noise assessment is in two parts: (a) a noise assessment procedure for the environmental impact analysis of high-speed rail systems and (b) a discussion of the noise characteristics of high-speed trains, including conventional steel wheel and steel rail trains and magnetically levitated (maglev) trains. Aerodynamic noise dominates the wayside noise levels at speeds above 150 mph. The result is that maglev and conventional tracked trains can have similar noise levels at high speeds. A procedure for estimating noise impact corridors for high-speed rail is used in an example.

The general environmental assessment procedure for new transportation projects and some of the noise information from high-speed rail systems that can be used for impact assessment purposes are described. The noise assessment procedure for high-speed rail (HSR), or any other rail project, has not been specified by any agency. UMTA is currently developing noise and vibration impact procedures to be applied to urban transit projects. A similar approach is proposed to be applied to HSR. Included in this paper are data on noise generated by operation of high-speed trains; the surprising result is that noise from maglev systems seems to be the same as that from conventional rail systems at high speeds.

PROJECT PHASE

The noise analysis is done in stages as a major project develops. At an early stage when alternatives are being analyzed, a more general treatment of the noise impacts is appropriate. Corridor screening can be used to identify potential problem areas and to contribute to a comparison of alternatives on an equal basis, with the use of simple screening distances and land use maps. Later, after alternatives have been defined, the noise analysis will focus on site-specific impacts. General assessment, the next refinement, is performed using the level of detail associated with preliminary engineering and the draft environmental impact statement (DEIS). At this intermediate stage, problem areas are identified before the final operational details are known. Detailed calculations are needed in the final design and for the final environmental impact statement (FEIS), when complete operational details and site details are known. This paper provides general information that could be used directly in the first step, corridor screening, and as background information in the more detailed stages.

Harris, Miller, Miller, & Hanson Inc., 429 Marrett Road, Lexington, Mass. 02173.

CRITERIA

Noise impact assessment is based on criteria for community acceptability for a new project. After reviewing the available noise criteria established by the various agencies, UMTA is considering a combination of absolute criteria and relative criteria based on L_{dn}, the day-night sound level (*1*). Shown in Figure 1 are proposed noise criteria for HSR based on the proposed UMTA criteria. The lower curve in Figure 1 represents the onset of noise impact. For conditions below this curve, noise impact is minimal and noise mitigation would not need to be considered. For conditions that fall in the area between the two curves in Figure 1, noise impact is identified. Under these conditions, mitigation would need to be investigated, but not necessarily provided (except for land use where serenity and quiet are of extraordinary significance or where mitigation costs are reasonable). Finally, the upper curve in Figure 1 represents the onset of severe noise impact. For conditions above this curve, noise mitigation would be necessary wherever it is feasible, according to the requirements of the applicable environmental enforcement authority.

HSR NOISE CHARACTERISTICS

Noise from tracked vehicles comes from a variety of sources, including the propulsion system, the wheel-rail interaction, the aerodynamics, and the guideway. The propulsion system tends to dominate noise at low speeds, with electric traction considerably quieter than diesel- or turbine-powered trains. Wheel-rail interaction becomes the dominant noise source for speeds higher than 50 mph for conventional electric trains, with an approximate noise versus (normalized) speed dependency according to the following relationship (*2*): Wheel-rail noise is proportional to 30 log speed.

Until recently, aerodynamic noise sources have been associated with aircraft and ignored in ground transportation vehicles. Airflow over vehicles generates noise for all vehicles, however. Furthermore, with the advent of HSR, this source comes into the picture very strongly as speed increases because of the following relationship (*3*): Aerodynamic noise is proportional to 60 log speed.

These relationships are shown in Figure 2 for typical trains. Both curves apply to conventional steel wheel and steel rail trains where wheel-rail sources dominate up to speeds of 150 mph, above which the aerodynamic noise becomes dominant. A magnetically levitated (maglev) train is subject to the same aerodynamic conditions as other trains, with the same noise generation characteristics. Consequently, the aerodynamic noise

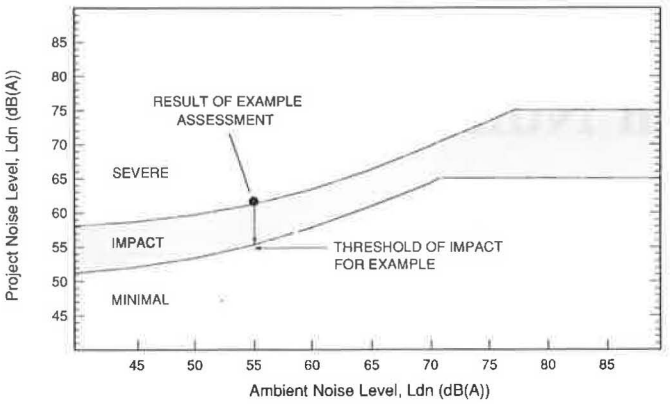

FIGURE 1 Proposed noise impact criteria for HSR projects (*1*).

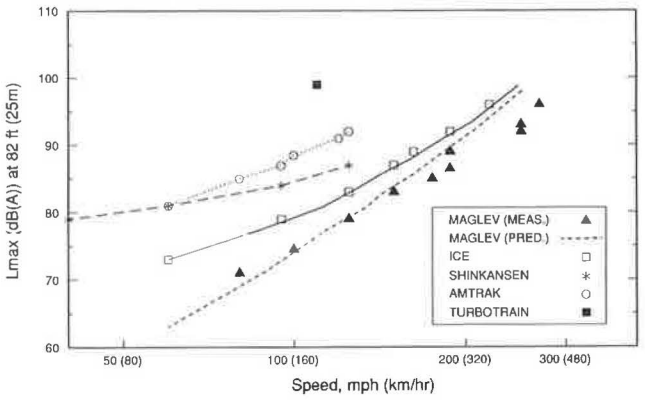

FIGURE 3 HSR noise data: maximum A-weighted sound level versus speed (*4*; *5*; W. Dickhart, TransRapid International, unpublished data; and C. E. Hanson, unpublished data).

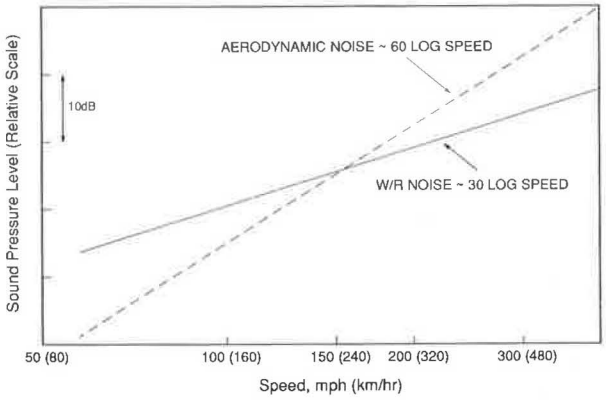

FIGURE 2 Speed relationship of the dominant sources of noise for electrically powered trains.

curve applies to maglev systems as well as to conventional tracked trains. The interesting conclusion is that at high speed, the noise characteristics of either type could be the same, depending on the shape and aerodynamic smoothness of the train.

Aerodynamic noise is related to the smoothness and shape of the train, as measured by the coefficient of drag. The noise is generated by rapidly fluctuating pressures in the turbulent air on or near the exterior surface. Contributions to the overall noise are made by turbulent boundary layer noise and flow separation noise. Some of the sources of aerodynamic noise are vortex shedding from wheel cut-outs and parts of the wheelset and truck frame that protrude into the airstream, the pantograph, and roughness elements on the surface, such as windshield wipers, that can trigger boundary layer separation. Much of the basic research on the sources of aerodynamically generated sound from trains was performed in Germany (*3*).

HSR NOISE DATA

Noise levels from representative HSR systems are shown in Figure 3. Data are shown for some of the fastest conventional trains on ballast and tie trackbed as well as predicted and measured levels from a maglev system on an aerial structure. The data are plotted as measured at an international standard distance of 25 m, corresponding to 82 ft. The curves illustrate the combination of noise sources found in HSR systems, including propulsion noise, wheel-rail noise, and aerodynamic noise.

The lowest noise levels are represented by the measured and predicted noise levels from the German TransRapid magnetically levitated demonstration vehicles, designated TR06 and TR07. The predicted curve is obtained using theory for aerodynamic noise, which includes assumptions about the size and shape of the body (*3*). Actual measured data show the predictions to be conservative by nearly 5 dB at the higher speeds, although the slopes of the curves are in essential agreement (W. Dickhart, TransRapid International, unpublished data).

The curve labeled *ICE* represents data measured on the new German Intercity Express, which has been operated at speeds over 250 mph. These data are representative of all high-speed steel wheel and steel rail systems, including those in operation in France (*4*). The curve of noise versus speed for this train illustrates the combination of wheel-rail noise and aerodynamic noise (*5*). At lower speeds, below 100 mph, the slope of the curve follows the 30 log speed relationship. As speed approaches 150 mph, the slope gradually changes to correspond to a sum of wheel-rail and aerodynamic noise, and at speeds greater than 180 mph, the slope approaches the 60 log speed relationship of aerodynamic noise. Contributions of the various sources of noise from the ICE have been measured with linear microphone arrays (*5*). The results confirm the expected behavior.

Noise from the high-speed trains in Japan has been reported in the documentation of the efforts by the Japanese National Railway to meet environmental constraints (*6*). The data shown here indicate a 20 log speed relationship as opposed to the more usual 30 log speed behavior found for tracked systems, although there is a hint of a change in slope at the highest speed reported. No explanation has been given for the anomalous behavior. It may be caused by a greater contribution of propulsion noise than expected to the low-speed data points.

The Amtrak data shown in Figure 3 are taken from a series of tests run on the then newly introduced electric locomotive from Sweden, the ASEA RC–4, on a long, straight section of track near Princeton, N.J., in 1978 (*7*). The train consist was five cars besides the new locomotive. The data followed approximately a 30 log speed relationship, except when the locomotive was accelerating under power, in which case the relationship was more like the Shinkansen result of 20 log speed.

A single data point represents a passby of an ANF Turboliner (RTG–2) measured by Harris, Miller, Miller, & Hanson, Inc., during a demonstration run on Amtrak's Northeast Corridor (C. E. Hanson, unpublished data). Here, unlike electrically powered trains, the wheel-rail noise and the aerodynamic noise components contributed less than the propulsion noise.

EXAMPLE OF NOISE IMPACT CORRIDOR FROM HSR

In view of public concern over noise from HSR, it is important to make a preliminary estimation of the noise impact corridor from various alternative systems. Expected community reaction is related to the noise criteria based on the L_{dn} metric. In order to estimate the L_{dn} caused by the introduction of high-speed trains, the operational schedule, speed profile, and train consists are required in addition to the L_{max} data. The following conditions are used as an example of the procedure for estimating a noise impact corridor:

Site: average suburban residential community, existing L_{dn} = 55 dBA;
Train: conventional HSR (e.g., the ICE), 780 ft long;
Guideway: ballast and tie, at-grade;
Schedule: one train every hour from 7 a.m. to 12 p.m.;
Speed: 180 mph.

From Figure 3, L_{max} = 91 dBA at 82 ft for this train. Conversion of the L_{max} of a single train passby to hourly equivalent sound level is done by assuming that the train acts like a dipole sound source and using an equation suggested by Peters (*8*). Calculation of the L_{dn} proceeds by summing the hourly noise exposure over the hours of operation, with a 10-dB penalty applied to hours between 10 p.m. and 7 a.m. For this scenario, there are 15 daytime hours and 12 nighttime hours. The project noise calculation yields L_{dn} = 62 dB at 82 ft.

For assessment of noise impact, the project noise level of 62 dB for this hypothetical example is plotted on Figure 1 together with the assumed existing ambient noise level of 55 dB. The point falls into the severe impact zone, which is understandable for a site just 82 ft from the tracks of a high-speed train. Referring again to Figure 1, the project noise level needs to decrease to 55 dB to fall on the threshold of impact, at the point where ambient noise level is 55 dB. Assuming a truncated line source and propagation over ground covered with vegetation, the project noise level would be 55 dB at a distance of 240 ft from the tracks. Consequently, the noise impact corridor for this scenario would have a total width of 480 ft. The corridor would be even wider for residential areas with lower ambient noise levels or for track sections with more train traffic. Typically, the noise impact corridor ranges between 200 ft and 1,000 ft, depending on existing ambient noise conditions, train schedule, operating conditions, and guideway configuration. This scenario is the unmitigated condition; the noise impact corridor can be narrowed considerably with the use of wayside noise barriers.

CONCLUSION

High-speed trains can cause severe environmental noise impact in residential areas; this needs to be considered thoroughly during the preliminary engineering and final design phases of a new system. Aerodynamic noise is the dominant source at speeds greater than 150 mph, and applies to trains whether or not they run on rails. Noise impacts may extend out to distances of 500 ft on either side of the tracks in otherwise quiet residential areas.

REFERENCES

1. *Guidance Manual for Transit Noise and Vibration Impact Assessment.* Report UMTA-DC-08-9091-1. UMTA, U.S. Department of Transportation, Sept. 1990.
2. B. Hemsworth. Prediction of Train Noise. In *Transportation Noise Reference Book* (P. Nelson, ed.), Butterworths & Co., London, 1987.
3. W. F. King and D. Bechert. On the Sources of Wayside Noise Generated by High-Speed Trains. *Journal of Sound and Vibration*, Vol. 66, No. 3, 1979, pp. 311–332.
4. *VDI Nachrichten*, No. 5, Feb. 1990, p. 23.
5. W. F. King and H. J. Lettman. On Locating and Identifying Sound Sources Generated by the German ICE Train at Speeds Up to 300 Km/H. *Proc., InterNoise 88*, Avignon, France, 1988.
6. Japanese National Railways. *Shinkansen Noise.* Aug. 1973.
7. C. E. Hanson. Measurements of Noise from High Speed Electric Trains in the United States Northeast Railroad Corridor. *Journal of Sound and Vibration*, Vol. 66, No. 3, 1979, pp. 469–471.
8. S. Peters. The Prediction of Railway Noise Profiles, *Journal of Sound and Vibration*, Vol. 32, 1974, pp. 87–99.

Publication of this paper sponsored by Committee on Intercity Passenger Guided Transportation.

Energy-Related, Environmental, and Economic Benefits of Florida's High-Speed Rail and Maglev Systems Proposals

THOMAS A. LYNCH

The environmental, energy, and economic benefits of specific, though different, proposed statewide high-speed rail (HSR) systems, to be combined with a proposal for a regional magnetically levitated (maglev) train under review in Florida, are examined. One of the HSR proposals and the maglev system are projected to be fully authorized within the next 18 months and operational by the 1994–1996 period. The specifics of each applicant's proposals are integrated into a complex computer model reflecting different (a) technologies and speeds, (b) energy demands and other resource needs, (c) system service-level characteristics, (d) ridership levels, and (e) modal splits, combined with (f) other system differences. This computer model then integrates the unique (a) fuel consumption and (b) emission levels of the actual electrical generation grid supplying the HSR and maglev systems in central and south Florida. Finally, the model quantitatively combines these data with equivalent emissions, energy, and other systems information on automobile and airplane transportation modes. These data and pertinent user characteristics enable the model to estimate precise environmental, energy, and economic benefits (expressed in 1990 dollars) for each unique HSR and maglev transportation system for the year 1999 alone.

The economic, environmental, and energy benefits of high-speed rail (HSR) and magnetically levitated (maglev) trains are directly related to the technology's energy supply, electricity, and the diversity and control of the sources of fuel that generate the power. Central station generation facilities use diverse sources of fuel in a more environmentally efficient form and can control their emissions far more effectively than competing automobile and aircraft sources.

A more detailed examination of potential HSR and maglev applications in Florida will fully clarify the potential range of energy, economic, and environmental benefits available and the nature of their interrelationships. All projections for this analysis are based on actual Florida-specific HSR applicant proposals submitted by the Florida High Speed Rail Corporation (FHSRC) (*1*, *2*) and TGV of Florida (*3*, *4*). (On October 27, 1989, TGV of Florida withdrew its application from further review in Florida. However, their proposal is included in this analysis because of the extensive amount of in-depth HSR analysis performed by the TGV Company, and because the results of their work are readily available.) The maglev system information is drawn specifically from the Florida maglev proposal submitted by Maglev Transit, Inc. (*5*). Where necessary, these reports are supplemented with information contained in a federally funded Florida HSR study completed in 1984 (*6*).

Florida High Speed Rail Transportation Commission, 311 S. Calhoun St., Tallahassee, Fla. 32301.

These data are further augmented with Florida-specific data and research on power plant (*7*), energy production (*8*), sources of fuel, emission levels (*9*, *10*), and cost of fuel. Other needed information, such as aircraft and automobile emissions, are adapted from standard U.S. Environmental Protection Agency (EPA) (*11*), U.S. Department of Energy (DOE) (*12*), and Florida Department of Environmental Regulation (DER) sources (*9*).

FLORIDA HIGH-SPEED RAIL AND MAGLEV APPLICANT PROPOSALS

Florida High-Speed Rail Corporation Proposal

The FHSRC proposes to use a Swedish HSR train manufactured by ASEA Brown Boveri and called Fastrain. It would be capable of operating in excess of 150 mph and would travel between Miami and Tampa in 160 to 175 min. The FHSRC proposal would ultimately include 13 stations. Ridership is forecast to increase from 1.6 million in 1995 to 2.78 million in 2020 (see Table 1). These preliminary forecasts are being revised on the basis of new surveys conducted by FHSRC in mid-1989. These preliminary estimates do not include induced ridership or short trips.

For purposes of the analysis in this paper, the ridership in 1999 of 1.7 million will be used as a baseline for the FHSRC emission benefit estimation. In addition, the FHSRC proposal indicates that Fastrain sets would carry 480 passenger seats and consume 14,000 kwh for each one-way trip between Miami and Tampa. Fastrain therefore would produce a gross energy consumption of 972 Btu per seat mile. If a passenger per seat occupancy ratio of 70 percent is assumed, the FHSRC Fastrain provides a consumption of 1,388 Btu per passenger mile. This value is higher than that of the original generic Florida High Speed Rail Study (*6*). FHSRC estimates total train weight at 1.31 million lb (1.36 tons) per seat.

Finally, FHSRC indicates that 61 percent of HSR trips systemwide would be diverted from the automobile, 29 percent from the airplane, and the remaining 10 percent from other modes—specifically bus and train (*2*). These will be the technical components of the FHSRC modal split, ridership, and energy needs used for analysis of net emission and energy trade-off reported in this paper for their system.

TGV of Florida Proposal

The Florida TGV proposes to use the French HSR train manufactured in France by Alsthom and Bombardier, Inc. The

TABLE 1 PRELIMINARY RIDERSHIP PROFILE: THE FHSRC HSR SYSTEM

Mode	FHSRC High Speed Rail Mode	Diversions From: Automobile Mode	Diversions From: Airline Mode	Diversions From: Other Masses	Induced Trips
Passenger Miles	391,529,000	238,832,690	113,543,410	39,152,900	N/A
# of Passengers	1,702,300	1,038,403	493,667	120,230	N/A
Passengers/Day	5,674	3,461	1,646	507	N/A
Average Trip Length (Miles)	230	230	230	230	N/A
Days Operation/Year	300	300	300	300	N/A
Mode Occupancy %*	70%	50%	60%	--	N/A

* Mode occupancy percentages based on FHSRTC calculations.

French system is referred to as *train à grande vitesse* (TGV). The train is capable of operating at 185 mph and would travel between Miami and Tampa in 160 min. The TGV proposal includes seven stations. Ridership is forecast to increase from 2.77 million in 1995 to almost 11 million in 2020. These estimates include (a) all intermediate and short trips and (b) an estimated 10.5 percent induced ridership.

For the analysis in this paper, the ridership in 1999 of 5.88 million, with the 617,000 induced riders removed, or 5.26 million trips, will be used as a baseline for the TGV emission benefit estimation. TGV states (*13*):

> The diversion of . . . four million passengers from auto (80% of diverted) and one million from . . . airplane (20% of diverted) in 1999 will result in consumption of 110 million kilowatt hours . . . to transport approximately 5 million passengers. . . . This is equivalent to roughly 11 million gallons of fuel . . . to transport TGV passengers a total of 705 million miles.

Finally, the TGV proposal indicates that each train set would carry 366 passenger seats and consume 9,000 kwh for each one-way trip between Miami and Tampa. The TGV train, therefore, would produce a gross energy consumption of 803 Btu per seat mile. If a passenger per seat occupancy ratio of 70 percent is assumed, the TGV would provide a consumption of 1,147 Btu per passenger-mile (see Table 2).

This energy consumption rate is also higher than the original generic Florida High Speed Rail Study levels (*6*). This system, however, proposes train speeds up to 185 mph, which is considerably above that of the generic Florida HSR systems examined in the study completed in 1984. This energy consumption level is also below that of the FHSRC Fastrain, even though at maximum speed the TGV proposes to operate 35 mph faster than the Fastrain. Most travel times between stations are, however, very close between these two competing systems. The TGV estimates total train weight at 0.975 million lb (1.33 tons) per seat. This is virtually identical to the FHSRC value of 1.36 tons/seat.

These technical components of the TGV modal split, ridership, and energy needs will be used for analysis of the net emission and energy tradeoff reported in this paper for their system.

MAGLEV TRANSIT, INC., PROPOSAL

The Maglev Transit, Inc., proposal was submitted to the FHSRTC by a consortium of Japanese and German manu-

TABLE 2 TGV HSR SYSTEM PROPOSED RIDERSHIP PROFILE

Mode	TGV HSR Mode	Automobile Mode	Airline Mode	Induced Trips
Passenger Miles	735,000,000	526,260,000	131,565,000	77,175,000
# of Passengers	5,262,000	4,210,000	1,052,520	617,400
Passengers/Day	19,600	14,034	3,508	2,058
Average Trip Length (Miles)	140	140	140	140
Days Operation/Year	300	300	300	300
Mode Occupancy %*	70%	50%	60%	0

* Mode occupancy percentages based on FHSRTC calculations.

facturing, banking, and business interests. The German Transrapid maglev system is proposed to operate between the Orlando Airport and the Walt Disney World Epcot Center, a distance of approximately 18 mi, and achieve speeds of 310 mph (see Table 3). The proposal indicates average travel time of 7½ min for the approximately 18 mi between Epcot and the Orlando Airport.

Maglev Transit's application indicates that the system could attract between 6½ and 8½ million (one-way) passenger trips a year during the first years of operation.

In the Maglev Transit system, each maglev coach would carry 100 passenger seats and each train would carry 400 passengers and on average consume 0.11 kwh per seat-mile. Again assuming a 70 percent ridership occupancy factor, the gross energy consumption rate would be 1,573 Btu per passenger mile on this maglev system (Table 4). The Transrapid 07 has an average weight of 0.75 ton per passenger seat for first class and 0.45 ton per passenger seat for second class (see Table 4) (*14*). These weights are considerably lighter than either the TGV- or FHSRC-proposed HSR system, being 34 and 56 percent, respectively, of these systems' average seat weight (see Figure 3).

The proposed operating speed of the Maglev Transit system is five to six times faster than that of the automobile, and as much as twice that of the HSR applicants. Surprisingly, this system consumes only 11 percent more energy than the FHSRC high-speed rail system, although operating at approximately 110 percent higher speeds. This capability is especially interesting given that energy consumption increases as the square of speed. The differences are obviously in weight and technology design. Similarly, although consuming 25 percent more energy than the TGV HSR train, the Maglev Transit system operates at almost 70 percent higher average speed. These are the technical components of the Maglev Transit proposal used in this analysis.

MODEL DEVELOPMENT

Tables 5 and 6 present an overview of the key transportation mode energy efficiencies and the fundamental assumptions and relationships that underlie the development of this model and the research conclusions in this paper. Each of the key HSR and maglev proposals discussed earlier is appropriately factored into the model's specification and summarized in these tables.

Cost of fuel and other pertinent electrical generation information were derived from the Florida Public Service Commission and Florida Power Coordinating Group sources (*7*). Other pertinent transportation modeling information, such as that developed for aircraft emissions and operating conditions, was developed from widely accepted industry standards using relatively conservative assumptions (*11*, *12*).

CENTRAL AND SOUTH FLORIDA-SPECIFIC ELECTRICAL ENERGY PRODUCTION SOURCES AND ESTIMATED EMISSION LEVELS

Perhaps one of the greatest secondary benefits of developing the HSR and maglev transportation networks is the substantial promise that these systems hold for improvements in the environment. These improvements may be second in importance only to slowing down the future increases in environ-

TABLE 3 MAGLEV TRANSIT, INC., PROPOSED SYSTEM

Mode	Maglev Mode	Automobile Mode	Induced Trips
Passenger Miles	144,000,000	144,000,000	0
# of Passengers	8,000,000	8,000,000	0
Passengers/Day	19,600	19,600	0
Average Trip Length (Miles)	18	18	0
Days Operation/Year	300	300	0
Mode Occupancy %*	70%	50%	0

*Mode occupancy percentages based on FHSRTC calculations.

TABLE 4 ENERGY EFFICIENCIES OF THE TRANSPORTATION MODES CONSIDERED

MAGLEV ENERGY CONSUMPTION		TGV ENERGY CONSUMPTION	FHSRC ENERGY CONSUMPTION	AUTOMOBILE ENERGY CONSUMPTION	
kWh per/seat mile	0.11 MIAMI-TAMPA kWh	9,000	14,000	PASSENGERS/AUTO	1.9
NET Btus/Seat Mile	366 #SEATS/PER TRAIN	366	480	MILES/GALLON	20
GROSS Btus/seat mile	1,099 MILES/TRIP	306	300	Btus/gallon	125,000
Assumed capacity factor	0.70 TOTAL SEAT MILES/TRI	111,996	144,000	PASSENGER MILE/GALLON	38
Reciprocal of cap factor	1.43 NET Btu/trip	30,000,000	46,666,666	Btus/PASSENGER MILE	3,289
GROSS Btus/pass mile	1,570 Gross Btu/trip	90,000,000	140,000,000		
	gross Btu/seat mile	804	972		
	gross Btu/pass mile	1,148	1,389		

TABLE 5 THE FLORIDA HIGH SPEED RAIL CORPORATION (FASTRAIN) AND MAGLEV ENERGY ESTIMATES

Mode	Max. Speed	Avg. Speed	Energy Consumption Btu's/Mile/ Passenger	Auto	Air Plane	Maglev	FHSRC
FHSRC (FAS-TRAIN)	150+	130	1,388	2.25	4.48	1.13	1.00
Maglev	311	144	1,570	1.99	3.96	1.00	0.88
Auto-mobile	65	45	3,125	1.00	1.99	0.50	0.44
Airplane	500	450	6,220	0.50	1.00	0.25	0.22

Maglev and HSR mode passenger mile energy consumption is estimated for gross energy consumed at electrical generation station.

TABLE 6 TGV AND MAGLEV ENERGY ESTIMATES

Mode	Max. Speed	Avg. Speed	Energy Consumption Btu's/Mile/ Passenger	Auto	Air Plane	Maglev	The TGV
The TGV	185	130	1,148	2.72	5.42	1.13	1.00
Maglev	311	144	1,570	1.99	3.96	1.00	0.73
Auto-mobile	65	55	3,125	1.00	1.99	0.50	0.37
Airplane	500	450	6,220	0.50	1.00	0.25	0.18

Maglev and HSR mode passenger mile energy consumption is estimated for gross energy consumed at electrical generation station.

mental degradation that are inevitable with expansion of conventional transportation systems. In other words, one benefit is displacement of existing higher-polluting automobile and air traffic and the second benefit is to reduce or displace future demand for these higher-polluting modes.

These potential environmental improvements, like the increases in economic efficiency, owe their existence to HSR and maglev use of relatively clean stationary sources of energy production. As described earlier, electric power plants use diverse fuel source mixes to produce efficient energy and can use and manage large and efficient emission control technologies. These abilities result in substantial improvements in air pollution emissions over conventional transportation technologies in all but one regulated pollutant. Figure 1 shows that 15.4 percent of electrical generation is from nuclear sources, whereas 32 percent is from coal. Fuel for over 47 percent of this region's electrical generation is from sources that are not foreign controlled. Given that much oil and natural gas is domestic, the actual total domestic supply of fuel is much higher.

All power plant emission estimates in this model are derived from averaging historic 2-year (1986–1987) actual emissions from all major power plants in operation in central and south Florida. Table 7 presents a summary of all electric generation facilities serving central and south Florida and the results of 2 years of emission monitoring for principal pollutants. These data were derived from the Florida Department of Environmental Regulation (*9*) and were systematically analyzed to derive weighted averages of annual emissions for the region.

Southeast and central Florida were divided into three geographic electrical service areas. The first is the Tampa Bay

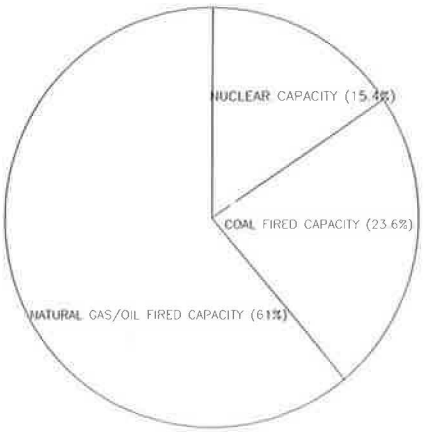

FIGURE 1 Central and south Florida available electric generation by fuel type.

TABLE 7 ELECTRIC POWER PLANT AND ANNUAL POLLUTION EMISSIONS INVENTORY 1986–1987

REGION #3 & OPERATOR	FACILITY NAME	TOTAL SITE MW	YEAR	VOC	SOx	PM	NOx	CO
3 FPL	CANAVERAL PL	800	1986	17	924	106	3,740	
3		800	1987	28	2,540	262	7,090	518
3 FPL	PT EVERGLADE	800	1986	80	12,061	4,657	9,019	991
3		1820	1987	45	7,759	666	6,369	490
3 FPL	LAUDERDALE	1400	1986	3	258	66	2,313	802
3		1400	1987	4	230	39	1,531	168
3 FPL	SANFORD	1000	1986	27	3,748	314	2,130	158
3		1000	1987	7	1,271	170	560	39
3 FPL	RIVIERA	700	1986	28	3,040	297	6,190	453
3		700	1987	17	1,115	131	4,820	351
3 FPL.	TURKEY POINT	2450	1986	64	9,340	833	10,300	757
3	1600 NUCLEAR	2450	1987	50	7,360	655	9,000	661
3 FPL	MARTIN	1600	1986	21	2,199	217	3,219	236
3		1600	1987	73	71,772	563	9,490	697
3 FPL	FT MYERS	1600	1986	33	6,949	484	3,020	246
3		1600	1987	73	10,214	839	4,436	340
3 FPL	ST LUCY	1800	1986	0	0	0	0	0
3	NUCLEAR	1800	1987	0	0	0	0	0
3 FPL	MANATEE	1600	1986	161	32200	2660	14220	1062
		1600	1987	102	20890	1711		
REGION 3 TWO YEAR TOTAL		29,540		830	193,870	14,670	106,457	8,642
ONE YEAR AVERAGE		14,770		415	96,935	7,335	53,229	4,321
FACILITIES' CAPACITY FACTOR=.75								
MWH ANNUAL AVERAGE=97,038,900								
REGION 3 LBS OF EMISSION/MWH				0.009	1.998	0.151	1.097	0.089

REGION #2				VOC	SOx	PM	NOx	CO
2 ORLANDO	INDIAN RIVER	618	1986		4,540	188	3,100	227
2	COAL	618	1987		1,192	98	1,879	121
2 ORLANDO	STANTON CENTER	460	1986					
2	COAL	460	1987		848	42	2,087	
2 ORLANDO	BARTOW	200	1986	0	0	3	6	1
2		200	1987	0	0	80	15	1
2 LAKELAND	LAKELAND	400	1986		2,327	161		
2		400	1987		312	23	49	
2 LAKELAND	MCINTOSH	400	1986		4,561	325		
2		400	1987		4,522	213	3,977	
2 FLORIDA POWER INTERCESSION		400	1986					
2		400	1987		64	13	173	
2 FLORIDA POWER	DELTONA	420	1986		2,382	53	773	
2		420	1987		2,347	97	620	
TOTAL 2 YEARS		5,796		0	18,302	1,133	11,113	350
ONE YEAR AVERAGE		2,898		0	9,151	567	5,557	175
POWER PLANT CAPACITY FACTOR=.75								
ANNUAL AVAILABLE MWH= 19,039,860								
				VOC	SOx	PM	NOx	CO
REGION 2 LBS OF EMISSIONS/MWH				0.000	0.961	0.060	0.584	0.018

REGION #1				VOC	SOx	PM	NOx	CO
1 FLORIDA POWER BARTOW		800	1986	14	23,069	480	3,719	
1		800	1987		18,550	523	2,607	
1 FLORIDA POWER HIGGINS		300	1986		1,983	44	665	
1		300	1987		2,254	67	637	
1 FLORIDA POWER BAYBORO		300	1986		1	11	142	
1		300	1987		42	5	70	
1 FLORIDA P. CRYSTAL RIVER		3,400	1986		84,564	1,524	41,306	
1 COAL & NUCLEAR (800)		3,400	1987		86,018	1,429	42,509	1,725
1 FLORIDA POWER ANCLOTE		1,200	1986		19,178	718	6,039	0
1		1,200	1987		17,742	1,123	5,521	557
1 TECO	HOOKER PT	250	1986	2	325	12	133	12
1	COAL	250	1987					
1 TECO	BIG BEND	1,880	1986	131	132,887	2,604	43,108	1,109
1	COAL	1,880	1987	160	152,151	2,770	48,404	1,347
1 TECO	GANNON	1,500	1986	77	44,584	1,663	39,810	647
1		1,500	1987	197	51,802	1,618	47,058	763
TWO YEAR TOTALS		19,260		581	635,150	14,591	281,728	6,160
ANNUAL AVERAGE		9,630		290	317,575	7,295	140,864	3,080
# MWH/YR 63,269,100								
ANNUAL FACILITIES CAPACITY FACTOR=.75				VOC	SOx	PM	NOx	CO
REGION 3 POUNDS OF EMISSIONS/MWH				0.009	10.039	0.231	4.453	0.097

SUMMARY	VOC	SOx	PM	NOx	CO
REGION 1 LBS/MWH-TAMPA	0.009	10.039	0.231	4.453	0.097
REGION 2 LBS/MWH-ORLANDO	0.009	0.961	0.060	0.584	0.097
REGION 3 LBS/MWH-SOUTH EAST FLORIDA	0.009	1.998	0.151	1.097	0.089

* CO AND VOC FOR REGION 2 AND VOC FOR REGION 3 ARE ADAPTED FROM REGION 1 DUE TO DATA

FHSRC AND TGV RAIL ALIGNMENT WITHIN EACH UTILITY REGION

HSR	CORRIDOR MILE	PERCENT OF TOTAL
TAMPA	30	9.09%
ORLANDO	220	66.67%
SOUTH	80	24.24%
TOTAL	330	100.00%*

	REGION 3		REGION 2		REGION 1		ALL REGIONS	
ANNUAL AVAILABLE MW CAPACITY	MW 9,630	PERCENT 100%	MW 2,898	PERCENT 100%	MW 14,770	PERCENT 100%	MW 27,298	PERCENT 100%
ANNUAL AVAILABLE NUCLEAR CAPACITY	3,400	35%	0	0%	800	5%	4,200	15%
ANNUAL COAL CAPACITY	2,130	22%	460	16%	6,150	42%	8,740	32%
ANNUAL OIL/NATURAL GA	4,100	43%	2,438	84%	7,820	53%	14,358	53%
TOTAL	9,630	100	2,898	100%	14,770	100%	27,298	100%

area, including all of the power stations of the Tampa Electric Company and some of those of the Florida Power Corporation. The second is the greater Orlando area, with power plants owned and operated by Orlando and Lakeland Utilities and some Florida Power Corporation facilities. The third and largest region is southeast Florida, containing all the generation capacity of Florida Power and Light. Table 7 presents data for the power plants within each region.

Next, a unique megawatt-hour (MWh) emissions factor was calculated for the five principal pollutants reported in the Florida Department of Environmental Regulation (FDER) and Environmental Protection Agency (EPA) air emissions inventory (*11*). They are volatile organic compounds (VOC), sulfur oxides (SO_x), nitrogen oxides (NO_x), total suspended particulates (TSP), and carbon monoxide (CO). In several cases, most notably VOC and CO, missing data were apparent for Regions 1 and 2. The VOC and CO emissions factors from Region 1 were used in these cases to avoid biased low emissions projections for these regions.

HSR and maglev mileage within each electrical generation service area was estimated. Then, each HSR and maglev system's energy requirements were calculated for each region. Total annual HSR and maglev MWh electrical demand for each system was combined with each unique region's emission factor to yield total system emission by region. The HSR and maglev transportation system emissions were then aggregated and finally compared with those of the automobile and airplane transportation emissions calculated earlier.

These regions and their unique fuel consumption mix also serve as the basis for estimation of fossil fuel consumption analysis, oil import demand differential, and net energy consumption estimation for the HSR and maglev modes.

ENERGY CONSUMPTION AND AIR POLLUTION EMISSIONS OF HSR AND MAGLEV COMPARED WITH OTHER TRANSPORTATION MODES AT FORECAST RIDERSHIP LEVELS

HSR and maglev systems generally have two to three times the gross energy efficiency of the automobile while offering average commuting speeds from three to six times faster. Comparably, HSR and maglev maintain considerable energy efficiency advantages over the airplane while offering competitive transportation time service levels. Florida HSR studies indicate that the HSR and maglev systems would enjoy a gross energy consumption (number of total Btu per passenger mile) efficiency between four and five times that of the airplane (*2*, *4*) (see Tables 5 and 6 and Figures 2 and 3).

As described earlier, the two proposed Florida HSR and maglev systems would consume 1,148 to 1,570 Btu per passenger-mile compared with 3,125 and 6,220 Btu per passenger-mile for the automobile and airplane, respectively. These efficiencies can vary according to the technology under examination, the average operating speed, occupancy rate, and a variety of other system characteristics. However, these general efficiency levels are most appropriate for the model reported in this paper, given the precise proposals designed for Florida-specific systems.

The total energy requirement to transport the 1.7 million FHSRC passengers annually is 0.53 trillion Btu. Comparable

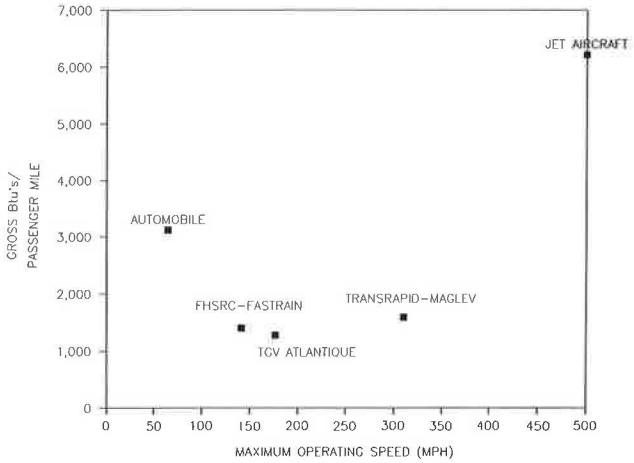

FIGURE 2 Comparative gross energy consumption per passenger mile for each transport mode considered.

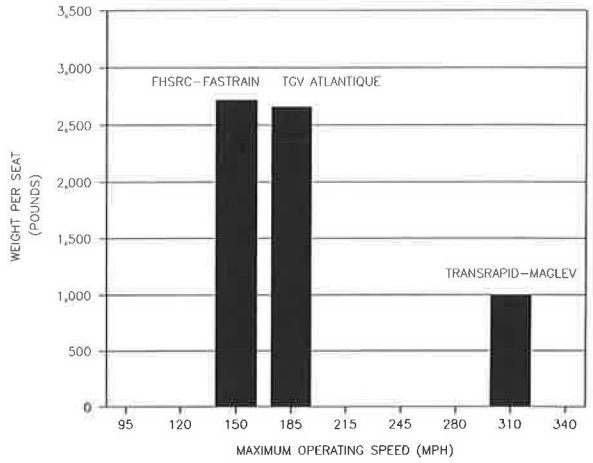

FIGURE 3 Weight per seat for the HSR and maglev transit systems.

automobile and air modes would consume 1.57 trillion Btu. By contrast, to transport the proposed 5.2 million TGV passengers annually would require 0.86 trillion Btu in Florida. The same volume of passengers using automobile and air modes would require 2.46 trillion Btu. Total energy consumption for the HSR proposals and the existing modal shares of passenger volume is only one-third that of the automobile and air modes.

The Orlando maglev proposal indicates that total fossil fuel consumption for movement of as many as 8 million one-way trips would consume 0.251 trillion Btu of energy compared with the 0.526 trillion Btu consumed by the automobile annually. Total net energy savings for the HSR and maglev systems in Florida for 1999 would range from 1.35 to 1.875 trillion Btu.

These comparisons suggest that a substantial reduction in energy consumption would result from diversion of automobile and air travel to HSR and maglev systems. In addition, the following benefits would result:

1. Consumption of nonfossil fuels for transportation (15 percent in central and south Florida).

2. Consumption of less expensive (unrefined oil and coal) domestic and foreign sources of fossil fuels for transportation systems.

3. Consumption of more plentiful and less expensive domestic sources of fossil fuels for transportation systems (reducing U.S. economic dependence on foreign sources of energy).

4. Substantial reductions in air pollution emissions (because central station fossil fuel emissions can more efficiently remove pollution than numerous small nonpoint mobile sources such as automobiles and airplanes).

5. Transportation of passengers, goods, and services over the same distance for approximately the same energy consumption level in one-third to one-sixth the time.

6. Enhancement of overall high-technology growth of the economy by raising the quality of economic productivity and competitiveness.

HSR AND MAGLEV ECONOMIC BENEFITS

General Economic Benefits

The central thrust of much economic study is the examination of the distribution and use of scarce resources among competing demands. These scarce resources can be a natural resource like fossil fuel and iron ore for manufacturing or the scarce human resources of skilled labor and time itself. Each has a value and each contributes to the economic value of the nation's gross national product (GNP). More efficient use of these resources increases the nation's productivity, quality of life, and the GNP itself as the economy's given annual net scarce-resource assets go further and further in creating wealth and human well-being.

This phenomenon is easily grasped by recalling the enormous strides in productivity that this country and the developed world have made since the end of World War II. War-induced scientific discoveries and large-scale automation of industrial production led to substantial growth in U.S. manufacturing output in the five decades after World War II.

These technological enhancements were coupled with considerable improvement in the skill level of American workers. Many of these improvements were given an artificial boost by the necessities of war and its associated need for large numbers of highly trained technicians to operate and maintain the increasingly complex mechanisms of war. A comparable push on the home front propelled large numbers of untrained workers into technical support jobs designing, manufacturing, and maintaining the machines of war within American factories.

These war-stimulated technological discoveries and broad-based gains in formal educational attainments and skilled worker training were unprecedented in world history and reached across a broad base of the American work force. These trends, which continued into the decades after the war and up to the present, were the underpinning of the giant gains in economic growth and improvements in the quality of life that this nation has achieved during the past 45 years.

In recent years, with the advent of computer automation, gains in productivity and quality of life are readily apparent. Computers have enhanced productivity in manufacturing, office automation, research and design, communications, medicine, the home, and a number of other important areas.

Energy efficiency has also evolved as a critical issue for resource conservation in the wake of the tripling of oil prices by the Organization of Petroleum Exporting Countries over the period 1973 to 1977. American productive economies responded well to this resource challenge even though energy prices are now as inexpensive as at any time in the past few decades. Between 1973 and 1985, the amount of energy needed to produce one unit of GNP within the industrialized world fell by 20 percent. In the United States alone, GNP grew by 40 percent during that period, whereas consumption of energy stayed relatively constant (*15*).

Each time a scarce resource such as an hour of time or a kilowatt-hour of energy is saved (because of the enhanced productivity of the computer or other advances), that resource is also liberated for additional productive use within the economy. That additional hour of labor or kilowatt-hour of energy can add more to productivity elsewhere within the economy. The wealth of the nation's GNP and the national quality of life are commensurately enhanced.

So it is with HSR and maglev transportation systems that conserve natural and productive resources and travel time. The general economic efficiencies of HSR and maglev systems would enable the state and national economies to do more with expenditure of fewer resources.

Integration of technological advances can dramatically reduce the amount of energy required to produce a given level of goods and services and simultaneously reduce energy demands worldwide. Innovations like HSR and maglev can enhance energy efficiency and help reduce American dependence on foreign sources of fossil fuel without sacrificing economic growth (*15*) or quality of life.

As Europeans know, the technical and commercial productivity for HSR systems is much higher than that of conventional train operations. In a recent report (*16*), the European HSR community indicated that HSR operation makes much more efficient use of rolling stock fleets. HSR rolling stock can operate over two to three times the distances of conventional rolling stock annually. Where conventional rolling stock operates over 100,000- to 200,000-km routes (60,000 to 120,000 mi) per year, HSR rolling stock can operate over 300,000- to 400,000-km routes (180,000 to 240,000 mi) annually.

Furthermore, fleet uniformity and specialized maintenance equipment enable the rolling stock to be more efficiently maintained and keep the existing stock in better condition and more available than average conventional train sets. Finally and most important, the high speed of the service enables much higher productivity of train crews, operational and commercial staff, and other administrative and technical support. Much more route, equipment, and passenger mileage per unit of labor is possible with the HSR systems than with conventional systems. As a result, productivity and profits are both considerably higher than for conventional systems.

HSR and maglev systems provide the safest and highest quality, time-efficient transportation services with a time savings factor of three to six times that of the automobile at one-third to one-half the level of energy and other resource consumption of the automobile and one-fifth that of the airplane. Stated differently, the HSR systems can transport three times as many persons or goods to any given destination on average three times faster than the automobile, using the same amount of energy. Maglev can deliver twice as many persons or goods

any distance at over five times the speed for equivalent energy. These savings of energy, time, money, and reductions in accident costs and vehicle wear can be released for other productive purposes within the economy and further stimulate the GNP. Furthermore, these gains would enhance the quantity and quality of leisure time and thereby add to the economy's quality of life and general productivity.

The value of a number of these benefits can be quantified and are the basis of some of the economic benefits projected and reported here for the HSR and maglev systems proposed for Florida.

Travel Time Savings

Tables 5 and 6 itemize the proposed HSR and maglev annual 1999 passenger miles traveled and list the travel mode splits for these passengers without high-speed systems. These travel levels are estimated and do not include induced ridership for any of the systems examined. The proposed TGV stations in the greater Orlando area involve the same market as the maglev system. Therefore, a net reduction of 241,000 TGV passengers in that market segment were removed from the TGV passenger estimates to avoid double-counting potential passenger miles when the systems are combined.

The average TGV passenger trip is 125 mi, whereas the FHSRC average length is 230 mi. This estimated length (derived from actual proposed length from origin to destination and passenger volume) is from each technology's respective travel forecasts in Florida. The FHSRC excluded all short-distance trips and induced ridership. The TGV included both long and short trips and induced ridership. Again, induced ridership was removed from the TGV projections to ensure comparability in evaluation of benefits. The average one-way travel length for the maglev rider is approximately 18 mi.

Researchers often equate the hourly value of time savings and the per capita earning potential of the traveler, which for Floridians in 1990 is $8.43. The value of travel time is the basis of estimated economic savings in this analysis. This 1990 estimate of value of time is likely conservative for a variety of reasons. First, a large segment of the HSR travelers are business-related travelers, and they and the recreational traveler would both have higher-than-average earning potential. Second, a number of travelers for either system would be out-of-state visitors. Again, such travelers would have considerably higher income, on average, than the Florida per capita level. Finally, AASHTO estimates that the annual savings for the traveling public should be $9.27 per hour saved (*17*). This AASHTO estimate and a higher FAA (*18*) estimate are also frequently used for such benefit estimation and were the basis for the original Barton-Aschman Florida HSR study (*6*). The conservative nature of the lower value used in these estimates helps understate the potential value of these time savings benefits.

The value of saved traveling time on each of the HSR and maglev systems is presented in Table 8. The additive value of time savings when the maglev system is combined with each HSR system is also presented in Table 8. Figures 4 and 5 show bar graphs of the value of the combined HSR and maglev system time savings benefits. All estimates include standard access time, en route time, and egress time determined by Barton-Aschman (*6*). The time savings values shown in Figure 4 are most dependent on access time, travel time, and number of passengers. FHSRC ridership levels have considerably less time savings because the number of passengers initially estimated for the FHSRC system is less than half that for the TGV system.

The TGV potential time savings value exceeds $77 million for 1999. Comparatively, the FHSRC time savings benefit for that year is 46 percent of that, or $33 million. Finally, the maglev time savings value is estimated at $59 million for 1999. Thus, travelers within Florida could receive between $92 and $136 million in travel benefits in 1 year alone from implementation of HSR and the maglev systems within the state.

Reduced Automobile Maintenance and Vehicle Wear

A second very important area of potential economic savings would result from reduced wear and tear and maintenance costs for millions of personal automobiles across the state. These estimated gross wear and maintenance costs are exclusive of any fuel costs, which are addressed elsewhere in this paper. Related reduced deterioration of existing roadways and other infrastructure (such as bridges) is also a potential area of savings but is beyond the scope of this analysis.

It is difficult, if not impossible, to estimate the costs of less wear and tear from substitution of the proposed HSR and maglev systems at these proposed levels of ridership, because neither system is operational within Florida, but clearly the magnitude of the expense of individual automobile deterioration far exceeds those of the proposed systems. Although the gross estimated automobile vehicle wear and maintenance costs may overstate the true net benefit of replacement of the automobile, other potential benefits not included (such as savings in roadway and other infrastructure wear costs) tend to make this estimate conservative.

These unknown benefit levels may very well balance out, and until more precise information is available, the AASHTO automobile wear and maintenance projection provides the best possible estimate of the benefits of lower automobile deterioration costs attributable to implementation of HSR and maglev systems in Florida (*17*). AASHTO estimates $0.165/mi for vehicle operating cost. One-fourth of this cost is fuel related; therefore, $0.118/mi is the final cost for automobile maintenance and wear.

Automobile operation and maintenance costs are estimated to be $34.3 and $25.5 million less for the TGV and FHSRC proposals, respectively, for the year 1999 alone (see Table 9 and Figures 4 and 5). The maglev proposal will lower automobile maintenance expenses for 1999 by an additional $9.9 million.

Statewide potential benefits from lower automobile wear and maintenance expenses for 1999 from a combined HSR and maglev system would range from $35.4 to $44.2 million for 1999 alone.

Fewer Automobile Accidents and Reduced Property and Injury Losses

Another important category of potential economic benefits would result from reduced automobile accidents and property

TABLE 8 MAGLEV VALUE OF TRAVEL TIME DIFFERENCE OVER THE AUTOMOBILE

		TRIP HOURS ENROUTE	ACCESS TIME BOTH TRIP ENDS	# HOURS ENROUTE	# HOURS ACCESSING MODE	# HOURS ENROUTE & ACCESSING	TRAVEL TIME CONSUMER COS
AUTO SPEED IN MPH	40	0.45	1.25	3,600,000	10,000,000	13,600,000	$114,648,000
MAG LEV AVERAGE SPEED	250	0.07	0.75	576,000	6,000,000	6,576,000	$55,435,680
					MAGLEV TRAVEL TIME SAVINGS=		$59,212,320
# PERSONS		8,000,000					
TIME VALUE PER HOUR TRAVEL		$8.43			**Time Travel Savings/Maglev Trip = $7.40**		
AVERAGE TRIP LENGTH (MILES)		18					

FLORIDA HIGH SPEED RAIL CORP VALUE OF TRAVEL TIME DIFFERENCE OVER THE AUTOMOBILE AND AIRPLANE

	TRANSPORT MODE AVER SPEED (MPH	TRIP HOURS ENROUTE	ACCESS TIME BOTH TRIP ENDS	# HOURS ENROUTE	# HOURS ACCESSING MODE	# HOURS ENROUTE & ACCESSING	TRAVEL TIME CONSUMER COS
AUTOMOBILE MODE	45	5.11	0.75	6,177,458	906,475	7,083,932	$56,124,471
AIRCRAFT MODE	400	0.51	1.75	252,319	863,917	1,116,236	$9,414,334
FHSRC HSR SYSTEM	135	1.53	0.75	2,610,038	1,276,649	3,886,688	$32,780,324
					MAGLEV TRAVEL TIME SAVINGS=		$32,758,480
# AUTO PERSON TRIPS/YEAR		1,208,633					
# HSR PERSON TRIPS/YEAR		1,702,199					
# AIRPLANE PERSON TRIPS/YEAR		493,667			**Time Travel Savings/HSR Trip = $19.24***		
TIME VALUE PER HOUR TRAVEL		$8.43					
AVERAGE TRIP LENGTH (MILES)		230 AUTO					

THE TGV OF FLORIDA VALUE OF TRAVEL TIME DIFFERENCE OVER THE AUTOMOBILE AND AIRPLANE

	TRANSPORT MODE AVER SPEED (MPH	TRIP HOURS ENROUTE	ACCESS TIME BOTH TRIP ENDS	# HOURS ENROUTE	# HOURS ACCESSING MODE	# HOURS ENROUTE & ACCESSING	TRAVEL TIME CONSUMER COS
AUTOMOBILE MODE	45	3.13	0.75	12,406,500	2,977,560	15,384,060	$129,749,162
AIRCRAFT MODE	400	0.31	1.75	328,913	1,841,910	2,170,823	$18,308,717
THE TGV HSR SYSTEM	135	0.93	0.75	4,650,556	3,766,950	8,417,506	$70,993,242
					TRAVEL TIME SAVINGS		$77,064,637 **
# AUTO PERSON TRIPS/YEAR		3,970,080					
# HSR PERSON TRIPS/YEAR		5,022,600					
# AIRPLANE PERSON TRIPS/YEAR		1,052,520			**Time Travel Savings/HSR Trip = $15.34***		
TIME VALUE PER HOUR TRAVEL		$8.43					
TRIP LENGTH EACH WAY=		125					

TOTAL HSR AND MAGLEV TIME SAVINGS

FHSRC & MAGLEV	$91,970,800
TGV & MAGLEV	$136,276,957

* Savings per trip are higher for the FHSRC than the TGV Company based predominantly on longer average trip length of the FHSRC estimates.

** The TGV Company total time savings values are higher than those of the FHSRC because of the considerably larger number of passenger trips estimated for the TGV system.

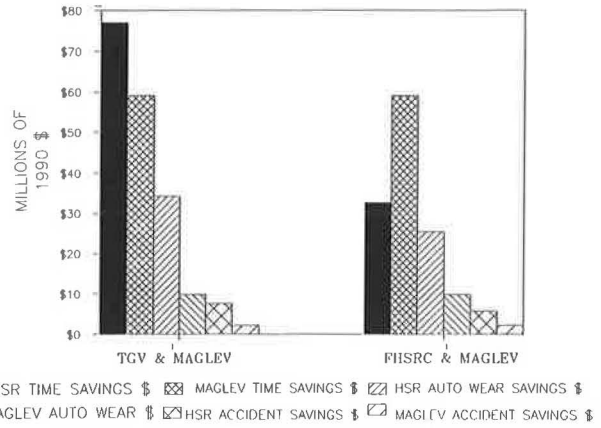

FIGURE 4 Comparison of individual economic benefits of operating the HSR and maglev systems in Florida for 1999.

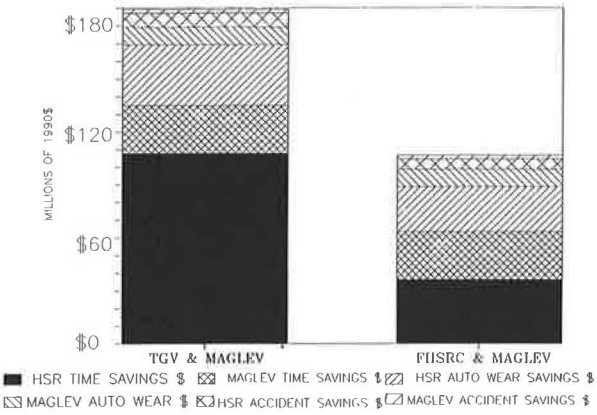

FIGURE 5 Comparison of total economic benefits of operating the HSR and maglev systems in Florida for 1999.

and injury losses. AASHTO estimates (using 1990 dollars) the per mile cost of automobile accident damage and injury costs at $0.0252 (*19*). Automobile accident cost savings (system benefits) for 1999 are presented in Table 10 and Figures 4 and 5 for each proposed HSR and maglev system. The TGV system's proposed highest system ridership again provides the highest level of potential benefits, $7.6 million annually by 1999; that for FHSRC is somewhat less at $5.7 million, and the maglev proposal savings is $2.2 million. Combining the HSR and maglev systems results in an annual 1999 statewide savings in automobile accident costs of $7.9 to $9.9 million.

Reduced Highway Infrastructure Expenditures in Florida

Florida, like America's other major areas of growth, is facing overwhelming increases in demand for transportation infrastructure. This demand, when combined with serious constraints on budgets and physical capacity to fulfill needed airport and roadway expansion, is one of the most serious issues that Americans collectively face. HSR and maglev may offer a workable alternative to help address these ever-increasing demands that must be met with shrinking resources. A recent study in Florida that examined demands for state

TABLE 9 AUTOMOBILE WEAR AND MAINTENANCE SAVINGS

	Savings ($)	
	TGV-Maglev	FHSRC-Maglev
HSR	34,276,145	25,499,389
Maglev	9,915,789	9,915,789
Total	44,191,934	35,415,178

TABLE 10 AUTOMOBILE ACCIDENT SAVINGS

	Savings ($)	
	TGV-Maglev	FHSRC-Maglev
HSR	7,672,317	5,707,742
Maglev	2,216,000	2,216,000
Total	9,888,317	7,923,742

public infrastructure estimated that the cost for the next 10 years for future growth alone will exceed $53 billion.

Transportation entails the largest share of that demand—a 1989 Florida Department of Transportation (FDOT) study that measures traffic volume by comparing the number of cars and paved miles in Florida indicated that vehicles per highway mile in Florida have increased by 50 percent in the last 8 years alone. For every paved mile in the state 8 years ago, there were two cars on the road. Now there are three. Highway capacity construction cannot keep up with the demand. HSR and maglev would complement other modes of travel in Florida by predominantly serving the intermediate-haul markets, whereas the automobile and airplane would dominate the short- and long-haul (over 300 mi) markets, respectively. Construction of a statewide HSR system could potentially save many millions and perhaps billions of public-sector dollars in highway capacity construction. For example, FDOT estimated that a $1 billion savings in highway capacity construction will result when the statewide HSR system is completed.

No comparable estimate is available for the Orlando maglev system, but after an established ridership develops, this system is also expected to result in local infrastructure savings.

Increased Employment and Income

Potential employment and income gains related to HSR and maglev may be viewed as transfers from other sectors of the Florida economy. It can be argued that if the HSR system were not completed, the monies would be expended elsewhere within the state's economy and would entail those of the same resources for other purposes. For example, these funds might be used for construction of new roads, tourist attractions, and service jobs to operate such facilities. Although the argument contains a certain logic, in this setting it is fundamentally flawed. Both the HSR and maglev systems are completely new concepts and would draw to the state both new financial resources and new bases of high-technology manufacturing and research. Most of the resources expended on these projects would not simply be reallocated within the

state if the systems were not built: The resources simply would not exist, because many of the dollars to construct these facilities would originate from sources outside the United States. It is therefore meaningful and important to examine the potential economic impact of increased employment and income resulting from construction and operation of the HSR and maglev systems.

The TGV of Florida proposal indicates that its system would typically generate employment of 4,558 persons, 29,980 man-years of direct construction employment, and secondary employment of 186,499 induced from construction.

The system proposed by TGV of Florida would typically generate $291 million annually in direct and indirect operations employment income, $800 million in total direct construction income, and $19.5 billion indirect income from construction.

The proposal submitted by Maglev Transit indicates that development and operation of their maglev system in Florida would typically result in $300 million in direct local expenditures, $75 million in indirect regional income, $15 million in state and local taxes, and $45 million in annual operating and maintenance costs. This system would also result in 1,500 construction jobs, 5,000 indirect full-time jobs, and 350 permanent jobs.

No comparable employment and income information is available from the FHSRC at this time, but the impacts would be considerable, long term, and of the same magnitude as those of the two other systems.

Reduced Dependence on Fossil Fuels for Transportation

Important to the HSR and maglev economic efficiency issues are the kind, source, and cost of competing energy supplies used in producing electricity to power the HSR and maglev technologies. Domestic sources of coal and nuclear-powered electrical energy enjoy a considerable economic advantage over predominantly imported residual fuel oil sources of power (*7*). The United States has sufficient coal reserves to fuel the economy for the next 260 years (*15*). In south and central Florida, 32 percent of the electrical energy produced is generated from domestic coal, whereas 15.4 percent is from nuclear power (*7*) (see Table 7 and Figure 6). Combining this advantage with the fact that HSR and maglev are two to three times more energy efficient at three times the service (speed) levels of the automobile and five times as efficient as the airplane at comparable travel times provides an insight into the technology's principal economic energy advantages.

As an example, to transport all of the proposed TGV-HSR and maglev passengers in 1999 by automobile and airplane would require up to $33.4 million in fossil fuels. To transport the same number of passengers the equivalent distance by maglev and HSR would cost only $3.1 million in fossil fuels. This translates into a potential fossil fuel savings within the economy of $30.3 million.

Although these are accurate facts in contemporary America, greater promise of substantial advances in areas of electrical energy production are on the horizon (*20*). These and other advances hold great promise of further accentuating the economic, environmental, and energy advantages of HSR and

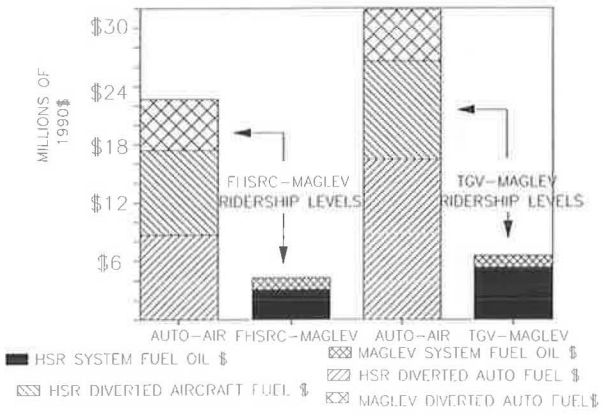

FIGURE 6 Comparison of oil import needs for the airplane and automobile versus the HSR and maglev transportation modes.

maglev over conventional transportation systems (*21*). This greater fossil fuel efficiency can be put to more productive use elsewhere in the economy and would result in even greater primary and secondary economic returns from the net national wealth.

Hand in hand with the HSR and maglev increased economic and energy efficiencies and related reliance on more diverse sources of energy production is the potential for substantial reduction in reliance on foreign sources of fossil fuels for U.S. transportation systems. Again, this would result because much of the HSR and maglev energy supply relies on non-oil-based fossil and nonfossil fuels for operation. Almost half, or 47.4 percent, of electrical power in central and south Florida is either coal fired or nuclear generated.

Development of an HSR and maglev system on the scale being examined in Florida would result in displacement of need for 14 to 20 million gal of expensive imported and then refined fuel oil for 1999 alone. Development of the HSR and maglev systems could reduce oil imports by well over 20 million gal annually by 2020 for Florida alone. These savings would translate into reduced purchases of foreign fossil fuels and therefore a reduced balance of payments of $24.3 and $31.5 million. Modal shifts to the new system offer prospects of annual foreign debt reductions in the future exceeding $50 million by 2020.

This substantial reduction in foreign imports would result in

1. Strengthening U.S. energy independence,
2. Helping to equalize the international negative balance of payments,
3. Increasing domestic security, and
4. Reducing the vulnerability of the American economy to international economic fluctuation such as oil price variations.

Reduced Negative Environmental Externalities

Concurrent with enhanced productivity are the systems-associated benefits of reductions in air and water pollution emissions, quantified in the other sections of this paper. These emission reductions would likely result in a reduction in fac-

tors associated with higher automobile emissions, such as respiratory illness, materials and crop damage, and a variety of other ecological stresses. These economic cost factors, called "negative economic externalities," are undesirable byproducts of pollution. As an example, it is estimated that acid rain-induced materials damage alone in the United States exceeds $16.25 per person annually (*22*).

Such projections are beyond the scope of this analysis given the complexity of developing air pollution dispersion models and risk assessment analysis of the individuals and receptors at risk. This paper does not attempt to estimate the potential range of the benefits from HSR and maglev on environmental externalities because of the complexity of such an undertaking. Nor does this paper attempt to examine some other potential environmental risks associated with these technologies, such as electromagnetic field exposures. Only net air pollution emissions tradeoffs among the transportation technologies are examined.

However, reduced negative externalities represent real HSR and maglev potential economic benefits. These benefits are achieved by substituting the lower HSR and maglev net per-passenger emissions for the higher automobile and airplane emissions. Because these benefits are not quantified, they are discussed qualitatively within the context of each reduction in air pollution emission estimated.

HSR and Maglev Elasticities and Growth in Economic Benefits

Needless to say, the economic benefits of the HSR and maglev systems grow as rapidly as the ridership of these systems expands. A logical question, then, is what principal factors influence the growth of these societal (ridership-related) benefits and at what rate do these benefits grow?

A detailed answer to these questions is beyond the scope of the analysis in this paper. Nevertheless, it is an important issue, and it is possible to creditably address these issues from a macroeconomic perspective with a brief discussion of system elasticities. An elasticity measures the amount of change in one dependent variable, such as ridership or revenue, as an independent variable, such as trip time, changes. Usually, ridership studies examine how much ridership and ridership-related revenue change as trip times increase or decrease by 10 percent.

Response to this issue is of special interest because both HSR applicants completed separate analyses in a competitive environment, and they concluded with very similar ridership elasticities. The conclusions of these ridership studies were completed by two consultants who specialize in ridership studies. (FHSRC employed Charles River Associates and the TGV employed Peat Marwick Main & Company.) The conclusions offer the clearest empirical insight into the benefits of increases in HSR and maglev ridership for markets in Florida and elsewhere in the United States. Maglev markets particularly seem to hold great promise if the ridership-trip time arc elasticity relationships discussed here continue to hold over the 185- to 300-mph speeds and over intermediate (100- to 500-mi) distances.

The TGV analysis demonstrates highly sensitive trip time ridership and revenue elasticities (*23*). TGV reports a positive ridership elasticity of +35 percent increase in ridership for every 20 percent improvement (reduction) in travel time. Even more striking is the projected +54 percent increase in ridership revenues with a 20 percent improvement (reduction) in trip travel times. TGV estimated trip time between Tampa and Miami is 160 min.

A ridership elasticity of −23 percent and a −32 percent ridership revenue elasticity were estimated for the TGV HSR system, assuming that it experienced an average 20 percent slowdown (increases in trip times) over proposed en route times.

Given the elasticity estimations of potential increases in societal benefits examined in this paper, HSR and maglev ridership revenues (private benefits) are straightforward. For instance, the distance between Miami and Tampa is approximately 315 mi. Both FHSRC and TGV estimate the total trip time between these points to be approximately 160 min. The TGV analysis assumes five intermediate stops of 6 min (2 min each for deceleration, dwell time, and acceleration). Therefore, the average en route trip speed is approximately 145 mph.

Figure 7 is a comparative bar graph of potential percentage changes in ridership and revenues as a result of increases or decreases in average transport trip speeds. These estimates indicate that if a steel wheel or maglev system could increase average trip speeds by 34 percent, to 195 mph, the ridership and societal benefits reported in this paper would all increase by 60 percent. Ridership revenues would jump by 93 percent.

This estimate assumes that the arc ridership and revenue elasticities reported by the TGV hold into the upper speed ranges, but they should, because they are in part predicated on the airplane, which offers even faster en route trip times. Presumably then, a maglev system operating at an average trip speed of 255 mph would anticipate a 132 percent increase in ridership and 205 percent increase in ridership revenue over the current proposed TGV Florida forecast.

Figures 8 and 9 provide ridership and revenue curves extrapolated from the proposed TGV Florida base case of 5.2 million riders and $152 million (1990 dollars) of ridership

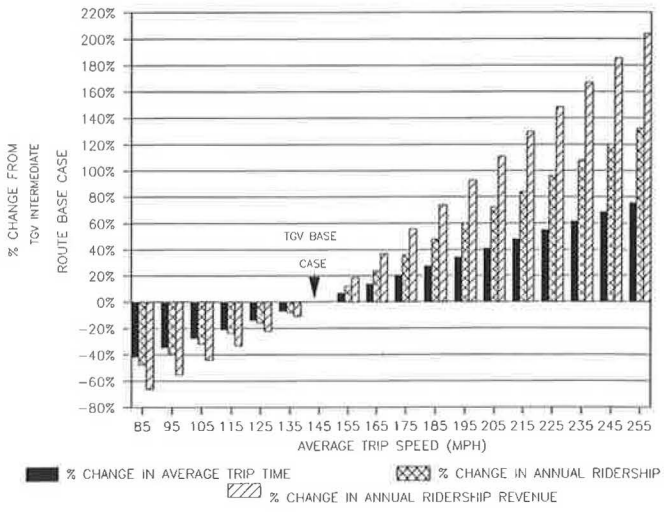

FIGURE 7 HSR and maglev potential changes in ridership and system revenues in Florida at different average trip speeds.

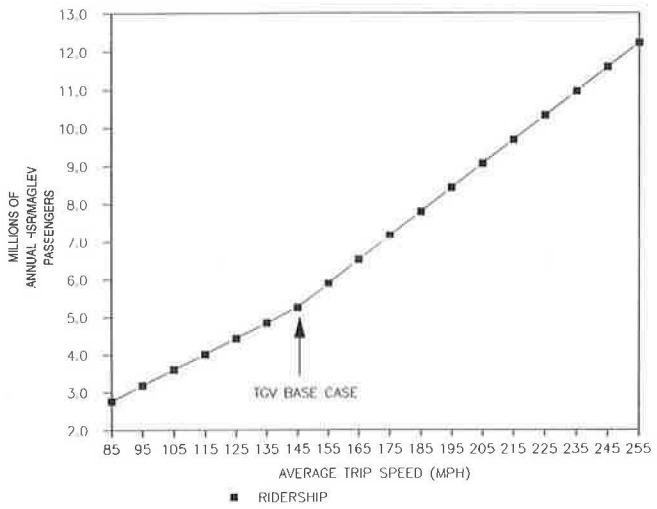

FIGURE 8 Annual ridership potential as a function of average trip speed using TGV estimated revenue elasticities.

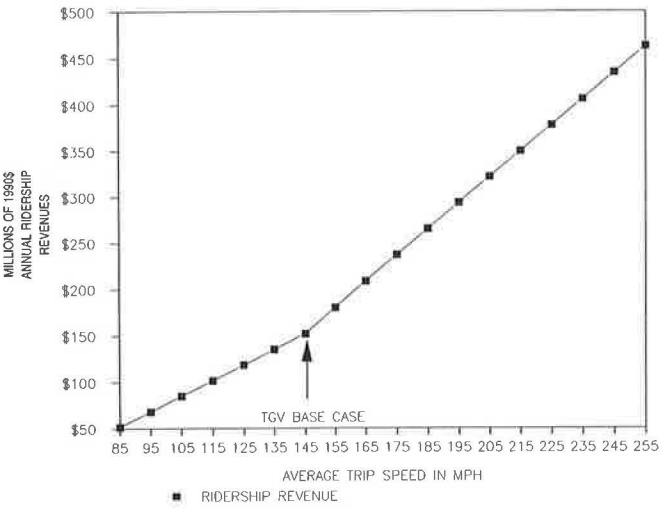

FIGURE 9 Potential HSR and maglev revenue versus speed projections extrapolated from TGV revenue elasticities.

revenue forecast for 1990. The bend at 145-mph average speed results from the higher elasticity rate of ridership and revenue gains above the TGV base case of 145 mph than below that value. Again as an example, annual average passenger levels would increase from 5.2 to 12.2 million in 1999 if a maglev system capable of operating at 255 mph were in place. The growth in ridership revenues would increase from the annual base case of $152 to more than $463 million for 1999 in such a system. This forecast seems to hold considerable promise for substantial increases in societal and ridership revenue benefits for any system offering a reasonable increase in speed.

This information is especially timely because the TGV Atlantique reported that it established a new world speed record of 299.9 mph in France during December 1989. TGV asserts it will be offering conventional passenger service with top speeds of 200 mph within the foreseeable future.

Societal benefits reported in this paper are also directly dependent on the HSR and maglev ridership levels. Therefore, each economic benefit estimated and reported in this paper would also increase by approximately 132 percent, the magnitude of ridership increase, if a maglev system operating at average trip speeds of 250 mph were in place in Florida.

For competitive reasons, the FHSRC does not report (as of this writing) as extensively on ridership elasticities as TGV. Nevertheless, when it does offer an insight into ridership modeling, the ridership elasticity is close to that of the TGV.

FHSRC alludes to an equivalent powerful trip time and ridership relationship (*1*). It indicates that a ± 10 percent change in HSR travel time was found to result in ± 13 percent change in HSR ridership. These estimates suggest that an increase of 20 percent change in trip time would result in a 26 percent increase in ridership. Although not as large as the TGV 35 percent ridership response, this elasticity does indicate strong concurrence with the direction and magnitude of the TGV HSR ridership study.

The obvious implication is that significant increases in HSR and maglev societal (and private sector) benefits are possible with any measurable improvements (reductions) in average trip times. These conclusions are drawn from several sources in a Florida context, and are corroborated by competing sources in a private enterprise setting. These findings are believed to be among the most significant to evolve from the Florida HSR and maglev proposals under review. These findings hold great promise for other transportation markets within the United States.

Air Pollution Emission Differences

Volatile Organic Carbons

VOCs consist of hydrocarbons, which are of local concern in many urban areas. HCs, along with NO_2 and CO, are major precursors of ozone, which is another principal local-area pollutant plaguing American urban areas.

The proposed Florida HSR and maglev transportation systems would result in reductions of between 671 and 749 tons of hydrocarbons per year by 1999. Another way to view these differences is to realize that virtually all of the estimated automobile hydrocarbon pollutants generated by the 1.7 to 5 million HSR and 4 million maglev passengers would be removed if these systems were in place in Florida (see Table 11 and Figures 10 and 11).

Carbon Monoxide

Carbon monoxide (CO) is another of the principal local-area pollutants of concern in many urban areas. Again, it is a precursor of ozone.

HSR and maglev transportation systems operating in 1999 in the reported passenger range would result in reductions of 3,724 to 5,417 tons of CO per year. Again, an HSR system in Florida would virtually eliminate these estimated levels of automobile and aircraft CO emissions for the passenger levels under consideration. This improvement is due to the much more complete burn associated with power plant fuel consumption than fuel conserved in automobile engines (see Table 11 and Figures 10 and 11).

TABLE 11 HSR AND MAGLEV TOTAL EMISSIONS REDUCTIONS (TONS/YEAR)

	VOC	CO	CO2	NOx	TSP	Tire TSP	SOx
MAGLEV	169	981	12,167	242	19	18	(41)
TGV	579	4,437	50,638	1,108	78	73	(160)
TOTAL	749	5,417	62,805	1,350	97	90	(201)
	VOC	CO	CO2	NOx	TSP	Tire TSP	SOx
MAGLEV	169	981	12,167	242	19	18	(41)
FHSRC	502	2,744	50,061	801	51	43	(118)
TOTAL	671	3,724	62,228	1,043	70	61	(163)

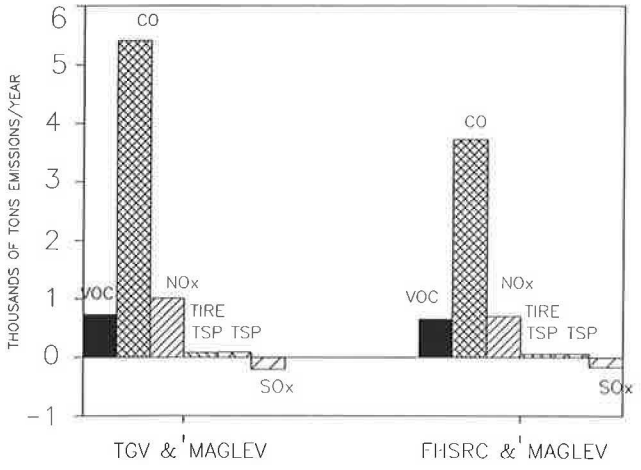

FIGURE 10 Florida net emissions reductions (excluding CO_2) resulting from HSR and maglev development.

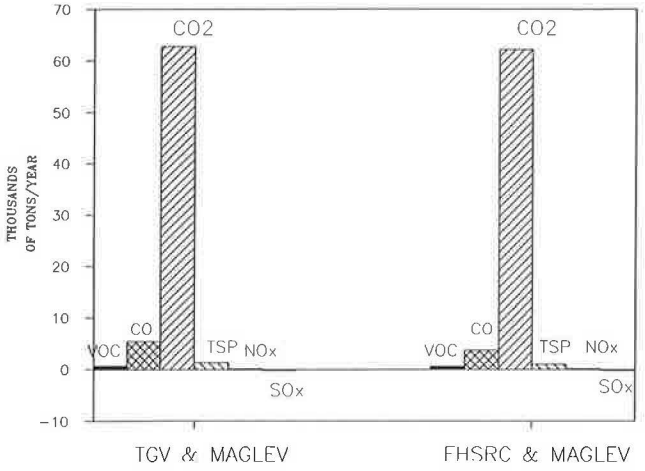

FIGURE 11 Florida net emissions reductions resulting from HSR and maglev development.

Total Suspended Particulates

Like hydrocarbons and CO, a serious concern in many urban areas in Florida (and elsewhere) is the level of total suspended particulates.

HSR and maglev transportation systems operating in the 1999 projected passenger range would reduce TSP emissions from the aircraft and automobile modes by 70 to 97 tons/year for 1999 alone. TSP, like the other pollutants examined, is a concern both as a localized pollutant and as a regional pollutant in many parts of Florida and throughout the United States (see Figures 10 and 11).

Here again, automobiles are widely recognized as one of the principal sources of this pollution. Aircraft operations are also a recognized important source of TSP in the vicinity of airports.

Suspended Particulates Related to Tire Wear

An HSR transportation system operating in the 1.7 to 5 million passenger range combined with the 8 million maglev passengers would produce no tire emissions because the systems are transported along the fixed guideway with no rubber-wheel–road friction or wear.

Automobiles and trucks again are widely recognized as the principal source of tire wear particulate pollution. Tire wear emissions within Florida could be reduced by 61 and 90 tons annually by 1999 if the HSR and maglev systems transported the projected passenger ranges in place of the automobile and airplane (see Table 11 and Figures 10 and 11).

Carbon Dioxide

CO_2 represents the largest quantified emission release from each of the transportation systems examined. CO_2 has only relatively recently become a pollution emission of some concern. Serious concerns about the links between CO_2 emissions and the greenhouse effect have gained growing acceptance in the world scientific community.

Gases such as CO_2, ammonia, and water vapor are relatively transparent to incoming short-wave radiation, but relatively opaque to outgoing long-wave radiation. The greenhouse effect occurs because these gases are radiatively active (*24*). Changes in their concentrations can alter the thermal balance of the earth's atmosphere. CO_2, in particular, though virtually transparent to incoming solar radiation, absorbs outgoing terrestrial infrared radiation that would otherwise escape to space. This trapping of radiation at the lower levels of the atmosphere results in a greenhouse effect caused by the increase in surface temperatures and cooling of upper levels of the atmosphere.

These concerns of global warming are creating intensified worldwide interest in CO_2 emissions. Proposals to examine

the effects and reduce the anthropogenic sources of CO_2 have taken on new prominence in the environmental sciences across the world. Combustion of fossil fuels is the primary source of CO_2. Efforts to shift from more fossil fuel and energy-intensive transportation modes, like the automobile and airplane, to less fossil-fuel-intensive modes, such as HSR and maglev, can significantly contribute to reductions in massive loading of CO_2 into the atmosphere.

The airplane and automobile transportation systems currently in place emit about 80,000 tons/year of CO_2 in transporting passengers at the levels proposed for the Florida HSR and maglev systems. By contrast, these advanced HSR and maglev transportation systems would emit only about 17,600 tons/year of CO_2. So although electrical generation facilities used to power these high-speed ground transport systems do emit CO_2, net state emissions could be reduced by as much as about 62,800 tons/year if an HSR and maglev system were implemented in Florida.

This HSR and maglev system combination is 35 to 58 percent more CO_2 efficient than the automobile and airplane transportation modes at similar passenger loadings. Clearly, this is potentially one of the largest emission reduction benefits that would result from implementation of the HSR and maglev systems in Florida (see Table 11 and Figures 10 and 11).

Nitrogen Oxides

Like the other pollutants, NO_x compounds are viewed as a principal concern in many urban areas across America. NO_x is also one of the principal precursors of acid rain. As mentioned earlier, NO_x compounds are also precursors of ozone.

Nitrogen oxides are a concern both as a localized pollutant and as a precursor to acidic deposition in many parts of this country. Automobiles are widely recognized as the principal and growing source of this pollution. Although power plants emit NO_x, implementation of the HSR and maglev systems in Florida would result in substantial reductions of this pollutant. For example, an HSR transportation system operating in the 1.7 to 5 million annual passenger level combined with the 4 million maglev passengers would reduce annual NO_x emissions statewide by 1,045 to 1,350 tons/year (see Table 11 and Figures 10 and 11).

Sulfur Oxides

Much like nitrogen oxides, sulfur oxides are a concern both as a localized pollutant and as a precursor to acidic deposition in Florida and many other parts of the country. Fossil fuel power plants are generally recognized as one of the principal sources of sulfur oxides.

SO_2 emissions are the single transportation-related pollutant that is estimated to increase somewhat if the HSR and maglev systems were developed in Florida. Although this potential increase in emissions may be of limited concern, several related and important points need to be considered with this projection to keep the potential increase in perspective.

The central point is that these potential increases are likely to diminish as new and more emission-efficient power plants are added to the Florida power plant grid, because of three important factors.

First, new power plants are required to meet stringent SO_2 (and other) pollution emission levels. These federally mandated New Source Performance Standards are resulting in increasingly cleaner total emissions per megawatt-hour as new capacity is added to the existing power plant mix and older facilities are retired.

Second, in addition to building more new power plants with the most stringent emission controls available to serve new and growing capacity, existing old dirty systems are also being replaced (*7*) or directed to operate at increasingly cleaner levels (*25*). These older plants with their historically authorized higher pollution emission levels are increasingly being either removed from service or replaced and upgraded by plants with cleaner emissions than the historic levels.

Third, and perhaps most important, new energy technologies that are both more energy and environmentally efficient are beginning to emerge in Florida and elsewhere across the country (*20*).

For example, improvements in emission controls and electrical generation capability from clean sources such as photovoltaics, other solar energy sources, nuclear sources, and clean-coal technologies are rapidly emerging. Solar markets in recent years are expanding significantly as price of production continues to decrease. Photovoltaics, although more expensive than conventional methods, cost $0.30/kWh and are common in small-source or isolated-source areas. In February 1990, a solar thermal plant is expected to generate power for less than $0.08/kWh, still greater than the $0.03/kWh fossil fuel price, but prospects for continuing declines are imminent.

Perhaps of more immediate interest and pertinence is the surge in recent years of the growth in highly efficient coal-burning technologies. Such is the case with fluidized-bed combustion and coal gasification technologies. Fluidized-bed combustion, which suspends coal in a stream of air, results in more efficient complete combustion, dramatically reduced emissions, and generation of inert byproducts from the burn. Both technologies are under active consideration in Florida and elsewhere for large-scale development. The first 300-mw fluidized-bed cogeneration power plant permitted in Florida will undergo final review during 1990–1991 (*8*).

The City of Tallahassee is also the site of a 120-mw fluidized-bed combustion plant, which is the largest of 13 clean-coal technology projects approved by the Department of Energy for 1990. It will reduce sulfur emissions by 99 percent. It is being built jointly by Tampa Electric (TECO) and CRSS Capital Inc. with the cooperation and support of the City of Tallahassee (*26*).

Finally, the potential increases in SO_2 must also be considered in the context of equivalent offsetting of net gains achieved elsewhere in net reductions of other air pollutants from HSR and maglev systems. Although substantial potential reductions exist in every other air pollution category, the considerable potential reductions in NO_x levels deserve special consideration at this juncture.

As described earlier, NO_2 and SO_2 are both of concern as sources of local and longer-range pollution. Both pollutants are also the principal precursors of acid rain (both wet and dry acidic deposition). Also, no well-accepted or highly efficient technology currently exists to control NO_x emissions. Meanwhile, literally billions of dollars of investment in equipment and substantial progress have been achieved with SO_x

emission reduction in Florida and elsewhere in the United States and in the world.

Therefore, it is both reasonable and desirable to support achievement of a substantial reduction in NO_x pollution at a slight cost of potentially moderate increases in SO_x emissions. This tradeoff is exactly what would result if HSR and maglev transportation systems were implemented in Florida and elsewhere to the extent that these modes would supplant trips by automobile and air.

Specifically, in the Florida setting the potential annual increase of 163 to 201 tons/year of SO_2 can be compared with the projected decrease of 1,043 to 1,350 tons/year of NO_x. A net reduction of localized and long-range pollutant and acid rain precursors could exceed 1,149 tons/year from the combination of these two pollutants (see Table 11 and Figures 10 and 11).

Again, this result would be provided by the development of the HSR and maglev proposed systems in the state of Florida alone. Stated differently, every potential ton of SO_2 emission increase would be matched with a 6.4- to 6.7-ton NO_x emission reduction. From a net environmental efficiency perspective, this tradeoff is desirable.

Total Annual Pollutants Emissions from Transportation

Simply stated, an HSR and maglev system would considerably improve net loadings of all pollutants (except SO_x) to the extent that it is implemented and diverts passengers from the automobile and airplane modes. HSR local area pollutants of CO, HC, NO_x, TSP, and SO_x estimated from these Florida studies are 6 to 16 percent of the automobile and airplane transportation technologies (see Table 11 and Figures 10 and 11).

Although these localized pollution emission loadings are important, of equal or of even greater long-run importance may be the net reductions in long-range pollutants of acid rain precursors (net reductions in the sum of NO_x and SO_x) and larger-scale CO_2 emissions that contribute to the greenhouse effect.

Reduction in these aggregate emission loadings, both localized and long-distance pollutants, could also have other, secondary environmental benefits from improvements in water quality (*27*). Potential reductions in levels of pollutant loadings, acid rain, and air pollution are the most directly visible environmental benefits of implementing such systems.

Other pollutants (such as heavy metals), however, can also contribute to lowering the quality of ambient water and potentially adversely affect other parts of the ecosystem. To the extent that HSR is substituted for the other transportation modes, these benefits would accrue to the environment.

Again, the total potential reduction in all pollutants including CO_2 from implementation of an HSR and maglev system is evident. Total automobile and airplane emissions exceed HSR and maglev emissions (excluding CO_2) by a factor of 14 and total emissions including CO_2 by a factor of 2. This magnitude of improvement can, if implemented in large scale, provide a significant contribution to improving ambient air quality in America's urban areas.

In the final analysis, the air and water environmental benefits of large-scale magnetic levitation technology substantially surpass the others evaluated in virtually every category examined.

CONCLUSION

The results of this Florida-specific analysis conclude that implementation of an HSR proposal and the maglev system would annually result in the following benefits.

Economic and Energy Benefits

- Time savings valued to $136 million.
- Automobile wear and maintenance savings valued to $44 million.
- Property and injury loss savings valued to $10 million.
- Reduction in annual transportation energy consumption of 1.35 to 1.875 trillion Btu.
- Reduced dependence of $33.4 million on fossil fuel to power the U.S. transportation systems.
- Reduction of $31.5 million in imported oil, thereby strengthening the U.S. domestic economy by (a) reducing the negative balance of payments, (b) increasing reliance on domestic sources of energy, and (c) increasing domestic security.
- Reduction in the annual economic damages (externalities) from transportation air pollution emissions.

In addition, HSR and maglev systems would provide the following benefits:

- Savings in new highway construction costs exceeding $1 billion.
- Up to 217,979 man-years of direct and indirect construction employment.
- Up to $20 billion in indirect construction income.
- As much as 9,908 annual permanent operations jobs created both directly and indirectly.
- Over $300 million annually in direct and indirect operation employment income.
- Enhanced transportation productivity by a factor of 3 over current modes.

Environmental Benefits

- Annual reductions of 671 to 749 tons/year of volatile organic carbon emissions.
- Annual reductions of 3,724 to 5,417 tons/year of carbon monoxide.
- Annual reductions of 62,228 to 62,805 tons/year of carbon dioxide.
- Annual reductions of 1,043 to 1,350 tons/year of nitrogen oxides.
- Annual reductions of 70 to 61 tons/year of total suspended particulate matter.
- Annual reductions of 61 to 90 tons/year of particulate matter due to tire wear.

- Annual increases of 163 to 201 tons/year of sulfur oxides.
- Total non-CO_2 automobile and airplane emissions exceed HSR and maglev emissions by a factor of 14.
- Total automobile and airplane emissions (including CO_2) that exceed HSR and maglev emissions by 200 percent.

Growth in Overall Benefits

All of these HSR and maglev social benefits would increase by a factor of 1.75 times any percentage of improvement in trip times, whereas ridership revenues to system owners could increase by a factor of 2.7.

REFERENCES

1. Florida High Speed Rail Corporation. *Franchise Component Volume One.* Submitted to Florida High Speed Rail Transportation Commission, Deerfield Beach, Fla., March 25, 1988.
2. Florida High Speed Rail Corporation. *Completeness Response.* Submitted to Florida High Speed Rail Transportation Commission, Deerfield Beach, Fla., April 3, 1989.
3. Bombardier Inc., Mass Transit Division. *A Presentation of the Florida TGV to The Florida High Speed Rail Transportation Commission, Franchise Component: Appendix-Market Study.* Washington, D.C., March 25, 1988.
4. Bombardier Inc., Mass Transit Division. *Response of the TGV of Florida, Inc.* Washington, D.C., March 31, 1989.
5. Maglev Transit, Inc. *Magnetic Levitation Demonstration Project, Volumes One and Two, Parts I–VI.* Orlando, Fla., March 1989.
6. Barton-Aschman Associates, Inc. *The Florida High Speed Rail Study, Final Report.* Prepared for the Florida Department of Transportation and the Florida High Speed Rail Committee, Tallahassee, 1984.
7. Florida Electric Power Coordinating Group and Florida Public Service Commission. *Florida Ten Year Electric Generation Plan.* Tallahassee, 1988.
8. AES/Cedar Bay, Inc. *The Cedar Bay Cogeneration Project. Volume 1.* Overland Park, Kan., Nov. 1986.
9. *Air Quality Report—1987.* State of Florida, Department of Environmental Regulation, Division of Air Resources Management, Tallahassee, 1988.
10. *Air Pollutant Information System Facility Emission Report.* State of Florida, Department of Environmental Regulation, Tallahassee, 1988.
11. *Procedures for Emission Inventory Preparation, Volume IV: Mobile Sources.* U.S. Environmental Protection Agency, Office of Air Quality, Planning and Standards, EPA-450/4-81-026D, Research Triangle Park, N.C., Sept. 1981.
12. *Carbon Dioxide and Climate, A Working Glossary.* Oak Ridge National Laboratory, U.S. Department of Energy, Oak Ridge, Tenn., 1987.
13. *Certification Component.* A Presentation of the Florida TGV to the Florida High Speed Rail Transportation Commission, Chapter 9—Energy and Electromagnetic Fields, TGV of Florida, Inc., Tallahassee, March 25, 1988, p. 9–1.
14. Transrapid Maglev System. Hestra-Verlag, Damstadt, Germany, 1988.
15. S. H. Gibbons, D. D. Blair, and H. L. Swin. Strategies for Energy Use. *Scientific American*, New York City, Sept. 1989.
16. *Proposal for a European High-Speed Network.* Community of European Railways, Brussels, Belgium, 1988, p. 22.
17. AASHTO. *A Manual of User Benefit Analysis of Highway and Bus-Transit Improvements.* Washington, D.C., 1977.
18. FAA. *Economic Analysis of Investment and Regulatory Decisions—A Guide.* Report FAA-APO 82.1. Washington, D.C., 1982.
19. AASHTO. *Estimating the Cost of Accidents.* Bull. T-113-82, National Safety Council, Chicago, Ill., 1982.
20. R. E. Balzhiser and K. E. Yegar. Coal-Fired Power Plants for the Future, *Scientific American*, New York City, Nov. 1987.
21. T. A. Lynch. Interregional Transportation Models Benefit Estimation for High Speed Rail in Florida. Presented at TRB Annual Meeting, Washington, D.C., Jan. 1987 (unpublished).
22. T. A. Lynch. *A Policy/Analysis Model Incorporating Acid Rain and Sulfur Dioxide Damages Associated with Power Plant Conversions From Oil to Coal in the State of Florida.* Florida State University, Tallahassee, Aug. 1984.
23. Peat, Marwick, Main & Co. *Technical Report: Patronage Estimation: Appendix—Market Study.* A Presentation of the Florida TGV to the Florida High Speed Rail Transportation Commission, Washington, D.C., March 1988.
24. *Carbon Dioxide and Climate, A Working Glossary.* Oak Ridge National Laboratory, U.S. Department of Energy, Oak Ridge, Tenn., 1987.
25. *Federal Clean Air Act.* S.1630, U.S. Senate, Washington, D.C., 1990.
26. *Fluidized Bed Combustion Power Proposal for the City of Tallahassee.* City of Tallahassee, Fla., 1989.
27. T. A. Lynch. *A Policy Analysis Model Incorporating Acid Rain and Sulfur Dioxide Damages Associated with Power Plant Conversions from Oil to Coal in Florida.* Florida State University, Tallahassee, Aug. 1984.

Publication of this paper sponsored by Committee on Intercity Passenger Guided Transportation.